

Identification and characterization of key regulatory components involved in the development of type VI glandular trichomes in *Solanum lycopersicum*

Dissertation

zur Erlangung des
Doktorgrades der Naturwissenschaften (Dr. rer. nat.)



der
Naturwissenschaftlichen Fakultät I – Biowissenschaften
der Martin-Luther Universität Halle-Wittenberg,

Vorgelegt von

Herr. M.Sc. Chandan Chiniga Kemparaju

geb. am 08 November 1985 in Hospet (Karnataka, India)

Gutachter:

1. Prof. Dr. Bettina Hause
2. Prof. Dr. Klaus Humbeck
3. PD. Dr. Axel Mithöfer

Tag der Verteidigung: 01 November 2018

SUMMARY

Plant glandular trichomes have gained a significant interest due to the storage and secretion of specialized compounds. To know how these epidermal structures are formed, which later turn into highly efficient biochemical factories, it is essential to understand the developmental factors involved in the formation of glandular trichomes. The current PhD thesis aims to dissect the molecular mechanisms involved in the formation of type VI glandular trichomes in tomato.

The molecular mechanism of type VI glandular trichomes is still not clear in the current plant science research. Substantial amount of data, corresponding to multicellular trichome formation (glandular and non-glandular) and density alterations in *Antirrhinum majus*, *Gossypium spp*, *Artemisia annua*, *Cucumis sativus* and Solanaceae states that transcription factors play a pivotal role in the initiation and development of trichomes. These transcription factors belong to the classes of MYB's, bHLH's and class IV HD-Zip's, which are also involved in the regulation of genes responsible for secondary metabolism. Unicellular trichome initiation process in the model plant, *Arabidopsis thaliana*, is tightly controlled by transcription factors within the MYB-bHLH-WD40 trimeric complex, activating the downstream trichome regulator AtGL2. However, a comparable role in the regulation of multicellular trichome formation remains speculative. Recent studies suggest that orthologs of Arabidopsis trichome regulators in the MBW complex were found to be expressed in the *Nicotiana tabacum* trichomes. This led to speculate that the orthologs of Arabidopsis trichome regulators might be linked in the formation of multicellular trichomes in tomato. Yet, in tomato, their transcript levels were extremely low, behaving explicitly different in young tomato leaves.

Among the factors that induce trichomes, phytohormones have a key role in elevating trichome numbers and density, and are considerably linked in the formation of trichomes. The plant hormone JA extensively contributes in the formation of trichomes. External application of JA on tomato leaves has led to elevated levels of type VI glandular trichomes. Type VI glandular trichome numbers are significantly reduced in the *jai1* mutant compared to wild type tomato plants. Although, there exist genotypes with significant differences in type VI glandular trichome numbers, the key regulators involved in the formation of glandular trichomes mediated through JA are still obscure.

In this research work, based on the RNA sequencing data, putative transcription factors or genes induced by JA were identified from wild type, JA-treated (2 hours and 24 hours) and *jai1* plants. Putative transcription factors upregulated shortly after JA treatment compared to *jai1* were predicted to contribute to the formation of glandular trichomes at the early developmental phase. The expression pattern of genes encoding putative MYB9, MYB4-like, MYC2 and PDF2 were validated using independent biological replicates. Validated putative candidates were transiently expressed in *N. benthamiana* leaves to analyze their subcellular localization.

For the first time, Arabidopsis epidermal specific promoter *ATML1* was used to control the activity of putative candidates in tomato. Initial *promoter-GUS* assays in tobacco and tomato showed its activity across the tomato leaf epidermis and basal regions of trichome cells, which was promising to take it further for the overexpression of putative candidates. Based on this, prime importance was given to MYB9 and PDF2 candidates under the control of constitutive 35S and epidermal specific *ATML1* promoters, in the wild type and *jai1* background, respectively. Overexpression of *pATML1::GFP:MYB9* and *35S::GFP:PDF2* showed no significant impact on type VI glandular trichome numbers compared to control. Further, secondary compounds were qualitatively analyzed to identify typical trichome related metabolites. Monoterpenes and sesquiterpenes were analyzed in the overexpression lines compared to wild type and *jai1* control leaves. From the qualitative analyses of these terpenoids, it was concluded that the putative MYB9 may significantly contribute to the synthesis of monoterpenes but not to class I sesquiterpenes. Furthermore, monoterpenes and class I sesquiterpenes were not significantly different across the individual lines of putative PDF2 compared to the control, indicating that PDF2 is not involved in the accumulation of monoterpenes and class I sesquiterpenes. Two of the genes encoding putative MYB4-like and MYC2 regulators were characterized for their loss-of-function by a TILLING approach. Mutations within the DNA-binding domain of putative MYB4-like and a premature stop codon in the N-terminus of putative MYC2 protein led to significant reduction in type VI glandular trichome numbers compared to control plants. This highlights the importance of (i) the functional DNA-binding domain of putative MYB4-like and (ii) the functional N-terminus of putative MYC2 protein for the formation of type VI glandular trichomes in the cultivated tomato. Taken together, the identification and functional characterization of putative transcription factors broadens the knowledge of the molecular mechanisms and their role in the formation of type VI glandular trichomes.

Zusammenfassung

Pflanzliche Drüsentrichome haben aufgrund der Speicherung und Sekretion von spezialisierten Verbindungen ein signifikantes Interesse erhalten. Um zu klären, wie diese epidermalen Strukturen gebildet werden, die später zu hocheffizienten biochemischen "Fabriken" werden, ist es wichtig die Entwicklungs-spezifischen 'Faktoren' zu verstehen, die bei der Bildung von Drüsentrichomen eine Rolle spielen. Die vorliegende Dissertation zielt darauf ab, die molekularen Mechanismen zu analysieren, die bei der Bildung von Typ VI glandulären Trichomen in Tomaten.

Die molekularen Mechanismen der Bildung von Typ-VI-Drüsentrichomen sind in der aktuellen pflanzenwissenschaftlichen Forschung noch nicht bekannt. Viele Daten zu multizellulärer Trichombildung (drüsig und nicht drüsig) und -dichte bei *Antirrhinum majus*, *Gossypium spp*, *Artemisia annua*, *Cucumis sativus* und Solanaceae (Tabak und Tomaten) bestätigen, dass Transkriptionsfaktoren eine zentrale Rolle bei der Trichombildung und -entwicklung spielen. Diese Transkriptionsfaktoren gehören zu den Klassen der MYB's, bHLH's und Klasse IV HD-Zip's, die auch an der Regulation der für den Sekundärstoffwechsel verantwortlichen Gene beteiligt sind. Die Initiierung einzelliger Trichome in der Modellpflanze *Arabidopsis thaliana* wird durch Transkriptionsfaktoren des MYB-bHLH-WD40-Trimärkomplexes strikt kontrolliert und aktiviert den nachgeschalteten Regulator GL2. Eine vergleichbare Rolle bei der Regulation der multizellulären Trichombildung bleibt jedoch spekulativ. Neuere Studien deuten darauf hin, dass Orthologe von *Arabidopsis* Trichomregulatoren im MBW-Komplex in *Nicotiana tabacum* Trichomen exprimiert werden. Dies ließ vermuten, dass diese Trichom-regulierenden Orthologe in die Bildung von mehrzelligen Trichomen in Tomate involviert sein könnten. Doch bei Tomaten waren die Transkriptionswerte extrem niedrig, insbesondere bei jungen Tomatenblättern.

Phytohormone spielen eine Schlüsselrolle bei der Erhöhung der Anzahl und Dichte von Trichomen und sind beträchtlich in der Bildung von Trichomen verbunden. Das Pflanzenhormon JA spielt eine bedeutsame Rolle bei der Bildung von Trichomen. Eine oberflächliche Behandlung von Tomatenblättern mit JA hat zu einem signifikanten Anstieg der Zahl der Drüsentrichome vom Typ VI geführt. Bei der Mutante *jai1* wurde ein erheblicher Unterschied in der Anzahl der Drüsentrichome vom Typ VI im Vergleich zur WT-Tomate beobachtet. Obwohl es Genotypen mit signifikanten Unterschieden in der

Anzahl der Drüsentrichome vom Typ VI gibt, sind die wichtigsten Regulatoren, die an der Bildung der durch JA vermittelten Drüsentrichome beteiligt sind, immer noch unklar.

In dieser Dissertation wurden durch JA induzierte vermeintliche Transkriptionsfaktoren oder Gene basierend auf RNA-Sequenzierungsdaten von Wildtyp, JA-behandelten (2 Stunden und 24 Stunden) und *jai1* Pflanzen identifiziert. Die entsprechende RNA-Seq-Analyse identifizierte Transkriptionsfaktoren, die für Gene kodieren, die sowohl im Wildtyp nach der JA-Behandlung als auch in der *jai1*-Mutante signifikant induziert sind. Es wurde angenommen, dass diese vermeintlichen Transkriptionsfaktoren bereits in einem frühen Stadium zur Bildung von Drüsentrichomen beitragen. Die Expressionsmuster von Genen, die mutmaßlich für MYB9, MYB4-like, MYC2 und PDF2 kodieren, wurden mit unabhängigen biologischen Replikaten validiert. Validierte mutmaßliche Kandidaten wurden transient in *N. benthamiana* Blättern exprimiert, um ihre subzelluläre Lokalisierung zu analysieren. Zum ersten Mal wurde der Epidermis-spezifische Promotor *ATML1* von Arabidopsis verwendet, um die Aktivität von vermeintlichen Kandidaten in Tomaten zu kontrollieren. Erste Promotor-GUS-Assays in Tabak und Tomaten zeigten Aktivität in der Epidermis der Tomatenblätter und in den Basalregionen der Trichomzellen, was vielversprechend für eine folgende Überexpression der Kandidaten war. Auf dieser Grundlage wurde den MYB9- und PDF2-Kandidaten unter der Kontrolle des konstitutiven *35S*- und des Epidermis-spezifischen *ATML1*-Promotors in Wildtyp- bzw. *jai1*-Hintergrund höchste Bedeutung beigemessen. Die Überexpression von *pATML1::GFP:MYB9* und *35S::GFP:PDF2* zeigte keinen signifikanten Einfluss auf die Trichomzahlen des Typs VI im Vergleich zur Kontrolle. Weiterhin wurden Sekundärmetaboliten qualitativ analysiert, um typische Trichom-relevante Metaboliten zu identifizieren. Monoterpene und Sesquiterpene wurden in den Überexpressionslinien im Vergleich zu Wildtyp und *jai1*-Blättern analysiert. Qualitative Analysen dieser Terpenoide kommen zu dem Schluss, dass das mutmaßliche MYB9 signifikant zur Synthese von Monoterpenen beitragen kann, nicht aber zu Sesquiterpenen der Klasse I. In der Folge unterschieden sich Monoterpene und Sesquiterpene der Klasse I nicht signifikant zwischen den einzelnen Linien des PDF2-Homologs im Vergleich zur Kontrolle, was auf keine signifikante Rolle bei der Akkumulation von Monoterpenen und Sesquiterpenen der Klasse I hinweist. Zwei der Gene, die für MYB4-like und MYC2-Regulatoren kodieren, wurden durch einen *loss-of-function* TILLING-Ansatz charakterisiert. Mutationen innerhalb der DNA-bindenden Domäne des mutmaßlichen MYB4-like und ein vorzeitiges Stoppcodon im N-Terminus des mutmaßlichen MYC2-Proteins führten zu einer signifikanten Reduktion der

Drüsentrichomzahlen vom Typ VI im Vergleich zu Kontrollpflanzen. Dies unterstreicht die Bedeutung von (i) der funktionellen DNA-Bindungsdomäne des mutmaßlichen MYB4-like und (ii) des funktionellen N-Terminus des mutmaßlichen MYC2-Proteins für die Bildung von Drüsentrichomen vom Typ VI in der kultivierten Tomate. Die Identifizierung von mutmaßlichen Kandidaten durch bioinformatische Methoden und ihre funktionelle Charakterisierung dienen als wichtige Werkzeuge, um Kandidatenprofile aufzudecken und JA-bezogene Typ-VI-Drüsen-Trichom-Phänotypen zu entschlüsseln. Zusammenfassend lässt sich sagen, dass durch die Untersuchungen in dieser Arbeit Identifizierung und funktionelle Charakterisierung von putativen Transkriptionsfaktoren hat einen Einblick in die molekularen Mechanismen gewonnen, die bei der Bildung von Drüsentrichomen vom Typ VI eine Rolle spielen.

TABLE OF CONTENTS

| | |
|--|-------------|
| SUMMARY | i |
| Zusammenfassung | iii |
| TABLE OF CONTENTS | vii |
| INDEX OF FIGURES | xiii |
| INDEX OF TABLES | xv |
| ABBREVIATIONS | xvi |
| 1 INTRODUCTION | 1 |
| 1.1 Plant trichomes | 1 |
| 1.1.1 Classification and morphological description of trichomes | 1 |
| 1.1.1.1 Non-glandular trichomes | 2 |
| 1.1.1.2 Glandular trichomes | 2 |
| 1.1.2 Importance of trichomes in the plant kingdom | 3 |
| 1.1.2.1 Significance of glandular trichomes | 3 |
| 1.1.3 Glandular trichomes in Solanaceae: Special emphasis on the <i>Solanum lycopersicum</i> cultivar 'MicroTom' | 4 |
| 1.1.4 Terpene levels in <i>Solanum lycopersicum</i> | 5 |
| 1.2 Role of phytohormones in trichome development | 6 |
| 1.2.1 Jasmonates (JAs) | 6 |
| 1.2.1.1 JA-deficient mutants affecting trichome formation | 7 |
| 1.2.2 Gibberellins (GAs) | 8 |
| 1.2.3 Cytokinins (CKs) | 9 |
| 1.2.4 Factors affecting trichome induction | 9 |
| 1.2.4.1 Insect herbivory and artificial damage | 9 |
| 1.2.4.2 Induction of trichomes by exogenous JA treatment | 10 |
| 1.3 The molecular mechanisms in the formation of trichomes | 10 |
| 1.3.1 Role of essential trichome regulators in <i>Arabidopsis thaliana</i> | 11 |
| 1.3.1.1 Positive regulators of the trichome regulatory complex | 11 |
| 1.3.1.2 Negative regulators of the trichome regulatory complex | 13 |

| | | |
|------------|---|-----------|
| 1.3.2 | Interaction of positive and negative regulators in trichome formation | 14 |
| 1.3.3 | Glandular trichome regulators in Solanaceae | 16 |
| 1.4 | Transcription factor families in <i>Solanum lycopersicum</i> | 17 |
| 1.4.1 | MYB transcription factor family | 17 |
| 1.4.2 | The basic helix-loop-helix (bHLH) transcription factor family | 19 |
| 1.5 | Thesis objectives | 20 |
| 1.5.1 | The importance of <i>jai1</i> mutant as a useful tool in the approach | 20 |
| 2 | MATERIALS & METHODS | 22 |
| 2.1 | Materials | 22 |
| 2.1.1 | Chemicals, enzymes and extraction kits | 22 |
| 2.1.2 | Microorganisms | 22 |
| 2.1.3 | Oligonucleotides and Plasmids | 22 |
| 2.1.4 | Buffers, media and solutions | 22 |
| 2.1.5 | Culture media and solutions | 23 |
| 2.1.6 | Plant transformation medium | 23 |
| 2.1.7 | Protein electrophoresis buffers and solutions | 24 |
| 2.1.7.1 | Western blotting buffers and solutions | 24 |
| 2.2 | Biological methods | 25 |
| 2.2.1 | Plant cultivation and growth conditions | 25 |
| 2.2.2 | Preselection of <i>jai1</i> mutant | 25 |
| 2.2.3 | Quantification of type VI glandular trichomes upon wounding | 26 |
| 2.2.4 | Phytohormone measurements upon wounding | 27 |
| 2.2.5 | Transcriptome sequencing | 27 |
| 2.3 | Microbiological methods | 27 |
| 2.3.1 | Production of chemically competent <i>Escherichia coli</i> cells | 27 |
| 2.3.2 | Transformation of <i>Escherichia coli</i> cells | 28 |
| 2.3.3 | Production of chemically competent <i>Agrobacterium tumefaciens</i> cells | 28 |
| 2.3.4 | Transformation of <i>Agrobacterium tumefaciens</i> cells | 29 |
| 2.4 | Molecular biological methods | 29 |
| 2.4.1 | Crude genomic DNA isolation and genotyping for <i>jai1</i> plants | 29 |
| 2.4.2 | Pure genomic DNA isolation | 30 |
| 2.4.3 | Total RNA extraction and Dnase I treatment | 30 |

| | | |
|------------|---|-----------|
| 2.4.4 | cDNA synthesis | 32 |
| 2.4.5 | Cloning the putative candidate genes | 32 |
| 2.4.6 | Isolation of plasmid DNA, Restriction digestion and ligation | 33 |
| 2.4.6.1 | Colony PCR for putative candidates | 33 |
| 2.4.7 | Agarose gel electrophoresis | 33 |
| 2.4.8 | Capillary gel electrophoresis | 34 |
| 2.4.9 | Quantitative real-time Polymerase Chain Reaction (qRT-PCR) | 34 |
| 2.5 | Bioinformatics analyses | 34 |
| 2.5.1 | Transcriptome database construction and expression profiling | 34 |
| 2.5.2 | Transcriptome data assembly and processing | 35 |
| 2.5.3 | Custom expression analysis and annotations | 35 |
| 2.5.4 | Gene Ontology (GO) analysis | 35 |
| 2.6 | Analytical techniques | 36 |
| 2.6.1 | Western blot | 36 |
| 2.6.1.1 | Protein extraction from Agro-infiltrated tobacco plants | 36 |
| 2.6.1.2 | Protein quantification by ESEN method | 36 |
| 2.6.1.3 | SDS- Polyacrylamide gel electrophoresis (PAGE) | 36 |
| 2.6.1.4 | Trans-Blot Semi Dry electrophoretic transfer | 37 |
| 2.6.1.5 | Immunostaining | 38 |
| 2.6.2 | Determination of jasmonate levels | 38 |
| 2.6.3 | Gas Chromatography-Mass Spectrometry (GC-MS) | 39 |
| 2.7 | Microscopy works | 39 |
| 2.7.1 | GUS histological assay | 39 |
| 2.7.2 | Paraplast embedding of leaf material | 39 |
| 2.7.3 | Polyethylene glycol (PEG) embedding of leaf material | 40 |
| 2.7.4 | Environmental Scanning Electron Microscopy (ESEM) | 40 |
| 2.7.5 | Localization of GFP- tagged proteins | 40 |
| 2.7.6 | Leaf imaging and counting glandular trichomes | 41 |
| 2.8 | Plant transformation | 41 |
| 2.8.1 | Transient transformation of <i>Nicotiana benthamiana</i> leaves | 41 |
| 2.8.2 | Transformation of <i>N. benthamiana</i> mesophyll protoplasts | 41 |
| 2.8.3 | Stable transformation of cultivated tomato | 42 |

| | |
|--|-----------|
| 2.8.3.1 Germination of seeds, plant growth and physiological conditions | 42 |
| 2.8.3.2 Pre-conditioning and transformation | 42 |
| 2.8.3.3 Callus cultivation and regeneration | 42 |
| 2.8.3.4 Plant acclimatization | 43 |
| 3 RESULTS | 44 |
| 3.1 Prerequisite experimental analysis | 44 |
| 3.1.1 Mechanical wounding | 44 |
| 3.1.2 Exogenous JA treatment | 45 |
| 3.1.3 Importance of third true leaf for downstream applications | 46 |
| 3.2 Validation of JA-induced genes to verify treatment conditions | 47 |
| 3.3 Validation of tomato homologs of trichome regulatory genes | 49 |
| 3.4 Validation of candidates from apex and glandular trichomes data set | 50 |
| 3.5 Transcriptomic data analysis from young tomato leaves | 53 |
| 3.5.1 Distribution of treatment biological replicates | 54 |
| 3.5.2 Differentially expressed genes in between treatment comparisons | 55 |
| 3.5.3 Functional enrichment analysis of differentially expressed genes between treatments | 57 |
| 3.5.4 Functional annotation putative transcription factors | 59 |
| 3.5.5 Clustering of differentially expressed genes | 60 |
| 3.6 Validation and selection of putative candidates | 62 |
| 3.6.1 Putative transcription factors up-regulated in the <i>jai1</i> mutant compared to JA_2h treatment | 64 |
| 3.6.2 Putative JA-regulated genes up-regulated in the JA_2h treatment | 67 |
| 3.7 Functional characterization of selected putative transcription factors | 69 |
| 3.7.1 Localization studies in <i>N. benthamiana</i> protoplasts | 71 |
| 3.7.2 Protein detection on the western blot from transiently transformed protoplasts | 72 |
| 3.8 Elucidation of loss-of-function of putative transcription factors through TILLING approach | 73 |
| 3.8.1 MYB4-like TILLING line | 73 |
| 3.8.2 MYC2 TILLING line | 75 |
| 3.8.3 Phenotypic characterization of TILLING mutant lines | 78 |
| 3.9 Cloning and characterization of <i>Arabidopsis thaliana</i> Meristem Layer 1 (ATML1) promoter | 80 |
| 3.9.1 Elucidation of ATML1 promoter activity in tomato | 82 |
| 3.10 Overexpression of putative transcription factors in tomato | 83 |

| | | |
|----------|--|------------|
| 3.10.1 | Localization studies for primary transformants under constitutive and <i>ATML1</i> promoter | 84 |
| 3.10.2 | Quantification of GFP levels in primary transformants (T0) | 85 |
| 3.10.3 | Localization of putative candidates in the F1 segregation lines | 87 |
| 3.10.4 | Quantification of putative candidate gene expression | 88 |
| 3.10.5 | Quantification of type VI glandular trichomes | 90 |
| 3.10.6 | Qualitative analysis of terpene levels on F1 transgenic lines | 91 |
| 4 | DISCUSSION | 94 |
| 4.1 | Importance of prerequisite experimental approach | 94 |
| 4.2 | Tomato homologs of key Arabidopsis trichome regulators behave explicitly different | 95 |
| 4.3 | Analysis of differentially expressed genes across sample treatments | 96 |
| 4.3.1 | Early JA response-related genes on young tomato leaves | 97 |
| 4.3.2 | Selection of putative candidates involved in trichome development | 97 |
| 4.3.3 | Validation of other significantly expressed JA regulated genes | 100 |
| 4.3.4 | Selected putative transcription factors are located in the plant cell nucleus | 101 |
| 4.4 | Functional characterization of selected putative transcription factors | 101 |
| 4.4.1 | Characterization of <i>ATML1</i> promoter activity in tomato leaves | 101 |
| 4.4.2 | Approaches for functional characterization of candidates: Overexpression and identification of mutants | 103 |
| 4.4.2.1 | MYB9 | 103 |
| 4.4.2.2 | PDF2 | 104 |
| 4.4.2.3 | Metabolic activity in <i>MYB9</i> and <i>PDF2</i> overexpressing plants | 105 |
| 4.4.2.3 | MYB4-like | 107 |
| 4.4.2.4 | MYC2 | 110 |
| 5 | CONCLUSIONS | 113 |
| | Future perspectives | 113 |
| 6 | APPENDICES | 116 |
| 6.1 | List of oligonucleotides | 116 |
| 6.1.1 | Primers for genotyping <i>jai1</i> mutant population | 116 |
| 6.1.2 | Primers for quantitative real time PCR (qRT-PCR) | 116 |
| 6.2 | List of antibiotics | 119 |
| 6.3 | Golden gate cloning strategy | 119 |
| 6.4 | Jasmonate measurements in young tomato plants | 120 |

| | | |
|----------------------------------|---|------------|
| 6.5 | Transcriptome sequencing analysis | 120 |
| 6.5.1 | Differentially regulated genes across WT control and JA- treatments | 120 |
| 6.5.2 | Clustering of highly significant genes across treatment conditions | 121 |
| 6.6 | Putative transcription factors encoding protein domains | 124 |
| 6.6.1 | Putative MYB9 protein homologs in closely related plant model species | 124 |
| 6.6.3 | Putative MYC2 protein homologs in closely related species | 126 |
| 6.6.4 | Putative PDF2 protein homologs in closely related species | 128 |
| 6.7 | Qualitative analysis of monoterpenes and sesquiterpenes | 131 |
| BIBLIOGRAPHY | | 134 |
| ACKNOWLEDGEMENTS | | 152 |
| Curriculum Vitae | | 154 |
| Eidesstattliche Erklärung | | 158 |

INDEX OF FIGURES

| | |
|---|----|
| Figure 1: Morphological description of trichomes in <i>Solanum</i> species | 5 |
| Figure 2: Distribution of trichomes on the wild type and <i>jai1</i> tomato leaves | 7 |
| Figure 3: Trichome regulatory model in <i>Arabidopsis thaliana</i> | 15 |
| Figure 4: Characterization of R2R3 MYB functional domains in tomato | 18 |
| Figure 5: Characterization of bHLH functional domains in tomato | 19 |
| Figure 6: Workflow for screening <i>jai1</i> mutant: | 26 |
| Figure 7: Qualitative estimation of leaf RNA samples | 31 |
| Figure 8: Artificial wounding experiments on tomato leaves | 44 |
| Figure 9: Quantification of type VI glandular trichomes | 45 |
| Figure 10: Quantification of type VI glandular trichomes upon JA treatment | 46 |
| Figure 11: Morphology of type VI glandular trichomes on the third true leaf | 47 |
| Figure 12: Transcript accumulation of JA-induced genes in treatment conditions | 48 |
| Figure 13: Transcript accumulation of the tomato homologs of Arabidopsis trichome regulatory genes | 49 |
| Figure 14: Transcript accumulation of putative tomato homologs from apex and glandular trichomes data set | 51 |
| Figure 15: Treatment biological replicates on Multidimensional scaling (MDS) plot | 54 |
| Figure 16: Representation of normalized dataset on smear plots | 55 |
| Figure 17: Representation of differentially expressed genes on Venn diagram | 56 |
| Figure 18: MAPMAN functional annotation significant transcription factors | 59 |
| Figure 19: Clustering of transcription factors on the heatmap | 61 |
| Figure 20: Transcript accumulation of putative transcription factors up-regulated after JA ₂ h treatment | 63 |
| Figure 21: Transcript accumulation of putative transcription factors up-regulated in the <i>jai1</i> _CO | 66 |
| Figure 22: Transcript accumulation of putative JA-regulated genes | 68 |
| Figure 23: Protein sequences of selected candidates | 70 |
| Figure 24: Localization of putative candidates in <i>N. benthamiana</i> protoplasts | 71 |
| Figure 25: Protein detection on the western blot | 72 |
| Figure 26: Putative MYB4-like protein sequence with mutation positions | 74 |
| Figure 27: Multiple sequence alignment of putative MYB4-like and its homologs | 75 |
| Figure 28: Putative MYC2 protein sequence with mutation positions | 76 |
| Figure 29: Multiple sequence alignment of putative MYC2 and its homologs | 77 |
| Figure 30: Characterization of MYB4-like and MYC2 TILLING lines | 78 |
| Figure 31: Cloning the promoter ATML1 using golden gate strategy | 80 |
| Figure 32: pATML1-GUS activity in tobacco and tomato leaves | 81 |

| | |
|--|-----|
| Figure 33: pATML1-GUS activity in the developing leaves of transgenic tomato plants | 82 |
| Figure 34: Generation of tomato transformants | 83 |
| Figure 35: Localization of putative candidates in the primary transformants | 85 |
| Figure 36: Relative transcript accumulation of GFP in primary transformants (T ₀)..... | 86 |
| Figure 37: Localization of putative candidates in the F1 generation..... | 87 |
| Figure 38: Relative expression of <i>GFP</i> in F1 transgenic lines | 88 |
| Figure 39: Relative expression of <i>MYB4</i> -like in F1 and F2 overexpression lines | 89 |
| Figure 40: Quantification of type VI glandular trichomes in F1 transgenic lines | 91 |
| Figure 41: Measurement of terpenes from the leaf extracts of F1 transgenic lines | 92 |
| Figure 42: Predicted secondary structures of putative MYB4-like protein | 109 |
| Figure 43: Predicted secondary structure of putative MYC2 protein | 111 |

APPENDICES

| | |
|--|-----|
| Figure A1: Assembly of modules for golden gate cloning..... | 119 |
| Figure A2: Determination of JA levels in young tomato plant organs. | 120 |
| Figure A3: Venn diagram scheme representation..... | 120 |
| Figure A4: Representation of gene clusters on heatmap..... | 123 |
| Figure A5: Multiple sequence alignment of putative MYB9 full-length and its homologs. | 124 |
| Figure A6: Multiple sequence alignment of putative full-length MYB4-like and its homologs..... | 125 |
| Figure A7: Multiple sequence alignment of putative full-length MYC2 and its homologs. | 127 |
| Figure A8: Multiple sequence alignment of putative full-length MYC2 and its homologs. | 130 |
| Figure A9: Analysis of the peak area of monoterpenes | 131 |
| Figure A10: Analysis of the peak area of sesquiterpenes..... | 132 |
| Figure A11: Analysis of the peak area of sesquiterpenes..... | 133 |

INDEX OF TABLES

| | |
|--|----|
| Table 1: List of micro and macroelements | 23 |
| Table 2: Media components for generating tomato (c.v MicroTom) stable transformants..... | 23 |
| Table 3: Buffers and staining solutions for protein electrophoresis | 24 |
| Table 4: Cycling conditions for genotyping <i>jai1</i> mutant plants | 29 |
| Table 5: Cycling conditions for genotyping <i>jai1</i> mutant..... | 30 |
| Table 6: Cycling conditions for candidates..... | 32 |
| Table 7: Cycling conditions for colony PCR | 33 |
| Table 8: Cycling conditions for qRT-PCR | 34 |
| Table 9: Reagents for separation and collection gel | 36 |
| Table 10: Antibodies for the detection of putative proteins | 38 |
| Table 11: Components for GUS staining solution | 39 |
| Table 12: Putative tomato homologs of key trichome regulators from apex and glandular trichomes data set..... | 50 |
| Table 13: Total read counts for treatment biological replicates generated by RNA-seq..... | 53 |
| Table 14: PAGEMAN functional enrichment analysis between JA_2h and <i>jai1_CO</i> | 58 |
| Table 15: PAGEMAN functional enrichment analysis between <i>jai1_CO</i> and JA_2h..... | 59 |
| Table 16: List of putative transcription factors upregulated shortly after JA treatment (JA_2h) compared to <i>jai1</i> mutant (<i>jai1_CO</i>). | 62 |
| Table 17: Putative transcription factors upregulated in <i>jai1_CO</i> compared to JA_2h treatment | 65 |
| Table 18: List of putative candidates selected for validation up-regulated after JA_2h treatment | 67 |
| Table 19: List of TILLING lines for putative MYB4-like | 73 |
| Table 20: List of TILLING lines for putative MYC2..... | 75 |

ABBREVIATIONS

| | |
|----------------|---|
| At | <i>Arabidopsis thaliana</i> |
| AOC | ALLENE OXIDE CYCLASE |
| ATML1 | <i>Arabidopsis thaliana</i> Meristem Layer 1 |
| BLAST | Basic Local Alignment Search Tool |
| bp | base pairs |
| bHLH | Basic Helix-Loop-Helix |
| CK | Cytokinins |
| DBD | DNA-Binding Domain |
| DNA | Deoxyribo Nucleic Acid |
| <i>E. coli</i> | <i>Escherichia coli</i> |
| EDTA | Ethylenediaminetetra acetic acid |
| EMS | Ethyl methanesulfonate |
| ESEM | Environmental Scanning Electron Microscope |
| ESTs | Expressed Sequence Tags |
| ERF | Ethylene Response Factor |
| For | forward |
| GA | Gibberellic Acid |
| GC-MS | Gas Chromatography-Mass Spectrometry |
| GFP | Green Fluorescent Protein |
| GUS | Beta-glucurodinase |
| HD-Zip | Homeo-Domain leucine zipper |
| JA | Jasmonic Acid |
| <i>jai1</i> | <i>jasmonic acid insensitive 1</i> |
| JAZ | Jasmonate ZIM Domain |
| kDa | Kilodalton |
| LAP A | Leucine Aminopeptidase |
| MeJA | Methyl jasmonate |
| MeOH | Methanol |
| µm | micrometer |
| MT | MicroTom |
| MYB | Myeloblastosis |
| NCBI | National Center for Biotechnology Information |
| OD | Optical Density |
| PAGE | Polyacrylamide Gel Electrophoresis |
| PBS | Phosphate Buffer Saline |
| PCA | Principal Component Analysis |
| PCR | Polymerase Chain Reaction |
| PDF2 | PROTODERMAL FACTOR 2 |
| qRT-PCR | Quantitative Real Time- Polymerase Chain Reaction |
| Rev | Reverse |

| | |
|----------|--|
| RIN | RNA Integrity Number |
| RNA | Ribo Nucleic Acid |
| RNAi | RNA interference |
| RNA-seq | RNA sequencing |
| rpm | Rotation per minute |
| RT | Room Temperature |
| SA | Salicylic Acid |
| SCF | S-Phase Kinase Associated Protein 1-Cullin-F-box Protein complex |
| SDS | Sodium dodecyl sulfate |
| SNP | Single Nucleotide Polymorphism |
| SPE | Solid Phase Extraction |
| Taq | <i>Thermus aquaticus</i> |
| TBS | Tris-Buffered Saline |
| TEMED | Tetramethylethylenediamine |
| TD | Threonine deaminase |
| TF | Transcription Factor |
| TRIS-HCl | Tris(hydroxymethyl)aminomethane hydrochloride |
| Vs | versus |
| WT | Wild-Type |
| X-Gal | 5-bromo-4-chloro-3-indolyl- β -D-galactopyranoside |
| Y2H | Yeast Two-Hybrid assay |

1 INTRODUCTION

1.1 Plant trichomes

Globally, life cycle of plants has constantly evolved and adapted to fluctuating environmental conditions. During the process of evolution, these fundamental sessile organisms have significantly strengthened to defend themselves from several biotic and abiotic factors. In order to thrive, sustain and cope up with various environmental risks, plants have vastly developed a strong protective sheath, with both hydrophobic and lipophilic qualities on their cuticular layer (Samuels et al., 2008). Plant cuticular layer not only consists of cutin and wax as major components to protect their epidermal surface, but also comprise hair-like projections or protuberances perpendicular to the plant surface (Samuels et al., 2008). These hair-like protuberances arising from plant epidermal surfaces are clearly defined as plant trichomes (Werker 2000; Wagner et al., 2004; Tissier, 2012).

1.1.1 Classification and morphological description of trichomes

Trichomes have been researched broadly since late 1950's. They evolve to form the basis of plant's first line defense with a unique defense mechanism, both physically and chemically (Uphof, 1962; Levin, 1973). Trichomes have been classified based on the number of cells they are structured. They vary greatly in their size and densities, scaling from few microns to several centimeters. The morphological features of trichomes are diverse in the plant kingdom and can be distinguished depending upon the species they vastly occur (Levin, 1973; Behnke, 1984; Payne, 2000; Werker 2000; Wagner 2004; Tissier 2012). Despite their minute size, they are majorly present on the leaves and stems but also on other plant organs like petioles, petals, fruits and peduncles (Werker, 2000; Wagner et al., 2004; Tissier, 2012). The basic morphological feature of trichomes is distinguished based on whether they are unicellular or multicellular. Further, they could appear in multitude forms such as spiral, straight, hooked or tortuous, simple, peltate or stellate (Levin, 1973; Southwood, 1986; Werker, 2000; Dalin et al., 2008). Since trichomes exist in indefinite morphological features, the main criteria to distinguish trichomes are simply based on whether they are glandular or non-glandular (Payne 2000; Werker, 2000; Glas et al., 2012; Tissier, 2012).

1.1.1.1 Non-glandular trichomes

The diversity of non-glandular trichomes with different morphological features was initially described (Fahn and Werker, 1972). They were mainly identified on most of the angiosperms, some gymnosperms and bryophytes (Uphof, 1962; Johnson, 1975). Unicellular trichomes on the model plant, *Arabidopsis thaliana* are referred as non-glandular trichomes, which are either branched, or unbranched (Mathur and Chua, 2000). Unicellular trichomes from *A. thaliana* were extensively considered as a model to study trichome cell differentiation process (Hülkamp, 1998; Mathur and Chua, 2000; Schwab et al., 2000; Schnittger and Hülkamp, 2002). However, unicellular trichomes have no specific role in the secretion and storage of specialized compounds (Schoonhoven et al., 1998; Werker, 2000; Wagner 2004).

1.1.1.2 Glandular trichomes

Glandular trichomes were initially formed on the seed ferns to defend from arthropod pests during the late Paleozoic and carboniferous era (Krings and Kerp, 1998; Krings et al., 2002, 2003; Tissier., 2012). The term 'gland' makes these trichomes an outstanding entity and these aerial appendages are present over the epidermal surfaces of about 30 % of all vascular plants in the plant kingdom (Fahn, 2000; Glas et al., 2012). Glandular trichomes are multicellular, varying between two to several cells, comprising a differentiated basal, stalk and apical stem (Fahn, 2000; Werker, 2000). Similar to non-glandular trichomes, glandular trichomes can either be branched or unbranched with varying sizes and shapes (Werker 2000; Tissier, 2012). Further, glandular trichomes are sub-divided into capitate and peltate trichomes (Tissier, 2012; Glas et al., 2012). Both capitate and peltate glandular trichomes, which differ slightly in their morphological features, were commonly identified among the Asteraceae, Lamiaceae, Cannabaceae and Solanaceae plant families but not widely known in monocotyledons (Glas et al., 2012; Tissier, 2012). An important feature of glandular trichomes is to secrete and to store large amounts of vivid specialized chemical compounds (Fahn. 2000; Schillmiller et al., 2008; Tissier, 2012; Glas et al., 2012). Both capitate and peltate trichome secretory cells possess different scale of volatile compounds within the species they occur (Maffei, 2010; Tissier, 2012).

1.1.2 Importance of trichomes in the plant kingdom

Since the evolution of plants, trichomes are significantly involved in the plant defense from insects and herbivores, and to cope up with adverse environmental conditions (Werker 2000; Wagner et al., 2004). Plants are frequently encountered with leaf eating insects, primarily beetles (Order: Coleoptera) or common herbivores such as caterpillars (Order: Lepidoptera), known as most common predators for leaf damaging activities (Schoonhoven et al., 1998). Unicellular trichome types, densely populated on leaves and stems are known to provide an extensive physical barrier for those plant-damaging predators (Levin, 1973; Schoonhoven et al., 1998). The chemical defense is achieved due to the presence of secretory components or glands that produce valuable chemical compounds known as secondary or specialized compounds (Uphof, 1962; Fahn, 2000; Schilmiller et al., 2008). With this unique feature of repellency, trichomes are capable of maintaining a barrier between plant epidermal surface and herbivorous insects.

Although trichomes play a prime role in providing a preliminary defense on the plant surface, they not only protect plants from insects and herbivores but also against abiotic factors (Hauser. 2014). Their extreme density on plant surface is crucial for water balance, stabilizing photosynthesis and photo-inhibition process (Werker, 2000; Tingey, 1991; Levin, 1973; Nobel, 1999; Karabouniotis et al, 1992). Further their safeguard activity extends to protect plant surfaces from UV rays, reduce transpiration rate and diffusion of carbon-dioxide (Ehleringer et al., 1976; Choinski and Wise, 1999; Benz and Martin, 2006; Galmes et al., 2007).

1.1.2.1 Significance of glandular trichomes

Glandular trichomes have gradually gained attention with respect to type of compounds they store and secrete (Schilmiller et al., 2008). Some of the specialized compounds such as terpenes, phenylpropanoids derivatives, acyl sugars, methyl ketones and flavonoids are the most synthesized and secreted secondary metabolites among gland-bearing trichomes (Gershenzon et al., 1992; Hallahan, 1998; van der Hoeven et al., 2000; Gang et al., 2001; Fridman et al., 2005; Schilmiller et al., 2008; Tissier., 2012). The secreting compounds from gland bearing trichomes could be a fragrance or toxic-based for insects and leaf herbivores (Schilmiller et al., 2008). The resultant feeding activity after ingesting secondary metabolites could drastically deteriorate taste sensory systems and intoxicate their immune system (Levin, 1973; Schoonhoven et al., 1998; Fürstenberg-Hägg et al., 2013). To avail

the potential benefits for mankind, these specialized compounds have been diversely extracted, utilized and valued in the areas of pharmaceuticals, agriculture, food processing, fragrance and essential oil production (Duke et al., 2000; Mahmoud and Croteau, 2002; Wagner et al., 2004).

1.1.3 Glandular trichomes in Solanaceae: Special emphasis on the *Solanum lycopersicum* cultivar 'MicroTom'

Glandular trichomes in *Solanum* species have drawn significant importance due to their role in producing specialized bioactive compounds (Iijima et al., 2004; Nagel et al., 2008; Sallaud et al., 2009). The genus *Solanum* comprises two main categories of trichomes – non-glandular and glandular. In tomato (*Solanum* spp), non-glandular trichomes (type II, III, V and VII) and glandular trichomes (type IV, VI and VII) are predominantly present. The morphological description of *Solanum* glandular trichomes was initially introduced (Luckwill, 1943) but later revised and classified based on the types (Fig. 1A) on different *Solanum* species (Channarayappa et al. 1992; Simons and Gurr 2005). The glandular trichome types differ among the tomato species and cultivars, and their morphological structures within the species are basically differentiated based on size, stalk length and number of secretory cells (Luckwill, 1943; Wilkens et al., 1996; Maluf et al., 2007; Kang et al., 2010). Interestingly, chemical compounds secreted by glandular trichome types differ among wild type and cultivated tomato species, and moreover quantitatively alters within the species (Schillmiller et al., 2009; Kang et al., 2010). The current thesis mainly focuses on the development of type VI glandular trichomes in cultivated tomato, *Solanum lycopersicum* cultivar (cv.) MicroTom (MT).

The dwarf tomato cultivar MicroTom (MT) has become popular in plant science research because of its short life cycle (≈ 10 weeks), compact size (≈ 15 cm), high fruit yield production and a compatible model for genetic studies (Meissner et al., 1997). Further, an up-to-date EMS and gamma rays mutant collection (Pino-Nunes et al., 2009), ESTs and SNP databases (Kazusa DNA research institute) and metabolite annotation profile (Iijima et al., 2008), is of great advantage for functional characterization studies. With this vast data, the MT cultivar has been utilized to study fruit development (Serrani et al., 2007), hormonal interactions (Campos et al., 2009), abiotic and biotic responses (Gratao et al., 2008; Hase et al., 2008), mycorrhizal colonization (Zsoegoen et al., 2008) and gene regulation activities, respectively (Zrachya et al., 2007).

INTRODUCTION

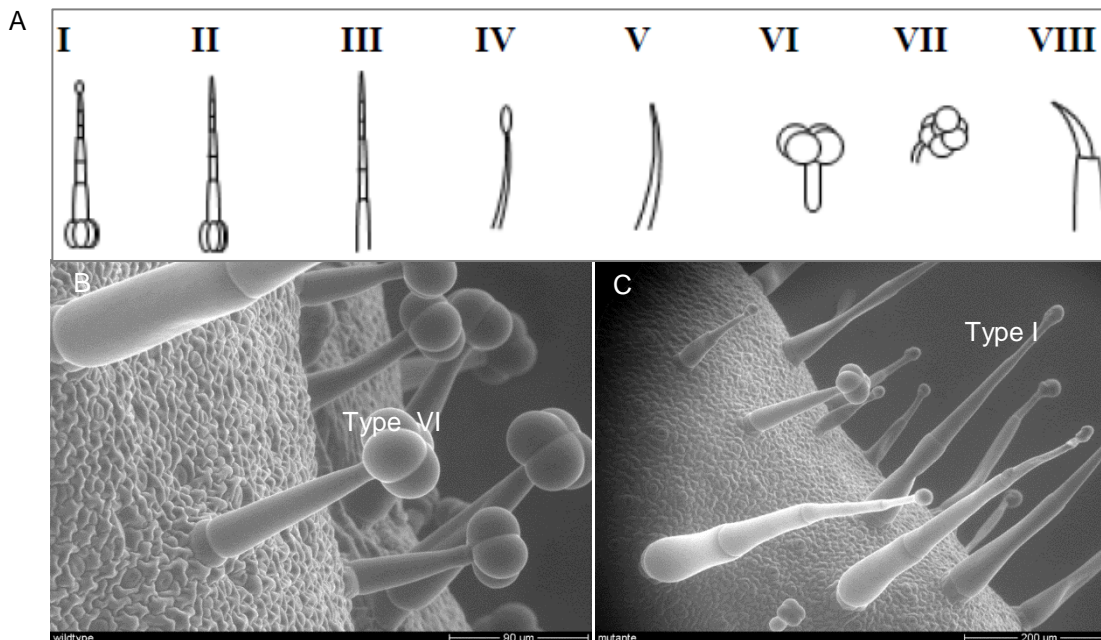


Figure 1: Morphological description of trichomes in *Solanum* species

(A) Eight-type of trichomes (glandular and non-glandular) revised by Channarayappa et al., (1992). (B, C) ESEM images of type VI and type I trichomes visualized on young leaf surface of *S. lycopersicum*. Scale bars represent 90 μm (B) and 200 μm (C).

The MT cultivar comprises type I - non-glandular (capitate) (Fig. 1A, C) and type VI and type VII - glandular trichomes (globular) (Fig. 1A, B) (Glas et al., 2012). Type VI glandular trichome numbers in the cultivated tomato are relatively higher compared to type VII and type I trichomes (Li et al., 2004; Glas et al., 2012; Bergau et al., 2015). Further, type VI glandular trichomes in cultivated tomato species mainly comprise monoterpenes and sesquiterpenes (Li et al., 2004; Schillmiller et al., 2009; Kang et al., 2010; Bergau et al., 2016; Balcke et al., 2017).

1.1.4 Terpene levels in *Solanum lycopersicum*

In tomato, various secondary metabolites like anthocyanin compounds and defense related volatile compounds have been identified (Thaler et al., 2002; Li et al., 2004; Chen et al., 2006). In the cultivated tomato, acyl sugars, flavonoids and terpenes are major secondary compounds produced in type I, IV and VI gland bearing trichomes (McDowell et al., 2011; Bergau et al., 2016; Balcke et al., 2017). Among terpenes, monoterpenes and class I sesquiterpenes like β - elemene, β - caryophyllene and α - humelene were known to be derived from type VI glandular trichomes of cultivated tomato leaves (Besser et al., 2009;

Schillmiller et al., 2010; Balcke et al., 2017). Further, the gland bearing trichomes from wild type and cultivated tomato lines show different metabolite accumulation patterns. For instance, accumulation of terpenoids are distinct and found to vary during each developmental phases of glandular trichomes within the two species (Besser et al., 2009; Schillmiller et al., 2009; 2010; Bergau et al., 2015; Balcke et al., 2017).

1.2 Role of phytohormones in trichome development

Plant hormones or phytohormones have an essential role in regulating trichome induction. The importance of phytohormones in the formation of trichomes in the below section is illustrated based on the discovery of respective deficient mutants across their hormone signaling pathways.

1.2.1 Jasmonates (JAs)

Jasmonates (Jasmonic acid, Jasmonic acid methyl ester, JA-amino conjugates and other JA metabolites) are a group of oxygenated compounds commonly referred as oxylipins, which are originated from α -linolenic acid, within the lipoxygenase pathway on chloroplast membranes (Creelman and Mullet, 1997; Wasternack, 2007). Jasmonates are primly known to regulate plant growth and developmental activities like, seed germination, root growth inhibition, lateral root formation, tuber formation, leaf senescence, flower development and trichome formation (Dathe et al., 1981; Staswick et al., 1992; Ueda and Kato, 1980; Stintzi and Browse, 2000; Li et al., 2004). The most important forms of bioactive molecules in JA signalling pathway are methyl jasmonate (MeJA), jasmonic acid (JA) and its conjugated amino acid JA-Isoleucine (JA-Ile), (Staswick and Tiryaki 2004; Wasternack, 2007; Fonseca et al., 2009a; Suza et al., 2010; Stitz et al., 2011). The modulation of JA biosynthesis is mainly decided based on the substrate availability, its circuitry feedback loop and tissue specificity (Wasternack, 2007; Browse, 2009a, 2009c). For instance, the CORONATINE INSENSITIVE1 (COI1) is an F-box protein within the frame of Skp1/Cullin/F-box (SCF) complex and functions as an E3 ubiquitin ligase. Further, COI1 sequentially recruits Jasmonate ZIM domain (JAZ) proteins for ubiquitination process (Chini et al., 2007; Thines et al., 2007; Yan et al., 2007). The Proteasomal degradation of JAZ proteins by JA or JA-Ile has relieved positive regulators like MYC2 transcription factors (TFs) to activate JA-responsive promoters and subsequent JA-responsive genes (Chung et al., 2008; Chini et al., 2009a). Characterization of JAZ proteins and their interaction with

INTRODUCTION

SCF^{COI1} complex has led to decipher regulatory events involved in the positive feedback loop of JA biosynthesis (Schaller and Stintzi, 2009; Stenzel et al., 2012; Wasternack and Hause, 2013).

1.2.1.1 JA-deficient mutants affecting trichome formation

Mutants impaired in JA deficiency has shown several roles corresponding to wounding and plant stress related activities (Stintzi and Browse, 2000; Stenzel et al., 2003b; Li et al., 2004; Wasternack, 2007). The Identification and functional characterization of *coronatine insensitive1 (coi1)* mutant in Arabidopsis initially paved the way to recognize the importance of *COI1* in JA signalling and perception (Xie et al., 1998). The *coi1* mutant is a male sterile with partial impairment in pollen production, deficient in wound responses and mainly insensitive to exogenous JA application (Xie et al., 1998). In tomato, JA response in trichome development was first recognized by characterizing *jasmonic acid in-sensitive (jai1)* mutant, a homolog of *COI1* in Arabidopsis (Li et al., 2004). The *jai1* mutant plants are insensitive to exogenous JA application, partially deficient in pollen production and majorly identified as female sterile (Li et al., 2004). The *jai1* mutant plants exhibited phenotypic characteristics like susceptibility to spider mites and improper growth and development of type VI glandular trichomes on leaves. This led to approximately 75 % reduction in type VI glandular trichomes in the *jai1* mutant compared to wild type (Li et al., 2004).

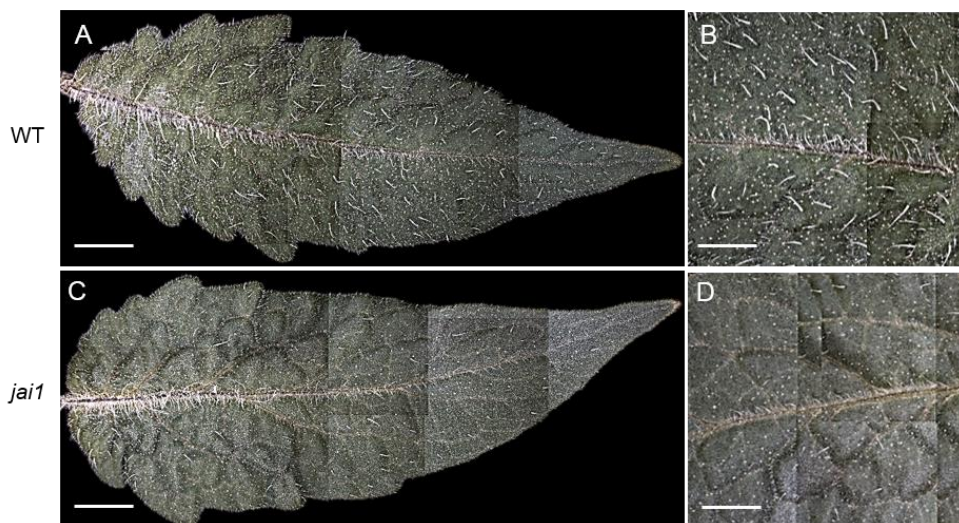


Figure 2: Distribution of trichomes on the wild type and *jai1* tomato leaves

(A, C) Wild type (WT) and *jai1* tomato leaves were compared after microscopy. (B, D) Visualization of trichome density between WT and *jai1* tomato leaves. Scale bars represent 200 μm (A, C) and 100 μm (B, D).

Another single recessive mutant, *odorless 2 (od-2)*, has shown defective and abnormal development in glandular trichome formation and density with altered secondary metabolite content in type VI glandular trichomes (Kang et al., 2010). Further, characterization of a highly conserved, specifically Rac1-associated protein subunit (SRA1) required for trichome development, strengthening actin-cytoskeleton dynamics, accumulation of flavonoids and sesquiterpenes, and resistance to insect attack, was known to be encoded by *Hairless (Hl)* gene (Kang et al., 2016). The loss-of-function of the *hl* mutant was similar to the *od-2* mutant. However, these previous studies speculate that both *od-2* and *hl* mutants are defective in JA-regulated pathway and affects glandular trichome development (Howe et al., 1996; Thaler, 1999; Li et al., 2002; Kant et al., 2004; Howe and Jander, 2008).

1.2.2 Gibberellins (GAs)

Gibberellins (GAs) are well known for their profoundness and diverse effects in plant developmental activities (Hooley et al., 1994). They play a key role in cell growth activities including seed germination to elongation of shoot meristem, to flower and fruit development and then seed reserve mobilization by aleurone cells (Hooley et al., 1994). Previous research on the model plant *Arabidopsis* (Koornneef and van der Veen, 1980) and tomato (Koornneef et al., 1981), has successfully led to identification of GA-deficient mutants (Koornneef et al., 1985). Role of GA towards trichome induction in *Arabidopsis* was first identified by observing variations in trichome numbers, particularly on the abaxial surface of cauline leaves while performing photoperiod experiments (Chien and Sussex, 1996). Evidence of GA in trichome induction and density was elucidated on one of the GA-deficient mutant, *ga1-3*, a null-allele of the locus encoding ent-kaurene synthase, which has shown a strong phenotype with total glabrous leaves (Chien and Sussex, 1996). The application of exogenous GA restored *ga1-3* mutant plants to retrieve WT phenotype behavior, suggesting that GA is involved in the epidermal cell layer and trichome development (Chien and Sussex, 1996).

In *Arabidopsis*, recessive alleles at the *SPINDLY (SPY)* locus were known to suppress trichome phenotypes due to GA deficiency (Jacobsen and Olszewski, 1993). Mutations in *spy* alleles have known to increase trichome numbers and trichome branching, particularly in four-branched trichomes on the rosette leaves of *A. thaliana*. This indicates that GA-deficient mutant *spy* negatively regulates GA signal transduction, signifying its role in

INTRODUCTION

trichome development (Perazza et al., 1998; Swain et al., 2001, 2002; Tseng et al., 2004; Greenboim-Wainberg et al., 2005; Silverstone et al., 2007).

1.2.3 Cytokinins (CKs)

Cytokinins were initially discovered in plant biological material during the mid-20th century. Since their discovery, various biological functions with respect to de novo organ culture (Skoog and Miller, 1957), stimulation of leaf and seed germination (Miller, 1961), senescence activity and apical dominance in shoots and roots (Richmond and Lang, 1957; Wickson and Thimann, 1958) were addressed. Understanding the role of cytokinins in the initiation of trichomes was first observed in floral meristems of *spy* mutant alleles in *A. thaliana*. The exogenous application of cytokinins, however, led to proliferation of trichomes on flowers, which was counteracted by mutations in the *SPINDLY*, showing a positive impact on cytokinin signalling (Greenboim-Wainberg et al., 2005). Subsequent supportive data showed that application of 6-benzylaminopurine (BA) led to proliferate trichomes on cauline leaves and stems (Gan et al., 2007). The cross-talk between GAs and CKs were mainly based on their counterparts, which is known to interact with downstream transcription factors (Greenboim-Wainberg et al., 2005; Gan et al., 2007).

1.2.4 Factors affecting trichome induction

Trichome numbers were found to be altered in plant hormone-deficient mutants. This indicates, at the endogenous level, molecular mechanisms are responsible for trichome induction process. Additionally, ecological factors play a substantial role in inducing trichome numbers. This includes insect-herbivory, wounding, and response to exogenous JA treatments.

1.2.4.1 Insect herbivory and artificial damage

Studies related to insect-herbivore damage caused either by Coleoptera or Lepidoptera was initially reported on several plant species, which has led to formation of new leaves with an increased trichome density (Baur et al., 1991; Traw and Dawson, 2002a; 2002b; Agrawal, 1999; 2000; Dalin and Björkman, 2003; 2008; Dalin et al., 2006;). This drastic increase in trichome numbers on newly developing leaves is defined as induced defense-regulated trichomes. Based on the previous data, trichomes are naturally induced and outnumbered due to damage caused by insect-herbivore feeding strategies. Besides herbivory, researchers have successfully attempted to reproduce herbivory damage both in

field and lab premises by conducting artificial or mechanical wounding experiments (Pullin and Gilbert, 1989; Dalin and Björkman, 2003; Valkama et al., 2005). Artificial damage-induced trichome numbers and density was stronger in field conditions than lab experiments in crop-oriented species (Dalin et al., 2008). In *A. thaliana* accessions, artificial wounding experiments have shown tremendous increase in trichome numbers and density (Traw and Bergelson, 2003). Further, they claim that quantification of trichome numbers and density by artificial wounding differs significantly from insect-herbivore feeding strategies (Cipollini et al., 2003; Dalin et al., 2008).

1.2.4.2 Induction of trichomes by exogenous JA treatment

Since artificial wounding and herbivory extensively triggers jasmonate-dependent responses (Bostock, 1999; Reymond et al., 2000; Yoshida et al., 2009; Erb et al., 2012), it was initially monitored for increase in trichome production in *A. thaliana* with the influence of exogenous JA application (Traw and Bergelson, 2003). They further report that trichome numbers can be significantly increased with lower concentrations of JA (Traw and Bergelson, 2003).

Another interesting group reported significant increase in type VI glandular trichomes in tomato upon MeJA treatment (Boughton et al., 2005). According to them, density of type VI glandular trichomes was analyzed on newly developed leaves at different day intervals (Boughton et al., 2005). Two to three weeks after MeJA treatment, the amount of type VI glandular trichomes were significantly higher (>9 fold) than control plants (Boughton et al., 2005). Exogenous JA or MeJA application, both in *Arabidopsis* and tomato indicate that trichome numbers and its density can be significantly altered.

1.3 The molecular mechanisms in the formation of trichomes

In *Arabidopsis*, unicellular trichomes were used as a model to investigate, understand and address cell developmental mechanisms, mainly aspects of cell-differentiation, cell-polarity and control of cell shape across the epidermal cell layer (Hülkamp, 2004). Trichomes on *Arabidopsis* have not only provided in-depth understanding towards dynamics of cellular mechanisms but also paved a way to discover regulatory mechanisms at the molecular level such as function of microtubules, actin cytoskeleton, cell-cycle and the role of transcription factors (Hülkamp, 2004). Specifically, the essential role of transcription factors has gained a special importance in plant science research past two decades and

INTRODUCTION

some of those involved in trichome initiation and development has been the scope of interest in the further sections of the current thesis.

To get a fundamental understanding on how the trichomes are initiated, protodermal cells from the plant epidermis undergo a series of endo-replication cycles after retardation of mitotic cell division. Repetitive endo-replication cycles modify and alter the cellular contents including the nucleus, leading to cell enlargement and thus directing cell growth perpendicular to the leaf surface (Hülkamp et al., 1994; 2008). The process of trichome initiation and patterning is controlled by a group of patterning and endo-replication genes, which were successfully identified by mutagenesis screens (Marks et al., 1997; Hülkamp et al., 1998). Several mutants have been previously described and characterized, specifically involved in the phenotypic properties of trichome development (Feenstra, 1978; Koornneef, 1981; Koornneef et al., 1982; Haughn and Somerville, 1988; Marks et al., 1991 and Hülkamp et al., 1994). Characterization of those mutants led to the identification of distinctive trichome morphogenesis phenotype (Feenstra, 1978; Koornneef et al., 1983; Hülkamp et al., 1994). Major striking trichome phenotypes were observed in the *glabra1* (*gl1*), *transparent testa glabra1* (*ttg1*) and the *glabra2* (*gl2*) mutants, affecting the epidermal cell fate, leaving behind glabrous surface and traces of trichomes on the leaves compared to the wild type (Hülkamp et al., 1994).

1.3.1 Role of essential trichome regulators in *Arabidopsis thaliana*

Trichomes inducing factors or genes were grouped based on the theoretical model established by Meinhardt and Gierer (1974). Their two-dimensional patterning model explains the *de novo* spacing pattern of trichome cells and classifies trichome inducing regulators based on their positive and negative roles in trichome induction (Hülkamp and Schnittger, 1998; Ishida et al., 2008; Larkin et al., 2003).

1.3.1.1 Positive regulators of the trichome regulatory complex

GLABRA1 (AtGL1)

Arabidopsis GLABRA1 or *AtGL1*, encodes a R2R3 MYB transcription factor with two repeats of MYB DNA-binding domain (Oppenheimer et al., 1991). Recessive mutation at the *AtGL1* loci resulted in very few or complete absence of trichomes on the rosette leaves of *A. thaliana* (Koornneef et al., 1982; Oppenheimer et al., 1991). Homozygous mutant plants also displayed trichome deficiency on stems, petioles and sepals (Koornneef et al.,

1982; Oppenheimer et al., 1991). The Relative transcript levels of *AtGL1* were found to be higher in young initiated trichomes than fully developed ones. The *AtGL1* protein is located in the nucleus (Larkin et al., 1993; Szymanski et al., 1998). Cloning and complementation studies of *AtGL1* not only confirmed its structural similarity to MYB transcription factor family, but the latter also provided evidence that *gl1* phenotype was successfully rescued by forming abnormal trichomes on cotyledons (Oppenheimer et al., 1991; Larkin et al., 1993; Kirik et al., 2001), suggesting that *AtGL1* might interact with other regulatory factors responsible for trichome induction (Kirik et al., 2001).

TRANSPARENT TESTA GLABRA 1 (AtTTG1)

Another single recessive mutation at the *AtTTG1* loci is known to affect the trichome initiation process (Koornneef et al., 1982). Mutation at the *AtTTG1* loci not only affected trichome formation but also showed loss of anthocyanin production, seed coat pigmentation and mucilage content (Koornneef et al., 1981; 1982). The *AtTTG1* locus encodes a WD-40 protein, which consists of four WD repeats (de Vetten et al., 1997; Walker et al., 1999) that are known to function as protein-protein interaction domain in various developmental processes (Neer et al., 1994; Walker et al., 1999). The constitutive expression of maize *R* gene in Arabidopsis wild type plants complemented *ttg1* mutant phenotypic characteristics, however overexpression of *R* protein in *ttg1* mutant background suppressed its mutational effects, thereby indicating the sequence homology between *R* and *AtTTG1* and also addressing their pleiotropic effects (Lloyd et al., 1992; Walker et al., 1999).

GLABRA3 (AtGL3)

AtGL3 was identified based on the sequence similarity search between maize *R* gene and the *AmDELILA*, a *Antirrhinum majus* (*A. majus*) basic helix-loop-helix (bHLH) anthocyanin regulatory gene loci (Payne et al., 2000; Lloyd et al., 1992; Goodrich et al., 1992). Cloning of *AtGL3* further proved that it encodes a bHLH transcription factor homologous to maize *R* and *AmDELILA* (Payne et al., 2000). Unlike *ttg1-1* and *gl1-1* mutants which are devoid of trichomes (Koornneef et al., 1982; Oppenheimer et al., 1991), *gl3-1* mutant plants exhibit fewer immature trichomes (Payne et al., 2000). The shortening of trichome branches compared to the wild type is a characteristic feature of *gl3-1* mutant plants due to shortened endo-replication cycles, which results in decreased cell size and the nucleus (Hülkamp et al., 1994).

INTRODUCTION

GLABRA2 (AtGL2)

Several years ago, *GLABRA2* or *AtGL2* was identified in the development of seed coat mucilage (Koornneef et al., 1982). The *gl2* mutant plants from *Arabidopsis* did not only affect production of seed coat mucilage but also showed its importance in the morphological development of smaller trichomes, reduced branching and maturation of trichomes (Rerie et al., 1994; Masucci et al. 1996). *AtGL2* encodes a homeodomain-leucine zipper (HD-Zip) protein, a motif corresponded with transcription factors which is responsible both in animal and plant development (Affolter et al., 1990; Vollbrecht et al., 1991; Rerie et al., 1994). Transcript levels of *AtGL2* were shown to be higher in the developing trichomes compared to young immature trichomes and its protein is located in the nucleus of developing trichomes (Rerie et al., 1994; Syzmanski et al., 1998). The expression of *AtGL2* was strongly suppressed in *gl1* and *ttg1* mutants, pointing its role as a key downstream regulator for *AtGL1* and *AtTTG1* (Rerie et al., 1994; Syzmanski et al., 1998; 2000).

1.3.1.2 Negative regulators of the trichome regulatory complex

TRYPTICHON (AtTRY)* and *CAPRICE (AtCPC)

Unlike positive regulators, regulatory factors like *TRYPTICHON (AtTRY)* and *CAPRICE (AtCPC)* inhibit formation of hair-cells on leaves and roots, a lateral inhibition mechanism in both root-hair and trichome patterning (Meinhardt and Gierer, 1974; Hülskamp et al., 1994; Wada et al., 1997; Schnittger et al., 1999; Lee and Schiefelbein, 1999; Schellmann et al., 2002; Kirik et al., 2004a). Initially, *AtTRY* was identified as the only negative regulator in the trichome formation due to its lateral inhibition of the epidermal cells, hence anticipating its involvement in cell to cell signalling (Hülskamp et al., 1994; Schnittger et al., 1999). Secondly, *AtCPC*, which encodes a MYB transcription factor lacking a transactivation domain, was found to inhibit the formation of root-hair cells (Wada et al., 1997). Although *AtTRY* and *AtCPC* encode a MYB-related protein, their sequences are homologous (Schellmann et al., 2002). Both *AtTRY* and *AtCPC* were known to be highly expressed in the leaf primordia and the developing trichome cells (Wada et al., 1997; Schellmann et al., 2002). However, based on *try* and *cpc* single and double mutant phenotypes, their role were complemented with the theoretical model established by Meinhardt and Gierer (1974), thus defining them as negative regulators (Schellmann et al., 2002). On an important note, both *AtTRY* and *AtCPC* perform common lateral inhibition roles in shoots and non-hair cells of roots (Lee and Schiefelbein, 1999; Kirik et al., 2004b). A known fact

that transcription of *AtCPC* and *AtTRY* are assisted by *AtTTG1* and *AtGL1* in the developing trichomes, and *AtTTG1* and *WEREWOLF (AtWER)* in the developing non-hair cells (Lee and Schiefelbein, 2002; Schellmann et al., 2002; Schiefelbein et al., 2003; Wada et al., 2002).

ENHANCER OF TRY AND CPC (AtETC1/ AtETC2)

ENHANCER OF TRY AND CPC 1 and *2 (AtETC1 and AtETC2)* are the important homologous regulators involved in the regulation of trichomes and root-hair patterning. Interestingly, *AtETC1* and *AtETC2* encode MYB transcription factor which possess a R3 MYB domain without an activation domain (Wada et al., 1997; Schellmann et al., 2002; Kirik et al., 2004a). Both *AtETC1* and *AtETC2* show high sequence similarity and functionally with the *AtTRY* and *AtCPC* genes (Kirik et al., 2004a; 2004b). Overexpression of *AtETC1/AtETC2* led to decrease in trichome numbers but increase in the root hair development (Kirik et al., 2004a; 2004b). Analysis of both *etc1* and *etc2* mutants displays no change in trichome branching or trichome numbers but slight reduction in the root hairs (Kirik et al., 2004a; 2004b). Based on the triple mutant analysis (*try/cpc/etc1* or *try/cpc/etc2*), *etc1/etc2* enhances the effect of *try* and *cpc*, hence shows redundancy in trichomes and non-hair cells of shoots and roots, respectively (Kirik et al., 2004a; 2004b).

1.3.2 Interaction of positive and negative regulators in trichome formation

The functionality of key regulatory components involved in trichome initiation and patterning is determined when both positive and negative key regulators collaboratively function together. Genetic analysis of key regulatory components has provided substantial data to address the genes that control trichome regulatory events and that are actually involved in the trichome initiation, spacing and developmental process.

Trichome initiation was hypothesized based on a mutual-inhibition mechanism, where the model explains interaction of both positive and negative regulators in the feedback circuit, playing the roles of activator and inhibitor (Schiefelbein, 2002; Larkin et al., 2003; Hülskamp et al., 2004). The role of activator is to activate the inhibitor and the inhibitor with the movement is able to inhibit the activator (Hülskamp et al., 2004).

Trichome regulatory complex model

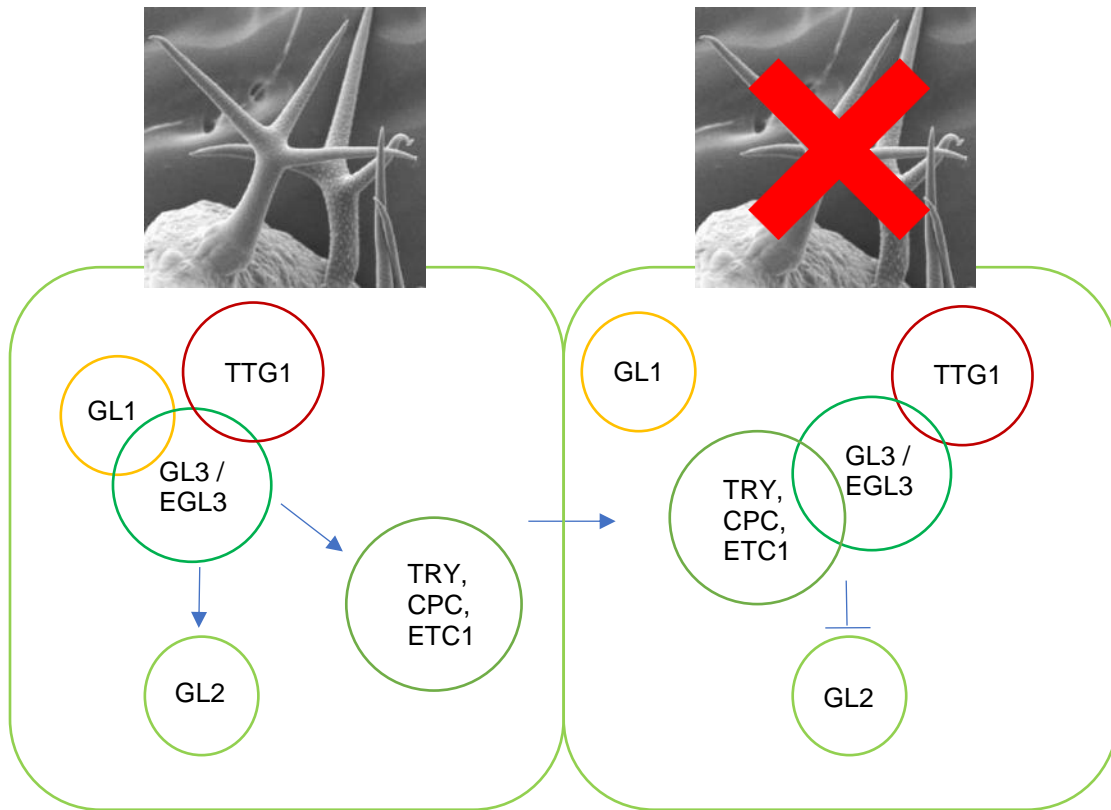


Figure 3: Trichome regulatory model in *Arabidopsis thaliana*

Positive regulator complex: *GL1*, *GL3* or *EGL3* and *TTG1* and negative regulator complex: *TRY*, *CPC* and *ETC1* competes together to regulate trichome inducing gene *GL2*. *GLABRA1* (*GL1*) encodes a MYB-related transcription factor, *GLABRA3* (*GL3*) encodes a basic helix-loop-helix (bHLH) transcription factor, *ENHANCER of GL3* (*EGL3*), a close homolog of *GL3* and *TRANSPARENT TESTA GLABRA1* (*TTG1*) encodes a WD-40 protein and *GLABRA 2* (*GL2*), encodes a homeodomain transcription factor (HD-Zip), respectively (adapted from Hülkamp et al., 2004).

The proposed model defines trichome patterning and root-hair differentiation involving similar set of regulatory factors (Hülkamp et al., 2004). The illustration of the regulatory complex model in this thesis is constrained to trichome initiation and formation. The interaction of positive and negative regulators have been clearly defined by elucidating their functional relationship at the molecular basis (Zhang et al., 2003; Schellmann et al., 2002; Wada et al., 1997; Kirik et al., 2004; Payne et al., 2000). According to their research, the prime regulator for trichome initiation is *AtGL2*, which has been regulated by three other

positive regulators including *AtGL1*, *AtGL3* or *AtEGL3* and *AtTTG1*, through a trimeric complex network (Fig. 3, Hülkamp et al., 2004). Further, the active complex comprising positive regulators that are thought to activate negative regulators (*AtTRY*, *AtCPC* and *AtETC1* or *AtETC2*), move into neighboring cells and compete with positive regulators to dissociate regulatory complex (Schellmann et al., 2002; Wada et al., 1997; Kirik et al., 2004b).

The proposed model supports the interaction of the *AtGL1* MYB domain with the N-terminal domain of bHLH proteins, *AtGL3* and *AtEGL3* in yeast (Payne et al., 2000; Zhang et al., 2003). The positive regulator, *TTG1* was known to interact with different domains of *AtGL3* and *AtEGL3* proteins in yeast and its regulation by *AtGL3* via intracellular co-expression studies (Payne et al., 2000; Zhang et al., 2003; Zimmerman et al., 2004; Balkunde et al., 2011). Likewise, *AtCPC* and *AtTRY* were shown to interact with the N-terminal domain of *AtGL3* and *AtEGL3* in yeast and their mobility to bind was confirmed through overexpression studies (Zhang et al., 2003; Diguni et al., 2008). The interaction and competition to bind positive regulators in the neighboring cells eventually detaches *AtGL1* and inactivates the positive regulatory complex, which leads to repression of *AtGL2* activity (Fig. 3) (Schellmann et al., 2002; Schiefelbein, 2003; Larkin et al., 2003; Kirik et al., 2004b; Diguni et al., 2008; Balkunde et al., 2011).

1.3.3 Glandular trichome regulators in Solanaceae

Trichomes in the Solanaceae family especially from *Nicotiana* and *Solanum* species are pre-dominantly multi-cellular, well known as glandular secreting trichomes (GSTs). Earlier, focus on tobacco GSTs was mainly harnessed to elucidate biosynthesis of specialized or secondary metabolic components and to produce their secretion. Successively, this has contributed to combat pest management and plant-insect herbivory complexities in order to benefit economic crop species (Wagner et al., 2004; Schillmiller et al., 2008; Besser et al., 2009; Tissier A, 2012). Both tobacco and tomato GSTs also provided significant gene expression data, identifying proteins related with photosynthesis and carbon fixation (Harada et al., 2010; Cui et al., 2011). There has been greater depth of understanding the regulatory mechanisms with respect to unicellular trichomes whereas, insufficient research knowledge is lacking in the regulation of multicellular trichomes and the mechanisms involved in it.

INTRODUCTION

An attempt was made to overexpress two heterologous closely related MYB-class genes, *AmMIXTA* from *Antirrhinum majus* and *CotMYBA* from *Gossypium hirsutum* in *Nicotiana tabacum* (Payne et al, 1999). The overexpression of *AmMIXTA* showed alterations (hyperdevelopment) in papillate cells, which are responsible for the initiation and differentiation of multicellular trichomes. Overexpression of *CotMYBA* resulted in excess trichomes with different morphological behavior (Payne et al., 1999). Both MYB-class genes played distinct role in altering the differentiation of multicellular trichomes but no successful proof has been established in trichome initiation process (Glover et al., 1998; Payne et al, 1999). In tomato, *SIMIXTA-Like* gene was shown to act as a positive regulator in the cutin biosynthesis of fleshy fruits but, lacks its characterization towards understanding the regulation of glandular trichomes (Lashbrooke et al., 2015). Overexpression of Arabidopsis MYB and bHLH TF Orthologs in tomato, *SITRY* and *SIGL3*, showed no change in trichome numbers and root hair development (Wada et al., 2013). An important regulatory gene in tomato, *Woolly (Wo)* encodes a HD-Zip protein has strong interaction with *B-type cyclin* gene (*SICycB2*). The woolly phenotype is caused due to the mutation in the *WO*. Silencing of either *WO* or *SICycB2* by RNAi experiments has affected type I trichomes and further cytological experiments has shown that *WO* is linked with seed development and embryo formation (Yang et al., 2011). Although knockdown experiments conferred significant decrease in type I trichomes, glandular trichome types were not affected by *WO* (Yang et al., 2011). Collectively, these findings indicate further work is necessary to identify the regulation of glandular trichomes in tomato.

1.4 Transcription factor families in *Solanum lycopersicum*

1.4.1 MYB transcription factor family

The genome sequencing of *Arabidopsis thaliana* has significantly gathered extensive data on MYB transcription factors (Du et al., 2009; Dubos et al., 2010). MYB proteins comprise MYB DNA-binding domains, which spans around 50-53 amino acid residues and forms a helix-turn-helix (HTH) folding with three regularly spaced tryptophan (W) residues (Kaneishii et al., 1990). MYB TFs have been classified into four major groups; R1, R2, R3 and R4; where R1-R4 refers to one to four MYB repeats (Dubos et al., 2010). Plants essentially contain R2R3-type MYB domain proteins (Paz-Ares et al., 1987; Lipsick 1996; Dubos et al., 2010)

INTRODUCTION

paved a way to identify clusters of comprehensive orthologous groups to the corresponding subgroups (Li et al., 2016).

1.4.2 The basic helix-loop-helix (bHLH) transcription factor family

The basic helix-loop-helix transcription factor family is considered as one of the super families among all other transcription factors, which were initially discovered in the mammalian systems (Atchley et al., 1997; Littlewood and Evan, 1998; Ledent and Vervoort, 2001). The bHLH proteins are referred to as important regulatory components involved primarily in the transcriptional networks, controlling diverse processes like cell proliferation and lineage development, stress responses, phytochrome and hormone signalling (Grandori et al., 2000; Massari and Murre, 2000; Feller et al., 2011).

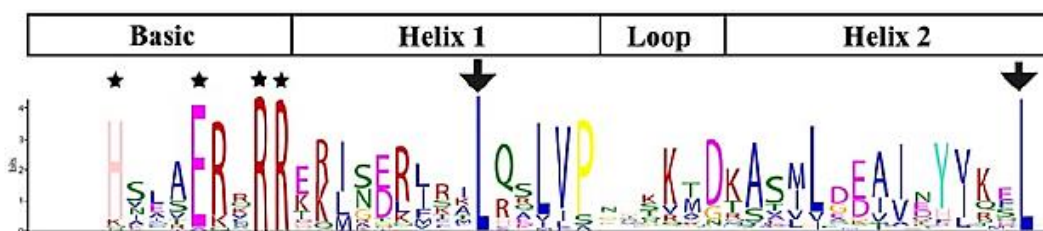


Figure 5: Characterization of bHLH functional domains in tomato

The H5, E9 and R12 amino acids starred indicate basic region important for DNA-binding. Amino acids indicated by arrows in the helix-loop-helix (HLH) region responsible for homo and hetero dimerization (adapted from Wang et al., 2015).

The initial genome-wide classification analysis in *Arabidopsis* consisted approximately 137 bHLH encoding genes (Reichmann et al., 2000; Wang et al., 2015), but later with thorough systematic phylogenetic analysis of bHLH protein family, there were at least 162 bHLH-encoding genes assigned to 21 subfamilies (Toledo-Ortiz et al., 2003; Bailey et al., 2003). The bHLH domain spans approximately 60 amino acids consisting of two distinct functional regions, a basic region at the N-terminus which is important for DNA-binding and a helix-loop-helix (HLH) region located at the C-terminus, which acts as a dimerization domain for homo and hetero dimer formation (Murre et al., 1989; Ferre-D'Amare et al., 1994; Jones, 2004). In tomato, the genome-wide phylogenetic analysis led to identify a total of 152 bHLH genes (Wang et al., 2015). The functional region indicates a basic region spanning approximately 17 amino acids, which encode 199 DNA-binding and 33 non-DNA-binding proteins (Fig. 5, Wang et al., 2015). The total number of tomato bHLH protein family

members were assigned to 24 subfamilies and mapped to the tomato genome (Wang et al., 2015).

1.5 Thesis objectives

The majority of previous research work was mainly contributed to understand the initiation and differentiation of single-cells using easily accessible model plant organ, unicellular trichomes of *Arabidopsis*. Identification of key regulatory factors in trichome development led to decipher the molecular mechanisms behind them. Interaction of one or more key regulatory factors indicated that regulation of trichomes does not solely depend on one prime regulator instead, with the interaction and cross-linkage of other key transcription factors. The substantial data on the formation and patterning of unicellular trichomes, and their molecular mechanisms clearly stated that the development of multi-cellular trichomes may follow different regulatory pathways. Over a decade, research on multicellular trichome-based plant species took a drastic step in the identification of genes involved in the development of glandular trichomes. Precisely, the identification of genes in tobacco and tomato dealt with understanding the process of secondary metabolite production. On an important note, it is clear that application of phytohormones elevates significant trichome numbers and numerous studies shows a strong connection between phytohormones and trichome formation. Based on previous research data and our preliminary analysis, JA has significantly contributed in elevation of type VI glandular trichome numbers and density. Currently, characterization of JA-induced regulatory components involved in the formation of glandular trichomes in tomato is still unknown. Therefore, current thesis work mainly focuses on identifying and characterizing the putative regulatory factors involved in the formation of type VI glandular trichomes in tomato, potentially regulated by exogenous JA treatment.

1.5.1 The importance of *jai1* mutant as a useful tool in the approach

Since the molecular characterization of *jai1* mutant in tomato, several characteristics like insensitiveness to JA, defective JA-induced gene expression and reduced number of type VI glandular trichomes and subsequent alteration of secondary metabolic compounds (Li et al., 2004), has gained interest to consider JA-deficient mutant as an important genotype in the current thesis work. The *jai1* mutant is a potential genotype for significant comparison

INTRODUCTION

of type VI glandular trichomes versus wild type, which could further facilitate to identify some putative key regulators involved in the development type VI glandular trichomes.

The specific objectives are as follows,

- Conducting RNA sequencing (RNA-seq) analysis on young tomato (cv MicroTom) leaves treated with JA at 2 hours (JA_2h) and 24 hours (JA_24h) time intervals, and untreated WT (WT_CO) and *jai1* mutant (*jai1_CO*). Further, identification of differentially regulated genes with more focus on putative transcription factors regulated by JA.
- Validation of putative candidate transcription factors and genes based on their transcript accumulation at different treatment conditions.
- Characterization of TILLING mutant population for the selected candidates of interest.
- Functional characterization of selected putative candidates by over-expression under tissue specific *ATML1* and constitutive promoters, through stable transformed tomato transgenic lines.

2 MATERIALS & METHODS

2.1 Materials

2.1.1 Chemicals, enzymes and extraction kits

Chemicals for the experimental work were ordered from the manufacturers: Merck, Sigma-Aldrich, Carl Roth, Serva, Roche and Fluka, respectively.

Enzymes for molecular biology methods (Taq DNA polymerases, Reverse-Transcriptase, ligases) were ordered from the manufacturers: Bio & Sell, Merck-Millipore, Invitrogen, Promega, and New England Biolabs.

Isolation of plant genomic DNA, RNA, plasmid DNA, cDNA from agarose gel electrophoresis and PCR purification was performed with Qiagen, Macherey-Nagel and Bio & Sell kits

2.1.2 Microorganisms

Escherichia coli - The *E. coli* strain DX10B was used for cloning.

Agrobacterium tumefaciens - The *A. tumefaciens* strain GV3101::pMP90 was used for both transient and stable transformation. Aliquots of *E. coli* and *Agrobacterium* liquid cultures were stored in 15% (v/v) glycerol at -80°C for long term.

2.1.3 Oligonucleotides and Plasmids

All Oligonucleotides were ordered from Eurofins MWG Operon. All primers were designed using Primer3 software (<http://primer3.ut.ee>). To control specific properties of primers, Oligo calc software (<http://www.basic.northwestern.edu/biotools/oligocalc.html>) was used. All primer sequences have been listed in the Appendix (see 6.1, Appendices). All-important plasmids described in the corresponding chapters are listed in the Appendix (see 6.3, Appendices)

2.1.4 Buffers, media and solutions

1XTAE DNA running buffer (1L) (pH 8.0)

Tris base - 4.84 g, Acetic acid – 1.14ml, EDTA – 0.37g

2.1.5 Culture media and solutions

Luria Bertani (LB) broth / medium (1 L) (pH 7.5)

Bacto-tryptone 10 g, Yeast extract 5 g, NaCl 10 g, Agar 10 g (for media)

Bacterial glycerol stock: LB medium and 30% (v/v) Glycerol

Super Optimal Broth (SOC) medium (1 L)

Tryptone 10 g, Yeast Extract- 2.5 g, 1 M NaCl 5 mL, 1 M KCl 1.2 µL, 1 M MgCl₂ 5mL,

1 M MgSO₄ 5 mL and 1 M Glucose 10 mL

Agro-infiltration medium (1 L) (pH 5.6)

For induction - 10 mM MES, 10 mM Glucose, 20 µM Acetosyringone

For infiltration - 10% (w/v) Sucrose, 20 mM Glucose, 8,6 g/L MS-Medium

Long Aston solution (20% phosphate) (1 L)

1 liter Long-Ashton solution contains 10 ml of stock solution microelements A, 1 mL of stock solution microelements B and 0.22 g Fe-EDTA, respectively. Amounts of micro and macroelements listed below were solved in H₂Odest [Hewitt, 1966].

Table 1: List of micro and macroelements

| Macroelements | Amount in (g) | Microelements A | Amount in (g) |
|---|---------------|---------------------------------------|---------------|
| KNO ₃ | 4.04 | MnSO ₄ ×1 H ₂ O | 1.60 |
| Ca(NO ₃) ₂ | 9.44 | CuSO ₄ ×5 H ₂ O | 0.25 |
| MgSO ₄ ×7H ₂ O | 3.68 | ZnSO ₄ ×7 H ₂ O | 0.33 |
| NaH ₂ PO ₄ ×7H ₂ O | 0.36 | H ₃ BO ₃ | 3.10 |
| Microelements B | | NaCl | 5.90 |
| (NH ₄) ₆ Mo ₇ O ₂₄ ×4 H ₂ O | 0.88 | | |

2.1.6 Plant transformation medium

Table 2: Media components for generating tomato (c.v MicroTom) stable transformants

SGM – shoot generation media, RGM – root generation media

| Media components | KCMS (pH 5.7) | Z-Media (pH 5.8) | SGM (pH 5.8) | RGM (pH 5.8) |
|---------------------------------|---------------|------------------|--------------|--------------|
| MS with Vitamins | 4.4 g/l | 4.4 g/l | 4.4 g/l | 4.4 g/l |
| Sucrose | 20 g/l | 30 g/l | 30 g/l | 30 g/l |
| KH ₂ PO ₄ | 200 mg/l | 100 mg/l | 100 mg/l | 100 mg/l |
| Agar | 8 g/l | 8 g/l | 8 g/l | 8 g/l |
| Thiamine | 0.9 mg/l | - | - | - |
| Nitsch Vitamins (1000x) | - | 1 ml/l | 1 ml/l | 1 ml/l |
| Kinetin | 100 µg/l | - | - | - |
| IAA | 0.5 mg/l | 0.1 mg/l | 0.1 mg/l | - |
| Zeatin-riboside | - | 2, 1 or 0.5 mg/l | - | - |
| Gibberellic acid | | | 0.1 mg/l | - |
| β-bactyl / Timentin | - | 300 mg/l | 250 mg/l | 200 mg/l |
| Kanamycin | - | 100 mg/l | 100 mg/l | 100 mg/l |

2.1.7 Protein electrophoresis buffers and solutions

Table 3: Buffers and staining solutions for protein electrophoresis

| SDS sample buffer components | Concentration |
|---|------------------------|
| Tris-HCL (pH 6.8) | 125 mM |
| SDS | 20 g/l |
| Glycerin | 50 % |
| β -Mercaptoethanol | 5 % |
| Bromophenol blue | 0.01 g/l |
| | |
| Electrode buffer (Running buffer) components | Concentration |
| Glycin | 14.4 g/l |
| Tris | 3 g/l |
| SDS | 1 g/l |
| | |
| Coomassie blue staining solution components | Volume (400 ml) |
| Serva Blue G | 0.2 g |
| Ethanol 96% | 200 ml |
| dH ₂ O | 160 ml |
| Acetic acid | 40 ml |

2.1.7.1 Western blotting buffers and solutions

Towbin transfer buffer

25 mM Tris, 192 mM Glycine, 20% (v/v) Methanol, 1.3 mM SDS

10X PBS buffer (pH 7.4)

1.39 M NaCl, 27 mM KCl, 125 mM Na₂HPO₄·2H₂O, 18 mM KH₂PO₄

10X TBS buffer (pH 7.5)

500 mM Tris-HCl, 1.5 M NaCl, 10 mM MgCl₂·6H₂O

For TBS-T buffer add 0.5% (v/v) Tween-20

Blocking Solution

3-5% (w/v) Milk powder in 1X TBS-T

2.2 Biological methods

2.2.1 Plant cultivation and growth conditions

Solanum lycopersicum c.v MicroTom (family: *Solanaceae*) was used during the thesis work. Both Wildtype (WT) and *jasmonic acid-insensitive 1 (jai1)* mutant seeds were kindly obtained by Dr. Greg Howe, Michigan state university, Ithaca. TILLING mutant lines for putative candidates were collaboratively obtained from Dr. Yoshihiro Okabe, generated at the University of Tsukuba, Japan.

Seeds of WT and *jai1* were germinated on moist expanded clay beads (2-5 mm) (Original Lamstedt Ton; Fibo ExClay, <http://www.fiboexclay.de>), for 8 days in phytochamber. Eight-days after germination, young tomato seedlings were transferred to pots filled with sterile coco-pit soil. The physiological parameters of plant growth conditions are; light intensity of $300 \mu\text{mol m}^{-2} \text{s}^{-1}$, a light phase of 16 hours at 28°C, a dark phase of 8 hours at 20°C and relative humidity of 50% were maintained during the plant growth activities. Plants were watered 3 times a week.

The physiological parameters of plant growth chamber housing transgenic tomato plants - light phase: 16 hours at 27°C, dark phase: 8 hours at 20°C and relative humidity of 22%, were maintained during the plant growth phase.

2.2.2 Preselection of *jai1* mutant

To identify *jai1* homozygous plants, initially third true leaves exceeding their size range (0.4-0.6 cm, Fig. 6C) were eliminated. Secondly, all plants showing anthocyanin production were excluded (Fig. 6D), since *jai1* fails to accumulate anthocyanins (Li et al., 2004). Homozygous *jai1* plants are generally female sterile, thus the mutation can only be maintained in the heterozygous state (Li et al., 2004) for further downstream applications.

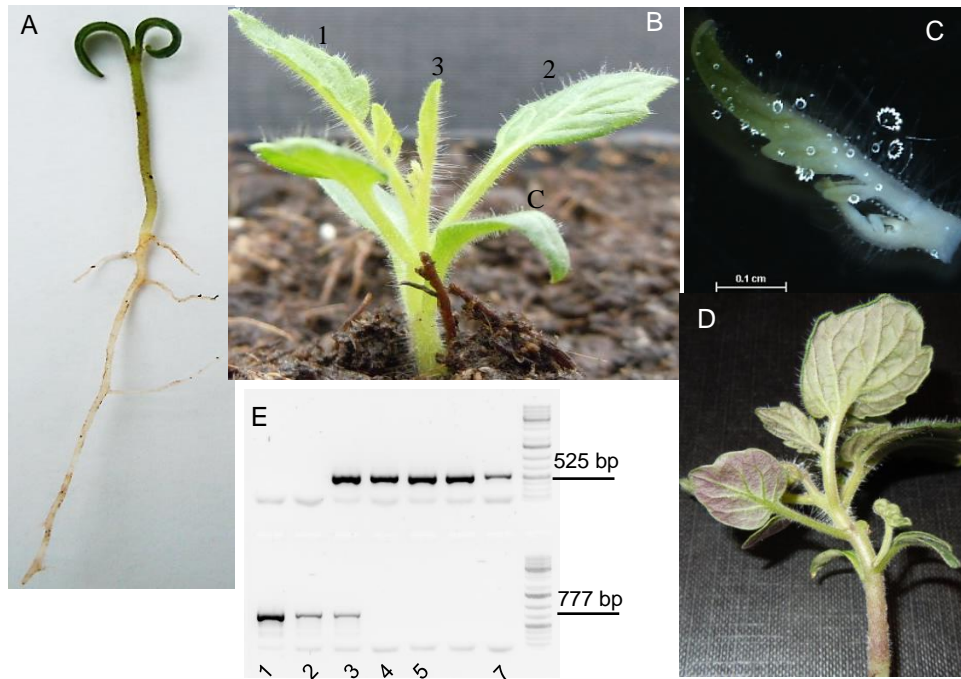


Figure 6: Workflow for screening *jai1* mutant:

(A) Eight-days-old seedlings were transferred to soil. (B) Five days after transfer on soil, young plant with true leaves (B1-3). (C) Size determination of third true leaf (0.4-0.6 cm) under light microscope. (D) Leaves showing anthocyanin phenotype on the abaxial leaf surface. (E) Agarose gel results of plants after genotyping, WT PCR product yielding 525 bp (E4-7), heterozygous *Jai1* yielding 525 bp and 777 bp (E3) and homozygous *jai1* yielding 777 bp (E1-2), respectively.

2.2.3 Quantification of type VI glandular trichomes upon wounding

Three-weeks after transfer to soil, plants were wounded to induce enhanced trichome formation in newly developed leaves. Leaflets of compound leaves (mature leaf and its neighboring leaflets) preferably bigger than 5 cm were considered for wounding using a pair of tweezers for five continuous days. Leaves were squeezed at 3 different leaf margins (basal-middle-frontal) with a scale of moderate to heavy. Two weeks after wounding, newly developed compound leaves were used to count glandular trichomes and compared to unwounded control plants.

2.2.4 Phytohormone measurements upon wounding

Cotyledons, first and second true leaves from young tomato plants (section 2.2.1) were considered for wounding using a pair of sharp tweezers, whereas control plants were unwounded. Thirty minutes post wounding, three biological replicates from each plant material (cotyledons, first, second, third, fourth-true leaves and stem) were rapidly harvested and frozen in liquid nitrogen. The frozen plant material was further subjected to grinding using mortar and pestle, and subsequent phytohormone measurements were performed.

2.2.5 Transcriptome sequencing

Young tomato plants (section 2.2.1) were sprayed twice with 50 μ M JA on the adaxial leaf surface, whereas the control plants were sprayed with double distilled water. Further, the third true leaves (n=3) were harvested 2 hours and 24 hours after the JA treatment. The harvested leaf material was quickly infiltrated in chilled absolute ethanol (100%) with the help of exsiccator. Furthermore, Leaf samples stored in ethanol were freeze dried on a lyophilizer (Christ LT-105, Germany), to evaporate the entire ethanol leaving behind dried leaves in a frozen state. Prior to lyophilization, the temperature in the lyophilizer is set to attain -102°C . Further. Leaf samples stored in chilled ethanol were sealed with paraffin, punched holes to ensure proper evaporation. After 2-3 hours, dried young third true leaves were stored at -20°C for RNA extraction.

2.3 Microbiological methods

2.3.1 Production of chemically competent *Escherichia coli* cells

MAX Efficiency DH10B *E. coli* strain, chemically competent cells (Life Technologies GmbH, Germany) were used for cloning procedures during experimental work. MAX Efficiency DH10B *E. coli* strain was cultured over night at 37°C . The cultured *E. coli* strain was measured 0.6 at OD_{600} and subsequently incubated in LB broth at 37°C for 3 hours. The cells were allowed to cool down on ice and centrifuged at 4°C , $3000 \times g$ for 10 minutes. Further, the culture was resuspended in 20 ml chilled TFB1 buffer (20 ml per 50 ml culture, Composition: 30 mM potassium acetate, 10 mM CaCl_2 , 50 mM $\text{MnCl}_2 \cdot \text{H}_2\text{O}$, 100 mM RbCl and 15% Glycerol, pH adjusted to 5.8, filter sterilize and stored at 4°C). Subsequently, the culture was centrifuged again and resuspended in $1/25^{\text{th}}$ of cool TFB2 buffer (2 ml per 50

ml culture, Composition: 100 mM MOPS or PIPES, 75 mM CaCl₂, 10 mM RbCl and 15% Glycerol, pH 6.5). Filter sterilized and stored at 4°C. Lastly, aliquots of 50 µL in 1.5 mL Eppendorf tubes were frozen in liquid nitrogen and stored at -80°C for transformation assays.

2.3.2 Transformation of *Escherichia coli* cells

Aliquot of 50 µL chemically competent (DH10B) cells were thawed on ice for 5 minutes. A 10 µL aliquot of ligation reaction mixture was added to thawed *E. coli* cells and incubated for half an hour on ice. The transformation mixture was incubated at 42°C in water bath for 90 seconds, as a heat shock. Immediately, the mixture was cooled on ice for 2 minutes and sterile 400 µL of SOC media were added. Further, the transformation mixture was incubated at 37°C, 350 rpm for 45 minutes. After the incubation, sterile LB plates with respective antibiotics and X-gal were used to plate spread nearly 100 µL of transformation mixture. The plates were incubated overnight at 37°C and the white colonies were analyzed by plasmid isolation and sequencing.

2.3.3 Production of chemically competent *Agrobacterium tumefaciens* cells

Agrobacterium strain GV3101::pMP90 was streaked out from glycerol stock to LB plates (containing antibiotics: 50 µg/mL rifampicin and 50 µg/mL gentamicin). The LB plates were incubated at 28-30°C overnight. A single colony was inoculated in 50 mL LB containing appropriate antibiotics and the inoculum was incubated at 28-30°C overnight. Further, the entire pre-culture inoculum was transferred to 500 mL LB with antibiotics and the OD₆₀₀ at 0.6 was measured. Further, the *Agrobacterium* culture was transferred to 250 mL bottles and centrifuged and cooled on ice for 15 minutes. The culture was centrifuged at 4°C for 15 minutes at 4000×g. After centrifugation, the supernatant was discarded and the pellet was gently re-suspended in 250 mL cold sterile water. In order to wash away the salts completely, centrifugation was repeated for three more times. Further, the pellets were dissolved gently in 25 mL ice cold 10% glycerol and transferred to single pre-chilled 50 mL falcon tubes. The pre-chilled culture mixture was centrifuged at 4°C for 15 mins at 3000×g and the pellet was re-suspended in 1 mL ice-cold 10% glycerol and aliquots of 50 µL in pre-chilled 1.5 mL sterile tubes were immediately frozen and stored at -80°C for transformation assays.

2.3.4 Transformation of *Agrobacterium tumefaciens* cells

Fifty microliters of electrocompetent *A. tumefaciens* cells was thawed on ice for 5 minutes. Five microliters of plasmid DNA (20 ng/ μ L) was added to the thawed cells. Further, the entire transformation mixture was transferred to pre-chilled electroporation cuvettes (VWR International GmbH, Germany) and the mixture was tapped down to eliminate air bubbles. A power pulse of 2.5 kV, with 200 Ω was applied until the beep and the cells were rejuvenated with 1 mL of LB broth. Further, the mixture was transferred carefully to 2 mL Eppendorf tubes and incubated for 3 hours at 28°C on a shaker at 350rpm. Lastly, the transformation mixture (300-350 μ L) was plated on LB plates (containing antibiotics: Rifampicin (50 μ g/mL) and Gentamicin (25 μ g/mL)) and incubated for 2-3 days at 28°C.

2.4 Molecular biological methods

2.4.1 Crude genomic DNA isolation and genotyping for *jai1* plants

Two-weeks-old tomato plants on soil (section 2.2.1) with small emerging, newly developing leaves or flower buds were excised with the help of forceps collected in PCR tubes. At first, a volume of 40 μ L of 0.25M NaOH was added to PCR tubes containing plant material. Samples were crushed with the pipette tips to become a homogenous pulp. The crude samples were further incubated at 95°C for 30 seconds on a thermal cycler (BIORAD Laboratories Inc., Munich, Germany). Further, 20 μ L of 0.5 N Tris- HCl (at pH 8.0 mixed prior with Igepal) was added to the crude mixture and vortexed. The crude samples were further treated with 40 μ L of 0.25 N HCl, mixed well and incubated at 95°C for 2 minutes on thermal cycler.

Table 4: Cycling conditions for genotyping *jai1* mutant plants

| Cycling conditions for <i>jai1</i> | | Temperature (°C) | Time |
|------------------------------------|-------------------|------------------|--------|
| Initial denaturation | | 94°C | 2 min |
| Denaturation | PCR for 39 cycles | 94°C | 30 Sec |
| Annealing | | 55°C | 30 sec |
| Extension | | 72°C | 45 sec |
| Final extension | | 72°C | 5 min |

Two microliters of crude DNA supernatant was used for PCR reactions. For genotyping crude DNA extracts of *jai1* plants, PCR components from Bio & Sell (Bio & Sell GmbH, Germany) were used. The protocol was followed according to manufacturer guidelines using BIORAD C1000 Touch™ Thermal Cycler (BIORAD Laboratories Inc., Munich, Germany), with following cycling conditions.

2.4.2 Pure genomic DNA isolation

Young leaves from 2-weeks-old plant on soil (section 2.2.1) were used to extract genomic DNA using Macherey-Nagel (MN) Plant DNA kit. The procedure was followed according to the manufacturer guidelines. Alternatively, a ready-to-use master mix (Phire Plant Direct PCR master mix, Life Technologies GmbH, Germany) was used to extract genomic DNA directly and perform PCR without undergoing DNA extraction. The procedure for Phire Plant Direct PCR master mix was followed according to manufacturer guidelines.

To increase the productivity of genotyping, an alternative method was employed for screening *jai1*, TILLING and stable transformants using Phire Plant Direct PCR Master Mix (Life Technologies GmbH, Germany). The protocol was followed according to manufacturer guidelines using BIORAD C1000 Touch™ Thermal Cycler (BIORAD Laboratories Inc., Munich, Germany), with following cycling conditions

Table 5: Cycling conditions for genotyping *jai1* mutant

| Cycling conditions | | Temperature (°C) | Time |
|----------------------|-------------------|---|--------|
| Initial denaturation | | 98°C | 5 min |
| Denaturation | PCR for 39 cycles | 98°C | 5 sec |
| Annealing | | 64.4°C (calculated based on Tm °C web calculator, ThermoScientific) | 5 sec |
| Extension | | 72°C | 20 sec |
| Final extension | | 72°C | 1 min |

2.4.3 Total RNA extraction and Dnase I treatment

Total RNA was extracted by pooling third-true leaves of 15 plants as one biological replicate. The leaf samples were lyophilized (section 2.2.5) and powdered with the help of steel beads (≈7mm) using bead mill (Retsch GmbH, Germany). The powdered material was further used for RNA extraction using RNeasy plant mini kit with Dnase I (Qiagen®),

MATERIALS & METHODS

The Netherlands). The RNA extraction procedure and Dnase I treatment was performed according to manufacturer guidelines Alternatively, the extracted RNA was subjected to Dnase I treatment by using TURBO™ DNase (Ambion® DNase kit, Life Technologies GmbH, Germany).The protocol was followed according to manufacturer guidelines.

To check the integrity and quality of RNA samples, aliquots (1µg/µL concentration) were analyzed on QIAxcel system (Qiagen®, The Netherlands). The RNA quality estimation was performed according to manufacturer guidelines. The RNA quality was distinguished based on RNA integrity number (RIN), which extends from a scale of 1 (totally degraded) to 10 (highly intact). An example of RNA quality estimation (Fig. 7) illustrates RIN values in the scale 8 to 10 (Fig. 7B).

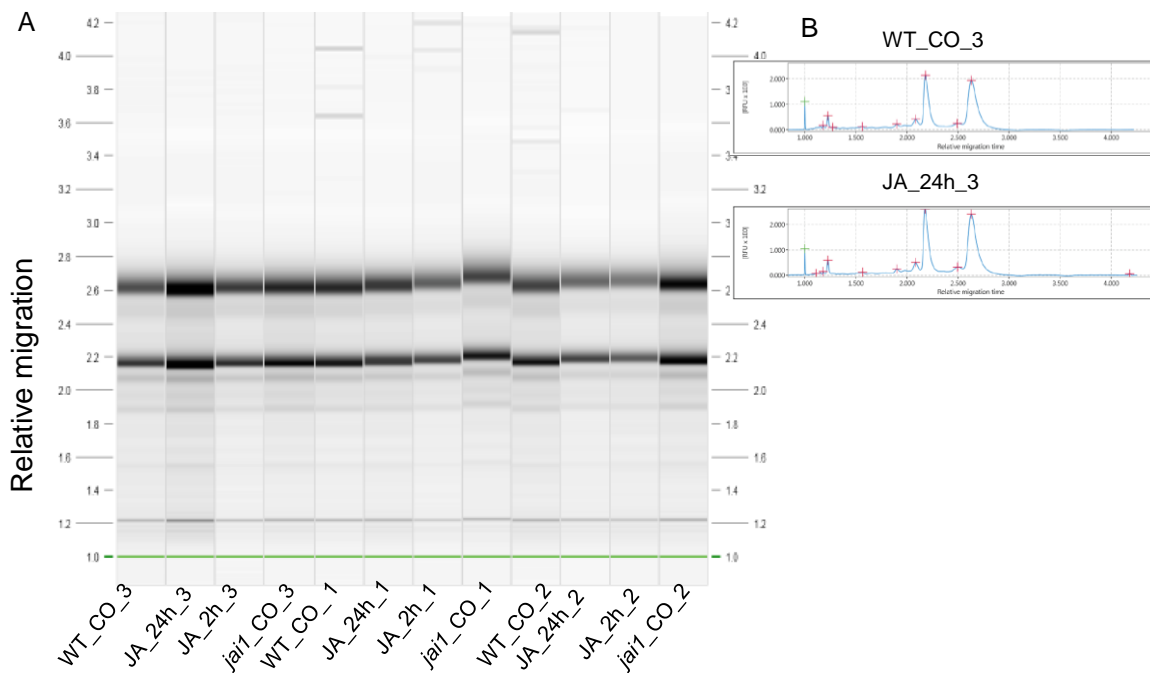


Figure 7: Qualitative estimation of leaf RNA samples

(A) RNA quality from Wild type control (WT_CO), JA treated (JA_2h and JA_24h harvest post treatment) and *jai1* control (*jai1_CO*) was estimated on QIAxcel screening gel, n=3. (B) RNA integrity peaks for WT_CO and JA_24h RNA samples. All RNA samples at WT_CO and JA_24h treatment belongs to RNA integrity scale from 8 to 10 respectively.

2.4.4 cDNA synthesis

One microgram of total RNA was used to synthesize cDNA by reverse transcription through oligo dT primers. Synthesis of cDNA was performed according to manufacturer guidelines (Promega GmbH, Germany). The cDNA concentration was examined at the NANODROP (PeqLab Biotechnology GmbH) and subsequent dilutions were made for the qRT-PCR. The samples were stored at -20°C for further downstream applications.

2.4.5 Cloning the putative candidate genes

All putative coding sequences of candidates of interest were cloned through 'one pot Golden Gate Cloning mechanism'. This cloning strategy employs type II restriction enzyme, which cuts outside the recognition site according to Engler and Marillonnet, 2008. Further, the sub cloning mechanism involves restriction and ligation in one step simplistic manner. All constructs were designed *in silico* using Geneious version 7.0.5 (<http://www.geneious.com>, Kearse et al., 2012).

The coding sequences of putative candidates of interest were amplified using a high fidelity KOD Hot Start DNA polymerase (TOYOBO Life Science department, Osaka, Japan). This proof-reading KOD DNA polymerase exhibits strong 3'-5' exonuclease activity, excellent processivity and elongation capability compared to other Taq DNA polymerase. The protocol was followed according to manufacturer guidelines using BIORAD C1000 Touch™ Thermal Cycler (BIORAD Laboratories Inc., Munich, Germany), with following cycling conditions.

Table 6: Cycling conditions for candidates

| Cycling conditions | | Temperature (°C) | Time |
|----------------------|-------------------|---------------------------------|------------------|
| Initial denaturation | | 95°C | 2 min |
| Denaturation | PCR for 34 cycles | 95°C | 20 sec |
| Annealing | | Lowest primer T _m °C | 10 sec |
| Extension | | 70°C | 10 - 25 sec / Kb |
| Final extension | | 72°C | 5 min |

2.4.6 Isolation of plasmid DNA, Restriction digestion and ligation

Plasmid DNA was isolated using NucleoSpin® Plasmid EasyPure kit (MACHEREY-NAGEL GmbH & Co. KG, Düren, Germany). The isolation was carried out according to the manufacturer guidelines. Putative candidate gene fragments were cloned using *Bpil* or *Bsal* restriction enzymes (Life Technologies GmbH, Germany) and T4 DNA ligase (Life Technologies GmbH, Germany), with necessary buffers in one step process. Subsequent plasmids were digested using *Bpil*, *Bsal* restriction enzymes along with CutSmart® and Buffer-G (New England Biolabs and Life Technologies GmbH, Germany). Protocol for restriction digestion and ligation reactions were performed according to manufacturer guidelines.

2.4.6.1 Colony PCR for putative candidates

Colonies from LB plates with respective antibiotics were picked and analyzed by PCR, through DreamTaq DNA Polymerase (Life Technologies GmbH). The protocol was followed according to manufacturer guidelines using BIORAD C1000 Touch™ Thermal Cycler (BIORAD Laboratories Inc., Munich, Germany), with following cycling conditions

Table 7: Cycling conditions for colony PCR

| Cycling conditions | | Temperature (°C) | Time |
|----------------------|-------------------|---------------------------|--------|
| Initial denaturation | | 95°C | 3 min |
| Denaturation | PCR for 30 cycles | 95°C | 30 sec |
| Annealing | | 55-59°C (primer Tm - 5°C) | 30 sec |
| Extension | | 72°C | 1 min |
| Final extension | | 72°C | 5 min |

2.4.7 Agarose gel electrophoresis

PCR products were separated by electrophoresis at 80 - 100 volts in 1 % Agarose (BIO & SELL GmbH, Germany), constituting 1× TAE buffer (section 2.1.4). Gel was pre-stained using Stain-G (Serva GmbH, Heidelberg, Germany) and the resultant bands were visualized under Fusion FX7 UV chemiluminescence (PeqLab Ltd, VWR Life Sciences Competence Center, Germany) detection machine.

2.4.8 Capillary gel electrophoresis

Alternatively, PCR products were separated on QIAxcel (Qiagen®, The Netherlands) machine using QIAxcel DNA screening cartridge provided by the manufacturer. The protocol for performing capillary gel electrophoresis was followed according to manufacturer guidelines.

2.4.9 Quantitative real-time Polymerase Chain Reaction (qRT-PCR)

Quantitative analyses of transcript levels from WT and JA-treated leaf samples was performed using 'EVA GREEN' master mix (BIO & SELL GmbH, Germany). Each biological replicate was estimated with two technical replicates and the PCR was performed on BIORAD CFX manager thermal cycler (BIORAD Laboratories Inc., Munich, Germany) using following conditions.

Table 8: Cycling conditions for qRT-PCR

| Cycling conditions for candidates | | Temperature (°C) | Time |
|-----------------------------------|-------------------|----------------------------------|----------|
| Activation of Taq DNA polymerase | | 95°C | 15 min |
| Denaturation | PCR for 39 cycles | 95°C | 15 sec |
| Annealing | | 58°C (optimal T _m °C) | 20 sec |
| Extension | | 72°C | 20 sec |
| Final extension | | 95°C | 10 sec |
| Melt Curve analysis | | 65°C - 90°C (increment of 0.5°C) | 0.05 sec |

2.5 Bioinformatics analyses

2.5.1 Transcriptome database construction and expression profiling

One µg/µL high quality total RNA was used to construct libraries for RNA sequencing (Qubit Fluorometer (Invitrogen Q32857, Carlsbad, CA, USA) use with Quan-IT DNA assay kit HS (Invitrogen, Q32851)), which was exclusively carried out at Jim Giovannoni lab, the Boyce Thomson Institute for Plant Research (BTI, Ithaca, NY, USA). The constructed libraries from RNA samples of different treatments were run on high-throughput Illumina HiSeq 2000 platform (Illumina, Inc. San Diego, CA, USA). The detailed procedure was

described and the same was performed according to protocol published in Cold Spring Harbor Protocols (Zhong et al., 2011).

2.5.2 Transcriptome data assembly and processing

Raw RNA-Seq reads were first processed to remove adaptors and low quality sequences using 'Trimmomatic' (Bolger et al., 2014). The processed RNA-Seq reads were then aligned to ribosomal RNA sequence database (Quast et al., 2013) using 'Bowtie' allowing two mismatches (Langmead et al., 2009), to remove any possible contaminations of these sequences. The resulting filtered reads were aligned to the tomato Heinz genome (The Tomato Genome Consortium, 2012) using 'TopHat' (Trapnell et al., 2009) allowing 1 segment mismatch. Following alignments, raw counts for each tomato gene were normalized to reads per kilobase of exon model per million mapped reads (RPKM). Differentially expression genes were identified with the 'EdgeR' package (Robinson et al., 2010).

2.5.3 Custom expression analysis and annotations

Although, differentially expressed genes (DEG's) were identified with EdgeR package as mentioned in section 2.5.2, a customized RNA-seq data analyses was performed to identify low abundant transcription factors and other differentially expressed genes according to thesis objectives. Here the raw read counts of each tomato gene were log (log₂ fold change (FC)) transformed and normalized to reads per kilobase of exon model per million mapped reads (RPKM). The normalized log transformed read counts were tested based on multiple statistical correction, Benjamini-Hochberg False Discovery Rate (FDR), by adjusting the p-value ≤ 0.05 . The statistical correction yielded 18,354 transcripts which were differentially regulated across the sample treatments. Further, these transcripts were annotated against International Tomato Annotation Group (ITAG, version 2.3).

2.5.4 Gene Ontology (GO) analysis

To identify putative jasmonic acid regulated transcription factors and genes, an efficient, fast and simple functional annotation software tool (<http://mapman.gabipd.org/web/guest/app/Mercator>) was used to perform gene ontology. For more details, please refer to (Lohse et al., 2014).

2.6 Analytical techniques

2.6.1 Western blot

2.6.1.1 Protein extraction from Agro-infiltrated tobacco plants

Agro-infiltrated leaves of tobacco plants were harvested 2 days post infiltration using a cork borer. About 50 mg of infiltrated tobacco leaf samples were frozen and grinded on bead mill (Retsch GmbH, Germany). Protein extraction buffer of 200 μ L was added to leaf powder and incubated at 95°C heat bath for 5 minutes. Further, the crude extract was centrifuged for 10 minutes at 13000 rpm and the supernatant was transferred to new 1.5 μ L tubes for further protein quantification.

2.6.1.2 Protein quantification by ESEN method

Protein extracts from tobacco-infiltrated leaves were quantified according to ESEN method. All necessary procedures for quantifying protein extracts of putative candidates was adapted to detailed protocol mentioned in Esen (1978). The eluted protein samples were incubated at room temperature overnight and their optical density at 578 nm was measured on spectrophotometer.

Calculation of protein concentration,

$$(\text{Excitation of probe} / \text{Excitation of standard}) * 2 = \mu\text{g} / \mu\text{L}$$

2.6.1.3 SDS- Polyacrylamide gel electrophoresis (PAGE)

The Polyacrylamide-Gel Electrophoresis was carried out using Minigel-Twin chamber Mini-PROTEAN Tetra Cell (BIORAD Laboratories Inc., Munich, Germany).

Table 9: Reagents for separation and collection gel

| Reagents for 12% gel (2 gels) | Separation gel | Collection gel |
|-------------------------------|----------------|----------------|
| Acrylamide (37, 5:1, 40%) | 1.5 mL | 200 μ L |
| dH ₂ O | 2.175 mL | 1.28 mL |
| Tris-HCl (1.5M, pH 8.8) | 1.25 mL | 500 μ L |
| SDS (20%) | 25 μ L | 10 μ L |
| TEMED | 2.5 μ L | 2.5 μ L |
| APS (10%) | 50 μ L | 20 μ L |

Stacking and collection gel

The gel cassettes were aligned and assembled vertically to Minigel-Twin chamber unit. Both separation and collection gel were prepared according to Table 9. Firstly, stacking or separation gel was mixed poured using a 5 mL pipette. To avoid air contact and oxidation, the gel was overlaid with water up to the surface of cassette. Once the stacking gel was polymerized after 2 hours, collection gel was mixed well and poured above stacking gel layer. Immediately, the comb was placed without forming any air bubbles and the gel was allowed to polymerize for 2 hours.

Loading the gel

Before loading the SDS-gel, the protein samples with a concentration of 10 µg were thawed on ice for 15 mins. For each protein sample, two volumes of SDS-sample buffer was mixed in a 1.5 mL tubes and incubated on thermo-block for 10 mins at 65°C. SDS gels were placed into Mini-PROTEAN Tetra Cell (BIORAD Laboratories Inc., Munich, Germany) containing electrode buffer and washed 2 to 3 times to eliminate air pockets. A Hamilton syringe was used to load a PageRuler Plus Prestained protein ladder (Life Technologies GmbH, Germany) at the corner wells and the protein samples. The electrophoresis was performed with following conditions: 45 volts for 15 minutes and 135 volts for 45 mins.

Coomassie blue staining

SDS-gel was stained with Coomassie blue staining solution. Here, the gel was heated in a microwave for 2-3 minutes at 600 watts. Similarly, excessive staining was removed by de-staining in 7% acetic acid solution at 150 rpm overnight for proper band visualization.

2.6.1.4 Trans-Blot Semi Dry electrophoretic transfer

Proteins were transferred to nitrocellulose or polyvinylidene difluoride (PVDF) membrane using Trans-Blot Semi Dry electrophoretic transfer apparatus (BIORAD Laboratories Inc., Munich, Germany). All necessary buffers and solutions are listed (section 2.1.4) and the protocol for Trans-Blot Semi Dry electrophoretic transfer was followed according to manufacturer guidelines.

2.6.1.5 Immunostaining

Table 10: Antibodies for the detection of putative proteins

| Antibodies | Dilution rate |
|---|----------------------|
| <i>For GFP</i> | |
| Primary antibody – anti GFP from Rabbit | 1:4000 |
| Secondary antibody – Goat anti-Rabbit (Alkaline phosphatase coupled) | 1: 5000 |
| <i>For c-Myc</i> | |
| Primary antibody – anti c-Myc from Mouse | 1:1000 |
| Secondary antibody – Goat anti-Mouse (Alkaline phosphatase coupled) | 1: 5000 |

Membrane subjected to semi dry electrophoresis described in section 2.6.1.4 was further washed with TBS buffer (100 mM Tris-HCl and 150 mM NaCl, pH 7.5) for 5 mins and blocked with 5% milk powder (BIORAD Laboratories Inc., Munich, Germany) in TBS buffer (pH 7.5). Further, the membrane was incubated overnight on shaker (150 rpm) at 4°C in TBS buffer (pH 7.5) consisting of primary antibody (dilution rate, Table 10) and 5% milk powder. The membrane was further washed 3 times with TBS T (TBS buffer, pH 7.5 + 0.05% Tween 20) and washed again with TBS buffer (pH 7.5) for 5 mins. Further, the membrane was treated with secondary antibody mixture, (diluted in TBS buffer (pH 7.5) containing 5% milk powder) for 2 hours at room temperature. The washing step was repeated with TBS T and TBS buffer (pH 9.5). Lastly, the membrane was further washed with reaction buffer (100 mM Tris-HCl (pH 9.5), 100 mM NaCl and 50 mM MgCl₂) for 5 mins. For staining the membrane, Nitro blue tetrazolium (NBT), and 5-Bromo-4-chloro-3-indolyl phosphate (BCIP) were diluted in 10 mL of reaction buffer and incubated on slow rotor at 150 rpm. The reaction was stopped using stop buffer (10 mM Tris-HCl (pH 8.0) and 1 mM EDTA) and stored in dark for further documentation

2.6.2 Determination of jasmonate levels

Young tomato plants were cultivated according to section 2.2.1. Wounding and collection of plant material were according to section 2.2.4. Determination of phytohormones from different plant parts of a young tomato plant was performed on ultra-performance liquid chromatography-mass spectrometry (UPLC-MS) device (Balcke et al., 2012). Reagents necessary for phytohormone measurements was prepared according to Balcke et al., (2012). Nearly 50 to 70 mg of frozen plant material powder was subjected to methanol extraction using internal jasmonates (OPDA, JA and JA-Ile) standards. Detection of phytohormones and validation of measured values were performed according to Balcke et al., (2012).

2.6.3 Gas Chromatography-Mass Spectrometry (GC-MS)

Whole leaf extracts of stable transformed F1 generation tomato lines were performed using n-hexane (Carl Roth GmbH). The protocol for hexane extraction and the data analysis was followed as described, according to Scheler et al., (2016).

2.7 Microscopy works

2.7.1 GUS histological assay

Table 11: Components for GUS staining solution

| Component | Stock solution | Final concentration |
|--|----------------|---------------------|
| X-Gluc | 100mM | 2mM |
| EDTA (pH 8.0) | 500mM | 10mM |
| Triton-X | 10% | 0.1% |
| Potassium ferricyanide ($K_3Fe(CN)_6$) | 100mM | 0.5mM |
| Potassium ferrocyanide ($K_4Fe(CN)_6$) | 100mM | 0.5mM |
| Disodium phosphate (Na_2HPO_4), pH-7.2 | 500mM | 50mM |
| Monosodium phosphate (NaH_2PO_4), pH-7.2 | 500mM | 50mM |

Leaf samples were harvested with a cock borer and placed in a 24-well plate (Greiner Bio one GmbH, Germany). Freshly prepared GUS solution was added to immerse the whole tissue. Further, the leaf tissues were vacuum infiltrated using a desiccator for 5-10 minutes. The infiltrated leaf tissues were then incubated at 37°C overnight, to obtain better staining. De-coloration of leaf samples to remove chlorophyll content was carried out by washing repeatedly with graded series of ethanol (50%, 60% and 70% respectively). The samples were documented under light microscope (Nikon AZ100, Japan) and stored at 4°C for further analyses.

2.7.2 Paraplast embedding of leaf material

Third true leaf samples were incubated in in small glass vials containing formaldehyde-acetic acid (FAA) solution and vacuum infiltrated for 10 minutes. Further, the leaves were washed in a graded ethanol series (10% for 30 minutes, 30%, 50%, 70%, 90% and 100% for 1 hour). The washed leaf samples were treated with 100% ethanol (Merck, Germany) plus 0.1 mg/mL Eosin (Merck, Germany) for one hour. The leaf specimens were washed in combination with 96% ethanol (Carl Roth GmbH, Germany) and pure rotihistol (Carl Roth GmbH, Germany) (in a mixture of 3:1, 1:1 and 1:3 ratios respectively), with each ratio

mixture for 1 hour. Subsequently, leaf specimens were washed with pure rotihistol for about 30 minutes and transferred to 60°C incubator to repeat with pure warm rotihistol. Further, liquid paraplast (Sigma-Aldrich) was added drop by drop until rotihistol was evaporated leaving pure paraplast. Lastly, the leaf specimens were embedded on silica blocks, solidified overnight and stored at 4°C for hybridization assays.

2.7.3 Polyethylene glycol (PEG) embedding of leaf material

All the chemical reagents and materials necessary for following PEG embedding procedure was considered according to Hause et al., (1996) and Isayenkov et al., (2005).

Leaf samples were cut into small pieces (approximately, 4mm length * 3mm breadth) in PBS solution containing 4% para-formaldehyde and 0.1% Triton X-100, using a sharp razor blade. Fine leaf tissues were vacuum infiltrated for 2hrs. The infiltrated leaf specimens were dehydrated in the graded series of ethanol (10% for 30 mins, 30% & 50% for 1 hour each and overnight at 4°C in 70% ethanol respectively). Further the dehydration process was continued with higher percentage of graded ethanol series (90% & 100% for 30 minutes each). In general, washing, dehydration in series of graded ethanol, infiltration of PEG1500 and final embedment was performed according to method published in Hause B et al., 1996 and modified according to Isayenkov et al., 2005 respectively.

2.7.4 Environmental Scanning Electron Microscopy (ESEM)

Surface of fresh young true leaves of WT and *jai1* homozygous mutant about 14 days old, showing detailed developmental phases of glandular trichomes were captured on scanning electron microscope ESEM XL-30 FEG by Mr. Frank Syrowatka at the ICMS, Halle (FEI/Philips, Eindhoven, The Netherlands). The ESEM was operated on wet mode and the gas pressure of 1.5 millibar was applied. For imaging, a gaseous secondary electron detector was used.

2.7.5 Localization of GFP- tagged proteins

Putative candidates fused with GFP reporters were infiltrated to *N. benthamiana* leaves. Three days after infiltration, leaf discs of 1 cm² were excised using a cork borer and the sub-cellular localization of GFP-tagged protein was visualized under laser scanning microscope (LSM 700, Zeiss, Jena, Germany) using a wavelength between 495-550 nm and excitation of 488 nm.

2.7.6 Leaf imaging and counting glandular trichomes

The third true leaves and the newly emerged young leaves at the apical meristem were imaged under bright field microscope (Nikon AZ100, Japan) with advanced Nikon software (NIS Elements AR version 4.51). Leaves of same developmental stages were chosen for imaging. Glandular trichomes were counted with the help of Image J (Image J version 1.48, <http://imagej.nih.gov/ij>).

2.8 Plant transformation

2.8.1 Transient transformation of *Nicotiana benthamiana* leaves

Single colonies from successful Agrobacterium-mediated transformation confirmed through colony PCR was incubated in LB with necessary antibiotics (see 6.2, Appendices) for 2-3 days at 28°C. The OD₆₀₀ of agro culture was measured at the spectrophotometer (Beckman DU@530, Beckman Coulter, USA) and the required culture volume was calculated using a simple formula,

$$\text{OD (Required)} * \text{Total Volume (Required)} = \text{OD (Measured)} * \text{Culture (Required)}$$

$$\text{Culture (Required)} = \frac{\text{OD (Required)} * \text{Total Volume (Required)}}{\text{OD (Measured)}}$$

$$\text{OD (Measured)}$$

The required culture volume for leaf infiltration was diluted with agro-infiltration buffer (5 mM MES, 10 mM MgCl₂ and 150 μM acetosyringone). Sterile syringes without needles were used to infiltrate young *N. benthamiana* leaves (4 to 5-week-old plants). Further, plants were transferred to green house to estimate the protein expression.

2.8.2 Transformation of *N. benthamiana* mesophyll protoplasts

Transient expression of putative candidate proteins was identified in mesophyll protoplasts of *N. benthamiana*. Five-week-old plants with well expanded leaves were used for protoplast isolation. Further isolation of protoplasts and PEG-mediated DNA transfection were performed by adapting the protocol according to Yoo et al., (2007). Transfected protoplasts were made into aliquots and used for sub-cellular localization under laser scanning microscope and subsequently frozen in -80°C for protein immunoblot.

2.8.3 Stable transformation of cultivated tomato

Stable transformation of tomato was generated by adopting and modifying the materials and methods according to Fernandez et al., 2009, Cermak et al., 2015 and Van Eck et al., 2006 respectively. Media components and antibiotics are described (Table 2, section 2.1.6).

2.8.3.1 Germination of seeds, plant growth and physiological conditions

Seeds of WT and *jai1* heterozygous were sterilized using 3% H₂O₂ in 70 % ethanol. Around 15 to 20 seeds were sterilized in a 50 mL falcon tube. With a 5 mL sterilizing solution and repeated washes with distilled water, the seeds were sterilized and placed in subsequent order on plant cultivation media (Plant agar, DUCHEFA BIOCHEMIE B.V, The Netherlands). Media plates were incubated in dark chamber for 3 days and transferred to growth chamber.

2.8.3.2 Pre-conditioning and transformation

Six days after germinating seeds on ½ MS media, Agrobacterium culture carrying constructs were inoculated with appropriate antibiotics (see 6.3, Appendices) overnight. Seven-days-old cotyledons were pre-conditioned by gently excising the both ends of cotyledons, placed upside down on KCMS media (Table 2, section 2.1.6) and incubated in dark overnight. The OD₆₀₀ of Agrobacterium culture was adjusted to 0.08 by diluting with liquid KCMS for transformation. The Agrobacterium culture was then poured into a petri-dish and the pre-conditioned cotyledons were incubated in Agrobacterium culture for 30 mins on rotor at 20 rpm. Further, the cotyledons were transferred to new KCMS, placed upside down and incubated in dark for 2 days.

2.8.3.3 Callus cultivation and regeneration

The inverted cotyledons after 2 days, were transferred on to 2Z-media (2 mg/l Zeatin riboside, Table 2, section 2.1.6) plates in upright position and incubated in plant growth chamber (growth parameters, see section 2.2.1) for 2 weeks until new callus were generated. Those newly formed callus was then transferred to 1Z-media (1 mg/l Zeatin riboside, Table 2, section 2.1.6) and incubated for 2 weeks. Once the callus was proliferated to form new meristems, they were further transferred to 0.5Z-media (0.5 mg/l Zeatin riboside, Table 2, section 2.1.6) containers for 2 weeks to develop shoots. Once the shoots start to develop from proliferating callus, single shoots were excised with a sharp

MATERIALS & METHODS

sterile razor and placed on shoot generation media containers, until the shoots were matured. Approximately after 2 weeks, every single transformants were transferred to root generation media until they formed stable roots. The transformants were renewed on new media once in a week to avoid any sort of contamination.

2.8.3.4 Plant acclimatization

Once the transgenic plants attained stable shoot and root system, they were moved on to pots containing expanded clay granules in phytochamber with controlled greenhouse containers. The plants were further allowed to adapt and acclimatize to phytochamber atmosphere conditions. Slowly, once acclimatized, the plants were transferred on to soil and watered thrice a week.

3 RESULTS

3.1 Prerequisite experimental analysis

The aim of preliminary analysis was to verify type VI glandular trichome numbers and to select the right leaf material for the transcriptome sequencing. Previous research reports that trichome numbers were significantly increased on newly developed leaves of *Arabidopsis* and tomato after artificial wounding and exogenous application of jasmonates (Traw and Bergelson, 2003; Boughton et al., 2005). In the current thesis, type VI glandular trichomes were monitored in cultivated tomato species (cv MicroTom) by both approaches, mechanical wounding and exogenous JA treatment.

3.1.1 Mechanical wounding

In order to quantify type VI glandular trichome numbers across the WT and *jai1* mutant, tomato leaves were mechanically wounded (Fig. 8).

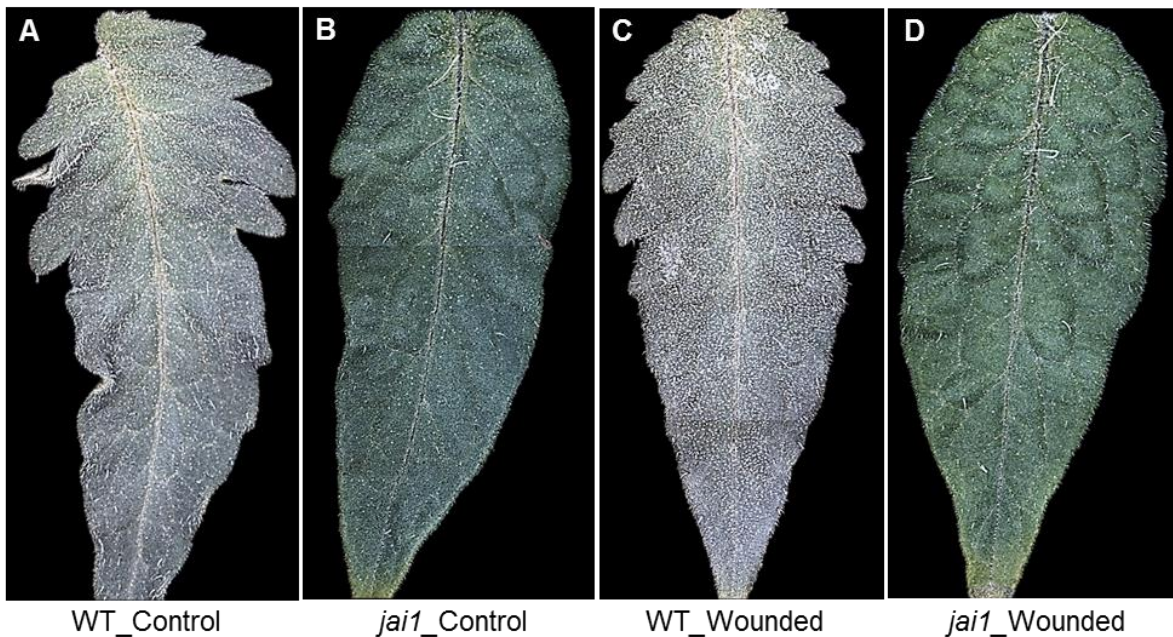


Figure 8: Artificial wounding experiments on tomato leaves

Three-week-old tomato leaves of WT and *jai1* mutant was observed under bright field microscope (3x magnification). (A) Control leaves of WT and (B) *jai1* unwounded, were compared with (C) WT and (D) *jai1* wounded leaves.

RESULTS

In the cultivated tomato, type VI glandular trichome numbers are significantly different between WT and *jai1* mutant (Li et al., 2004). During mechanical wounding, three-week-old tomato leaves from the WT and *jai1*, both control and wounded were compared (Fig. 8). Fine and densely populated white heads were distinguished between WT and *jai1* control leaves (Fig. 8A-B). Two weeks after wounding, an abrupt increase in the type VI glandular trichomes was observed on the newly developed leaves of WT plants (Fig. 8C). By contrast, type VI glandular trichome heads remain unchanged on *jai1* leaves (Fig. 8D). During trichome quantification, type VI glandular trichomes were found to be significantly different between control and wounded WT leaves (Fig. 9). Further, trichome quantification showed that there was a 10 fold difference between WT and *jai1* leaves after wounding (Fig. 9). Overall, mechanical wounding experiments indicate significant changes in type VI glandular trichome numbers between WT and *jai1* leaves but no difference in type VI glandular trichome numbers was observed within the *jai1* control and wounded leaves (Fig. 9).

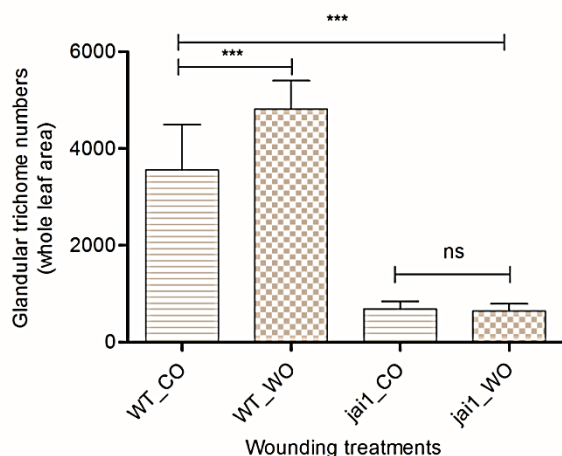


Figure 9: Quantification of type VI glandular trichomes

Type VI glandular trichomes were quantified after wounding tomato leaves. WT_CO and WT_WO represents control and wounded for WT leaves and same applies for the *jai1* mutant. Test of significance (** $p < 0.001$), ($n=8$) was determined by students t-test.

3.1.2 Exogenous JA treatment

In Arabidopsis and tomato, jasmonates (JA and MeJA) treatment has led to significant increase in the trichome numbers and density (Traw and Bergelson, 2003; Boughton et al., 2005). During preliminary analysis, twelve-days-old tomato plants with four true leaves were treated with JA. To analyze the effect of JA, a minimum concentration of 50 μ M was exogenously sprayed on every true leaves of young tomato plants. Type VI glandular trichome numbers from JA-treated and control (water) leaves were estimated on the whole leaf surface area (Fig. 10). Based on the quantitation data, type VI glandular trichome

numbers across four individual true leaves were found to be higher compared to control leaves (Fig. 10). For instance, type VI glandular trichome numbers on the second and third true leaves were significant but not with the first and fourth true leaves due to high standard deviations (Fig. 10). Further, type VI glandular trichome numbers were significantly higher on JA-treated third true leaves compared to control leaves (Fig. 10). This indicates that increase in type VI glandular trichome numbers at an early plant developmental stage after JA treatment enables to select the right leaf material for the further downstream analysis.

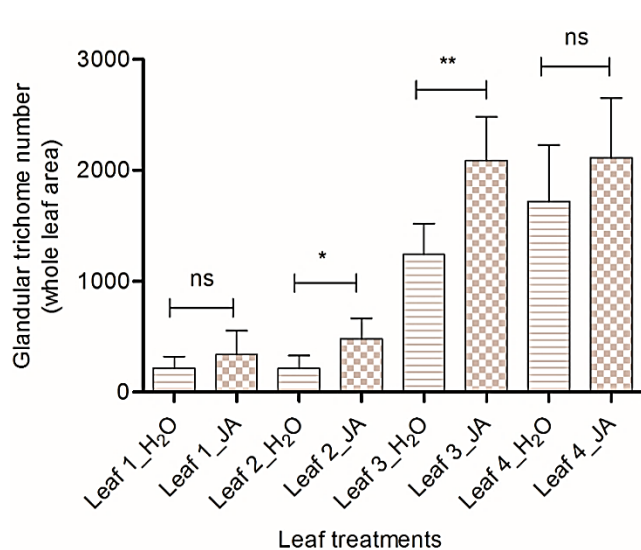


Figure 10: Quantification of type VI glandular trichomes upon JA treatment

Type VI glandular trichomes were quantified from JA-treated true leaves. Leaf 1-4 depicts four true leaves of a 12-days-old young tomato plant. Young leaves treated with water and JA (50 μ M) shown on the x-axis and glandular trichome number determination per whole leaf area on the Y-axis. Test of significance (* $p < 0.05$, ** $p < 0.01$), $n=3$, was determined by student t-test.

3.1.3 Importance of third true leaf for downstream applications

Choosing the right leaf material for downstream applications was certainly essential. This was inferred through preliminary data obtained based on the significant changes in type VI glandular trichome numbers after JA treatment (Fig. 8). A young tomato plant, preferably twelve-days-old with four true leaves (Fig. 11A) was suitable for harvesting leaf samples. Since the quantification of type VI glandular trichome numbers on the third true leaves showed striking difference compared to other true leaves (Fig. 10), third true leaves were initially investigated under bright field microscope (Fig. 11B). Interestingly, the adaxial and abaxial leaf surface of third true leaves (0.6 cm) were densely populated with non-glandular (type I) and glandular (type VI) trichomes (Fig. 11B). Further, the magnification of third true leaves under ESEM indicated both trichomes (type I and type VI) at different developmental phases, from initiation to maturation (Fig. 11C). Collectively, the

RESULTS

quantification of type VI glandular trichomes and its morphological features, third true leaves were considered as a right leaf material for further downstream applications.

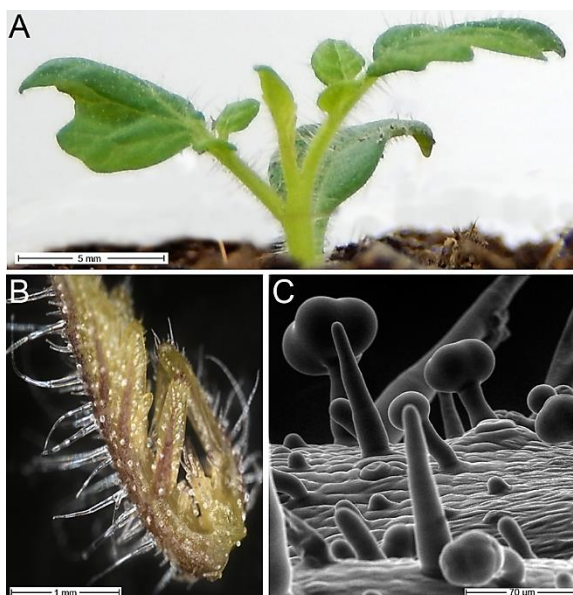


Figure 11: Morphology of type VI glandular trichomes on the third true leaf

(A) Twelve-days-old plant with true leaves. (B) Third true leaf under bright field microscope after harvest. (C) Magnification of third true leaf surface under environmental scanning electron microscope (ESEM).

3.2 Validation of JA-induced genes to verify treatment conditions

The contribution of JA has been remarkable in the area of plant molecular functions and mechanisms. By exogenous application, JA has proven to enhance and induce trichome numbers significantly (Traw and Bergelson, 2003). To evaluate the transcript abundance of JA-induced genes, RNA extracted from WT_CO, JA-treated (JA_2h and JA_24h) and *jai1*_CO third true leaves were considered. Relative expression of early JA-induced genes including *Allene oxide cyclase* (AOC) (Fig. 12A) and late induced genes like *Proteinase Inhibitor 2* (PIN2), *leucine aminopeptidase A* (LAP-A), *Threonine deaminase* (TD) (Fig. 15B, C and D) were analyzed for their transcript abundance across the treatment conditions. AOC transcript levels were up-regulated shortly after JA treatment (JA_2h) and decreased after 24 hours (JA_24h) (Fig. 12A). Further, AOC transcript levels were found at the basal level in WT_CO and *jai1*_CO treatment conditions (Fig. 12A), however presence of huge standard deviation led to no significant fold changes across treatment conditions. Similarly, LAP-A transcript levels were up-regulated after JA-2h treatment and decreased after JA_24h treatment (Fig. 12B). The elevated transcript levels shortly after JA treatment showed a fold change of 1.4 compared to WT_CO and *jai1*_CO conditions (Fig. 12B). Further, as a late JA-induced gene, PIN2 showed lower transcript accumulation after

JA_2h treatment and increased transcript levels after JA_24h treatment (Fig. 12C). There was no significant fold change observed in comparison to control and treatment conditions due to huge standard deviation (Fig. 12C). Similar to *LAP-A*, transcript levels of *TD* were significantly up-regulated after JA_2h treatment and decreased after JA_24h treatment. Concurrently, transcript levels of *TD* were at the basal level across WT_CO and *jai1*_CO treatment conditions (Fig. 12D). The validation of potential JA-regulated genes not only signifies transcript accumulation after JA-treated time points but also confirms the quantitative estimation of RNA samples necessary for transcriptome sequencing.

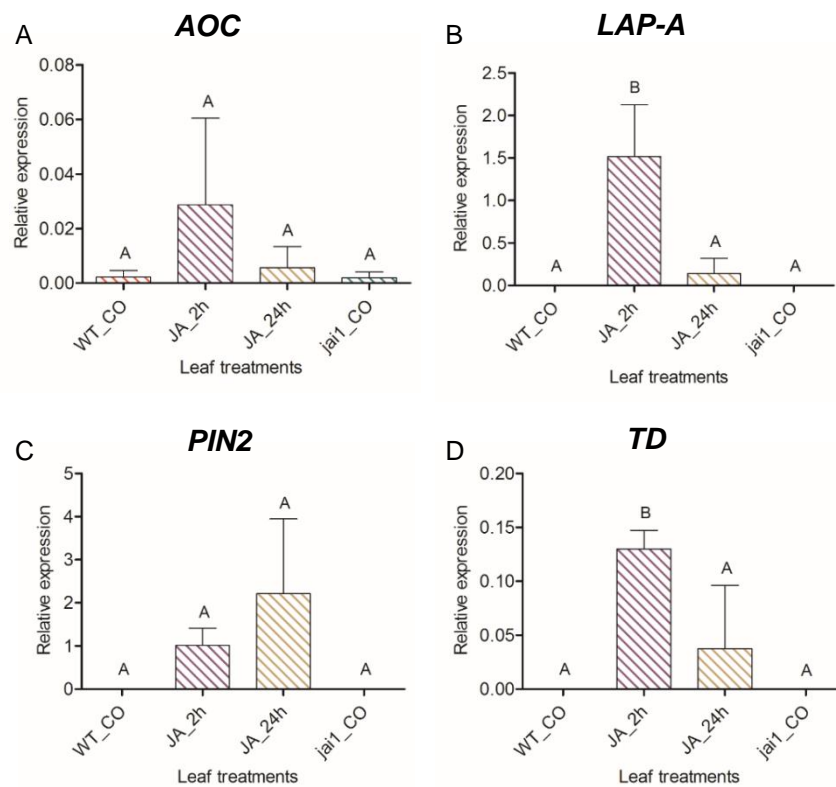


Figure 12: Transcript accumulation of JA-induced genes in treatment conditions

(A-D) Total RNA samples from WT, JA-treated and *jai1* third true leaves were considered to estimate transcript levels of JA induced genes, with reference to *Solanum lycopersicum* *ELONGATION FACTOR (EF)* house-keeping gene. Leaf treatments on the X-axis correspond to wild type control (WT_CO), wild type treated with JA (50 μ M) and harvested after 2 hours (JA_2h) and 24 hours (JA_24h), and lastly *jai1* control (*jai1*_CO), respectively. JA-induced genes: *Allene oxide cyclase (AOC)*, *leucine aminopeptidase A (LAP-A)*, *Proteinase Inhibitor 2 (PIN2)* and *Threonine deaminase (TD)*. Error bars indicate mean values \pm SD (n=3), statistical significance was determined by the analysis of variance (ANOVA) with a post hoc test (Newman-Keuls multiple comparison test).

3.3 Validation of tomato homologs of trichome regulatory genes

The molecular mechanisms of key regulatory factors involved in the initiation and induction of unicellular trichomes in *Arabidopsis* have been previously well described. The key regulatory factors are primarily involved in forming trimeric complex, commonly referred as MYB-bHLH-WD40 (MBW) regulatory complex (Ramsay et al., 2005; Serna et al., 2006; Balkunde et al., 2010; Feller et al., 2011 and Wada et al., 2011). To validate tomato homologs of key trichome regulators, protein sequences of *Arabidopsis* key trichome regulatory factors were blasted for sequence similarity against *Solanum lycopersicum* genome database using BLAST tool (Altschul et al., 1990).

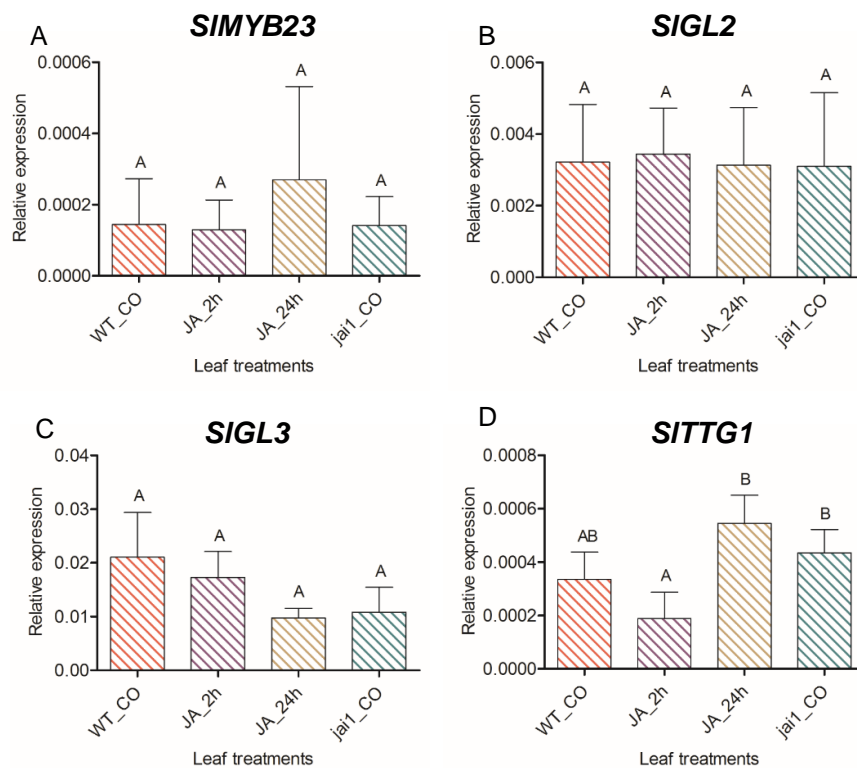


Figure 13: Transcript accumulation of the tomato homologs of Arabidopsis trichome regulatory genes

Total RNA samples from corresponding leaf treatments, descriptions of leaf treatments, validation with reference to house-keeping gene and statistical significance test were according to description in Fig. 12. The tomato homologs of Arabidopsis trichome regulatory genes abbreviated as, (A) MYB family transcription factor (*SIMYB23*), (B) *GLABRA2* (*SIGL2*), (C) *GLABRA3* (*SIGL3*) and (D) *TRANSPARENT TESTA GLABRA1* (*SITTG1*), respectively.

The transcript accumulation of tomato homologs showed different expression profiles across treatments conditions. Transcript levels of *SIMYB23*, which encodes a R2R3 MYB transcription factor, were not significantly different across treatment conditions (Fig. 13A). Tomato homolog of key trichome inducing gene, *SIGL2* encoding a homeo-box leucine zipper protein showed equal distribution of transcript levels with no significant changes across JA-treated and control samples (Fig. 13B). Another important tomato homolog of MBW trimeric complex, *SIGL3* encoding a bHLH transcription factor (Fig. 13C) showed varying levels of transcript accumulation across JA-treated and control samples without any apparent significant changes (Fig. 13C). The last homolog of MBW trimeric complex, *SITTG1*, encodes a WD-40 protein. Transcript levels were significantly higher in JA_24h compared to JA_2h treatments, but no significant difference in *SITTG1* transcript levels were observed among WT_CO and *jai1*_CO treatment conditions (Fig. 13D). Collectively, the transcript abundance of trichome regulatory factor homologs in tomato was found to be very low or merely basal across the treatment conditions.

3.4 Validation of candidates from apex and glandular trichomes data set

Tomato species predominantly comprise three different kinds of trichomes, type I (non-glandular), type VI and VII (glandular) (Channarayappa et al., 1992). Within the species and respective cultivars of tomato, common trichome types are shared. For instance, wild type *S. habrochaites* share its glandular trichome types with cultivated tomato *S. lycopersicum* cultivars (Channarayappa et al., 1992; Glass et al., 2012).

Table 12: Putative tomato homologs of key trichome regulators from apex and glandular trichomes data set

| Attributes | Human readable-description | Apex/Trichome ratio |
|--------------------|---|---------------------|
| Solyc01g095640.1.1 | Myb, Myb family transcription factor IPR015495 | 125.00 |
| Solyc03g120620.2.1 | GL2 / Homeobox-leucine zipper protein ATHB-15 , IPR002913 Lipid-binding START | 5.73 |
| Solyc08g081140.2.1 | GL3 / Myc-like anthocyanin regulatory protein, IPR001092 bHLH dimerization region | 3.78 |
| Solyc03g097340.1.1 | TTG1 / WD-repeat protein IPR017986 | 0.84 |
| Solyc07g008010.2.1 | CPC/ Myb transcription factor IPR015495 Myb transcription factor | 99.52 |

RESULTS

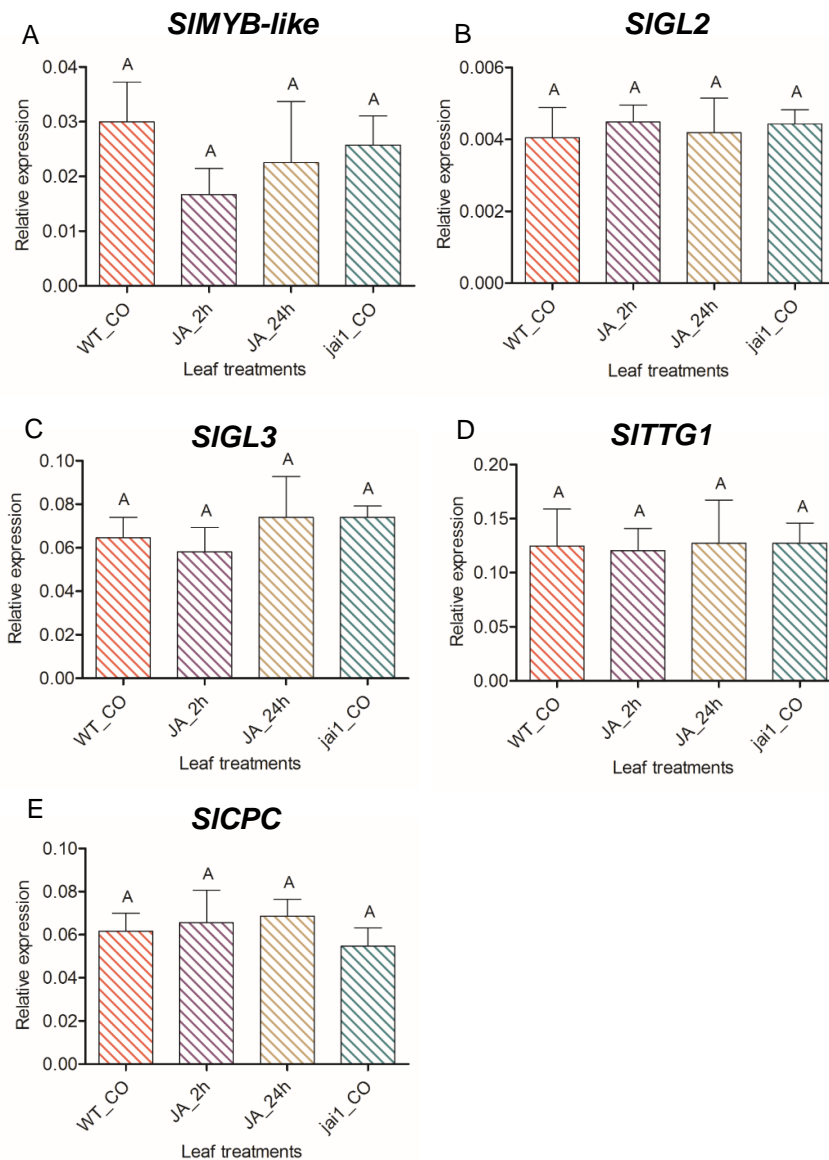


Figure 14: Transcript accumulation of putative tomato homologs from apex and glandular trichomes data set

Putative tomato homologs were identified from wildtype (*S. habrochaites*) and cultivated tomato (*S. lycopersicum*) apex and glandular trichomes transcriptomic data. Total RNA samples from corresponding leaf treatments, descriptions of leaf treatments, validation with reference to house-keeping gene and statistical significance test was performed according to Fig. 12. Tomato homologs of Arabidopsis trichome regulatory genes abbreviated as, (A) R2R3 MYB transcription factor (*SIMYB23*), (B) *GLABRA2* (*SIGL2*), (C) *GLABRA3* (*SIGL3*), (D) *CAPRICE* (*SICPC*) and (E) *TRANSPARENT TESTA GLABRA1* (*SITTG1*), respectively.

Unlike previous experiments, tomato homologs were selected based on the similarity search, whereas here, the respective homologs of Arabidopsis key trichome regulatory factors were selected based on the Solyc ID attributes through SOL genomics network database. An overview and methodology for RNA-seq data has been described in the upcoming section (section 3.5). Putative tomato homologs were identified from the RNA-seq data of apices and glandular trichomes, harvested from wild type (*S. habrochaites*) and cultivated tomato (*S. lycopersicum*) (personal communication, Dr. Stefan Bennewitz, IPB, Halle). Apex signifies young leaf meristems, which is a hotspot for trichome initiation and development. The identified putative tomato homologs of Arabidopsis trichome regulatory factors were explicitly upregulated in the apex region, with significant \log_2 fold changes (\log_2 FC), but not up-regulated in the trichomes (Table 12). The selected candidates were validated on qPCR with two sets of biological replicates harvested from WT, JA-treated and *jai1* third true leaves, respectively. Transcript accumulation of *MYB-like* transcription factor varied across JA-treated (JA_2h and JA_24h), WT_CO and *jai1*_CO treatments with no significant changes (Fig. 14A). Tomato homologs of other key regulators such as, *GL2*, *GL3*, *TTG1* and a negative regulator *CPC* (Table 12) showed almost equal levels of transcript accumulation pattern across the treatment conditions (Fig. 14B-E), without showing any significant changes. To conclude, validation of Arabidopsis trichome regulatory homologs in tomato either by sequence similarity search (Fig. 13) or identifying through transcriptomic data set (Fig. 14) showed no significant changes. Interestingly, the relative expression of these transcription factors was found to be very low in control and JA-treated samples (Fig. 13 and Fig. 14).

3.5 Transcriptomic data analysis from young tomato leaves

The RNA-seq data analyses was conducted by Dr. Benedikt Athmer at the IPB, Halle. The objective of candidate gene profiling was to identify genes that are differentially regulated across control and JA-treated RNA samples. The key regulators involved in the initiation and induction of trichomes in *A. thaliana* were collaboratively a group of transcription factors. With this perspective, differentially regulated transcripts were predicted to play a potential role in the formation of glandular trichomes in tomato. A robust and emerging sequencing platform, RNA sequencing, is capable of more accurate quantification of differential transcript expression and retrieving low-abundance transcripts in the course of sequencing compared to other next-generation sequencing platforms.

In order to obtain a complete transcriptome analysis of WT, JA-treated (JA_2h and JA_24h) and *jai1* leaves, three biological replicates from each treatment condition was subjected to paired-end RNA sequencing (2× 50 bp), performed at the Boyce Thompson Institute collaborative partner. The resultant sequencing yielded one to several millions of reads across each sample biological replicates (Table 13). Using a Trimmomatic software tool (Bolger et al., 2014), raw reads were processed to remove low-quality reads, cut-down adapter sequences and eliminate poor-quality bases. Further, the processed reads were aligned to tomato reference (Heinz) genome.

Table 13: Total read counts for treatment biological replicates generated by RNA-seq

| Paired-end RNA sequencing (2×50 bp reads) | | Alignment to tomato (Heinz) genome | |
|---|------------------------|------------------------------------|-------------------------|
| Biological replicates | Total raw reads | Mapped reads | Mapped reads (%) |
| <i>jai1</i> _CO_1 | 3,308,070 | 2,207,950 | 78.16 |
| <i>jai1</i> _CO_2 | 2,837,015 | 2,030,803 | 83.56 |
| <i>jai1</i> _CO_3 | 3,692,437 | 2,705,871 | 81.99 |
| WT_CO_1 | 2,712,123 | 2,050,466 | 83.06 |
| WT_CO_2 | 2,499,873 | 1,716,841 | 77.42 |
| WT_CO_3 | 13,036,802 | 6,622,078 | 65.63 |
| WT_JA_2h_1 | 3,572,201 | 2,485,002 | 81.49 |
| WT_JA_2h_2 | 2,464,533 | 1,645,703 | 76.13 |
| WT_JA_2h_3 | 11,292,490 | 7,297,856 | 72.69 |
| WT_JA_24h_1 | 3,240,957 | 2,166,467 | 81.48 |
| WT_JA_24h_2 | 4,394,476 | 3,096,444 | 81.18 |
| WT_JA_24h_3 | 1,142,861 | 758,639 | 82.18 |

3.5.1 Distribution of treatment biological replicates

The aim of transcriptome analysis in tomato was to compare and identify transcripts or genes that are differentially regulated among four different treatments, WT_CO, JA_2h, JA_24h and *jai1*_CO, respectively. To achieve this, estimation of biological coefficient of variation (BCV) is highly essential, reliable and crucial to assess the biological replicates within treatment conditions. BCV represents the variation in true abundance of genes across sample biological replicates (Chen et al., 2008; McCarthy et al., 2012), which is represented on a multidimensional scaling (MDS) plot. The MDS plot realistically depicts WT control, JA-treated (JA_2h and JA_24h) and *jai1* control biological replicates allotment in the given dimensions (Fig. 15). The distribution and spacing of biological replicates at different treatment conditions, however, explains batch effects. The distant allotment of biological replicates from different treatments is due to technical variations, physiological and growth parameters of plants.

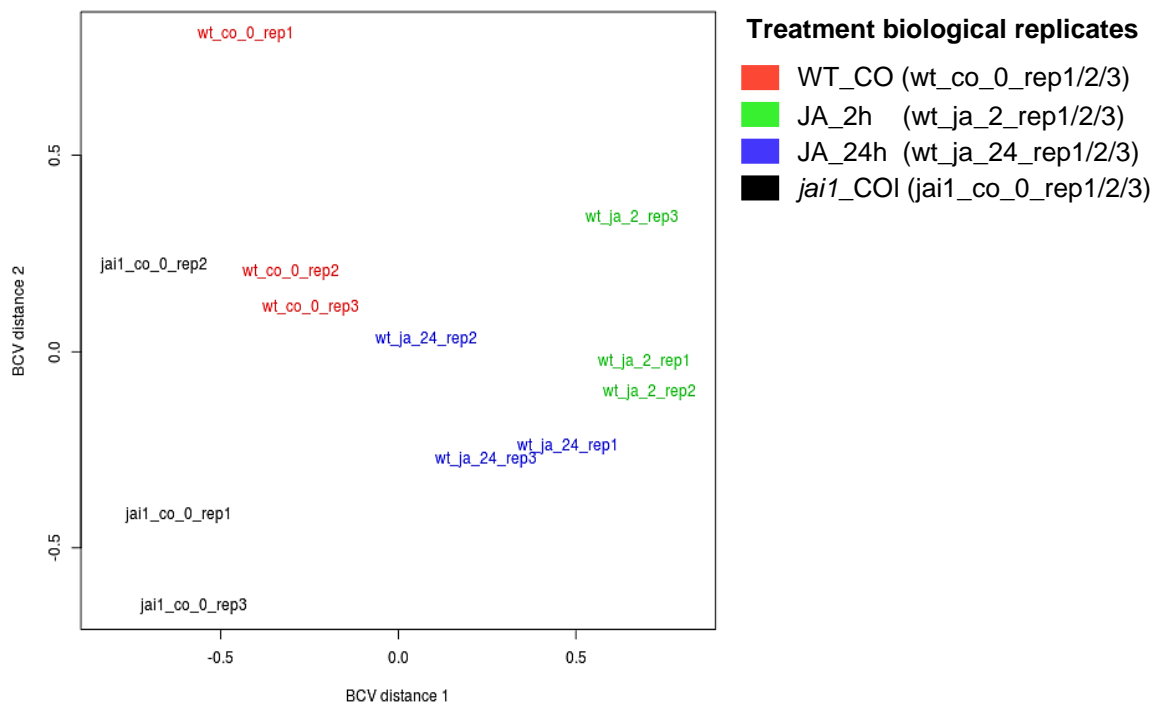


Figure 15: Treatment biological replicates on Multidimensional scaling (MDS) plot

Distribution of WT_CO, JA_2h, JA_24h and *jai1*_CO treatment biological replicates. The plot dimension BCV distance 1 (X-axis) refers to biological coefficient of variation across treatment conditions and the second dimension (Y-axis) BCV distance 2 refers to differences and distances in biological coefficient of variation in treatment biological replicates (generated by Dr. Benedikt Athmer)

3.5.2 Differentially expressed genes in between treatment comparisons

Processing and normalization of read counts are critical for differential gene expression (DGE) analysis. DGE analysis was performed by incorporating edgeR[®] package on the R platform (Chen et al., 2008). Through edgeR, using smear plot function, an entire set of mapped genes were visualized on X-Y dimensional plots (Fig. 16). Smear plots provides an overview of normalized count data (CPM) with their corresponding \log_2 fold change for each gene whether they are regulated differentially or non-differentially.

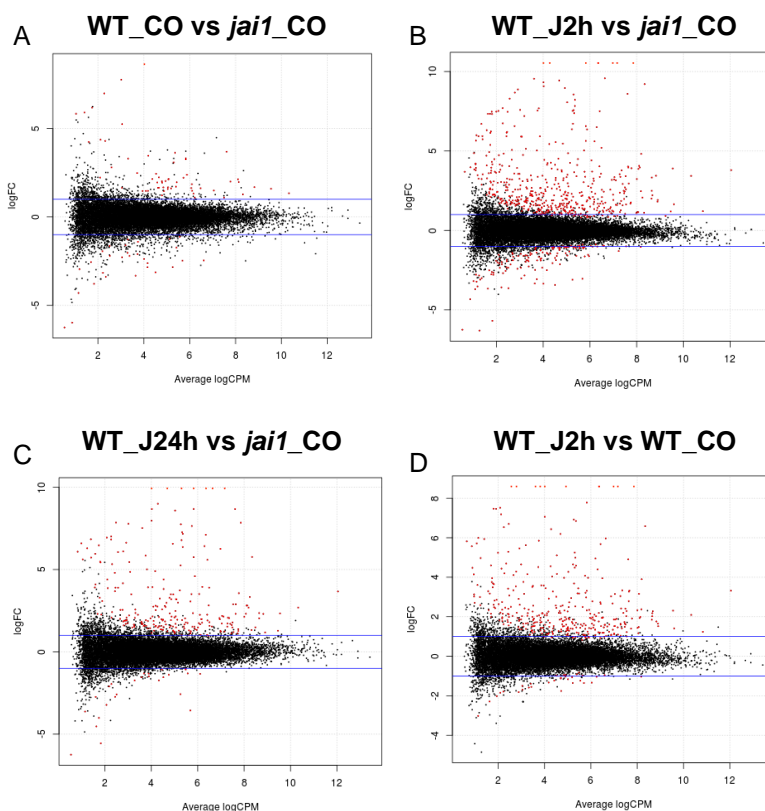


Figure 16: Representation of normalized dataset on smear plots

Differentially and non-differentially expressed genes between the treatment comparisons according to Benjamini-Hochberg correction (false discovery rate, FDR<0.05). (A) WT_CO (B) JA_2h and (C) JA_24h treatments were exclusively compared with *jai1*_CO (A-C), respectively. Further comparisons include JA_2h vs WT_CO (D). Horizontal blue lines indicate threshold \log_2 fold change (\log_2 FC). Red dots above and below threshold cut-off line indicates differentially regulated genes. Dispersion of black dots between threshold lines represents non-differentially regulated genes (generated by Dr. Benedikt Athmer).

Smear plots were based on average logarithmic count per million (logCPM) of every single gene, which is plotted against their fold change expression values (logFC). The blue lines

above and below zero signifies threshold \log_2 fold change (logFC), with an allotment of (logFC = -1 and 1) cut-off values, for genes at the FDR<0.05, p <0.001, respectively. Most differentially regulated genes significantly up and down regulated, are depicted with red and black dots above and below threshold \log_2 FC cut-offs, across treatment comparisons (Fig. 16A-D). However, a huge mass of genes between threshold \log_2 FC indicate genes that are not differentially regulated (Fig. 16A-D). Quantitative estimation of total number of genes, which are most differentially regulated across treatment comparisons are correlated with the representation of Venn diagrams (Fig. 17).

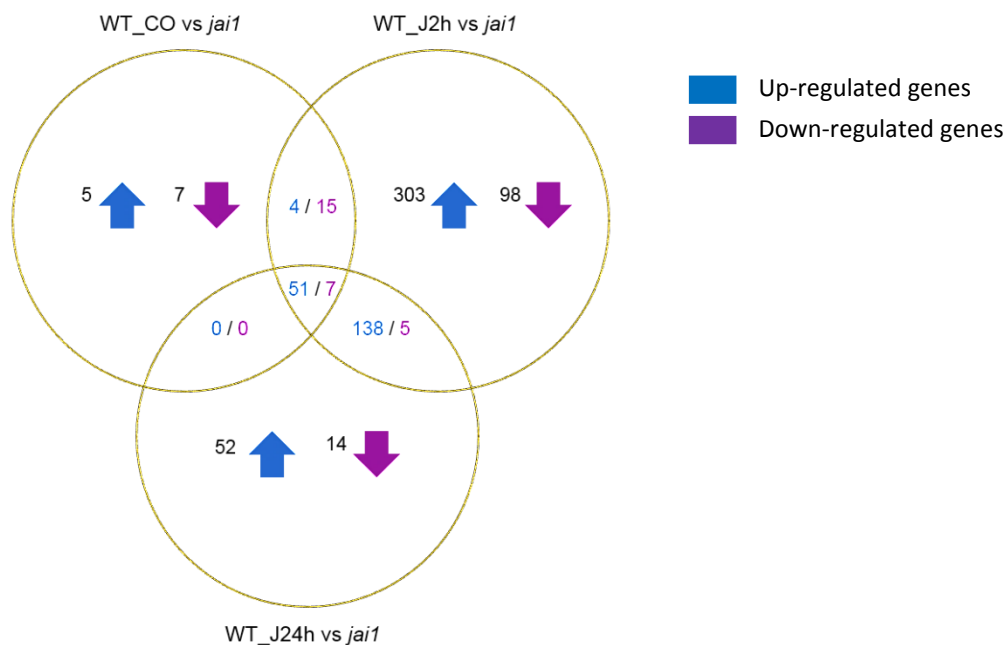


Figure 17: Representation of differentially expressed genes on Venn diagram

Differentially expressed genes across treatment conditions, Benjamin-Hochberg corrected at the FDR<0.05. Blue and violet arrows indicate genes that are up and down regulated across treatment conditions. (Differential gene expression analysis conducted by Dr. Benedikt Athmer).

In total 36,007 transcripts were expressed after mapping the reads to the tomato reference genome (Heinz). Clearly, 17,800 genes were up-regulated and 18,207 genes were down-regulated across wild type control (WT_CO), *jai1* control (*jai1*_CO) and JA treated (JA_2h and JA_24h) samples, respectively. DGE analysis confirmed about 850 genes that were significantly up-regulated across four individual treatment conditions. JA-insensitive mutant, *jai1* with significant decrease in glandular trichomes was kept as a reference for identifying differentially expressed genes between treatment conditions. Comparison of WT_CO,

RESULTS

JA_2h and JA_24h were exclusively made with *jai1_CO* samples, as represented in the Venn diagram (Fig. 17). Comparison between WT_CO and *jai1_CO* (Fig. 17) yielded a total of 89 significantly expressed genes, of which 60 genes were significantly up-regulated across the WT_CO and 29 genes across *jai1_CO* treatments (Fig. 17). Interestingly, we found that around 621 genes were highly significant and differentially regulated between JA_2h treated and *jai1_CO* samples. Among those, 496 genes were significantly up-regulated after JA_2h treatment and the remaining 125 genes were up-regulated across *jai1_CO* (Fig. 17). Lastly, comparison between JA_24h treated and *jai1_CO* resulted around 255 genes that were differentially regulated, of which 229 genes were significantly up-regulated after JA_24h treatment and only 26 of them were significantly upregulated across *jai1_CO* samples (Fig. 17). The genes that are significantly upregulated across the aforementioned treatment comparisons are also correlated with the smear plots (Fig. 16). Subsequently, comparisons were made between JA_2h vs WT_CO, JA_24h vs WT_CO as well as JA_2h vs JA_24h treatment conditions (Fig. A3, Appendices).

3.5.3 Functional enrichment analysis of differentially expressed genes between treatments

Functional enrichment analysis of DEG's is essential for further downstream experimental analysis and drawing the hypothesis. To perform the functional enrichment analysis of DEG's from different sample treatments, a multi-platform fast and efficient user-friendly graphical interface called PAGEMAN[®] (Usadel et al., 2006) was adopted.

With the use of a mapping file generated for DEG's from four different treatments, genes that are significantly up and down regulated between JA-treated (JA_2h) (Table 14) and *jai1_CO* (Table 15) samples were compared with different gene ontology (GO) platforms. Further, DEG's were scrutinized with Fisher's exact statistical test for over and under representation (ORA) and allotted to respective BINs for their functionality (Table 14, 15). The elements in the PAGEMAN[®] functional analysis correspond to number of candidates which fall into particular functional BIN. For example in Table 14 under 'Cell wall synthesis' - cellulose synthesis, 11 elements were identified, which are over-represented in JA_2h samples compared to the *jai1_CO*. The over-representation of elements in JA_2h samples were apparently not expressed in the *jai1_CO* condition (Table 15). However, with the PAGEMAN[®] analysis, more gene elements were over-represented under different gene categories (Table 14). Most gene elements were identified in the gene categories: cell wall synthesis, secondary metabolism, hormone metabolism, UDP glucosyl transferases and

protein degradation, respectively (Table 14). By contrary, over-representation of gene elements across *jai1_CO* mainly corresponded to protein degradation function (Table 15). Further, all the gene elements corresponding to their gene categories have shown a significant \log_2 fold change in JA_2h and *jai1_CO* treatment conditions (Table 14 and 15).

Table 14: PAGEMAN functional enrichment analysis between JA_2h and *jai1_CO*

Significant over-representation of genes in JA_2h compared to *jai1_CO* treatment conditions Data points in each BIN which exceeded the value of 1.0 were tested for over representation using Fisher's exact test. The p-values were adjusted according to Benjamini-Hochberg correction (FDR <0.05).

| Bin code | Gene Category | Elements | Log2 FC |
|----------|---|----------|-----------|
| 10.2 | Cell wall. cellulose synthesis | 11 | 2.0469947 |
| 10.2.1 | Cell wall. Cellulose synthesis. cellulose synthase | 19 | 3.082369 |
| 11.8 | Lipid metabolism. 'Exotics' (steroids, squalene etc.) | 23 | 2.260566 |
| 16 | Secondary metabolism | 1 | 8.996315 |
| 16.1 | Secondary metabolism. Isoprenoids | 14 | 3.4146688 |
| 16.1.2 | Secondary metabolism. Isoprenoids. mevalonate pathway | 1 | 2.8141317 |
| 16.1.5 | Secondary metabolism. Isoprenoids. terpenoids | 40 | 2.5737693 |
| 16.2 | Secondary metabolism. Phenylpropanoids | 38 | 6.879835 |
| 16.7 | Secondary metabolism. Wax | 25 | 2.0891528 |
| 16.8 | Secondary metabolism. Flavonoids | 20 | 2.9557612 |
| 17 | Hormone metabolism | 4 | 3.7853312 |
| 17.2.1 | Hormone metabolism. Auxin. synthesis -degradation | 15 | 2.05578 |
| 17.3 | Hormone metabolism. Brassinosteroid | 1 | 3.4733658 |
| 17.3.1 | Hormone metabolism. Brassinosteroid synthesis-degradation | 21 | 3.9437618 |
| 17.3.1.2 | Hormone metabolism. Brassinosteroid synthesis-degradation. sterols | 17 | 3.7683117 |
| 17.7 | Hormone metabolism. Jasmonate | 1 | 4.584445 |
| 17.7.1 | Hormone metabolism. Jasmonate. synthesis-degradation | 30 | 2.7069879 |
| 17.7.1.3 | Hormone metabolism. Jasmonate.synthesis-degradation.allene oxidase synthase | 1 | 2.6850462 |
| 17.7.2 | Hormone metabolism. Jasmonate.signal transduction | 7 | 3.8305435 |
| 20.1.3 | Stress. Biotic.signalling | 5 | 2.5737693 |
| 22 | Polyamine metabolism | 1 | 2.0891528 |
| 22.1 | Polyamine metabolism. synthesis | 1 | 2.1813207 |
| 26 | Misc. | 1 | 7.2282376 |
| 26.2 | Misc.UDP glucosyl and glucoronyl transferases | 166 | 5.470038 |
| 26.1 | Misc.cytochrome P450 | 27 | 2.778395 |
| 26.28 | Misc.GDSL-motif lipase | 58 | 2.5329518 |
| 29.5.3 | Protein.degradation. cysteine protease | 45 | 2.1813207 |
| 34.13 | Transport.peptides and oligopeptides | 67 | 2.7407417 |

RESULTS

Table 15: PAGEMAN functional enrichment analysis between *jai1_CO* and JA_2h

Significant over-representation of genes in *jai1_CO* compared to JA_2h treatment conditions. Data points in each Bin which exceeded the value of 1.0 were tested for over representation using Fisher’s exact test. The p-values were adjusted according to Benjamini-Hochberg correction (FDR <0.05).

| Bin code | Gene Category | Elements | Log2 FC |
|----------|-------------------------------|----------|------------|
| 29 | Protein | 1 | -3.9437618 |
| 29.2 | Protein.synthesis | 2 | -3.7853312 |
| 29.5.11 | Protein.degradation.ubiquitin | 45 | -2.8225207 |

3.5.4 Functional annotation putative transcription factors

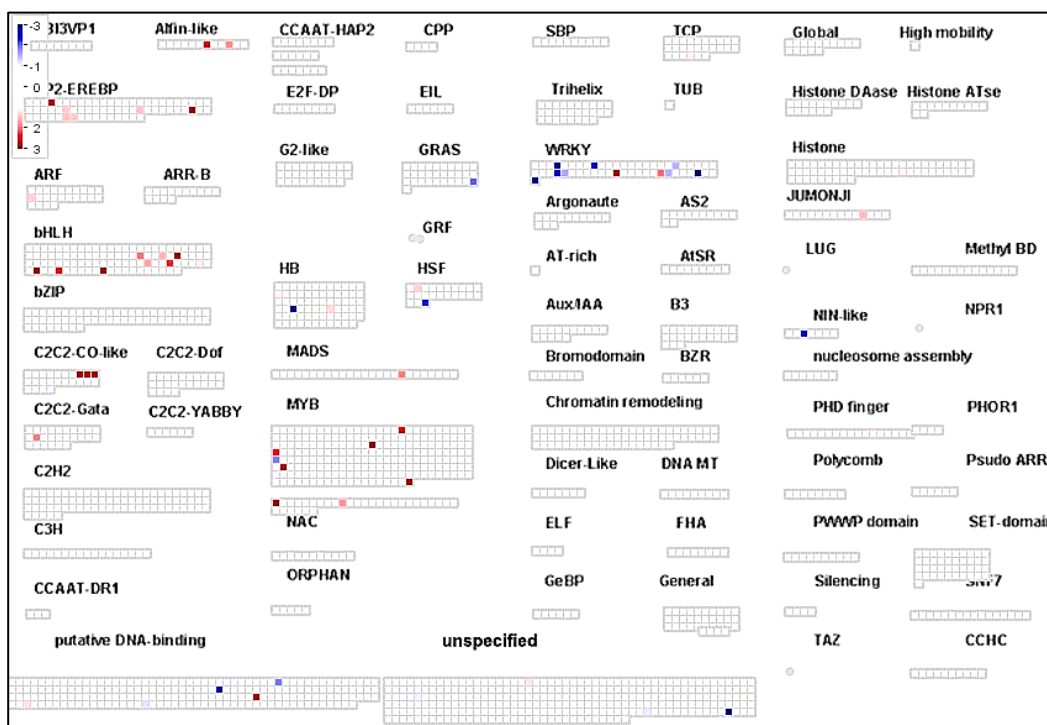


Figure 18: MAPMAN functional annotation significant transcription factors

Most significantly up and down regulated (Benjamini-Hochberg corrected, FDR<0.05) transcription factors in JA-treated (JA_2h) vs *jai1* mutant (*jai1_CO*) conditions. Color code scale: red and blue bars on scale indicate high and low scores or expression levels of genes according to log₂ scale transformation, across both treatment comparisons, respectively.

Differentially expressed genes through Mercator pipeline were assigned to functional categories called as ‘BINS’ in the MAPMAN® ontology suite (Thimm et al., 2004 and Lohse et al.,2014). An important feature of Mercator tool is to search unknown sequences against

known reference databases including blast-based and protein domain searches (Lohse et al., 2014). To substantiate further, sequences with significant similarities to reference proteins or domains were assigned to MAPMAN BIN (Lohse et al., 2014). The identification of significantly regulated transcription factors within the treatment conditions, JA_2h and *jai1_CO* were majorly annotated to the classes of Myb, bHLH, WRKY and AP2/ERE BP transcription factor families, and few were identified as putative DNA-binding factors (Fig. 18).

3.5.5 Clustering of differentially expressed genes

Clustering of normalized data from RNA-seq analysis was performed by incorporating edgeR[®] package in R program. Clustering of normalized count data such as fragment per kilobase million (FPKM), read per kilobase million (RPKM) or transcripts per million (TPM), is an added advantage to elucidate novel molecular players or networks by comparing two library groups or treatment conditions. Two factors are important prior to clustering: \log_2 transformation, which helps the expression values attain closer to normal distribution and convenient for statistical tests and secondly, scaling the expression values by Z-transformation. Here, scaling refers to scale the rows by calculating Z-scores within genes but across the samples. This actually clarifies the hypothesis for genes expressed across different treatment conditions and weighs equally when clustering. Therefore, Z-transformed expression values (Row-Z-Score, Fig. 19) for each gene was used to generate heatmaps.

Since our objective was to identify potential transcription factors which were in low-abundance with significant expression levels, DGE analysis paved the way to identify considerable number of transcription factors (Fig. 19). To substantiate this claim, clustering yielded most highly variant and significantly expressed differentially regulated genes across four treatment conditions, depicted on the heat maps (Fig. A4, Appendices). However, significantly expressed transcription factors (FDR<0.05) across four treatment conditions were aligned based on their Z-transformed scores (Fig. 18), indicated by color key intensity based on the gene expression level. For functional annotation, these significantly expressed transcription factors were performed with a homology search against plant transcription factor reference database (Jin et al., 2017).

RESULTS

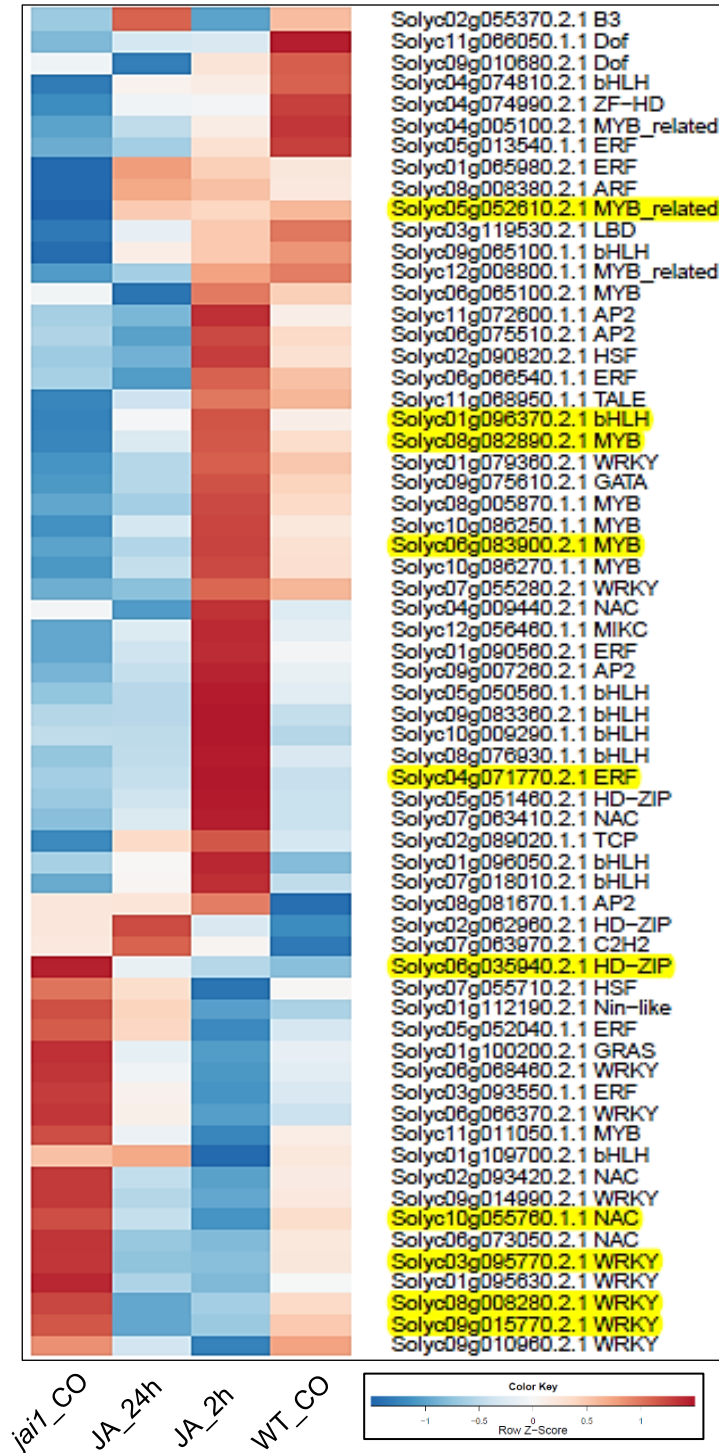


Figure 19: Clustering of transcription factors on the heatmap

Cluster depicting list of transcription factors that were differentially regulated across treatment conditions with p-values adjusted to Benjamini-Hochberg correction (FDR<0.05). Color key represents Row-Z-Score for each transcription factor that has been scaled and transformed to each treatment condition. Red indicates high expression (log2FC = 1) and

blue indicates low expression ($\log_2FC = -1$) for each candidate across particular treatment condition, respectively. Transcription factors highlighted in yellow were chosen for validation analysis (generated by Dr. Benedikt Athmer).

3.6 Validation and selection of putative candidates

Table 16: List of putative transcription factors upregulated shortly after JA treatment (JA_2h) compared to *jai1* mutant (*jai1_CO*).

The p-values were adjusted according to Benjamini-Hochberg correction (FDR<0.05).

| Gene ID | Annotations | Log ₂ FC – RNA-Seq | p-values | Log ₂ FC – qRT-PCR |
|--|---|-------------------------------|------------|-------------------------------|
| Transcription factors | | | | |
| <i>Solyc05g052610.2.1</i> | MYB transcription factor (<i>DIVARICATA</i>) | 6.74 | 8.79E-08 | 0.62 |
| <i>Solyc06g083900.2.1</i> | Myb-related transcription factor (<i>MYB4</i>) | 6.36 | 5.43E-35 | 16.97 |
| <i>Solyc08g005870.1.1</i> | MYB transcription factor (<i>MYB308</i>) | 4.16 | 6.85E-05 | 3.65 |
| <i>Solyc08g082890.2.1</i> | MYB transcription factor (<i>MYB9</i>) | 4.75 | 6.50E-11 | 5.74 |
| <i>Solyc01g096370.2.1</i> | BHLH transcription factor Helix-loop-helix DNA-binding (<i>MYC2</i>) | 5.03 | 3.63E-20 | 1.22 |
| <i>Solyc04g071770.2.1</i> | Ethylene responsive transcription factor 2a Pathogenesis-related, DNA-binding (<i>ERF2a</i>) | 2.93 | 7.16E-18 | 2.52 |
| <i>Solyc04g076720.1.1</i> | WD-repeat domain phosphoinositide-interacting protein 3 .WD40 repeat-like (<i>WD-40</i>) | 5.65 | 0.00492751 | 0.90 |
| <i>Solyc08g076930.1.1</i> | Transcription factor IPR011598 - Helix-loop-helix DNA-binding (<i>TF</i>) | 2.31 | 1.63E-15 | 3.1 |
| JA-induced genes (Reference validation) | | | | |
| <i>Solyc02g085730.2.1</i> | Allene oxide cyclase IPR009410 - Allene oxide cyclase (<i>AOC</i>) | 11.58 | 129.98 | 1.25E-18 |
| <i>Solyc00g187050.2.1</i> | Leucyl aminopeptidase IPR011356 - Peptidase M17, Leucyl aminopeptidase (<i>LAP A</i>) | 9.81 | 4.26 | 6.43E-16 |
| <i>Solyc09g089510.2.1</i> | Proteinase inhibitor I IPR000864 - Proteinase inhibitor I13, potato inhibitor I (<i>PIN1</i>) | 3.53 | 945.01 | 2.09E-15 |

RESULTS

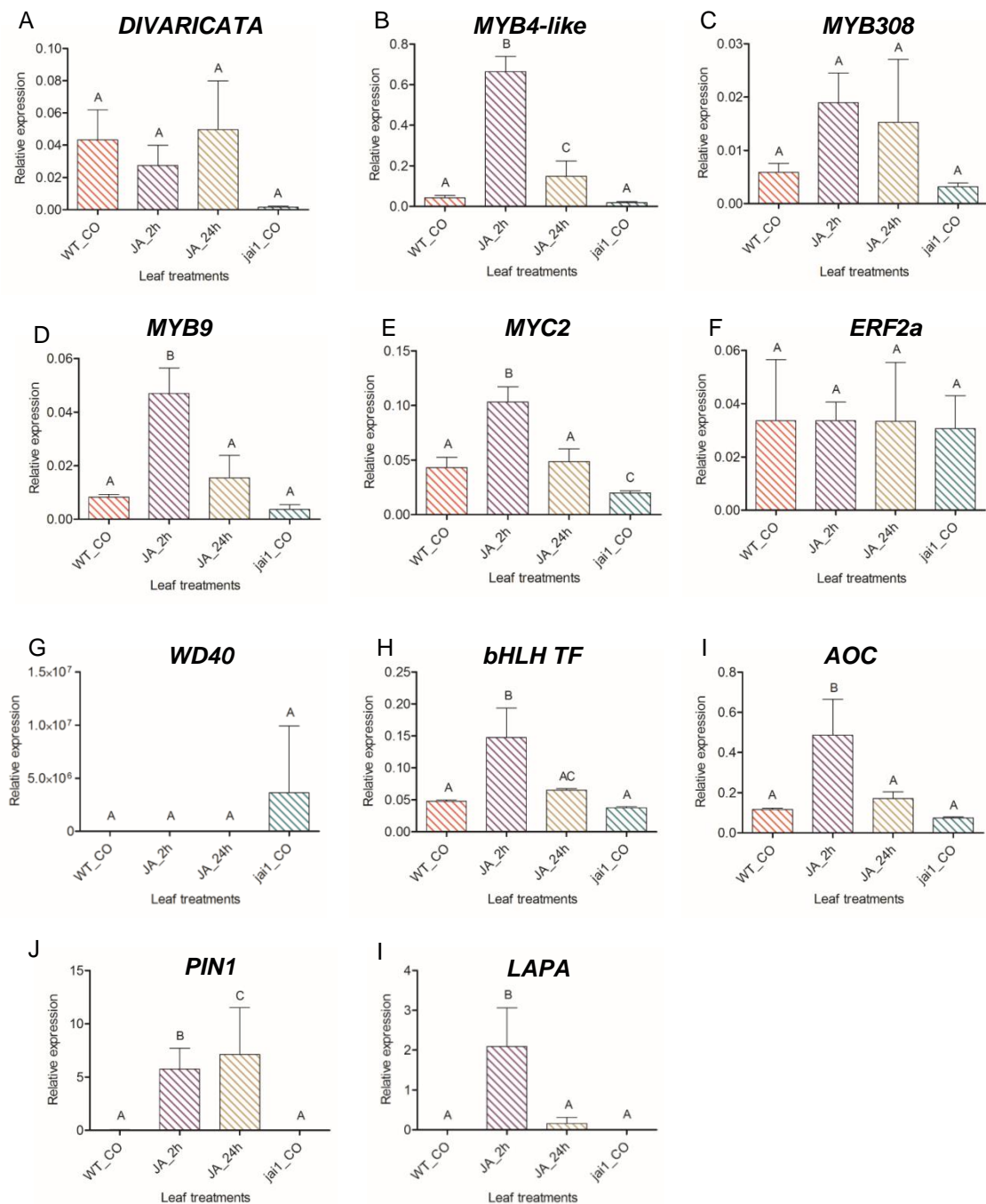


Figure 20: Transcript accumulation of putative transcription factors up-regulated after JA_{2h} treatment

Relative expression levels of transcription factors (A-F, G & K) and JA-regulated genes (H-J) estimated with reference to *S. lycopersicum* *ELONGATION FACTOR (EF)* house-keeping gene. Error bars indicate mean values \pm SD (n=3), statistical significance was determined by ANOVA with a post hoc test (Newman-Keuls multiple comparison test). Genes encoding putative TF's abbreviated as (A-D) MYB TFs (*DIVARICATA*, *MYB4-like*, *MYB308* and *MYB9*), Ethylene responsive factor (F) (*ERF2a*), (E, H) bHLH TF's (*MYC2*

and *bHLH* unknown TF) and (G) Phosphoinositide-interacting protein (WD-40) and (I-K) JA regulated genes abbreviated according to Fig. 13, respectively. Treatment conditions were described according to Fig. 12.

Seven transcription factors and three JA-regulated genes were selected for estimating their transcript levels across treatment conditions. According to the statistical hypothesis, putative transcription factors in the MYB, bHLH, ERF, WD-40 and Helix-loop-helix families were selected based on the criteria, p -value <0.05 and respective \log_2 fold changes (Table 16). According to the RNA-seq expression data, all putative transcription factors and corresponding JA-regulated genes were significantly up-regulated after JA_2h (Table 16, Fig. A4, Appendices) and severely down-regulated in the *jai1_CO* after clustering (Fig. 19).

Validation of transcription factors led to the identification of transcript accumulation patterns across WT_CO, JA_2h, JA_24h and *jai1_CO* treatment conditions. The significance level and the fold changes of transcription factors were higher in the RNA-seq data (Table 16). The transcript levels of putative *DIVARICATA*, *MYB308*, *ERF2a* and *WD-40* (Fig. 20A, C, F and G) showed variations in transcript accumulation and were not significant across different treatment conditions. Their significance level could not be correlated with the RNA-seq data. Other putative transcription factors like, *MYB4-like*, *MYB9*, *MYC2* and unknown helix-loop-helix transcription factor (*TF*) were significantly up-regulated after JA_2h treatment compared to *jai1_CO* (Fig. 20B, D, E and K), hence, validated according to RNA-seq data. However, the relative expression of co-related transcription factors showed no significant transcript accumulation between WT control and *jai1* mutant (Fig. 20 - B, D, E and H). As a reference, transcript levels of JA induced genes were validated and correlated with the RNA-seq data (Fig. 20I-K).

3.6.1 Putative transcription factors up-regulated in the *jai1* mutant compared to JA_2h treatment

As declared in the thesis objectives and possible hypothesis, putative transcription factors showing negative responses to JA treatment were also selected. According to the RNA-seq data, putative transcription factors were found to be significantly up-regulated in the *jai1_CO* compared to JA_2h treatment (Table 17). The allocation of Z-transformation scores after data normalization and transformation has led to depict \log_2 FC values in a negative manner, which is correlated with clustering analysis (Row Z score color key, Fig. 19).

RESULTS

Table 17: Putative transcription factors upregulated in *jai1_CO* compared to JA_2h treatment

The p-values were adjusted to Benjamini-Hochberg correction (FDR<0.05).

| Gene ID | Annotations | Log ₂ FC – RNAseq | p-values | Log ₂ FC – qRT-PCR |
|----------------------------------|--|------------------------------|------------|-------------------------------|
| Transcription factors | | | | |
| <i>Solyc06g035940.2.1</i> | Homeobox-leucine zipper protein PROTODERMAL FACTOR 2 IPR002913 - Lipid-binding START (<i>PDF2</i>) | -3.04 | 2.67E-15 | 12.67 |
| <i>Solyc10g055760.1.1</i> | NAC domain protein IPR003441 - No apical meristem (NAM) protein (<i>NAC</i>) | -3.63 | 5.37E-07 | 2.85 |
| <i>Solyc09g015770.2.1</i> | WRKY transcription factor 6 IPR003657- DNA-binding WRKY (<i>WRKY6</i>) | -3.42 | 5.38E-05 | 1.64 |
| <i>Solyc09g014990.2.1</i> | WRKY-like transcription factor IPR003657 - DNA-binding WRKY (<i>WRKY-like</i>) | -3.35 | 3.90E-06 | 7.03 |
| <i>Solyc08g008280.2.1</i> | WRKY transcription factor-30 IPR003657 - DNA-binding WRKY (<i>WRKY30</i>) | -2.50 | 0.00142220 | 2.98 |

Putative *PROTODERMAL FACTOR 2 (PDF2)* encodes a homeo-box leucine zipper protein (HD-Zip), has shown approximately 5-fold expression in *jai1_CO* compared to JA_2h treatment conditions (Fig. 21A). The relative expression of putative *PDF2* correlates with the RNA-seq expression profile (Table 17). Another putative *NAC* domain transcription factor, which encodes for NO APICAL MERISTEM (NAM) protein, has significantly up-regulated in the *jai1_CO* compared to the WT_CO (Fig. 21B). Concurrently, putative *PDF2* and *NACD* TFs showed no significant transcript accumulation between JA_2h and JA_24h treatment conditions (Fig. 21A-B). A group of *WRKY* TFs, particularly showing significant up-regulation in the *jai1_CO* were also selected for validation (Table 17). Transcript levels of putative *WRKY* TFs in WT_CO, JA_2h and JA_24h treatments compared to *jai1_CO* showed variations (Fig. 21C-E). For instance, putative *WRKY6* shows equal transcript levels in *jai1_CO* and WT_CO, low transcript levels in JA_2h and high transcript levels in JA_24h treatment conditions (Fig. 21C). A similar transcript accumulation trend was also observed for *WRKY-like* TF (Fig. 21D). Lastly, transcript levels of putative *WRKY30* were found to be equal across all four treatments (Fig. 21E). Among the putative *WRKY*'s, none of them showed significant transcript accumulation during JA treatment conditions

compared to *jai1_CO* treatment, therefore putative *PDF2* was found to be promising for further characterization.

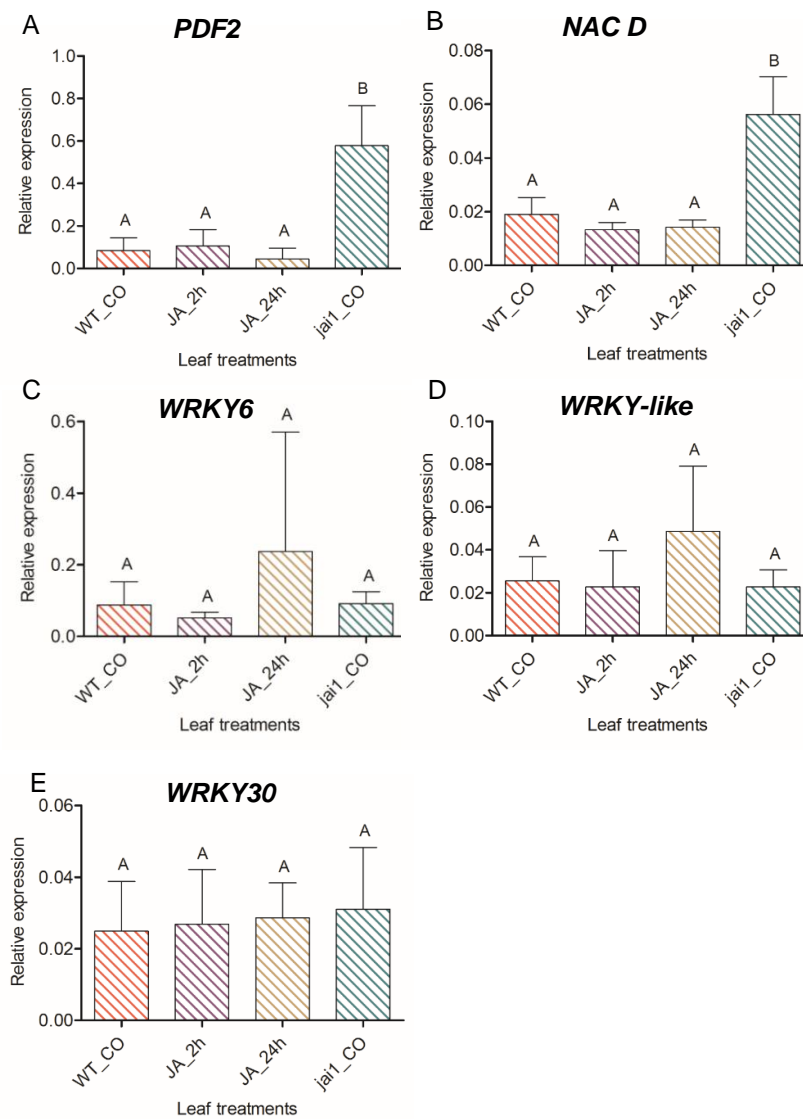


Figure 21: Transcript accumulation of putative transcription factors up-regulated in the *jai1_CO*

Relative expression levels of transcription factors (A-E) estimated with reference to *S. lycopersicum* *ELONGATION FACTOR (EF)* house-keeping gene. Error bars indicate mean values \pm SD ($n = 3$), statistical significance was determined by ANOVA with a post hoc test (Newman-Keuls multiple comparison test). Genes encoding putative transcription factors were abbreviated as *PROTODERMAL FACTOR 2 (PDF2)*, *NO APICAL MERISTEM (NAC D)* protein and WRKY TF's (*WRKY6*, *WRKY-like* and *WRKY30*). Treatment conditions were described according to Fig.12.

3.6.2 Putative JA-regulated genes up-regulated in the JA_2h treatment

Besides validating a set of significantly expressed transcription factors (Table 16, 17), putative genes explicitly up-regulated after JA treatment (JA_2h and JA_24h) were also considered for validation. Putative JA responsive candidates were up-regulated shortly after JA treatment and showed a higher \log_2 fold change values both in RNA-seq expression profile and qRT-PCR validation (Table 18, Fig. 22).

Table 18: List of putative candidates selected for validation up-regulated after JA_2h treatment

The p-values were adjusted to Benjamini-Hochberg correction (FDR<0.05).

| Gene ID | Annotations | Log ₂ FC – RNAseq | p-value*** | Log ₂ FC – qRT-PCR |
|----------------------------------|--|------------------------------|------------|-------------------------------|
| JA-regulated genes | | | | |
| <i>Solyc09g005770.1.1</i> | F-box family protein IPR001810 - Cyclin-like F-box | 7.58 | 9.55E-10 | 4.16 |
| <i>Solyc03g098780.1.1</i> | Kunitz-type protease inhibitor IPR002160 - Proteinase inhibitor I3, Kunitz legume | 8.6 | 1.04E-19 | 10.45 |
| <i>Solyc03g098720.2.1</i> | Kunitz trypsin inhibitor IPR011065 - Kunitz inhibitor ST1-like | 10.15 | 7.24E-12 | 28.34 |
| <i>Solyc07g008570.2.1</i> | Purple acid phosphatase IPR008963 - Purple acid phosphatase-like, N-terminal | 5.46 | 3.05E-19 | 347.24 |
| <i>Solyc07g007250.2.1</i> | Metallo-carboxypeptidase inhibitor IPR004231 - Proteinase inhibitor I37, carboxypeptidase A | 9.43 | 1.58E-15 | 3.09 |
| <i>Solyc01g006390.2.1</i> | Cysteine-rich extensin-like protein-4 | 4.13 | 1.36E-07 | 46.42 |

Putative, *cyclin-like* F-box protein transcript levels were too low (Fig. 22A), and the transcript accumulation pattern across four treatment conditions were almost similar due to varying standard deviations. Expression of *Kunitz-type protease inhibitor* and *Metallo-carboxypeptidase*, a group of plant protease inhibitors (PIs) (Habib and Khalid, 2007), were up-regulated after JA treatment (JA_2h and JA_24h, Fig. 22 B & E). These inhibitors were found to be down-regulated in the WT_CO and *jai1*_CO conditions (Fig. 22B & E), however, only *Kunitz-type* PI showed significant transcript accumulation after JA_2h and JA_24h treatments (Fig. 22 B). Transcript accumulation of both, putative *Kunitz-Trypsin* and *Purple Acid Phosphatase*, were significantly higher after JA_2h treatment compared to WT_CO, JA_24h and *jai1*_CO treatment conditions whereas, a gradual decrease in

transcript levels was observed after JA_24h treatment (Fig. 22C-D). For the last candidate, putative *Cysteine-rich extensin-like* was found to be upregulated after JA_2h and JA_24h treatments, showing significant transcript levels after JA_2h treatment compared to WT_CO and *jai1*_CO treatment conditions (Fig. 22F).

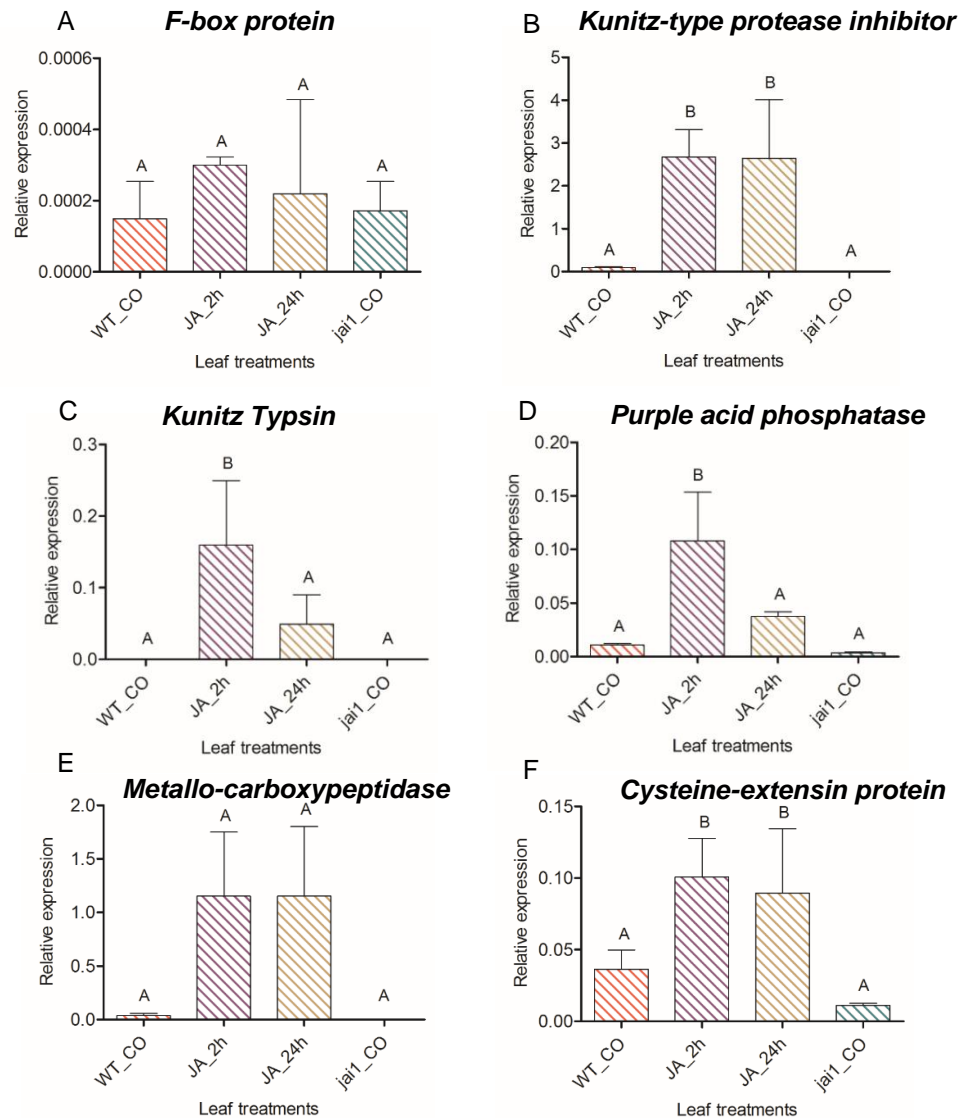


Figure 22: Transcript accumulation of putative JA-regulated genes

Relative expression levels of putative JA-regulated genes up-regulated after JA treatment (A-F) were estimated with reference to *S. lycopersicum* *ELONGATION FACTOR (EF)* house-keeping gene. Error bars indicate mean values \pm SD (n = 3), statistical significance was determined by ANOVA with a post hoc test (Newman-Keuls multiple comparison test). Treatment conditions were described according to Fig.12.

RESULTS

As per the validation data obtained for putative transcription factors, *MYB4-like*, *MYB9*, *MYC2* and *bHLH TF* were significantly up-regulated shortly after JA-treatment (JA_2h) compared to the *jai1* mutant (*jai1_CO*) (Fig. 20). By contrary, putative *PDF2* and *NACD* transcription factors showed significant up-regulation in the *jai1* mutant (*jai1_CO*) compared to JA-treated samples (JA_2h) (Fig. 20). These validated transcription factors were positively correlated with the fold change expression values of RNA-seq data (Table 16, 17). Based on validation and significant correlation, putative *MYB4-like*, *MYB9*, *MYC2* and *PDF2* were further selected for their functional characterization.

3.7 Functional characterization of selected putative transcription factors

Protein sequences of putative candidates were analyzed on PROSITE database tool. Each putative protein, encoded by transcription factors comprises DNA-binding domain, which is crucial for regulating downstream genes, which are predicted to be involved in the formation of type VI glandular trichomes.

A MYB9



```
MGRAPCCAKEGLRKGPWSTKEDLLLTNYINQYGEGQWRSLPKNAGLLRCGKSCRLRWVNY  
LKPGIKRGNFSEDEEDLIVRLHSLGNRWSLIAGRLPGRTDNEIKNYWNTHLTKKLRSTG  
IEPKPHKNLTKLKEKSRKQTKKEKSRKEVGKKSNDKLGQIAQVEKIKVFAPKPIRISC  
GISRNNSFENDTLSTTTCSSNSNFEEKVDDGKDREKEVKLFPRELDDELLEGGGFYDEFL  
MGESC�FSNKVEMNDNMVEKVYEEYLLLLSEIQEDQTEQKFSM
```

B MYB4-like



MGRSPCCEKLGLKRGWPWSKEEDYLLINYIKKNGHPNWRALPKLAGLLRCGKSCRLRWNTNY
LRPDIKRGNFTHQEEDTIIKHLQVLGNSWSAIAARLPGRTDNEIKNIWHTRLLKKKRNESQ
LKETQSEPENTNVDVHLEEANNSNDKHSEISNLKINIEIQQQPSPSSSVSSSESDSCSNT
TATSSESRNQIMSDNLEIDDDIWSEVVWAQVDDNYVDLSLMEDNYHINSSFDDNWFWD
LFTRSNEMLLELPEL

C MYC2



MEQLAVSSSPMAVAPPVVDVNVQVPLGLQQLQYVVKSQPEWWAYAIFWQTSNDDEGKNFL
AWGDGYFQGDGVVINNKGSSSSSLKSQAQSERKKVIKGIQALMDGNGDIDLVDGDVDT
DTEWFYVMSLARSFSAGDGSVTGKAFGSDDFLWITGPDQFQLHYSERAKEAQIHGIQTL
VSIPTSNQVFEFGSTQLIKQNLQVQVKSFLFCCPPIQFLEKTI SFADIGLVTGLQDD
NDYKLRNSRKPFPVAVAKRGRKPKGGEEDAHMAALNHVEAERQRREKLNHRFYALRSVV
PNVSRMDKASLLSDAVSYINQLKAKVDELELQLIDHTKKPKIVTESSADNQSATTSSDD
QVIKAANPTAAPEVEVKIVGTDAMIRVQSENVDYPSAKLMIALQNLQMQVHHASISSVNH
LVLHDVVVRVPQGLSTEDLRTALLTSYDL

D PDF2



MEKSTMELSNNRDGGVSGDELTSPLDGSSERRHKFSVNQIHELESVFKVSSHDPDEKTKQEL
ATKFSVDKKQVQFWFQNKRSISKTSERYNKRVLQQENEKLRTYEAAMREVMKKSICDPC
RNKDTTIRNENVDEKEILNEHARLKDELARIAIHADKSLGSSSFLEGLTSMMEKFGLEL
NEVDFGKYLSSPLPTNLDVTLDKSMLNLALDALNELLLKAMSDEPLWVRNLDGGGEMLN
MEEYATTFIPIIGIKPSHFTTEATRSSGTVVGNLTLVEMLMNESQWVEAFPCIIGKVNT
FDVISTGIGEGKSGTLLIEAELQIISNVVPVREIKFLRFCQKHAEDSWIIVDVSVDTIK
EGSQQYKIEKCRRLPSGCI IQDMSNGYSKVTWIEHMEYDEIFVDHLYRPLIRAGLGFQAQ
RWMSSLQRQSELLRVMASFVNSTVDPKGEIGMGI LSQRMTRSFCAVICATSHKWITIQKE
NGKDANLMMRRNISDAGEPIGVILSATKTIQLPIKSQCLFQFFTNKNLRRQWDILSCSGA
MENI IHINKDENLESSVSLLCANGGANENMMIFQDTCTDATGSLLVYAIVDSSKMNTVM
KGGDPSCVELLPNGISILPDL SANNKEFGSGSLVTIMFQMLVDNISTADLPQKSIVDAN
DIISHTIHKIKSALLI

Figure 23: Protein sequences of selected candidates

DNA-binding domains of (A) MYB9, (B) MYB4-like, (C) MYC2 and (D) PDF2 transcription factors are highlighted in red. Protein domains were identified and generated using PROSITE protein database tool.

RESULTS

3.7.1 Localization studies in *N. benthamiana* protoplasts

Nicotiana benthamiana is a well-known plant model to conduct transient assays in plant molecular biology (Yang et al., 2000). One of the important purposes of candidate gene profiling is to determine the area of localization of the selected putative transcription factors. To achieve this, coding sequences (CDS) of selected putative transcription factors were cloned according to Golden Gate cloning technique, using cloning modules kindly provided by Dr. Sylvestre Marillonnet, IPB, Halle.

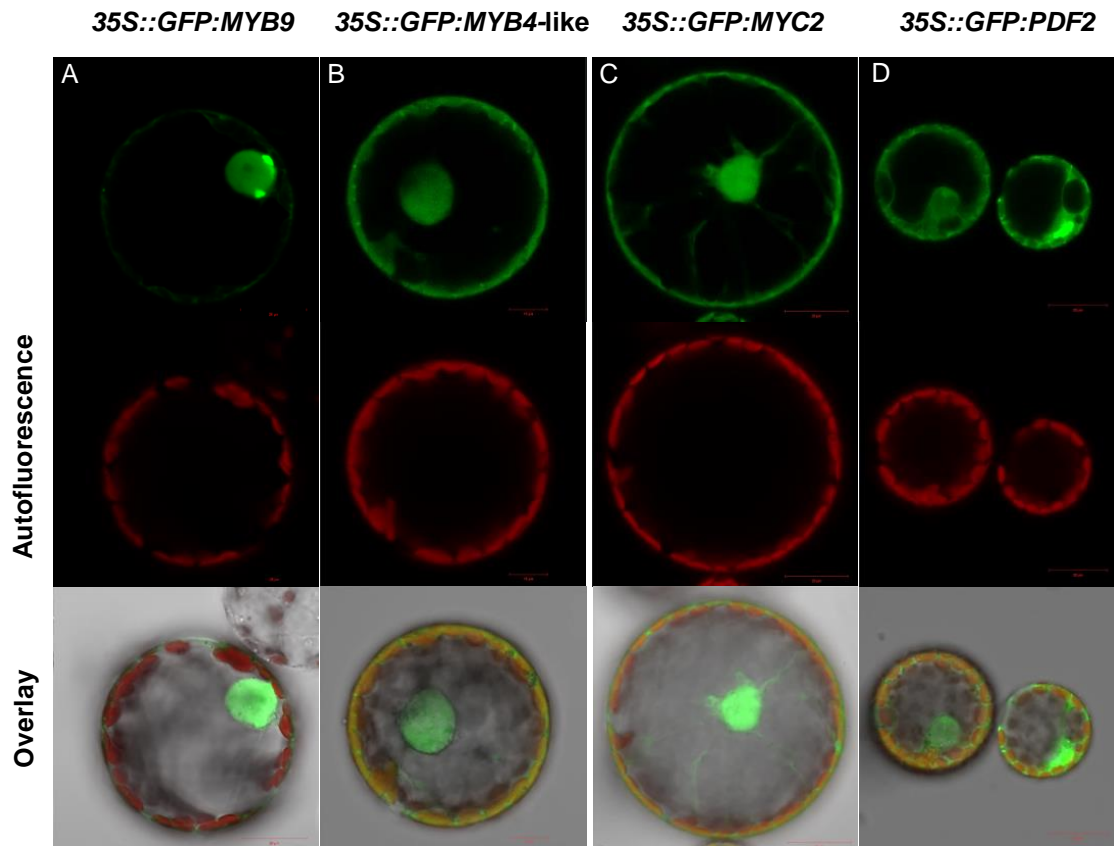


Figure 24: Localization of putative candidates in *N. benthamiana* protoplasts

Localization of putative (A) *MYB9*, (B) *MYB4-like*, (C) *MYC2* and (D) *PDF2* tagged to GFP reporter under the control 35S CaMV promoter, respectively. All protoplasts expressing putative TFs were visualized between 480-550 nm using laser scanning microscope (LSM).

To elucidate putative TFs intracellular localization, GFP reporter was fused to the N-terminus of putative transcription factor coding sequence, driven under the guidance of 35S CaMV promoter. For transient expression, 4 to 5-week-old, developed leaves were considered for Agro-infiltration. The first attempts of Agro-infiltration through leaves led to

unclear localization. For clarity and specificity, mesophyll protoplasts from young *N. benthamiana* leaves with the same age was used. All selected putative transcription factors were localized at the nucleus as predicted (Fig. 23). Interestingly, putative TFs such as *MYB4-like*, *MYC2* and *PDF2* were also found to be strongly localized at the cytoplasm (Fig. 23B-D).

3.7.2 Protein detection on the western blot from transiently transformed protoplasts

To confirm the respective sizes of putative proteins, aliquots of transformed protoplasts from transient expression assay were further used to detect proteins on the SDS-PAGE (Fig. 25). The sizes of putative proteins were detected with the help of anti-GFP antibody (Fig. 25). For reproducibility, two lanes or aliquots from each putative candidate were considered. As a positive control, GFP localized to plastids in tobacco (FNR: GFP) was compared between the putative candidate proteins (Fig. 25), which confirms the selected protein of interest.

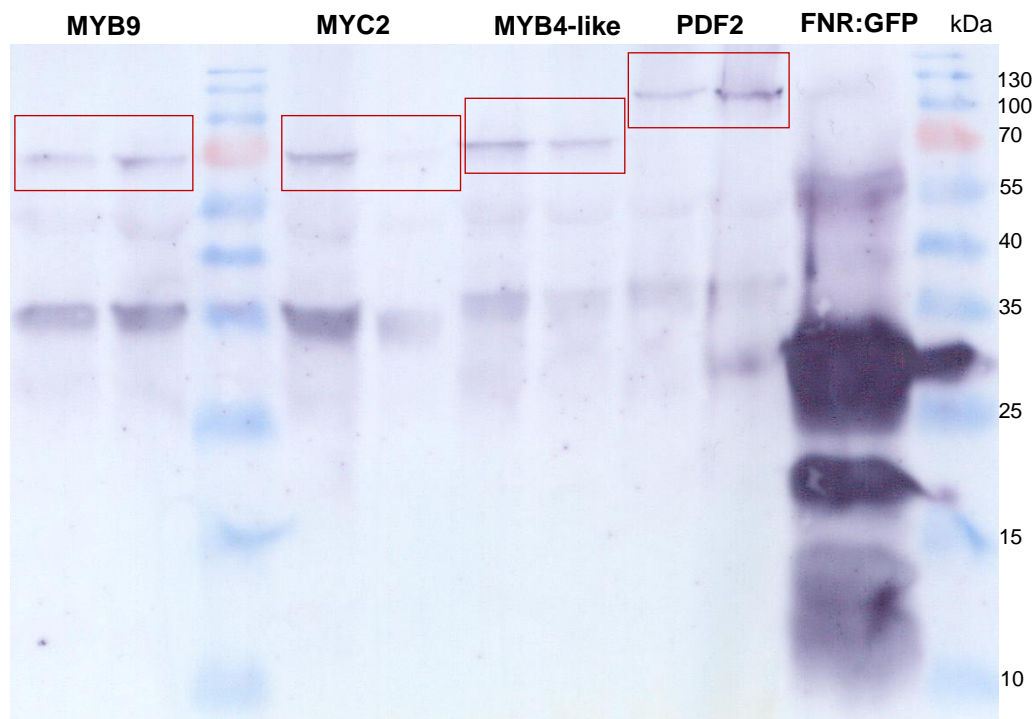


Figure 25: Protein detection on the western blot

Sizes of putative candidate proteins: MYB9 (59.67 kDa), MYB4-like (76.31 kDa), MYC2 (56.5 kDa) and PDF2 (102.1 kDa) respectively. As a positive control, a tobacco protein localized to plastids with a size of 27 kDa was used. Proteins were detected using anti GFP antibodies. PreStained Page ruler ladder was used to confirm the size of the protein.

3.8 Elucidation of loss-of-function of putative transcription factors through TILLING approach

Establishment of MicroTom TILLING platform has facilitated the analysis of tomato genes (Okabe et al., 2011). To elucidate the loss-of-function of selected putative transcription factors, TILLING mutant lines for putative MYB4-like (Solyc06g083900.2.1) and MYC2 (Solyc01g096370.2.1) were generated through EMS mutagenesis (Okabe et al., 2011) from Dr. Yoshihiro Okabe at the University of Tsukuba, JAPAN. The screening resulted in 8448 lines harboring mutations for each candidate. Around 3-4 random mutations were induced through mutagenesis for each selected candidate. Two out of three lines had mutations in putative MYB4-like, showed a base exchange at the genome positions 379 bp (W3551) and 645 bp (W2998), respectively (Table 19). For putative MYC2, two out of four mutations, line W2529 and W2267, resulted in silent mutation without any amino acid substitution (Table 20). Remaining two mutant lines from putative MYC2 had a base exchange at the genome positions, 649 bp (line W6269) and 458 bp (line 7811), respectively.

3.8.1 MYB4-like TILLING line

Table 19: List of TILLING lines for putative MYB4-like

| Line | Mutation position (genome) | Mutaion position (Protein) |
|-------------|-----------------------------------|-----------------------------------|
| W3551 | G379A | V84I |
| W3419 | G516T | intron |
| W2998 | C645T | S119F |

Since DNA-binding domain is important for a gene to function without interruption, out of three random mutations in the MYB4-like protein, line 3551 had a mutation within the DNA-binding domain (Fig. 26B). The mutation caused an exchange of amino acid from valine (V) to isoleucine (I) at the 84th position of MYB4-like protein. Another random mutation, in the line 2998, was induced few base pairs downstream of MYB4-like DNA-binding domain. The mutation had an amino acid exchange from serine (S) to phenylalanine (F) at the 119th position of MYB4-like protein (Fig. 26B).

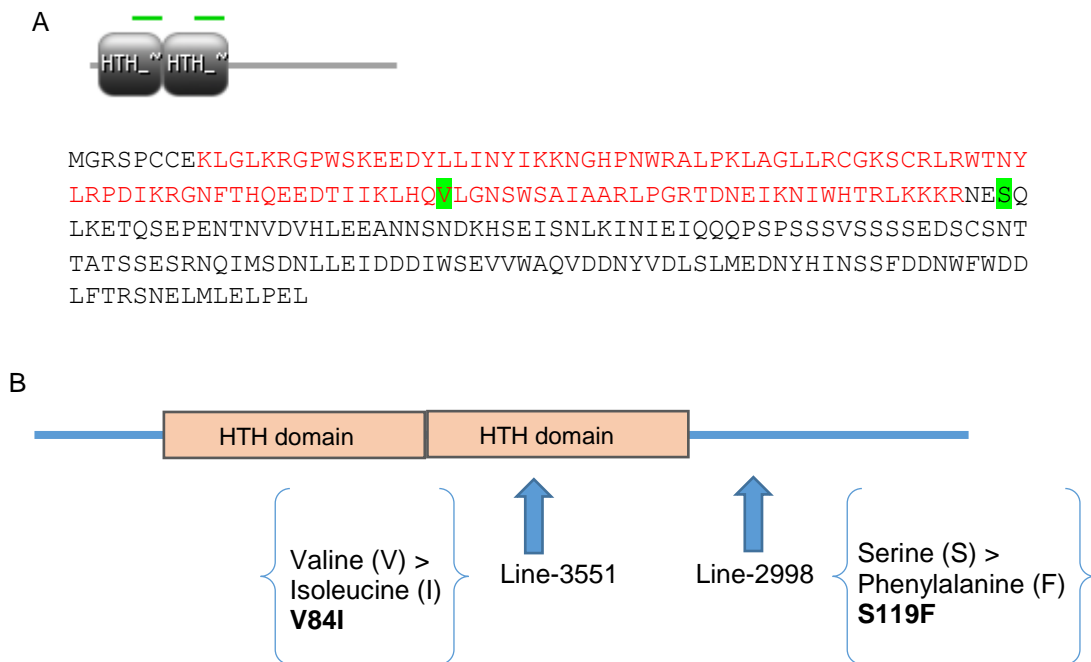


Figure 26: Putative MYB4-like protein sequence with mutation positions

(A) Putative MYB4-like sequence indicating the domain for DNA-binding activity highlighted in red. Mutation positions on the protein sequence are marked in green. (B) Outline depicting mutation positions and exchange of amino acids for the TILLING lines 3551 and 2998, respectively.

MYB4-like closely related homologs in different plant model species were identified using PLANT ENSEMBL database (version 2.0). Further, MYB4-like protein sequence was aligned with other closely related MYB protein homologs such as, *Glycine max* (GmMYB4-like), *Populus trichocarpa* (PoptriMYB190), *Theobroma cacao* (TcMYB13), *Arabidopsis thaliana* (AtMYB13) and *Solanum tuberosum* (StMYB15), using Clustal-Omega tool (version 1.2.1) (Fig. 27). Mutation position, valine (V), within the DNA-binding domain, was highly conserved between tomato and potato, showing high similarity (91%) to StMYB15 protein and less similar (49%) to AtMYB13 protein (Fig. 27). The degree of similarity was low between tomato and other plant (soybean, cotton and cacao) MYB protein homologs. For the second mutation position, serine (S), outside the DNA-binding domain of MYB4-like, is highly conserved between Arabidopsis and potato MYB homologs (Fig. 27). A similar highly conserved asparagine (N) was found among soybean, Populus and cacao MYB homologs, but they were less similar with tomato MYB4-like protein (Fig. 27).

RESULTS

| | | |
|--------------------|---|-----|
| GmMYB4-like | MGRAPCCEKMG LKRG PWTPEEDQILIN YINTYGHANWRALPKLAGLLRCGKSCRLRWINY | 60 |
| PoptrMYB190 | MVRAPCCEKMG LKKG PWTAEEDQILIN YIQLHGHGNWRALPKQAGLLRCGKSCRLRWINY | 60 |
| TcMYB13 | MVRAPCCEKMG LKKG PWTPEEDQILIN YIKLYGHGNWRALPKQAGLLRCGKSCRLRWINY | 60 |
| AtMYB13 | MGRRPCCEKIG LKKG PWSAEEDRILIN YISLHGHPNWRALPKLAGLLRCGKSCRLRWINY | 60 |
| SlMYB4-like | MGRSPCCE KLGLKRG PWSKEEDYLLIN YIKKNGHPNWRALPKLAGLLRCGKSCRLRWITNY | 60 |
| StMYB15 | MGRSPCCEKLG LKRG PWSKEEDLLIN YIKKNGHPNWRALPKLAGLLRCGKSCRLRWITNY | 60 |
| | * * * * * : * * * : * * * : * * * : * * * * * * * * * * * * * * * * * * | |
| GmMYB4-like | LRPDIKRGNF TREEDTIIISLHE MLGNRWSAIAARL SGRTDNEIKNVWHTLKKRLPQ NY | 120 |
| PoptrMYB190 | LRPDIKRGNFS REEDTIIKLHE MLGNRWSAIAARL PGRTDNEIKNVWHTLKKRLEK NH | 120 |
| TcMYB13 | LRPDIKRGNF TREEDTIIINLHE MLGNRWSAIAARL PGRTDNEIKNVWHTLKKRLKQ NH | 120 |
| AtMYB13 | LRPDIKRGNF TPHEEDTIIISLHQ LLGNRWSAIAAKL PGRTDNEIKNVWHTLKKRLHH EQ | 120 |
| SlMYB4-like | LRPDIKRGNF THQEEDTIIKLHQ VLGNWSAIAARL PGRTDNEI IKNIWHTRLKKKRNE EQ | 120 |
| StMYB15 | LRPDIKRGNF THQEEDTIIKLHQ VLGNWSAIAARL PGRTDNEI IKNIWHTRLKKKMNE EQ | 120 |
| | ***** : . ***** . * * : * * * ***** : * ***** : * * * * * : . . | |

Figure 27: Multiple sequence alignment of putative MYB4-like and its homologs

Closely related protein homologs of putative MYB4-like compared during multiple sequence alignment. DNA-binding domains are marked in red. The mutation positions among closely related species in the mutant line 3551 and 2998 are highlighted in yellow and green, respectively. Asterisks and dots represent conserved domains and degree of similarity during sequence analysis.

3.8.2 MYC2 TILLING line

For the putative MYC2, two out of four TILLING lines had point mutations several base pairs or amino acids before bHLH DNA-binding domain. The mutant line 7811 had an amino acid exchange from tryptophan to a stop codon (Fig. 28B) at the 153rd position of MYC2 protein. This is claimed to be important since a stop codon before DNA-binding activity can lead to protein dis-function. The second mutant line, W6269 had an amino acid exchange from proline to serine at the 215th position of MYC2 protein (Fig. 28B).

Table 20: List of TILLING lines for putative MYC2

| Line | Mutation position (genome) | Mutaion position (Protein) |
|-------|----------------------------|-------------------------------|
| W2529 | G267A | Q89= (= means no a.a change) |
| W6269 | C649T | P215S |
| W2267 | G876A | R292= (= means no a.a change) |
| 7811 | G458A | W153stop codon |

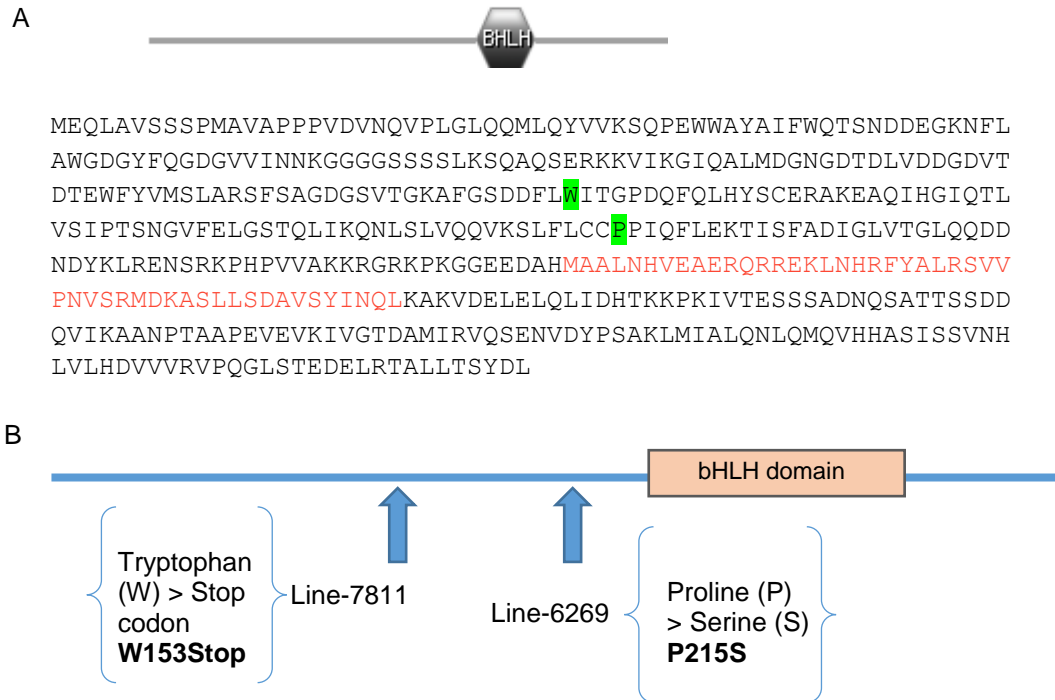


Figure 28: Putative MYC2 protein sequence with mutation positions

(A) Putative MYC2 DNA-binding domain highlighted in red and corresponding mutation positions are marked in green (W153 and P215). (B) Outline corresponding to (A) depicting mutation positions and exchange of amino acids for the TILLING lines 7811 and 6269, respectively.

The putative protein, MYC2, was aligned with closely related protein homologs of other model plant species using Clustal-Omega tool (Fig. 29). Interestingly, tryptophan (W153), highlighted in yellow, was found to be highly conserved among the closest MYC2 homologs in other plant species. Another mutation, proline (P215), highlighted in green, was found to be conserved between tomato, potato and soybean but not with Arabidopsis, cotton and cacao MYC2 homologs, respectively (Fig. 29). However, both *Populus* and cacao share conserved amino acid (Fig. 29).

3.8.3 Phenotypic characterization of TILLING mutant lines

For characterization, a PCR-based simple technique called dCAPS (Neff et al., 1998) was employed. Primers for dCAPS were designed using dCAPS finder version 2.0 web tool (Neff et al., 2002). The dCAPS PCR assay and subsequent restriction digestion confirmed homozygous, heterozygous and wildtype genotypes for *MYB4-like*. Transcript levels of *MYB4-like* were investigated among the homozygous lines: *Myb4-like_2998*, *Myb4-like_3551* and the WT (Fig. 30A). Transcript accumulation of *MYB4-like* in homozygous WT, *Myb4-like_2998* and *Myb4-like_3551* was almost equal due to high standard deviations without showing any significant changes (Fig. 30A)

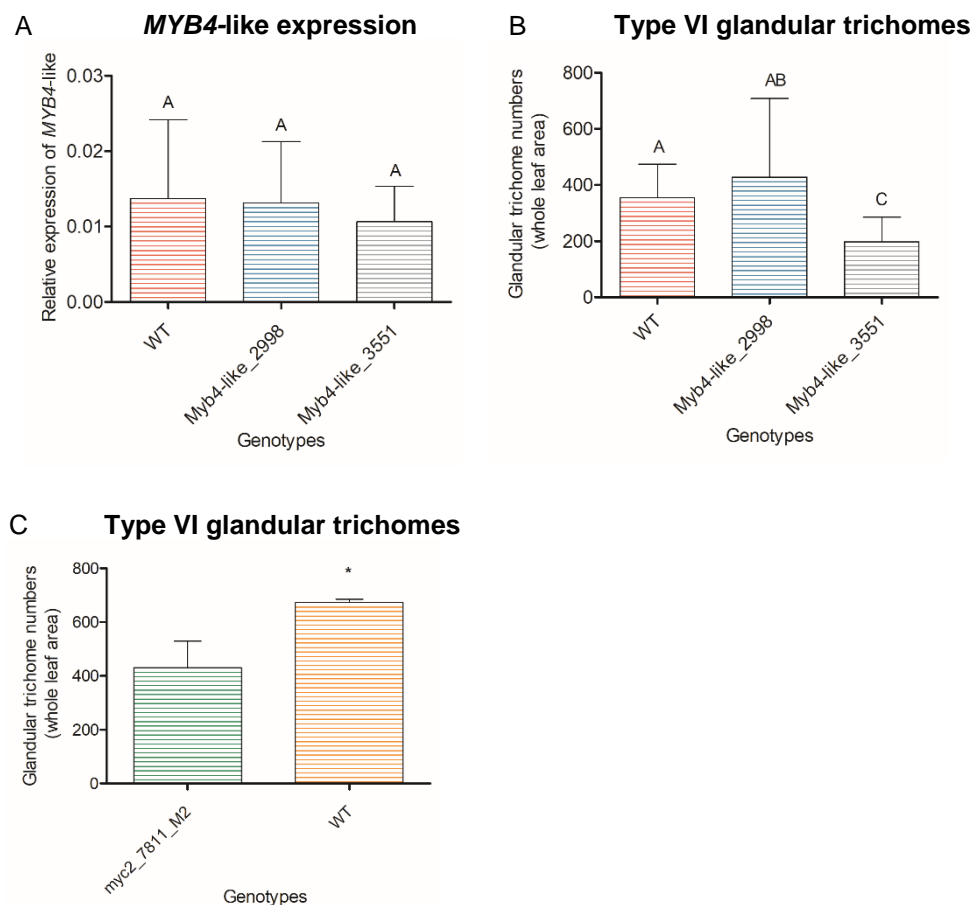


Figure 30: Characterization of MYB4-like and MYC2 TILLING lines

(A) *MYB4-like* Transcript levels in the homozygous *Myb4-like* and WT mutant lines. (B) Quantification of type VI glandular trichomes in *Myb4-like* mutant lines (*Myb4-like_2998* and *Myb4-like_3551*) compared to WT. (C) Quantification of type VI glandular trichomes in the *myc2_7811_M2* mutant line compared to WT. Number of biological replicates for quantifying *MYB4-like* transcript levels and glandular trichomes, n=10 and for

RESULTS

myc2_7811_M2, n=3. Error bars represent mean \pm SD, test of significance for *Myb4*-like was determined by ANOVA with Newmann-Keul's multiple comparison post hoc test and T- test for *myc2* line.

Type VI glandular trichomes were quantified to verify the effect of point mutations in the homozygous mutant lines of putative MYB4-like and MYC2 candidates. Ten biological replicates were considered for the quantification of type VI glandular trichome numbers in the *Myb4*-like and WT lines. WT, as a reference was recorded with an average of 356 type VI glandular trichomes (Fig. 30B). The mutant line, *Myb4*-like_2998 yielded an average of 429 type VI glandular trichomes compared to the WT without any significant changes (Fig. 30B). Interestingly, with an average of 198 type VI glandular trichomes, *Myb4*-like_3551 showed significant reduction in glandular trichomes compared to WT, as well as with *Myb4*-like_2998 mutant line (Fig. 30B). Concerning putative MYC2 TILLING line, initial screening with M1 population resulted in no homozygous plants to *MYC2*. Screening of M2 population yielded three individual homozygous plants, which were considered to quantify glandular trichome numbers. Quantification data recorded an average of 600 type VI glandular trichomes in the WT as a reference. Strikingly, *myc2_7811_M2*, representing a stop codon, showed a significant reduction in type VI glandular trichomes compared to the WT, recording an average of 400 type VI glandular trichomes per leaf (Fig. 30C).

3.9 Cloning and characterization of *Arabidopsis thaliana* Meristem Layer 1 (ATML1) promoter

Trichome formation takes place at the plant epidermal surface. Noting this, it was essential to clone and examine the activity of *Arabidopsis thaliana* Meristem L1 layer (ATML1) promoter among the putative candidates in tomato (Fig. 31). The ATML1 is a homeo-box gene, which shares its close sequence homology with Arabidopsis homeo-box gene and a key trichome regulator, *AtGL2*, (Rerie et al., 1994). The characterization of ATML1 promoter regulatory elements by Sessions et al., (1999) paved a way to clone the entire promoter region for further functional studies.

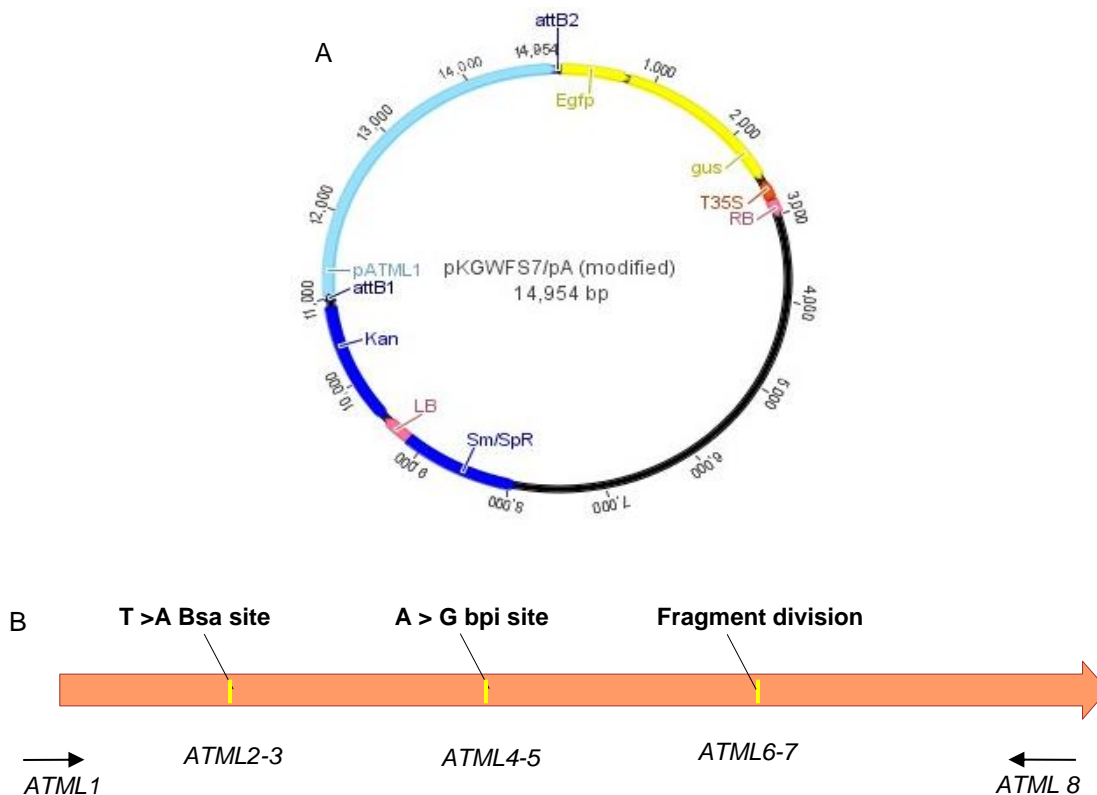


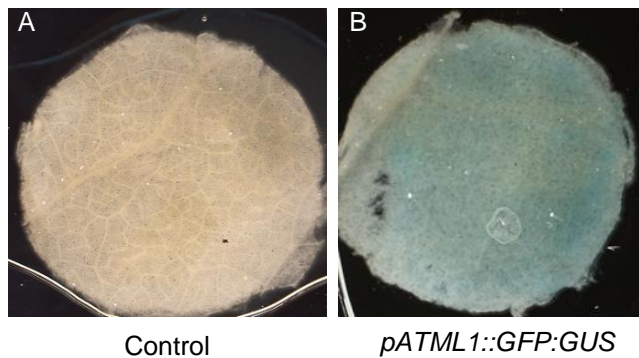
Figure 31: Cloning the promoter ATML1 using golden gate strategy

(A) A 3908 bp promoter initially cloned to a destination vector using Gateway cloning mechanism, (B) was modified to clone using golden gate cloning strategy. Black arrows represent primer sequences necessary for the amplification of promoter fragments. Modification of bases at the enzyme recognition sites by BsaI and BpiI are shown.

RESULTS

The *pATML1::GFP:GUS* construct, cloned in the GATEWAY destination vector (Fig. 31A), was kindly provided by Prof. Dr. Thomas Schmülling lab, Freie University, Berlin. Initially, the Agro construct harboring *pATML1::GFP:GUS* was used for transient GUS expression in *N. benthamiana* leaves (Fig. 32A, B). Further, the same construct was used to determine the GUS activity in transgenic WT tomato plants (Fig. 32C, D). The transient GUS expression was found to be lower in the epidermal surface of *N. benthamiana* leaves compared to transgenic tomato leaves (Fig 32B, D). A strong activity of promoter *ATML1* in transgenic tomato leaves was promising to fuse them with the selected transcription factors of interest. Therefore, the entire *ATML1* promoter sequence was re-cloned using golden gate cloning modules. In the golden gate cloning strategy, the huge promoter sequence (3908 bp) was fragmented into 4 parts and ligated to final vector after sequencing (Fig. 31B).

GUS assay on *N. benthamiana* leaves



pATML1::GFP:GUS in transgenic tomato leaves

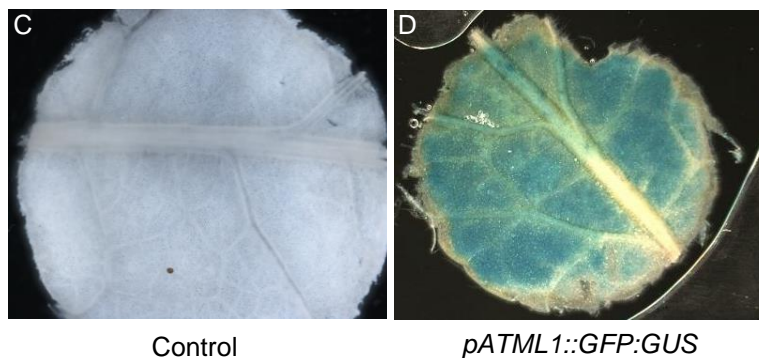


Figure 32: *pATML1*-GUS activity in tobacco and tomato leaves

(A, B) Promoter *ATML1* induced GUS activity in transiently transformed *N. benthamiana* leaves and transgenic tomato leaves (C and D). Scale bars represent 50 μm (A, B and D) and 65 μm for C, respectively.

3.9.1 Elucidation of *ATML1* promoter activity in tomato

ATML1 plays a significant role during different stages of shoot meristem development, apex and floral meristems (Lu et al., 1996). To elucidate *ATML1* promoter activity, GUS assay was performed with 4-week-old mature and young developing leaves of WT transgenic tomato lines (Fig. 33). The majority of the GUS activity was detected across the basal region and a minor detection at the apex region of developing leaves (Fig. 33A, C). Subsequently, both mature and young leaves were subjected to embedding through PEG. Interestingly, transverse sections of mature and young leaves showed GUS activity towards lower epidermis, palisade mesophyll cells and trichome stalk cells (Fig. 33B, D). The signal strength differs according to GUS activity on the leaf samples.

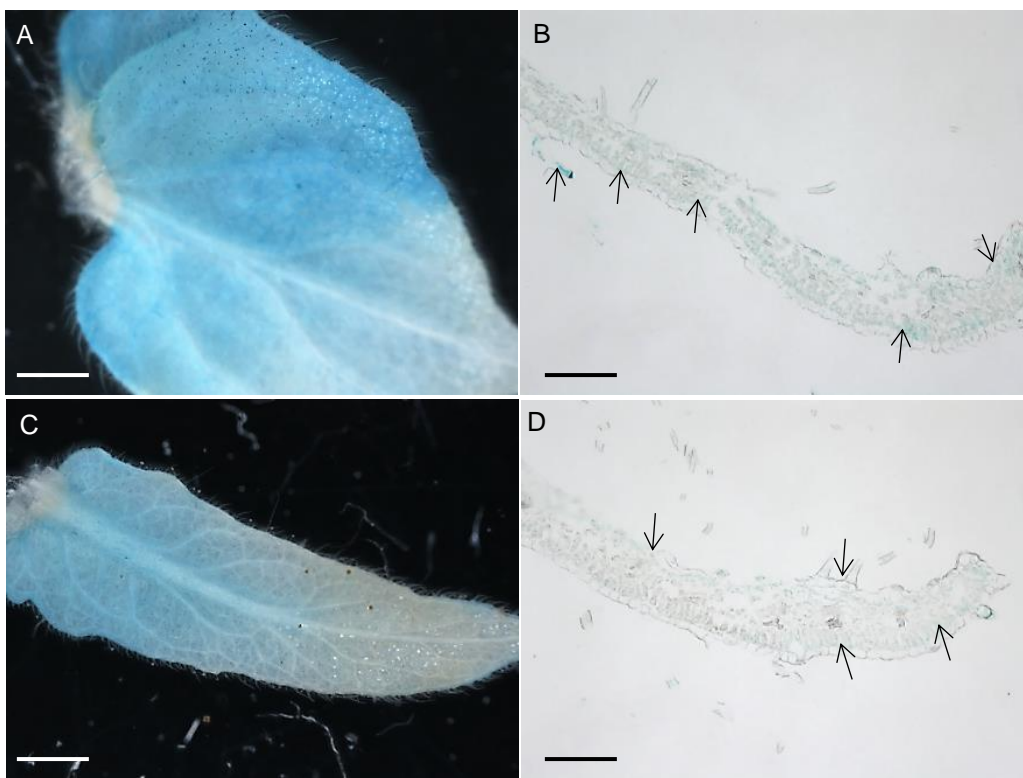


Figure 33: pATML1-GUS activity in the developing leaves of transgenic tomato plants

(A) Four weeks-old mature tomato leaves and (B) subsequent cross-section through PEG embedding. (C) Young tomato leaf and (D) subsequent cross-section through PEG embedding. Cross-sections of PEG embedded tomato leaves were 9 μm thickness. Black arrows indicate *pATML1::GUS* expression across lower epidermis, palisade mesophyll cells and trichome stalk cells. Scale bars represent (A) 50 μm , (B and D) 10 μm and (C) 20 μm , respectively.

RESULTS

3.10 Overexpression of putative transcription factors in tomato

According to the hypothesis of current thesis, putative transcription factors, MYB9, MYB4-like, MYC2 and PDF2 were selected for functional characterization by generating stable transgenic tomato lines. Since homozygous *jai1* are known to be female sterile and are impaired in seed production for future generations (Li et al., 2004), stable tomato transformants were generated in the heterozygous *jai1* background.

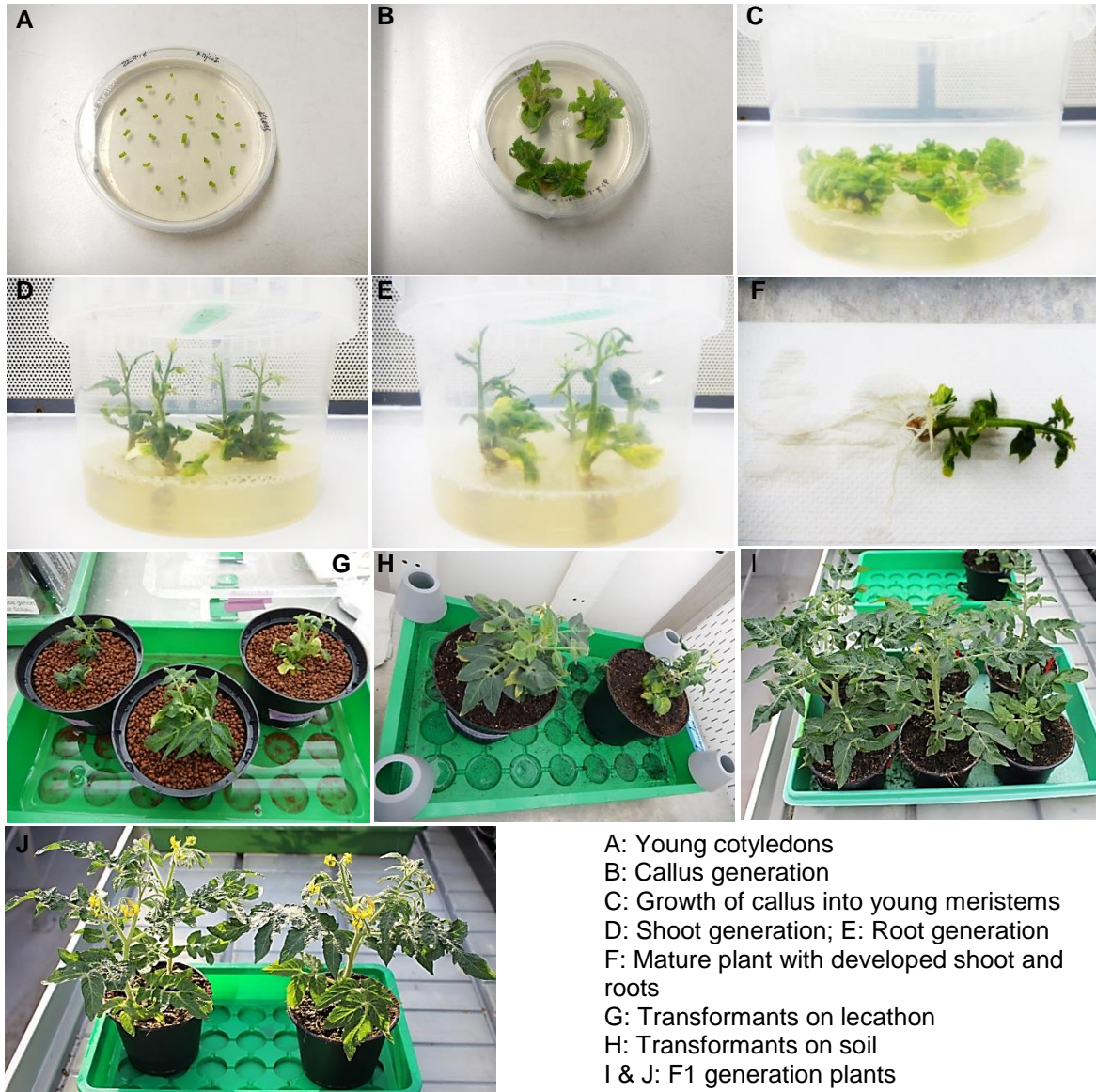


Figure 34: Generation of tomato transformants

(A) Eight-day-old tomato cotyledons pre-conditioned on KCMS media. (B) Formation of young callus from cotyledons on zeatin-riboside (2-Z) media. (C) Callus growth and

proliferation to form young meristems. (D) Shoot induction on shoot generation media. (E) Root induction on root generation media. (F) Transformants with developed shoots and roots. (G) Primary transformants transferred to lecathon for acclimatizing phytochamber conditions. (H) Primary transformants transferred to soil. (I and J) Successful transgenic lines in the F1 generation.

Eight-day-old tomato seedlings with young cotyledons were pre-conditioned on the KCMS media before transforming agro-constructs harboring putative candidates (Fig. 34A). Media necessary for growth and proliferation of the callus was maintained with descending concentration of zeatin-riboside and subsequent exchange of media with antibiotics: *kanamycin* for plants and β -bactyl for avoiding agro-contamination (Fig. 34B-C). Each callus formed with several shoots was separated and numbered prior to being transferred into shoot generation media (+GA) (Fig. 34D). Individual transformants were then transferred to root generation media (+IAA) (Fig. 34E) until the transformants were fully developed (Fig. 34F). To acclimatize from the plant growth cabinets to phytochamber, primary transformants were transferred initially onto expanded clay pots (Fig. 34G) and then to soil (Fig. 34H). Presence of transgene and the plant genotype was confirmed through genotyping PCR, in primary transformants (Fig. 34H) and in F1 segregated lines (Fig. 34I-J).

3.10.1 Localization studies for primary transformants under constitutive and *ATML1* promoter

Developing transgenic tomato lines and assessing the functionality of putative candidates in *planta* was an estimated objective for functional characterization. In order to achieve this goal, transgenic tomato lines harboring putative candidates were overexpressed under the control of constitutive (*35S*) and tissue specific *pATML1* promoters. During plant acclimatization period in the phytochamber, tomato leaf disc's of *35S::GFP:MYB9* (Fig. 35A) and *35S::GFP:PDF2* (Fig. 35B) primary transformants were examined under a laser scanning microscope (LSM) at a wavelength between 480-550 nm, respectively. The primary transformants harboring *35S::GFP:MYB9* and *35S::GFP:PDF2*, showed their localization at the nucleus of mesophyll cells (Fig. 35A-B). Similarly, primary transformants of *MYB9*, *MYC2* and *MYB4-like*, overexpressed under the control of tissue-specific promoter *pATML1*, were also found to be localized at the nucleus of mesophyll cells (Fig. 35C-D).

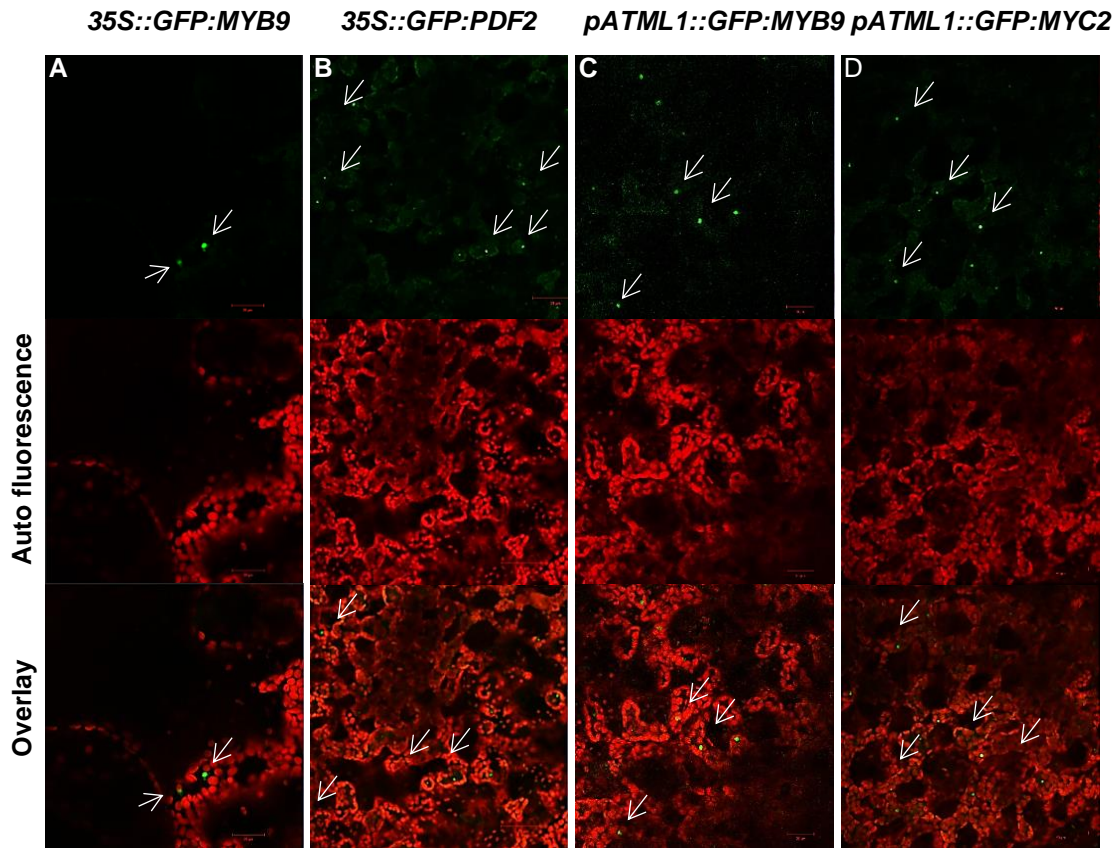


Figure 35: Localization of putative candidates in the primary transformants

Overexpression of putative transcription factors under the control of 35S and *ATML1* promoters in the heterozygous *Jai1* background. (A) Subcellular localization of putative MYB9 and (B) PDF2 under the control of 35S promoter. (C) MYB9 and (D) MYC2 under the control of *ATML1* promoter. White arrows indicate localization of putative candidates. Scale bars represent 50 μm .

3.10.2 Quantification of *GFP* levels in primary transformants (T_0)

To assess *GFP* reporter gene expression analysis, relative expression of *GFP* reporter gene from individual primary transformants *35S::GFP:MYB9* and *35S::GFP:PDF2* showed little or no expression (Fig. 36A-B). However it was found that, only line 8 from *35S::GFP:MYB9* (Fig. 35A) and line 4 from *35S::GFP:PDF2* (Fig. 36B) showed higher expression levels. Variations in transcript accumulation of *GFP* reporter gene were observed among individual transgenic lines of *MYB9*, *MYC2* and *MYB4-like* under the control of *ATML1* promoter (Fig. 36 C, D and E). As a control, empty vector without *GFP*-

tag was used for comparison between primary transformants. The individual lines with highest expression levels of *GFP* were considered for characterizing in the F1 generation.

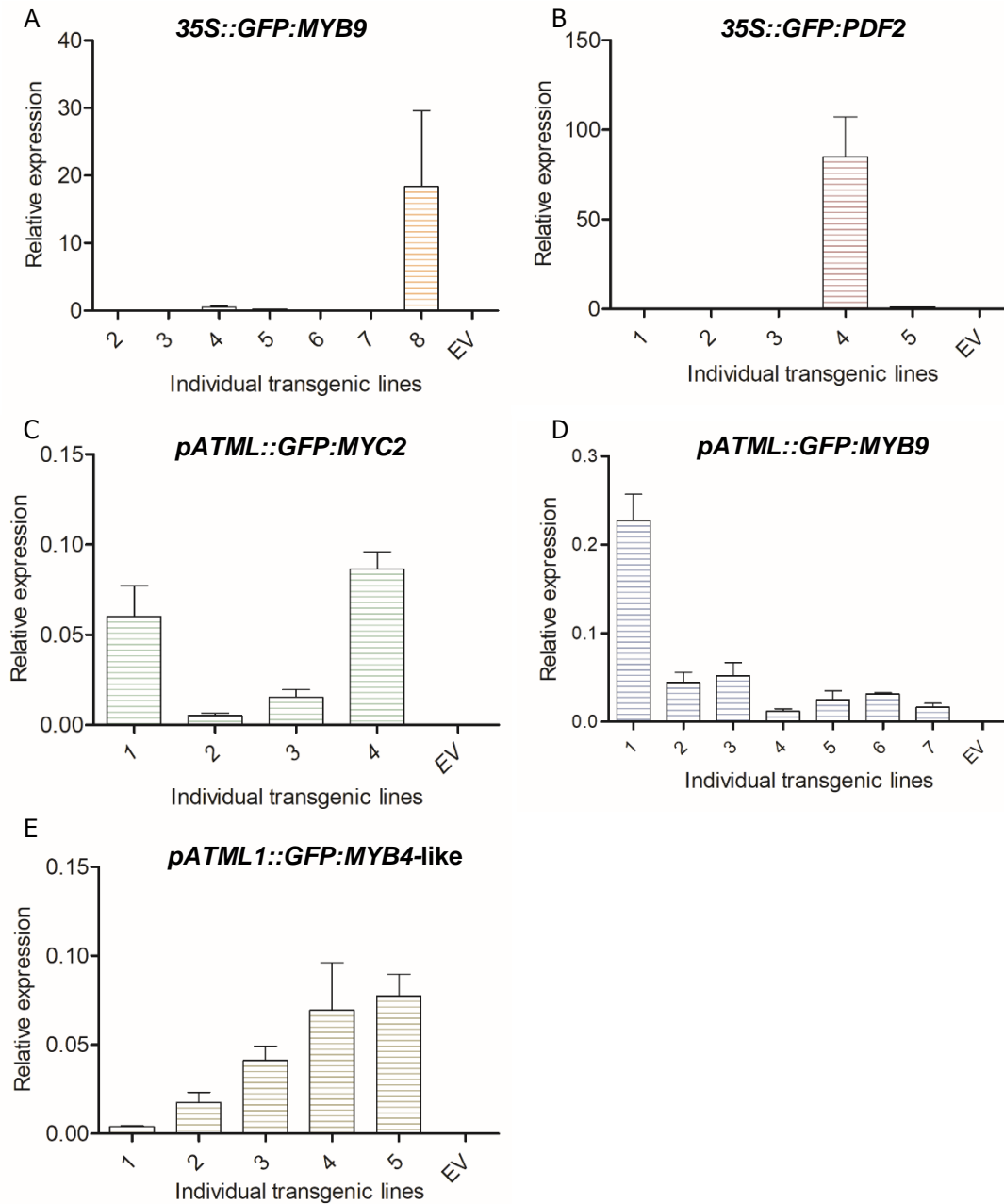


Figure 36: Relative transcript accumulation of GFP in primary transformants (T_0)

Relative expression of *GFP* reporter gene in primary transformants. (A) *35S::GFP:MYB9*, (B) *35S::GFP:PDF2*, (C) *pATML1::GFP:MYC2*, (D) *pATML1::GFP:MYB9* and (E)

RESULTS

pATML1::GFP:MYB4-like, respectively. Numbers on the X-axis represent individual transformants in the respective transformation event. EV represents empty vector.

3.10.3 Localization of putative candidates in the F1 segregation lines

According to the hypothesis, it was important to know the functionality of overexpression lines in the homozygous *jai1* and WT background. Therefore, Individual transgenic lines from primary transformants batch with highest expression levels of GFP were selected to validate and characterize subsequent lines in the F1 generation.

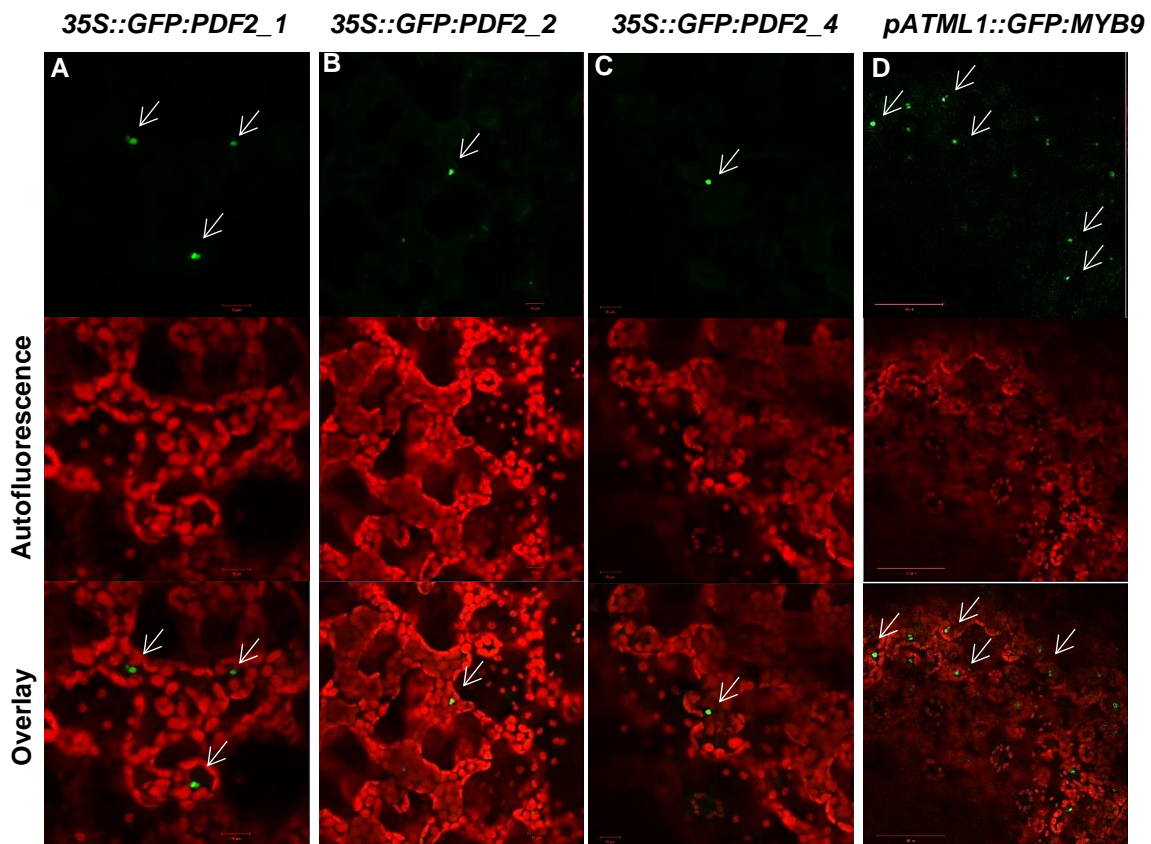


Figure 37: Localization of putative candidates in the F1 generation

(A, B and C) Transgenic lines *35S::PDF2_1/2/4* in the WT background and (D) *pATML1::MYB9* in the *jai1* mutant background showing their localization. White arrows indicate GFP signals of putative transgenic candidates (A-D), scale bar represents 20 μ m. Data was reproduced with three biological replicates.

Transcription factors corresponding to MYB and HD-Zip families are known to be involved in the formation of multicellular trichomes in other model plant species. Due to lack of time, seed setting in some individual lines (Fig. 36) and a varying number of individual lines

across primary transformants, putative MYB9 and PDF2 were selected for functional characterization. Three- lines from $35S::PDF2_F1$ (Fig. 36B) and one-line from $pATML1::MYB9_F1$ transformation event were considered (Fig. 36D). Young developing leaves from three-week-old F1 transgenic plants were used for localization studies (Fig. 37). All three individual lines from $35S::PDF2_1/2/4$ (Fig. 37A-C) and one individual line from $pATML1::GFP:MYB9$ (Fig. 37D), were found to be localized at the nucleus of mesophyll cells (Fig. 37A-D).

3.10.4 Quantification of putative candidate gene expression

To assess expression levels of individual F1 transgenic lines, *GFP* reporter gene expression from individual selected lines of $35S::PDF2_1/2/4$ and $pATML1::MYB9_F1$ was quantified. To remind again, according to the hypothesis in overexpression lines, expression of $35S::PDF2_1/2/4$ was vital if over-expression in WT could rescue and increase type VI glandular trichomes and vice versa with respect to $pATML1::MYB9$ in *jai1* background.

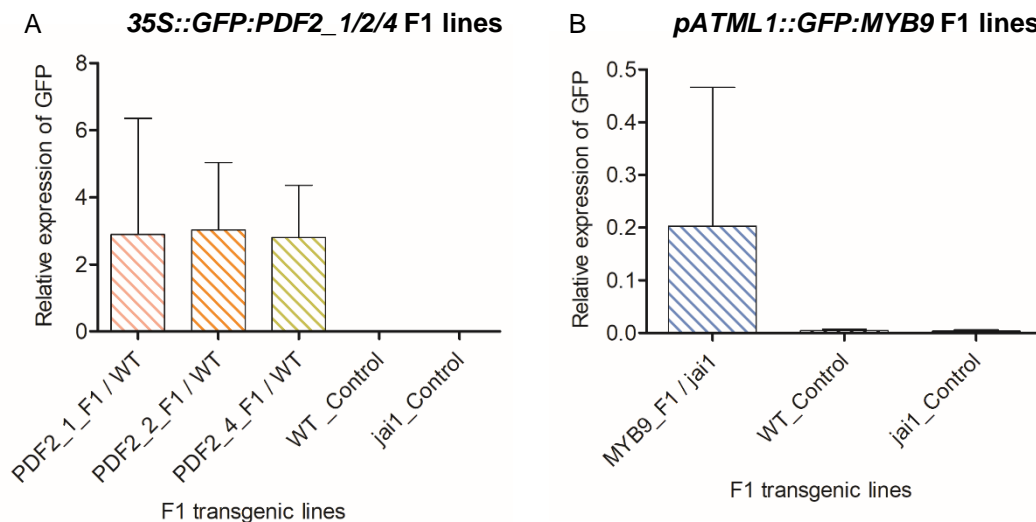


Figure 38: Relative expression of *GFP* in F1 transgenic lines

(A) $35S::GFP:PDF2_1/2/4$ and (B) $pATML1::GFP:MYB9$ showing their relative transcript accumulation of *GFP* in the F1 generation. Non-transformed WT and *jai1* were used as control for F1 transgenic lines. X-axis represents individual F1 transgenic lines. Test of significance was determined by ANOVA with post hoc test (Newmann-Keul's). Error bars represent mean \pm SD, n=7 for $35S::GFP:PDF2_1/2/4$ (A) and n=3 for $pATML1::GFP:MYB9$ (B), respectively.

RESULTS

Young developing leaves for RNA extraction (Section. 2.9.3) from seven-biological replicates for each individual lines of *35S::PDF2_1/2/4_F1* (37A) and three-biological replicates from *pATML1::MYB9_F1* (37B), were considered. For cDNA synthesis, protocol and synthesis kit from ProtoScript II (NEB Inc.) was adopted where RNA concentration was scaled down to 300 ng/μL instead of 500 ng/μL (Section 2.9.4). From the inference of real time analysis, transcript accumulation of *GFP* reporter remained nearly equal among 3 individual lines of *35S::PDF2_1/2/4* (Fig. 37A). The transcript levels of *GFP* reporter in putative *pATML1::MYB9* showed low expression levels. However, a huge standard deviation exists among *35S::PDF2_1/2/4* and *pATML1::MYB9* transgenic individuals. Nevertheless, as a control, WT and *jai1* mutant showed no *GFP* expression. This conclusion also confers the level of significance between transformed and non-transformed lines.

Putative *MYB4*-like transcription factor was over-expressed under the control of constitutive *35S* promoter initially in the homozygous *jai1* background. To rescue the primary transformants, they were crossed with WT for retrieving the seeds and to characterize of segregation events of *35S::MYB4-like:Flag* overexpression lines.

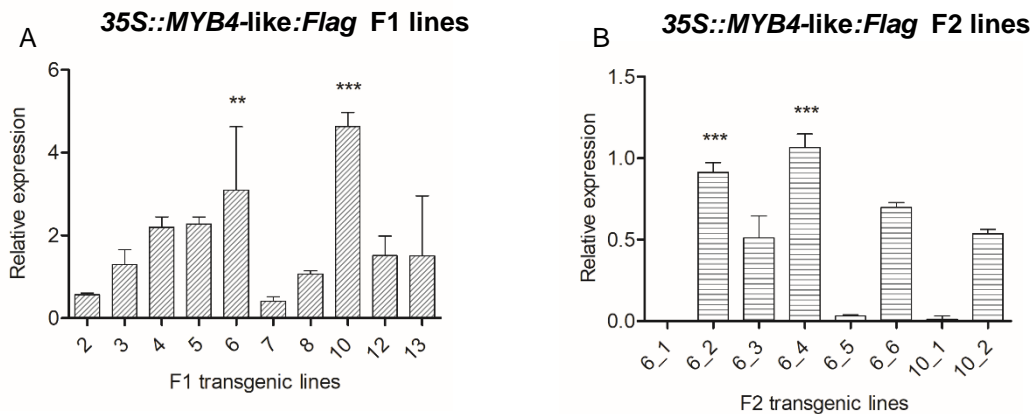


Figure 39: Relative expression of *MYB4*-like in F1 and F2 overexpression lines

(A) F1 and (B) F2 transgenic lines over-expressing *35S::MYB4-like::Flag*. Numbers on the X-axis represent individual transgenic lines in F1 and F2 generations, respectively. Significant expression from line 6 and line 10 F1 segregation events (A) were further considered for characterization in F2 generation (B). Error bars represent mean±SD, n=3, significance test was determined by ANOVA with post hoc test (Newmann-Keul's). ** and *** indicates $p < 0.01$ and $p < 0.001$, respectively.

Since, primary transformants of *MYB4*-like was in the homozygous *jai1* background, further crossing with WT yielded only transgenic heterozygous lines (*Jai1*) across F1 generation (Fig. 39A). The quantity of seeds was less in the F1 generation. This led analyze nearly 10-11 individual plants for *MYB4*-like expression (Fig. 39A). Among 10 individual lines, line 6 and line10 accumulated significant levels of *MYB4*-like transcripts (Fig. 39A), therefore, respective lines were considered for further characterization in the F2 generation. Although seed production in line 6 and line 10 from F1 segregation was too low, six plants for line 6 and two plants for line 10 were selected for validation. Prior to validation on the real-time PCR, genotyping for *jai1* homozygosity and transgene PCR confirmed that individual lines from line 6 and line 10 were in the heterozygous *jai1* background. The relative expression of *MYB4*-like in sub-individual lines of 6_2 and 6_4 showed significant transcript accumulation (Fig. 39B). By contrast, line 6_1, 6_5 and 10_1 showed nearly basal or no transcript accumulation (Fig. 39B). Functional characterization of *MYB4*-like over expression lines indicate that further characterization of homozygous lines in the F3 generation is necessary to address the overexpression status of putative *MYB4*-like.

3.10.5 Quantification of type VI glandular trichomes

A primary objective of this thesis is to quantify and compare the modifications in type VI glandular trichome numbers transgenic overexpression lines against control lines (Fig 40). Third true leaves, harvested from seven biological replicates of *35S::PDF2_1/2/4* F1 lines (Fig. 40A) and three biological replicates from *pATML1::MYB9* F1 lines (Fig. 40B) were considered to quantify type VI glandular trichomes against control WT and *jai1* lines. Type VI glandular trichomes among three individual F1 lines of *35S::GFP:PDF2* was recorded with an average of 150-200 glandular heads. Although, there was minor variations in type VI glandular trichome numbers, there was no significant difference in trichome numbers between *35S::GFP:PDF2_1/2/4* individual lines compared to WT control (Fig. 40A). The second candidate transgenic line, *pATML1::GFP:MYB9* in the F1 generation was assessed in the *jai1* background. Type VI glandular trichome numbers were almost equal number compared to control *jai1* leaves (Fig. 40B), showing an average of 160 type VI glandular heads. Subsequently, type VI glandular trichome numbers were assessed between control WT and *jai1* lines. Interestingly, a significant difference in type VI glandular trichome numbers was observed between control WT and *jai1* genotypes, with nearly 75% increase in the WT compared to *jai1* (Fig. 40 A), hence drawing the correlation with the previous research work (Li et al., 2004).

RESULTS

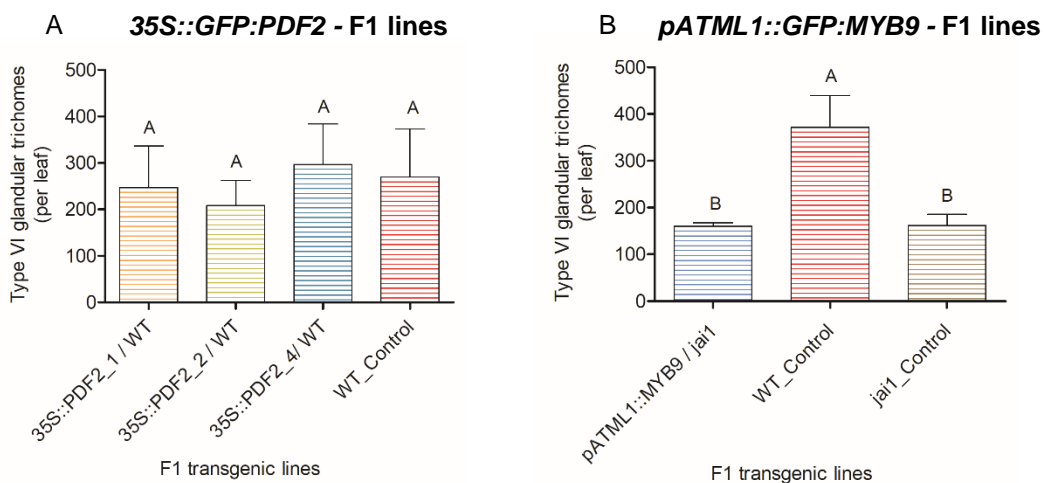


Figure 40: Quantification of type VI glandular trichomes in F1 transgenic lines

Type VI glandular trichomes on (A) *35S::GFP:PDF2* and (B) *pATML1::GFP:MYB9* F1 transgenic lines. Third true leaves with $n=7$ for *35S::GFP:PDF2* and $n=3$ for *pATML1::GFP:MYB9* F1 lines, respectively. Non-transformed WT and *jai1* were used as control in comparison to F1 lines. Test of significance was determined by ANOVA with post hoc test (Newmann-Keul's). Error bars represent mean \pm SD.

3.10.6 Qualitative analysis of terpene levels on F1 transgenic lines

To determine the secondary metabolites like monoterpenes and sesquiterpenes, young leaves from the individual biological replicates of *35S::GFP:PDF2* and *pATML1::MYB9* F1 lines, control WT and *jai1* lines, were subjected to hexane extraction to analyze terpene levels on gas chromatography-mass spectrometry (GC-MS) platform. Comparisons were made according to the hypothesis: WT control was compared with *35S::GFP:PDF2_1/2/4* F1 lines and *jai1* control was compared with *pATML1::GFP:MYB9* F1 lines. Monoterpenes like α - pinene and 3, 4- Carene, with the molecular weight 136.12 was measured at the retention time (RT) 5.42 (Fig. 41A). Class I sesquiterpenes like β - caryophyllene and α - humelene, with the molecular weight 204.18 was measured at the retention time (RT) 15.22 (Fig. 41B). Content of monoterpenes (α - pinene and 3, 4- Carene) between WT and *35S::GFP:PDF2_1* and *35S::GFP:PDF2_2* were not significant due to huge error bars, whereas significant levels between WT and *35S::GFP:PDF2_4* were observed (Fig. 41A). In order to analyze monoterpenes levels between control *jai1* and overexpression line, *pATML1::GFP:MYB9* in *jai1* background were found to be non-significant either. Sesquiterpenes, on the other hand, were found to have almost equal levels across WT and

35S::GFP:PDF2 F1 lines without any significant changes, which also holds true for *jai1* and *pATML1::MYB9* lines, respectively (Fig. 41A-B).

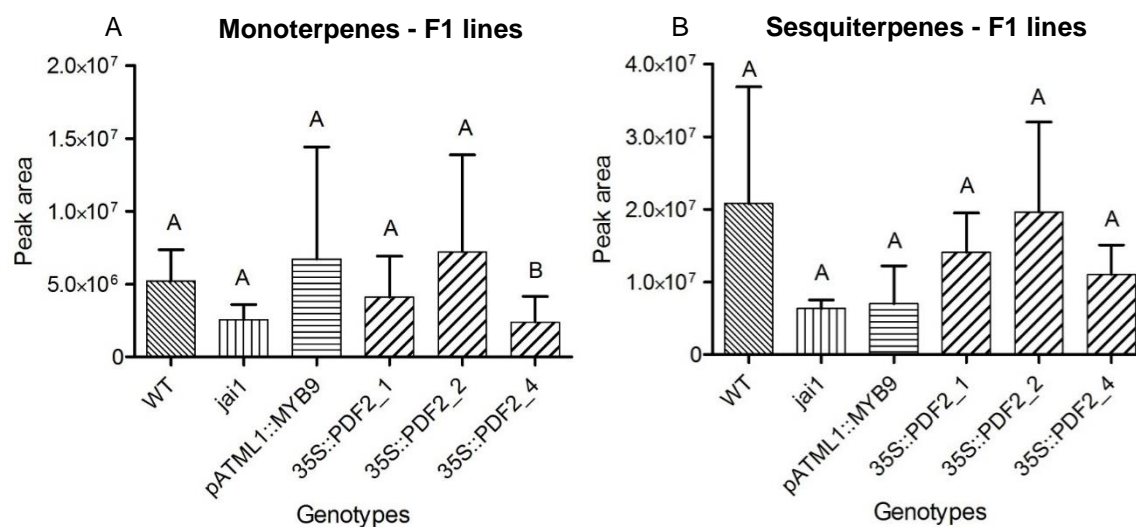


Figure 41: Measurement of terpenes from the leaf extracts of F1 transgenic lines

(A) Analyses of peak area of monoterpenes (α – pinene, 3, 4 –Carene, M.W – 136.12, R.T – 5.42) and (B) sesquiterpenes (β - caryophyllene and α -humelene, M.W – 204.18, R.T - R.T – 15.22) from hexane leaf extracts of F1 transgenic lines. Biological replicates, n=3 for WT, *jai1* and *pATML1::GFP:MYB9* F1 lines and n=7 for *35S::GFP:PDF* F1 lines. Test of significance was determined by T-test. Metabolite comparisons were made between WT and *35S::GFP:PDF2_1/2/4* F1 lines and *jai1* and *pATML1::GFP:MYB9* F1 lines. Error bars represent mean \pm SD.

4 DISCUSSION

This thesis addresses novel regulatory players involved in the formation of tomato glandular trichomes, potentially induced by JA. External application of jasmonates (JA and MeJA) are known to induce trichome numbers in Arabidopsis and tomato (Traw and Bergelson, 2003; Boughton et al., 2005). Thorough molecular characterization of *jai1* mutant in tomato showed a significant reduction in type VI glandular trichomes compared to WT (Li et al., 2004). However, potential regulators of type VI glandular trichomes in tomato, influenced primarily by JA were still an unanswered question. Serna and Martin predict that development of multicellular trichomes are operated under unique regulatory mechanisms unlike unicellular trichomes (2006), although there is a plausibility that common regulators exists between uni- and multicellular trichome initiation processes (Maes et al., 2011). To fill this gap, current thesis focuses on the identification and characterization of fundamental molecular regulators of type VI glandular trichomes in tomato. To achieve this primary objective, an approach with the current state-of-the-art transcriptome sequencing and its analysis concerning gene ontology and differentially expressed genes was performed. Subsequently, putative candidate transcription factors, preferentially regulated by JA, indicate possible outcomes based on the trichome quantification data.

4.1 Importance of prerequisite experimental approach

Mechanical wounding and insect-herbivory are known to trigger JA dependent responses in plants (Bostock, 1999; Reymond et al., 2000). In this view, trichome numbers and densities were reported to be significantly higher in mechanically wounded Arabidopsis accessions compared to equivalent leaves of control plants (Traw and Bergelson, 2003). Our experimental approach in the preliminary phase led to quantify type VI glandular trichomes on the WT and *jai1* leaves of cultivated tomato (MT) using both approaches: mechanical wounding and exogenous JA treatment. In the first approach, mechanically wounded plants showed a striking increase in type VI glandular trichome numbers, nearly a 10-fold increase in wounded WT leaves compared to control leaves (Fig. 9). Further, type VI glandular trichome numbers between wounded and control leaves of *jai1* mutant were found to be unchanged. This lies in agreement with Arabidopsis JA-deficient mutants like *aos* and *coi1*, where both JA deficient mutants failed to increase trichome numbers after wounding (Park et al., 2002; Yoshida et al., 2009). The correlation between Arabidopsis and tomato JA-

DISCUSSION

deficient mutants indicates that JA might play an important role in the formation of trichomes. In the second approach, young tomato plants with four true leaves were treated with JA instead of MeJA due to its high volatility and chances of contaminating other batch experiments. JA-treated leaves showed a striking difference in type VI glandular trichome numbers between older and younger leaves (Fig. 10). Newly developed leaves, such as third and fourth true leaves showed nearly a 10-fold increase in type VI glandular trichomes compared to first and second true leaves (Fig. 10). The quantification of JA-treated type VI glandular trichomes holds true with previous work, where newly developed leaves upon MeJA treatment yielded a 9-fold increase in type VI glandular trichome numbers compared to control plants (Boughton et al., 2005; Maes et al., 2008; 2011). Furthermore, type VI glandular trichomes on the third true leaves, observed under ESEM interestingly showed different developmental phases from initiation till maturation. Collectively, we hypothesized that JA functions as hormonal signal to induce type VI glandular trichome formation on young tomato leaves. The analyses of underlying molecular mechanisms may substantially contribute to identify key regulators involved in the formation of glandular trichomes. With this perspective, third true leaves were selected as right physiological material for transcriptome analysis and further downstream applications.

4.2 Tomato homologs of key Arabidopsis trichome regulators behave explicitly different

Both Arabidopsis and tomato comprise different types of trichomes: unicellular and multicellular, respectively. Previous studies reported that either MeJA or JA induce the expression of *AtGL3* or *AtEGL3*, positive regulators of MBW trimeric complex in Arabidopsis (Maes et al., 2008; Yoshida et al., 2009). Although trichome morphological features and types are distinct in Arabidopsis and tomato, there is a likelihood of common molecular regulators involved in unicellular and multicellular trichome initiation processes (Maes et al., 2011). According to phylogenetic analyses, key trichome regulatory gene homologs are considerably related between Arabidopsis and tomato (Tominaga-Wada et al., 2013). For instance, *SIGL3* shares 45% amino acid sequence with *AtGL3* and 46% with that of *AtEGL3* (Tominaga-Wada et al., 2013). The bHLH motif of *SIGL3* shares 46% and 50% amino acid identity with *AtGL3* and *AtEGL3*, respectively (Tominaga-Wada et al., 2013). Furthermore, both *SIGL3* and *SITRY* were known to be expressed in the aerial regions of tomato plant (Tominaga-Wada et al., 2013) but their transcript levels was not specifically detected in young leaves. Based on qPCR validation analysis, transcript levels

of *SIMYB23*, *SIGL2*, *SIGL3* and *SITTG1* were detected at the basal level with variations in transcript accumulation pattern across treatment conditions (Fig. 13). The variation and the accumulation of low number of transcripts was compared with JA reference genes (Fig. 12). Similar validation was performed for the tomato homologs of Arabidopsis trichome regulators detected by RNA-seq data of *S. habrochaites* young leaves vs glandular trichomes (S. Bennewitz, personal communication). The tomato homologs of Arabidopsis trichome regulators showed extremely low transcript levels with equivalent transcript patterns across treatment conditions (Fig. 14). This indicates that tomato homologs, identified from two different sources (BLAST and RNA-seq data), follows similar transcript accumulation trend which means no potential role in young tomato leaves. Although a close sequence similarity exists between Arabidopsis and tomato trichome inducing gene homologs, *SIGL3* and *SITRY* were found to have higher transcript levels in older leaves (Tominaga-Wada et al., 2013) compared to young tomato leaves. Therefore, it is speculated that there might be different homologs responsible for the formation of glandular trichomes in tomato leaves at different developmental stages. In future, tomato homologs of Arabidopsis trichome regulators can be considered for complementation experiments in Arabidopsis trichome inducing mutant background. In addition to this, exogenous treatment of JA could potentially uncover the role of trichome regulatory components induced by JA in trichome formation.

4.3 Analysis of differentially expressed genes across sample treatments

Identification of key regulatory factors of type VI glandular trichomes potentially regulated by JA treatment in young tomato leaves was one of the prime goals of the current thesis. In order to identify those putative regulatory factors, a high throughput, state-of-the-art Illumina sequencing platform was employed. Initial analysis of the RNA-seq dataset was normalized by TMM strategy (Robinson and Oshlack, 2010). This was essential to know if there was any distant clustering of individual biological replicates across the treatment conditions (Fig. 15). Distant clustering and variations across the biological treatment samples are well represented on MDS plot (Fig. 15), which indicates biological variability within the sample type. This could be affected due to the plant physiological and growth parameters. However, there was no data concerning variance decomposition (Shi et al., 2013) reported during the analysis.

4.3.1 Early JA response-related genes on young tomato leaves

The transcriptome analysis led to identify differentially expressed genes across JA-treated and non-treated leaf samples, which is clearly represented on smear plots (Fig. 16). This result confers both up and down regulation of genes based on the \log_2 fold cutoff values. In the current dataset, shortly after exogenous JA treatment (JA_2h), 496 genes were significantly upregulated compared to control *jai1* (*jai1_CO*). Most of the genes upregulated were known to have diverse functions such as cell wall synthesis, secondary metabolism, protein degradation, UDP glucosyl transferases reaction, hormone metabolism and degradation of auxins, brassinosteroids and jasmonates. Further, based on the PAGEMAN functional enrichment analyses, there were 39 gene elements exclusively identified as JA dependent. These genes within the gene elements correspond to lipases, lipoxygenases, 12-OPDA reductases, methyltransferases and JAZ's, which are known to be involved in signal transduction, biosynthesis and degradation activity (Table 14). A similar set of JA-dependent genes was found to be upregulated in the RNA-seq data generated from JA treated tomato stem trichomes (Spyropoulou et al., 2014), supporting our RNA-seq data. Further, the functional enrichment analyses indicated 45 gene elements that were significantly upregulated in *jai1_CO* samples. Most of the genes within the gene elements were categorized in protein degradation and ubiquitination process. Lastly, to confirm the normalized expression levels of JA-dependent genes from RNA-seq data, initial validation of JA reference genes (*AOC*, *LAP A* and *PIN1*) was performed on qPCR and the transcript accumulation was found to be significantly elevated in JA-treated leaf samples compared to control WT and *jai1*, respectively (Fig. 20).

4.3.2 Selection of putative candidates involved in trichome development

Clustering of significantly expressed genes that are differentially regulated across treatment conditions revealed set of genes and transcription factors that were primarily detected in the pathways of hormone metabolism, secondary metabolism, cell wall and protein synthesis (see Appendices, Table A10). The large number of putative genes upregulated after JA treatment (JA_2h and JA_24h) indicates JA involvement in several biological functions of plant development. JA has a potential role in altering glandular trichome density, induction of defense compounds such as monoterpenes and sesquiterpenes (Kang et al., 2010; Tian et al., 2012) and regulation of one of the key trichome formation regulator GL3 in *Arabidopsis* (Yoshida et al., 2009). These activities influenced by JA were mainly mediated by transcription factors. Based on this evidence, a detailed index of

transcription factors was analyzed to select transcription factors significantly upregulated shortly after JA treatment against down regulation in *jai1* biological replicates. Based on the expression scale between 2h_JA and *jai1_CO*, clusters representing transcription factors from MYBs, bHLHs, WD40, ethylene, WRKYs and HD-Zip families were hypothesized as positive and negative regulators of JA, according to Meinhardt and Gierer (1974). Putative TFs upregulated by JA, such as *Myb4-like*, *Myb9*, *MYC2*, an unknown bHLH TF, and the TFs upregulated in *jai1* mutant (*jai1_CO*) like *PROTODERMAL FACTOR 2* and to some extent *NAC D* TFs, were shown to have similar trend in transcript accumulation between RNA-seq data and qPCR validation (Fig. 20 and 21).

Recently, genome-wide classification of R2R3 MYB transcription factor superfamily in *S. lycopersicum* led to identify putative MYB4-like and MYB9 TFs, assigned as MYB14 and MYB66, respectively (Li et al., 2016). Putative MYB4-like and MYB9 TFs upregulated after JA_2h share nearly 40% sequence identity and represents conserved amino acids in R2R3 domain. These characteristics remain in concurrence with recently classified MYB14 and MYB66 TFs, which show no gene duplication within the tomato genome and were strongly upregulated after 2 hours MeJA treatment (Li et al., 2016), supporting the candidate validation. Further, based on the phylogenetic analyses, putative candidates were found to have high sequence homology with Arabidopsis TFs with known function. Putative MYB9 was found to have sequence homology with AtMYB3 (AT1G22640.1) (38.5%) and AtMYB4 (AT4G38620.1) (40.3%) DNA-binding domain. They are highly expressed in most of the tissues, preferentially in young leaves responding to phytohormones like JA and indulging in stress related activities (Kranz et al., 1998; Chen et al., 2006). Secondly, putative MYB4-like shares close homology with two MYB protein homologs, AtMYB13 (AT1G06180) (49%) and AtMYB14 (AT2G31180.1) (67.4%). Though both MYB homologs are involved in stress tolerance, AtMYB14 loss-of-function mutants are negatively regulated during cold treatment, inducing cold-resistant (CBF) genes (Chen et al 2013).

Third potential candidate significantly upregulated shortly after JA treatment was MYC2, a bHLH TF primarily targeted by JAZs and a master regulator involved in the activation and repression of distinct JA-responsive genes in Arabidopsis (Dombrecht et al., 2007; Lorenzo et al., 2004; Kazan and Manners, 2013). Putative MYC2 shares sequence homology with AtMYC4 (AT4G17880.1) (57%), which is known to be regulated by JA and interacting with JAZ proteins (Fernandez-Calvo et al., 2011; Schweizer et al., 2013). Similar JAZ interaction domains (JID) were identified in other bHLH TFs, like AtGL3, AtEGL3 and AtTT8, which are

DISCUSSION

potential regulators of trichome initiation in *Arabidopsis* (Qi et al., 2011). During the classification of bHLH TF superfamily in *S. lycopersicum*, putative MYC2 was assigned as bHLH13 within the subfamily III (d+e) (Wang et al., 2015). Further, differential gene expression analysis showed that members of subfamily III (d+e) were involved in JA-signaling network and defense against tomato yellow leaf curl virus (Wang et al., 2015). This gives a hint that MYC2 upregulated by JA treatment may have potential roles in glandular trichome formation.

The fourth putative candidate, *PROTODERMAL FACTOR2 (PDF2)* is a HD-Zip class IV TF family member, found to be significantly upregulated in control *jai1* leaves compared to control WT leaves (Fig. 21A). Most of the HD-Zip class IV genes identified in the past are exclusively involved in the formation of epidermal structures (Javelle et al., 2011, Nadakuduti et al., 2012). For instance, *AtGL2* is specifically expressed in leaf trichomes. Further, both *ATML1* and *PDF2*, are expressed in the epidermal layer of most plant parts (Rerie et al., 1994; Masucci et al., 1996; Lu et al., 1996). Putative PDF2 has shown highest sequence homology with HDG11 (AT1G73360.1) (60.2%). *AtHDG11* is known to exhibit highest degree of amino acid similarity with *AtGL2* and both function redundantly in trichome branching and development in *Arabidopsis* leaves (Khosala et al., 2014). Based on the candidate validation, *PDF2* transcript levels were slightly increased at JA_2h time point compared to the WT, whereas transcript levels at JA_24h were decreased compared to JA_2h time interval (Fig. 21A). This subtle change in *PDF2* transcript levels after JA treatment led to the prediction that putative PDF2 negatively regulates JA responses. Another tomato homolog in *Arabidopsis*, *ANTHOCYANINLESS (ANL2)*, expressed in the sub-epidermal layer of vegetative meristem, rosette leaves and the seedling roots (Kubo et al., 2008), was found to have a close homology with putative PDF2. This gives a hint that the putative PDF2 might have a potential role in the formation of epidermal structures.

Some of the key transcription factors involved in the formation of glandular trichomes in other model plants have also been reported in previous studies. For instance, AmMIXTA, an R2R3 MYB TF from *A. majus* is known for its ectopic expression in the development of tobacco glandular trichomes (Glover et al., 1998). Further, GoPGF, a bHLH transcription factor from *Gossypium* spp., acts as a positive regulator in the formation of glandular trichomes (Ma et al., 2016). Furthermore, AaHD1, a homeodomain-Leu Zipper TF is known to regulate glandular trichome initiation in *A. annua* through jasmonates (Yan et al., 2017). Furthermore, overexpression of AaMYB1 from *A. annua* induces increased number of

trichomes (Matias-Hernandez et al., 2017). Similarly, mutation at the CsGL3 locus, which encodes a HD-Zip TF in cucumber, has led to glabrous phenotype (Cui et al., 2016). Overall, these supportive data led to consider above described putative TFs as the candidates of interest for validation and functional characterization.

4.3.3 Validation of other significantly expressed JA regulated genes

Among the list of differentially expressed genes that are significantly regulated across biological treatments (see Appendices, Table A10), few proteinase inhibitors were found to be upregulated shortly after JA treatment. For instance, most prominent JA responsive defense-related protein PIN2, was found to be significantly expressed in the tomato glandular trichomes upon herbivore feeding (Tian et al., 2012). Further, *SaPIN2b* from *Solanum americanum* has close homology with *S. habrochaites PIN2*. Furthermore, promoter *SaPIN2b::GUS* was found to be constitutively expressed in the glandular trichomes of *S. americanum* and tobacco plants, respectively (Liu et al., 2006). As there is a growing circumstantial evidence that PIN2 might be involved in trichome development and plants defense against herbivory, essential proteinase inhibitors (PIs): *Kunitz trypsin*, *Cysteine-extensin*, *Metallo-carboxypeptidase (MCP)* PI's, a phosphatase activity candidate, *purple acid phosphatase (PAP)* and an unknown F-box protein were validated based on their extreme \log_2 fold changes ($p < 0.001$) against *jai1_CO* (Table 18). All PI's transcript levels were found to be responsive after JA treatment (Fig. 22B, C, E and F). Most importantly, *Kunitz type*, *Metallo-carboxypeptidase* and *Cysteine-extensin* PI's had a significant transcript accumulation in JA_2h and JA_24h treatments compared to WT_CO and *jai1_CO* (Fig. 22B, E and F), raising a possibility that PI's are coordinately expressed during the wound response for certain period of time. Precisely, putative MCP was also found to be upregulated in the type VI glandular trichomes of tomato stem (Schilmiller et al., 2010). This indicates that putative MCP is responsive to JA and might be active in stem glandular trichomes for secondary metabolite production. Two other putative candidates, *Purple acid phosphatase* ($>5 \log_2$ fold) with phosphatase activity in tomato due to phosphate stress response and a *Kunitz Trypsin* PI ($>10 \log_2$ fold), were significantly upregulated shortly after JA treatment, but the transcript levels were declined after JA_24h compared to WT_CO and *jai1_CO* (Fig. 22C, D). As PI's are positively upregulated upon JA treatment, functional analyses of validated putative proteinase inhibitors could possibly lead to discover their potential role in the trichome developmental process. Apart from the PI's, another well-known JA responsive candidate, F-box protein was significantly

DISCUSSION

upregulated after JA_2h and JA_24h treatment ($>7 \log_2$ fold higher), compared to *jai1_CO* (Fig. 22A). The role of F-box protein in the development of glandular trichomes is still unknown (Suen et al., 2015).

4.3.4 Selected putative transcription factors are located in the plant cell nucleus

Initially, tomato and tobacco Agro-infiltration experiments were found to be non-promising and fairly difficult to visualize putative candidate proteins. Later, successful localization of putative candidate proteins in mesophyll protoplasts of tobacco led to draw few conclusions: Putative MYB9 TF was localized to the nucleus encompassing bright speckles (Fig 24A). Putative MYB4-like, MYC2 and PDF2 proteins were not only localized to the nucleus but also towards the cytoplasm (Fig 24B, C, and D). A similar kind of localization was found with Woolly::GFP, expressed in onion epidermal cells under the control of 35S promoter (Yang et al., 2011). There could be two possible reasons where putative protein localization could its localization pattern. Firstly, tagging of GFP reporter to the N-terminus of the candidate coding sequence might affect the localization and secondly, the overexpression by using constitutive 35S promoter itself. Based on these anticipations, it is concluded that selected putative transcription factors were localized to the nucleus.

4.4 Functional characterization of selected putative transcription factors

4.4.1 Characterization of ATML1 promoter activity in tomato leaves

ATML1 belongs to HD-Zip TF family, which is expressed in the outermost cell layer (L1) of shoot meristems (Lu et al., 1996; Sessions et al., 1999). Since the characterization of ATML1 and its promoter activity, *cis*-elements in the promoter region are essential to regulate the outer cell layer (L1) of embryo, shoot epidermis and floral meristems (Abe et al., 2003; Takada et al., 2007; 2013). ATML1 was reported to transactivate its native promoter, especially binding to the L1-box region. Similar transactivation mechanism was also identified with other HD-ZIP class IV transcription factors *in vitro*, which suggest that ATML1 and its closest homologs are involved in the differentiation of epidermal cells (Abe et al., 2001; Nakamura et al., 2006; Takada et al., 2013). In a recent study, using live-imaging, quantitative image analyses and mathematical modeling, ATML1 was shown to play an important role, specifying cell-fate in Arabidopsis sepal development (Meyer et al.,

2017). In the current thesis, for the first time in tomato, a full-length *ATML1* promoter (3908 bp) was used to elucidate its functional activity as suggested by Sessions et al (1999) (Fig 31). Although a minimal promoter (179 bp), comprising *cis*-regulatory elements like L1-box and WUSCHEL-binding site is sufficient to promote *ATML1* expression in different stages of *Arabidopsis* embryo development (Takada et al., 2007), it is predicted that other promoter-binding elements might be essential for leaf epidermis activity in tomato. Therefore, initial transient expression experiments of *ATML1* promoter driving GFP and GUS reporter expression in tobacco showed low levels of GUS expression in leaf discs (Fig. 32A, B), and distinctly towards lower palisade mesophyll cells in transverse longitudinal sections (data not shown), whereas the GUS signal was stronger in transiently expressed mature WT tomato leaves (Fig. 31C, D). Interestingly, in transgenic WT tomato leaves, *ATML1* promoter was active both in mature and young leaves, where the GUS signal was majorly observed at the basal region and slightly at the leaf tip (Fig. 33A, C). The microscopic data showed GUS staining in type I non glandular trichomes of mature and young leaves but not in type VI glandular trichomes. By contrast, *AaHD1::GUS*, an *A. annua* HD-Zip class IV TF, was reported to be strongly active at the basal region of glandular and non-glandular trichomes in young leaves of *Artimisia annua* (Yan et al., 2017), which suggests, HD-ZIP class IV TFs may have distinct functions in different plant epidermal surfaces. Further, transverse sections of mature and young tomato leaves expressing *ATML1::GUS* revealed promoter activity not only in lower epidermis and palisade mesophyll cells but also in the trichome stalk cells (Fig. 33B, D). This indicates that *ATML1* promoter can be active at different layers of plant epidermis which lies in argument with the promoter activity at different embryonic differentiation phases in *Arabidopsis* (Takada and Juergens, 2007). As modification of *ATML1* promoter elements leads to varied GFP expression at specific embryonic cell divisions (Takada and Juergens, 2007), similar method could be employed to analyze the activity of promoter targeting trichome specific cells in tomato.

In *Arabidopsis*, HD-ZIP class IV transcription factors, *ATML1* and *PDF2* were shown to auto-regulate themselves by binding to their promoter L1-box elements (Abe et al., 2003; Takada et al., 2013; Ogawa et al., 2015). Recently, recognition of L1-box elements from the promoter sequence of *AaHD1* was shown to be required for JA mediated glandular trichome initiation (Yan et al., 2017). Based on this knowledge, in future experiments, it is worth to consider HD-Zip class IV TFs in tomato for similar transcriptional activation

mechanism using their native promoters to determine its effect on glandular trichome formation.

4.4.2 Approaches for functional characterization of candidates: Overexpression and identification of mutants

The functionality of putative candidate proteins was elucidated based on gain-of-function and loss-of-function characteristics. According to the hypothesis, putative candidates were overexpressed in heterozygous *jai1* background under the control of ubiquitous 35S and tissue specific *ATML1* promoters. Relative transcript levels of GFP among primary transformants (T_0) of putative MYB9, MYC2 and MYB4-like under the control of *ATML1* promoter and ubiquitous 35S promoter were found to be fluctuated (T_0 , Fig. 36). Genotyping and localization studies could confirm the presence of the transgenes and their expression in leaves (Fig. 35). Further, only few individual lines out of actual number of primary transformants were able to bear the minimum seeds for the next generation (T_1). Moreover, putative 35S::*GFP:MYC2* successive T_0 lines were unable to survive on the potting mix, indicating that the transgenic lines were stressed due to the transformation process and failed to cope up with the regeneration process.

Based on the transcription factors role in other model plant species, MYBs and HD-Zip TFs were anticipated to have a greater role in the development of glandular trichomes, therefore, *pATML::GFP:MYB9* and *35S::GFP:PDF2_1/2/4* overexpression lines were predicted to have a stronger impact on tomato type VI glandular trichome development. Apart from putative MYB9 and PDF2 TFs, further sections emphasize on putative MYB4-like and MYC2 with two approaches – overexpression and characterization of TILLING mutants.

4.4.2.1 MYB9

Putative MYB9 was found to be upregulated shortly after JA treatment (JA_2h). MYB9 transcript levels were significantly higher compared to *jai1* mutant in young tomato leaves, according to our RNA-seq data. Similarly, putative MYB9 closest homologs in Arabidopsis, AtMYB3 and AtMYB4 were found to be active in young leaves and responded to JA (Kranz et al., 1998; Chen et al., 2006a). AtMYB3 was known to interact with ABA-stress related protein, Arabidopsis CTD protein Like (AtCPL1) (Bang et al., 2008) but there was no functional proof related to trichome initiation and induction. Similar to AtCPL1-AtMYB3 protein-protein interaction, it is predicted that putative *Solanum* MYBs might also be

involved in the protein interaction at the conserved domains of JA responsive genes (Fig. 20).

Since putative MYB9 was upregulated 2 hours after JA-treatment in WT compared to other sample treatments, its overexpression was intended to be analyzed in the mutant *jai1*. Putative MYB9 was overexpressed under the control of ubiquitous 35S promoter and epidermal specific *ATML1* promoter. Most of the *35S::GFP:MYB9* primary transformants with relatively low GFP expression had low or no seeds for further characterization in F1 generation, whereas transgenic lines of *pATML::GFP:MYB9* with sufficient seed material were considered for further characterization. Interestingly, type VI glandular trichome numbers were found to be more or less similar between *jai1* plants expressing *pATML::GFP:MYB9* and control *jai1* lines (Fig. 40B). In a recent study, one of the uncharacterized homologs of putative MYB9 in Arabidopsis, *AtMYB17* was found to be the ortholog of *AmMIXTA1*. *AmMIXTA1*, under the control of native promoter was localized at the cuticular layer and basal region of glandular secreting trichomes in young leaves of *A. annua* (Shi et al., 2017). It is assumed that putative *MYB9* might be a far-related ortholog of *AmMIXTA1*. Further, an unaltered number of type VI glandular trichomes indicates that putative MYB9 has subtle or no role in glandular trichome initiation. With this perspective, to decipher a possible role of putative MYB9, *MYB9::GUS* assay gives an overview of putative *MYB9* expression in leaf tissues. Further, generating MYB9 knockout lines either by RNAi or through CRISPR/Cas9 will be essential to look at the protein functionality in tomato.

4.4.2.2 PDF2

Significant *PDF2* transcript accumulation in the *jai1* mutant compared to control WT and JA treatments, and further depletion of *PDF2* transcript levels after JA treatment in the WT, raise the possibility that *PDF2* might act in a negative manner (Fig. 21A). Such a negative activity was also observed for HOMEODOMAIN GLABROUS11 (HDG11) in Arabidopsis, where *hdg11* mutants showed excessive trichome branching (Khosala et al., 2014). According to the hypothesis, there were no significant differences in the quantification of type VI glandular trichome numbers between *35S::GFP:PDF2_1/2/4* overexpression lines, in the WT background, compared to control WT lines (Fig. 40A). The inference indicates that putative PDF2 in the WT has no significant contribution in the formation of type VI glandular trichomes. However, being strongly upregulated in the *jai1* mutant, it would be

DISCUSSION

worth to analyze the overexpression effects of putative PDF2 in the *jai1* background. By contrast, one of the far-related putative PDF2 homolog in *A. majus*, *AaHD1*, was highly expressed in young leaves. Overexpression of *AaHD1* in transgenic *A. majus* was found to promote glandular trichomes under the control of its native promoter. Further, increase in *A. majus* glandular trichomes was reported upon exogenous MeJA treatment (Yan et al., 2017). This indicates that further experimentation is required to prove the functionality of putative PDF2 in tomato.

Previous studies report that HD-Zip class IV TFs like *ATML1* and *PDF2* in Arabidopsis are involved in the transactivation mechanism with their native promoters for epidermal specific activity. For instance, successive overexpression of HDG11 under the control of *ATML1* promoter in *gl2-5* mutant background has led to regain trichome branching on leaf margins (Khosala et al., 2014). The transactivation method could be employed by putative *PDF2* with its native promoter which may be beneficial for overexpression studies. Additionally, developing leaves of putative *PDF2* transgenic lines could be treated with JA for monitoring type VI glandular trichome numbers in tomato. Since MeJA was known to increase glandular trichomes in transgenic *A. majus* lines, to prove whether there exists a link between putative candidates and JA-signalling perception, yeast two-hybrid assays with tomato JAZ proteins could facilitate and strengthen the functional analyses.

4.4.2.3 Metabolic activity in *MYB9* and *PDF2* overexpressing plants

Leaf epidermis of young developing leaves is responsible for the formation of higher densities of type VI glandular trichomes. This is not just limited to glandular trichome numbers alone but also contributing towards high terpene levels, since young leaves are known for producing volatile compounds in response to plant defense (Andersson et al., 1980; Buttery et al., 1987). Application of methyl jasmonate (MeJA) has shown to induce tremendous accumulation of caffeoylputrescine (CP), which is synthesized in WT tomato (MT) leaves and flowers but not in *jai1* mutant. This signifies that accumulation of CP might be mediated by JA biosynthetic pathway (Chen et al., 2006). The *jai1* mutant with significant reduction in type VI glandular trichomes compared to WT also indicated absence of monoterpenes like α - and β - pinene, limonene and *cis*-ocimene from type VI trichome exudates of tomato fruits and sepals (Li et al., 2004). These important secondary metabolites from cultivated tomato lines, elucidated from previous researchers motivated to uncover whether overexpression of putative *MYB9* and *PDF2* affects secondary metabolite

composition. Although there were minor fluctuations but no significant differences in type VI glandular trichome numbers between putative *pATML1::GFP:MYB9*, *35S::GFP:PDF2* and control leaves, occurrence of monoterpenes and sesquiterpenes were qualitatively analyzed (Fig. 40). Though monoterpenes like α - pinene and 3,4- carene were known to be absent in homozygous *jai1* (Li et al., 2004; Besser et al., 2009), leaf-surface extracts of control *jai1* still possess nearly half of monoterpene levels compared to *pATML1::GFP:MYB9* in *jai1* background, whereas leaf-surface extracts of *pATML1::GFP:MYB9* in *jai1* background shows slightly higher levels of monoterpenes compared to control *jai1* and WT (Fig. 40A). This indicates, although glandular trichome numbers are not significantly higher, the amount of terpenes produced is significantly higher in *pATML1::GFP:MYB9* across the homozygous *jai1* background. Further, higher levels of monoterpenes in *pATML1::GFP:MYB9* might be due to the activity of putative MYB9. Monoterpene levels across the leaf extracts of individual F1 transgenic lines of *35S::GFP:PDF2_1/2/4* in the WT background were at varying levels compared to control WT (Fig. 40A). Among the three individual lines of *35S::GFP:PDF2_1/2/4*, monoterpene terpene levels were significantly lower in the leaf extracts of *35S::GFP:PDF2_4* compared to *35S::GFP:PDF2_1* and *35S::GFP:PDF2_2* lines, respectively. This indicates, although three individual lines from *35S::GFP:PDF2_1/2/4* shows varying monoterpenes levels to that of type VI glandular trichome numbers, density of type VI glandular trichomes may not be significantly involved in the variation of monoterpenes levels. Fluctuations in both type VI glandular trichomes and monoterpene levels in three individual lines of *35S::GFP:PDF2_1/2/4* led to anticipate that putative PDF2 may not significantly contribute for terpene production rather it may be constrained to epidermal specific activity in tomato.

Class I sesquiterpenes were found to be strongly accumulated in the WT leaves compared to *jai1* mutant (Fig. 40B). Class I sesquiterpenes like β - elemene, β - caryophyllene and α - humelene, were found to be significantly elevated in the type VI glandular trichomes of WT leaves compared to stem trichomes (Schillmiller et al., 2010). Leaf-surface extracts of *pATML1::GFP:MYB9* showed equivalent levels of class I sesquiterpenes compared to control *jai1* (Fig. 40B), which correlates with the quantification data (Fig. 39B). This indicates that minimum number of type VI glandular trichomes on *jai1* leaves may be sufficient for accumulating class I sesquiterpenes. Furthermore, due to unchanged type VI glandular trichome numbers and class I sesquiterpene levels, *pATML1::GFP:MYB9* may not have a vital role either in glandular trichome development or towards sesquiterpene

DISCUSSION

synthesis. Constitutively overexpressed *PDF2* in the WT background, with three individual lines showed different accumulation patterns of class I sesquiterpenes compared to control WT leaves (Fig 40B). Although, sesquiterpenes levels were found to be lower in the cultivated tomato lines compared to LA1777 (WT) (Besser et al., 2009), overexpression of putative *PDF2* in the WT background failed to contribute for significant sesquiterpenes levels compared to control WT. This indicates, overexpression of both putative *MYB9* and *PDF2* may not significantly contribute to class I sesquiterpenes synthesis.

Use of tissue specific promoters could contribute significant role in the expression of terpene synthase genes. For instance, Monoterpene synthase 1 (MTS1) promoter was known to drive the expression of zingerberene synthase enzyme (ShZIS) in transgenic tomato type VI glands (Bleeker et al., 2012). Further, JA-regulated transcription factors like *SIMYC1* and *SIWRKY73* were known to transactivate terpene synthase promoters in *N. benthamiana*, specifically via G-box elements (Spyropoulou et al., 2014; Y. H Xu et al., 2017). Therefore, the transactivation mechanism supports that epidermis specific *ATML1* promoter may partially contribute to monoterpene accumulation in transgenic young cultivated tomato leaves. Secondly, putative transcription factors role in the production of terpenes can be estimated by selecting glandular trichome specific expression promoters. Further, it is important to analyze relative expression of both monoterpenes and sesquiterpenes synthase genes in the overexpression lines across WT and *jai1* background. To strengthen further, employing yeast one-hybrid and ChIP assays to analyze binding activity of putative tomato TF with that of terpene synthase promoters could indicate their role in the synthesis of mono- and sesquiterpenes.

4.4.2.3 MYB4-like

Putative MYB4-like was a candidate of interest due to its JA responsiveness, characterized for tomato flower development from another member of the same lab. Initially, *35S::MYB4-like:Flag* primary transformants were generated in the homozygous *jai1* background. In the *35S::MYB4-like:Flag* overexpressing plants, low expression of *MYB4-like* was detected during flower development but high levels were found in the leaves (R. Schubert, personal communication). One of the closest homologs of MYB4-like in Arabidopsis, AtMYB13 showed strong activity at the shoot branching points and in the young flowers before anthesis, in the AtMYB13::GUS lines. Further, under the control of constitutive 35S promoter, AtMYB13 was found to be active in the inflorescence and showed distorted

phenotype in the aerial development (Kirik et al., 1998). Although both AtMYB13::GUS and AtMYB14::GUS fusions were active during different stages of seedling, shoot and inflorescence development in Arabidopsis, no function corresponding to trichome initiation and development was reported. In this work, the offspring of individual transgenic *35S::MYB4-like:Flag* F1-lines showing high *MYB4-like* transcript levels was analyzed (Fig. 39B), but none of the lines were homozygous for *jai1*. Therefore, putative MYB4-like was considered for TILLING approach.

Two mutant lines harboring amino acid substitutions within and downstream of the DNA-binding domain were identified in putative MYB4-like. Both point mutations, V84I and S119F (Fig. 26A) are located at the C-terminus region of MYB4-like. According to the multiple sequence alignment (clustalWomega), putative MYB4-like DNA-binding domain was highly conserved among its close homologs, AtMYB13 (56%) and with other plant MYB homologs (Fig. 27). The V84I is located within the DNA-binding domain and appears to be weakly conserved among other plant MYB homologs (Fig. 26A). According to the predicted DNA-binding domain structure, V84I substitution occurs on the outer-surface layer of second Helix-Turn-Helix α -helix domain (Fig. 41). Substitution of valine with isoleucine (V84I) may not induce a greater conformational change, since both valine and Isoleucine possess similar structural properties and belong to aliphatic chain group (Betts and Russel, 2003). Relative transcript levels of *MYB4-like* were found to be almost equal in homozygous mutant lines, *Myb4-like_3551* and *Myb4-like_2998*, as well as the WT, without any significant difference (Fig. 30A). Interestingly, quantification of type VI glandular trichome numbers revealed significant differences between *Myb4-like_3551* and WT (Fig. 30B). This raises the possibility that substitution from valine to isoleucine within the MYB4-like DNA-binding domain could partially de-regulate protein function and lead to nearly 50% reduction in type VI glandular trichome numbers (Fig. 30B).

In the second mutant line, two amino acid positions downstream of putative MYB4-like DNA-binding domain, was found to be tightly conserved among the AtMYB and potato homologs, AtMYB13 and StMYB15, respectively, whereas, other MYB4-like homologs carry an asparagine (N) at position 119 in the *Myb4-like_2998* mutant line compared to the WT (Fig. 26). Substitution of serine to phenylalanine (S119F) may cause greater conformational change due to substitution from polar nature to hydrophobic nature (Betts and Russel, 2003) and also based on the predicted DBD protein structure (Fig. 41). The average type VI glandular trichome numbers were found to be equal between *Myb4-*

DISCUSSION

like_2998 and WT but significantly different between *Myb4-like_2998* and *Myb4-like_3551* (Fig. 30B). Although S119F could cause greater conformational change, equivalent levels of type VI glandular trichomes between *Myb4-like_2998* and WT might indicate no significant effect of S119F mutation on the MYB4-like function. This characteristic point mutation could lead to either positive or negative impact on plant meristematic activity, where trichome cell differentiation takes place (Dai et al., 2016). By contrary, no significant impact was observed in the quantification of type VI glandular trichomes in tomato, possibly due to the mutation outside the DNA-binding domain which may not affect the functionality of MYB4-like protein.

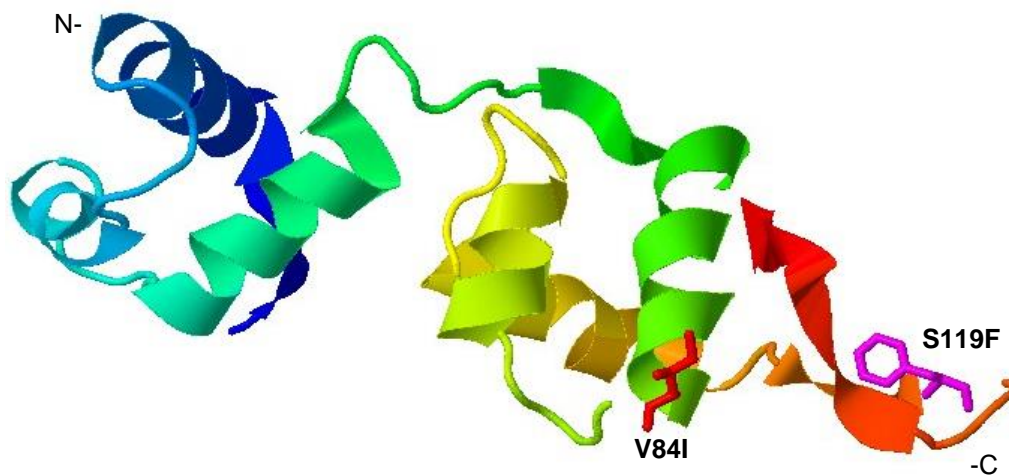


Figure 42: Predicted secondary structures of putative MYB4-like protein

The DNA-binding domain of putative MYB4-like depicts mutation positions at valine (V84I) and serine (S119F). Rainbow color scheme for MYB4-like domain protein is indicated by blue (N-terminus) and red (C-terminus) (generated on Phyre2 server).

Taken together, there were no significant changes in *MYB4-like* transcript levels in both mutant lines compared to WT. Significant reduction in type VI glandular trichomes was observed in the *Myb4-like_3551* compared to WT and *Myb4-like_2998* line, but not in between *Myb4-like_2998* and WT. This indicates that V84I within the DNA-binding domain is important for proper MYB4-like function. Phenotypic effects are obscure with the TILLING approach which may lead to minimal or no changes. Therefore, in future, characterization of MYB4-like loss-of-function mutants generated through CRISPR/Cas9 genome editing technology would be highly beneficial.

4.4.2.4 MYC2

Primary transformants overexpressing putative MYC2 failed to survive on plant regeneration media, which is assumed that overexpression of *35S::GFP:MYC2* might cause stress in transgenic plants. Alternatively, putative MYC2 was characterized through TILLING approach. In tomato, putative MYC2 full length protein was found to have a high similarity (41%, E-value<0.001) with uncharacteristic homolog, AtBhlh14 (Fig. 29). The N-terminus of the putative MYC2 protein (5-242 aa), necessary for repressing MYC2 activity by JAZ was highly similar (69%) to AtMYC2 and AtMYC3 (Zhang et al., 2015; Lian et al., 2017). Arabidopsis MYC2 and its closest homologs, MYC3 and MYC4, are highly similar on the protein level, but their functional properties differ from each other (Zhang et al., 2015; Lian et al., 2017).

Two TILLING mutation lines were obtained, a W153stop mutant in MYC2_7811 and a P215S exchange in line MYC2_6269 (Fig. 28B). Proline was conserved within *Solanum* and cotton MYC2 homologs but not with other plant bHLH encoding homologs. Unfortunately, there were no homozygous mutants obtained after genotyping for line MYC2_6269. Interestingly, mutation position at tryptophan (pos. W153) in putative MYC2_7811 generated a stop codon, which was also a conserved amino acid among other homologs (Fig. 29). According to the predicted secondary structure of putative MYC2 in tomato, the sequence similarity gives an idea that, tryptophan (pos. W153) might form a bridge between two α -helices by a beta-sheet at the C-terminus region of the predicted domain (5-242 aa) (Fig. 42). Bridging between two α -helices by a beta-sheet was shown to be important on resolved secondary structure of AtMYC3, due to its strong interaction site for JAZ proteins (Zhang et al., 2015). Therefore, protein disintegration due to stop codon may hinder MYC2 interaction with its Bhlh domain. On the phenotypic level, homozygous *myc2_7811* plants were quantified for type VI glandular trichomes on third true leaves (Fig. 30C). Interestingly, type VI glandular trichomes on *myc2_7811* mutant lines were significantly lesser, nearly 40% reduction compared to WT (Fig. 30C). This significant reduction in type VI glandular trichomes compared to WT could lead to possible predictions that there might be other putative trichome regulators, preferentially TFs forming a complex with MYC2 without depending on JAZ interaction complex on the N-terminus end. This could potentially activate downstream genes necessary for trichome formation. Furthermore, it is speculated that other putative MYC2 homologs in tomato could act redundantly and subsequently, bind the promoter G-box elements, to initiate the trichome

DISCUSSION

formation genes as shown by Lian et al. (2017). Taken together, stop codon at the N-terminus of putative MYC2 protein in *myc2_7811* lines has resulted significant reduction of type VI glandular trichome numbers. Further, mutational analysis in the N-terminus region of putative MYC2 protein could decipher alterations in type VI glandular trichome numbers.

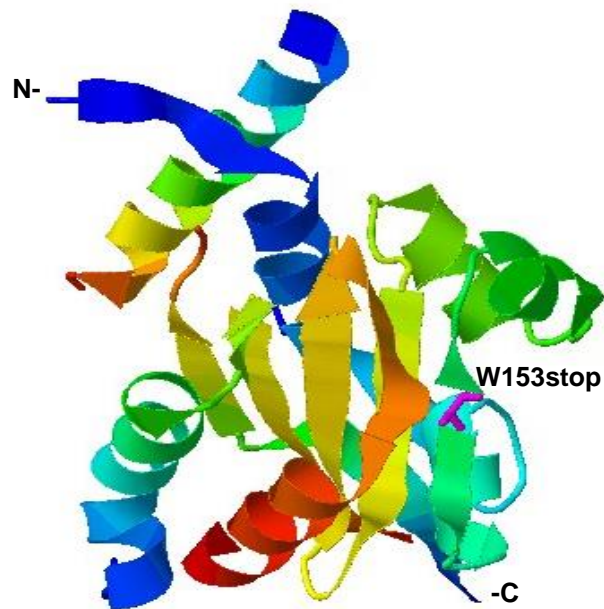


Figure 43: Predicted secondary structure of putative MYC2 protein

N-terminus (5-242 aa) of putative MYC2 protein showing mutation at tryptophan (W153Stop) to a stop codon. Rainbow color scheme for MYC2 domain protein is indicated by blue (N-terminus) and red (C-terminus).

Based on previous data, a conserved amino acid signature, [D/E]L*2[R/K]*3L*6L*3R, in the R3 domain of MYB proteins was found to interact with bHLH TFs in Arabidopsis (Zimmerman et al., 2004). Further, single amino acid substitution (S92F) in the R3 domain of GL1 affected trichome initiation, without forming any interaction with GL3 or EGL3 (Dai et al., 2016). It is speculated that type VI glandular trichomes are still produced irrespective of JAZ repression at the N-terminus or with the truncated repression complex. This speculation could be clarified considering future experiments like yeast-two-hybrid (Y2H) assays, bimolecular fluorescence complementation (BiFc) assays and pull-down experiments, to analyze not only the N-terminus of MYC2 protein but also the C-terminus end with the JAZ interaction (jas motif) domains of JAZ proteins, as there is an evidence that JAZ motifs interact with the C-terminus of Bhlh domain encoding TFs like TTG8, GL3

and EGL3, as well as the MYB75 in Arabidopsis (Qi et al., 2011). Along with protein-protein interaction experiments, abolishment of JAZ interaction by exogenous JA in planta could provide significant evidence that JA might play a potential role in glandular trichome formation. These ground breaking experiments could reveal much information not only with JAZ-MYC2, but also with other transcription factors which could potentially regulate glandular trichome formation in tomato.

Overall, there were positive remarks obtained by TILLING approach for putative MYB4-like and MYC2 transcription factors. Point mutations in putative MYB4-like and MYC2 candidates led to understand the modifications in the type VI glandular trichome numbers. TILLING approach has provided successive hints that putative MYB4-like and MYC2 candidates are involved in the formation of type VI glandular trichomes.

5 CONCLUSIONS

Understanding the regulation of molecular genetic network in the development of glandular trichomes is an essential aspect for biotechnological applications. Most of the work related to glandular trichomes is exceptionally carried out towards elucidating biochemical pathways of secondary metabolism. The current thesis provides a fundamental path for identifying regulatory components involved in the formation of type VI glandular trichomes mediated by the plant hormone JA. Transcription factors play a pivotal role in regulating gene expression for various plant developmental activities. The regulatory mechanisms are complex and hence poorly understood with respect to multicellular trichome formation. High throughput sequencing techniques like RNA sequencing has facilitated to uncover the expression patterns of low abundant transcription factors. According to the working hypothesis, transient assays and generation of stable transformants served as important tools to unveil candidate profiling towards understanding the JA regulated type VI glandular trichome phenotypes. Subsequently, characterization of candidate gene mutants identified in a TILLING approach supported loss-of-functionality of putative transcription factors with respect to type VI glandular trichome formation. Since transcription factors are usually part of complex regulatory networks involving redundancy or pleiotropism, partial effects in the formation of type VI glandular trichomes may be obtained in single mutants. Certainly, further experimental evidences are required to strengthen the functional analysis of putative candidates in future.

Future perspectives

With the high throughput sequence analyses of RNA-seq data, the enormous list of differentially expressed genes provides a footprint to identify closely related trichome regulatory orthologs from other plant species bearing multicellular trichomes. Novel trichome regulatory orthologs can be further validated to elucidate their functional properties. To strengthen the functional aspects of putative candidates, some experimental validation and characterization is necessary. This can be achieved by utilizing appropriate gene specific promoters for transactivation assays, functional interaction assays like yeast two-hybrid assay, co-immunoprecipitation assay (co-IP) and bimolecular fluorescence complementation (BiFC) to prove the interaction of putative transcription factors domains with JAZ proteins. Deleting specific interaction domains of putative transcription factors

using CRISPR/Cas9 technology may result in drastic phenotypic changes of type VI glandular trichome formation and density in comparison to conventional TILLING approach. Using exogenous JA treatments either on knockdown or overexpression lines would be advantageous to identify further genes involved in trichome formation. Lastly, re-considering *in situ* hybridization using RNA probes and performing GUS histological assays could lead to visualization of expression patterns of putative candidates across the tomato leaf epidermis. On a final note, identification of key regulators of trichome formation could contribute to breeding for enhanced resistance against phytophagous pathogens in the agronomic field or to produce valuable compounds, which is of immense interest in the biotech industries.

6 APPENDICES

6.1 List of oligonucleotides

6.1.1 Primers for genotyping *jai1* mutant population

Table A1: Genotyping *jai1* mutant population

| | |
|----------------------|--------------------------------|
| WT_For | 5'-CCATGGAGTCCATCACCTAACAGT-3' |
| <i>jai 1</i> _For | 5'-GTGGAGACGATATGTTGAGACTAA-3' |
| WT_ <i>jai1</i> _Rev | 5'-GTGGTCAGATCAGAGCCCTCTATT-3' |

6.1.2 Primers for quantitative real time PCR (qRT-PCR)

Table A2: Jasmonic acid-dependent genes for reference

| | |
|-------------------------------------|--------------------------------|
| Allene oxide cyclase (AOC)_For | 5'-TTCTACTTCGGCGATTACGGTC-3' |
| Allene oxide cyclase (AOC)_Rev | 5'-GGTTAAGTACGCTCCCTGAACG-3' |
| Threonine deaminase (TD)_For | 5'-CTTTATGCCGTTACCGTAATCAGG-3' |
| Threonine deaminase (TD)_Rev | 5'-GGAATCTGGAATCCCATCAACA-3' |
| Proteinase Inhibitor 1 (PIN1)_For | 5'-TCCTGGTATGATTAGGCCACT-3' |
| Proteinase Inhibitor 1 (PIN1)_Rev | 5'-GGGAGTAACTCGAACAATGCG-3' |
| Leucine Amino Peptidase (LAP A)_For | 5'-CCTGGTAATGGCGGTGCTATAA-3' |
| Leucine Amino Peptidase (LAP A)_Rev | 5'-TCGAGATGCAACCACTGAACC-3' |

Table A3: Genes involved in trichome initiation and induction: Orthologous of Arabidopsis in tomato

| | | |
|--------------------|----------------|------------------------------|
| Solyc05g053150.1.1 | MYB23-like_For | 5'-TGTGCCAAAACAAGACATGACC-3' |
| | MYB23-like_Rev | 5'-ACCACCTTGTTGATCTTGCTC-3' |
| Solyc08g081140.2.1 | GL3-like_For | 5'-TTGTGCGCCAATCAAGAGGCA-3' |
| | GL3-like_Rev | 5'-CCCCAATACCGTCTACCACC-3' |
| Solyc03g015440.2 | TTG1-like_For | 5'-ACTTCTTCCCTCACAAACCG-3' |
| | TTG1-like_Rev | 5'-CCCGATTGTTGAACTCTTCG-3' |
| Solyc01g095640.1.1 | SITRY_For | 5'-ACAGGTGGGGGCTTATAGCA-3' |
| | SITRY_Rev | 5'-TTCTTCTGCTGTTCTCCCTGG-3' |

Table A4: Putative transcription factors identified from apex/ trichome RNAseq data (upregulated in wild type and cultivated trichomes)

| | | |
|--------------------|------------|---------------------------------|
| Solyc08g081140.2.1 | GL3_For | 5'-AGTGAAGAAGACCTGCAGCC-3' |
| | GL3_Rev | 5'-CTTCCCTGGTAACCCTTGCC-3' |
| Solyc01g095640.1.1 | MYB Tf_For | 5'-ACTTGTTGGAGACAGGTGGG-3' |
| | MYB Tf_Rev | 5'-TCTTGTGTGCAAACCCATCAC-3' |
| Solyc03g120620.2.1 | GL2_For | 5'-CGCGTTCTTACCCCGTTATT-3' |
| | GL2_Rev | 5'-AAAGCATGAAGAAGAGAAGGAAAGA-3' |

| | | |
|--------------------|----------|----------------------------|
| Solyc03g097340.1.1 | TTG1_For | 5'-TGGCTGAACTGGAAAGGCAT-3' |
| | TTG1_Rev | 5'-CGTCATCCCCACCAGAACAA-3' |
| Solyc07g008010.2.1 | CPC_For | 5'-TCAGACCGAACATCAAGCGA-3' |
| | CPC_Rev | 5'-CCAGCAATTAGCGACCATCG-3' |

Table A5: Putative transcription factors identified from the leaf RNA-seq data

| Selected putative candidates | | |
|--|-----------|--------------------------------|
| Solyc11g069700.1.1 (Reference gene) | EF_For | 5'-ACCACGAAGCTCTCCAGGAG -3' |
| | EF_Rev | 5'-CATTGAACCCAACATTGTCACC -3' |
| Solyc08g082890.2.1 | MYB 9_For | 5'-CGGACGATTACCTGGTCAA -3' |
| | MYB 9_Rev | 5'-TCCTTATGGGCTTTGGTCAA -3' |
| Solyc01g096370.2.1 | MYC 2_For | 5'-ACAACCAGAGCGCCACCACCT -3' |
| | MYC 2_Rev | 5'-CTCCGGGGCTGCTGTGGGAT -3' |
| Solyc06g083900.2.1 | MYB 4_For | 5'-CAACCAAGTCCATCATCGTCAGT -3' |
| | MYB 4_Rev | 5'-TCGACTCTGAACTCGTTGCAGT -3' |
| Solyc06g035940.2.1 | PDF 2_For | 5'-GTGTGCTAATGGGGGTGCTA -3' |
| | PDF 2_Rev | 5'-AGCTCCACACAAGAAGGGTC -3' |
| GFP | sGFP_For | 5'-GGGCACAAGCTGGAGTACAAC-3' |
| | sGFP_Rev | 5'-ATGTTGTGGCGGATCTTGAAGT-3' |

| Other putative candidates from RNA-seq data | | |
|--|--------------------|--------------------------------|
| Solyc05g052610.2.1 | DIVA_For | 5'-CGATCGATGAAGACCTAATGGC -3' |
| | DIVA_Rev | 5'-CCAAGATTGAGGTGAGAATAGCA -3' |
| Solyc08g005870.1.1 | MYB 308_For | 5'-CCACATGCACAGGATTTTCGC -3' |
| | MYB 308_Rev | 5'-AGGTTGAGCTACTTGTGCCA -3' |
| Solyc04g076720.1.1 | PIP 3_For | 5'-GGAGACCACCCAAAATATCCGCG -3' |
| | PIP 3_Rev | 5'-GGCGCACCTCCGACCAGAAA -3' |
| Solyc09g005770.1.1 | Fbox_For | 5'-GGTAATGAGGTGGGAGCCGT-3' |
| | Fbox_Rev | 5'-CTCCATCCGCTCCGTCTTGT-3' |
| Solyc04g071770.2.1 | ERF 2a_For | 5'-CCTCTGTTAAGCTCGAAGAAGA -3' |
| | ERF 2a_Rev | 5'-CTCCTCTTCTCCTCCCCTGT -3' |
| Solyc03g098780.1.1 | Kunitz Type_For | 5'-GGAGACTGGAGGAAGCATAGGG-3' |
| | Kunitz Type_Rev | 5'-CCCTTACGGCAAAATGGACAGA-3' |
| Solyc03g098720.2.1 | Kunitz Trypsin_For | 5'-CCCCGCGTGAATTTGACAGA-3' |
| | Kunitz Trypsin_Rev | 5'-ACCTTCCACCATCCACACGT-3' |
| Solyc07g008570.2.1 | PAP 27-like_For | 5'-GTTGAATGGGGTTGGAAGGGC-3' |
| | PAP 27-like_Rev | 5'-TGAATCCAGGATCGCGCCAT-3' |
| Solyc07g007250.2.1 | MCPI_For | 5'-AGATGCAACTCTGACGAACTTT-3' |
| | MCPI_Rev | 5'-ACATGTCCCCGCGAACCTC-3' |
| Solyc01g006390.2.1 | CRE_For | 5'-CACCACCAACACCATCCCCT-3' |
| | CRE_Rev | 5'-GGCAACTAGTCCCAAGTGTACT-3' |
| Solyc08g076930.1.1 | TF unknown_For | 5'-TGGGGCTGGGGAGGAGAATA-3' |
| | TF unknown_Rev | 5'-CCGCCTCCACCTGACTTCAT-3' |
| Solyc10g055760.1.1 | NAC D_For | 5'-GGCTGAACTGCAAGTACCCA-3' |
| | NAC D_Rev | 5'-GCTACGCAATTGCATCCACA-3' |
| Solyc09g015770.2.1 | WRKY 6_For | 5'-CAACATTTGAAGCCTCCGGC-3' |
| | WRKY 6_Rev | 5'-AGTTCCAAAGACCCTCCTCA-3' |
| Solyc09g014990.2.1 | WRKY 26_For | 5'-GTCTCAACCAGCAGCCAGAT-3' |
| | WRKY 26_Rev | 5'-TCGTTGTGGAAGTGTGGCT-3' |
| Solyc08g008280.2.1 | WRKY 30_For | 5'-TGCCAGTAGTTCCAAGGCCT-3' |
| | WRKY 30_Rev | 5'-GGAGGGTGATTGGTGGTTGGA-3' |

| | | |
|---------------------------|-------------|------------------------------|
| Solyc05g050560.1.1 | Bhlh 13_For | 5'- CATTGAAGCCGCCAGTGATG -3' |
| | Bhlh 13_Rev | 5'- TCCCACGGCAAGTTTTGACT -3' |
| <u>Solyc07g018010.2.1</u> | Bhlh 35_For | 5'- TCTGGGAGGCTTCTCAAGAC -3' |
| | Bhlh 35_Rev | 5'- ACTCATCGGGCTATCGGGA -3' |

Table A6: Putative TILLING mutant lines

| | | |
|--------------------|----------|--------------------------------|
| Solyc06g083900.2.1 | 3551_For | 5'- GAATTTTTCTTCAACATTATA -3' |
| | 3551_Rev | 5'- TCATAATTCAGGCAATTCTAAC -3' |
| | 2998_For | 5'- GAATTTTTCTTCAACATTATA -3' |
| | 2998_Rev | 5'- TCATAATTCAGGCAATTCTAAC -3' |

Table A7: Primers for cloning putative candidates via Golden Gate cloning mechanism

| | | |
|--------------------|------------|--|
| Solyc08g082890.2.1 | MYB 9_For | 5'- TTAGAAGACAAAATGGGAAGAGCACCATGTTG TGC-3' |
| | MYB 9_Rev | 5'- AATGAAGACTTAAGCTTACATTGAGAATTTTTG CTCCGTTTGATC- 3' |
| Solyc01g096370.2.1 | MYC 2_For1 | 5'- TTAGAAGACAAAATGGAACAACCTCGCGGTTTC C -3' |
| | MYC 2_Rev1 | 5'- AAAGAAGACTCCATCTCCCAAGCTAAAAAGT TTTTTC -3' |
| | MYC 2_For2 | 5'- TTAGAAGACGAGATGGATATTTCCAAGGAGAT GGTGTAG -3' |
| | MYC 2_Rev2 | 5'- AATGAAGACTTAAGCTTACAAATCATAGCTAG TAAGAAGAGCAGTCCTTAG -3' |
| Solyc06g083900.2.1 | MYB 4_For1 | 5'- TTTGAAGACAAAATGGGGAGATCTCCTTGC -3' |
| | MYB 4_Rev1 | 5'- TTTGAAGACATCAGGCCTCAAGTAATTAGTCC -3' |
| | MYB 4_For2 | 5'- TTTGAAGACGGCCTGATATTAAGCGAGG -3' |
| | MYB 4_Rev2 | 5'- TTTGAAGACAAAAGCTCATAATTCAGGCAATT CTAACATCAACTC -3' |
| Solyc06g035940.2.1 | PDF 2_For1 | 5'- TTAGAAGACAAAATGGAGAAATCGACAATGGA ATTGAGTAAC -3' |
| | PDF 2_Rev1 | 5'- TTTGAAGACTATTGCGTTTTTCGATATGGATCG TTTA -3' |
| | PDF 2_For2 | 5'- TTTGAAGACAAGCAATCGGAACGATATAATAA GAGAGTG -3' |
| | PDF 2_Rev2 | 5'- AATGAAGACTTAAGCTCAAATTAAGAGAGCAC TTTTAATCTTATGAATGGTATGC -3' |

Table A8: Primers for cloning ATML1 promoter

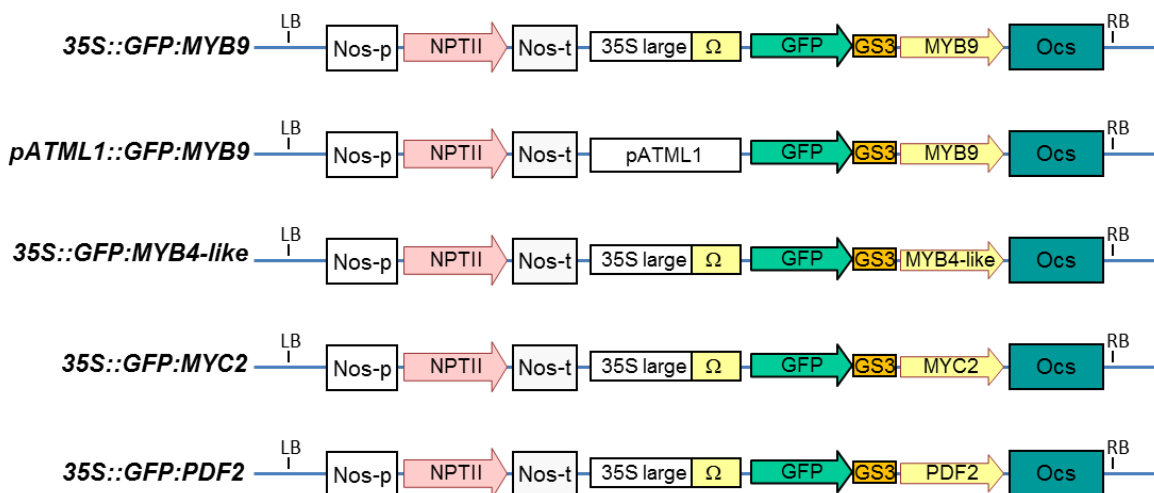
| | |
|-----------|--|
| ATML_For1 | 5'- TTTGGTCTCAACATAATGACAAGCCGTAGATGATTGGTTTTTC -3' |
| ATML_Rev1 | 5'- TTTGGTCTCAAGAGGAGTCCGGTAATCATATAG -3' |
| ATML_For2 | 5'- TTTGGTCTCACTCTTTATAAGCAACCACAGTT -3' |
| ATML_Rev2 | 5'- TTTGGTCTCAACAATGTCGTCCTCCTCGTGAATT -3' |
| ATML_For3 | 5'- TTTTGGTCTCAACATGACAAATGCAAGGAAACACAGC -3' |
| ATML_Rev3 | 5'- TTTGGTCTCAACAATTATAGTATACACTGATGTTAATTAATTTTTG -3' |
| ATML_For4 | 5'- TTTGGTCTCAACATATAATTACTACTCTAGCCAACAAG -3' |
| ATML_Rev4 | 5'- TTTGGTCTCAACAACATTATAGCCGGTCAAGACATAACC -3' |

6.2 List of antibiotics

Table A9: List of antibiotics used in bacterial and plat growing media

| Antibiotic | Stock concentration | Work concentration |
|---------------|---------------------|--------------------|
| Rifampicin | 50 mg/mL | 50 µg/mL |
| Ampicillin | 50 mg/mL | 50 µg/mL |
| Carbenicillin | 50 mg/mL | 50 µg/mL |
| Kanamycin | 50 mg/mL | 50 µg/mL |
| Gentamycin | 25 mg/mL | 25 µg/mL |
| Spectinomycin | 100 mg/mL | 100 µg/mL |
| IPTG | 1 M | 0.5 mM |
| X-Gal | 50 mg/mL | 50 µg/mL |

6.3 Golden gate cloning strategy

**Figure A1: Assembly of modules for golden gate cloning.**

Individual modules were assembled to clone putative candidates under the control of 35S and *ATML1* promoters using golden gate cloning strategy. Nos-p: Nopaline synthase gene promoter; Nos-t: Nopaline terminator; NPTII: Neomycin phosphotransferase (kanamycin

resistant) reporter gene; 35S large Ω : Large 35S constitutive promoter; pATML1: *ATML1* promoter; GFPxGS3: GFP reporter with one glycine and 3 serine repeats; Ocs: Octopine synthase gene terminator and LB / RB: left and right borders, respectively.

6.4 Jasmonate measurements in young tomato plants

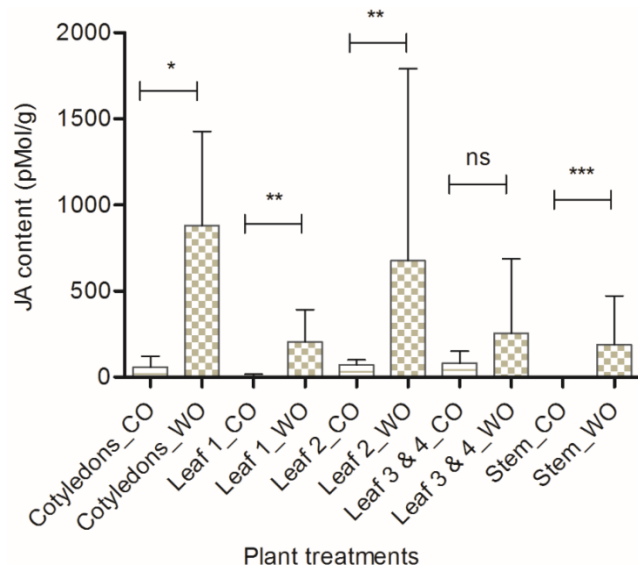


Figure A2: Determination of JA levels in young tomato plant organs.

Cotyledons, four true-leaves and stem of 2-weeks old young tomato plants were used for treatments, control (CO) and wounded (WO). Error bars represent SD, $n = 3$. Significance test determined by students t-test (asterix represent *** $p < 0.001$, ** $p < 0.01$ and * $p < 0.05$)

6.5 Transcriptome sequencing analysis

6.5.1 Differentially regulated genes across WT control and JA- treatments

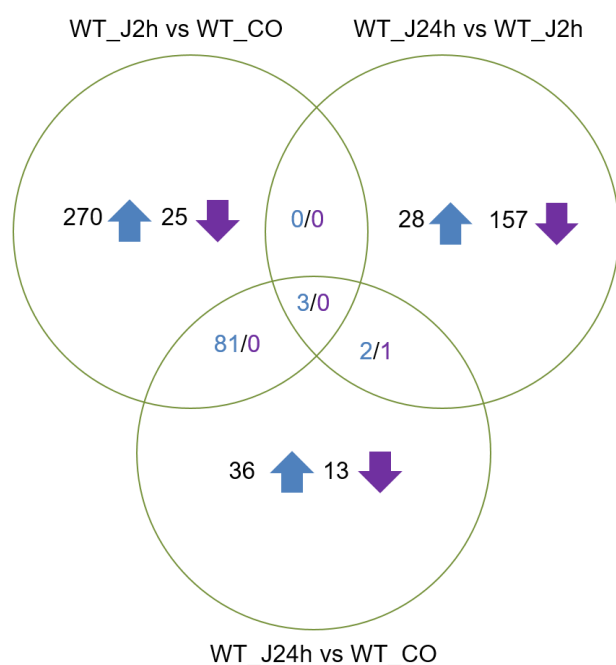


Figure A3: Venn diagram scheme representation.

Differentially expressed genes among the treatment conditions, WT_CO, JA_2h and JA_24h, respectively. Genes were normalized according to Benjamini-Hochberg correction at the $FDR < 0.05$, across treatment conditions. Blue and violet arrows indicate up and down regulated genes across treatment conditions, respectively.

█ Up-regulated genes
█ Down-regulated genes

6.5.2 Clustering of highly significant genes across treatment conditions

Table A10: List of highly significant genes differentially regulated across WT_CO, JA_2h, JA_24h and jai1_CO treatment conditions

| Solyc ID | Gene annotations |
|--------------------|---|
| Solyc08g076970.2.1 | Acetylornithine deacetylase or succinyl–diaminopimelate desuccinylase |
| Solyc09g084490.2.1 | Proteinase inhibitor I |
| Solyc03g098710.1.1 | Kunitz–type proteinase inhibitor A4 (Fragment) |
| Solyc09g089510.2.1 | Proteinase inhibitor I |
| Solyc09g089490.2.1 | Proteinase inhibitor I |
| Solyc07g007250.2.1 | Metallocoxy-peptidase inhibitor |
| Solyc03g098780.1.1 | Kunitz–type protease inhibitor |
| Solyc09g089530.2.1 | Proteinase inhibitor I |
| Solyc11g022590.1.1 | Kunitz trypsin inhibitor 4 (Fragment) |
| Solyc07g006380.2.1 | Defensin–like protein |
| Solyc08g080040.2.1 | Anthocyanidin synthase |
| Solyc12g088170.1.1 | Hydroxycinnamoyl CoA quinate transferase |
| Solyc02g085020.2.1 | Dihydroflavonol 4–reductase |
| Solyc07g043460.2.1 | Cytochrome P450 |
| Solyc12g006470.1.1 | Aminotransferase–like protein |
| Solyc02g086180.2.1 | Sterol C–5 desaturase |
| Solyc10g008410.1.1 | RING finger protein 5 |
| Solyc02g069490.2.1 | FAD linked oxidase domain protein |
| Solyc12g096770.1.1 | Hydroxycinnamoyl CoA quinate transferase |
| Solyc09g008670.2.1 | Threonine ammonia–lyase biosynthetic |
| Solyc02g086880.2.1 | Formate dehydrogenase |
| Solyc11g071480.1.1 | Hydroxycinnamoyl CoA shikimate |
| Solyc03g007240.2.1 | Spermidine synthase 1 |
| Solyc06g083900.2.1 | Myb–related transcription factor |
| Solyc01g105890.2.1 | (E)–beta–ocimene synthase |
| Solyc03g121270.2.1 | IAA–amino acid hydrolase |
| Solyc05g052610.2.1 | MYB transcription factor |
| Solyc09g005770.1.1 | F–box family protein |
| Solyc05g032660.2.1 | Dehydrogenase/ reductase 3 |
| Solyc09g005540.1.1 | NAD–dependent epimerase/dehydratase |
| Solyc02g090350.2.1 | Cytochrome P450 |
| Solyc08g076930.1.1 | Transcription factor |
| Solyc10g005320.2.1 | Tryptophan synthase beta chain 1 |
| Solyc04g071770.2.1 | Ethylene responsive transcription factor 2a |
| Solyc09g015070.2.1 | Reductase 1 |
| Solyc06g083890.2.1 | Pre–mRNA–splicing factor SLU7–A |

| | |
|--------------------|--|
| Solyc01g007640.2.1 | Ycf2 29.8 protein assembly and cofactor ligation |
| Solyc11g008780.1.1 | Acetolactate synthase small subunit |
| Solyc02g062960.2.1 | Homeobox-leucine zipper protein |
| Solyc02g044030.1.1 | 60 kDa chaperonin |
| Solyc11g072250.1.1 | Unknown Protein |
| Solyc05g053100.2.1 | Dihydrolipoyl dehydrogenase |
| Solyc04g051280.2.1 | F16G16.9 protein (Fragment) |
| Solyc01g007370.2.1 | Chloroplast envelope membrane protein A |
| Solyc12g088010.1.1 | Aberrant pollen transmission 1 |
| Solyc01g007600.2.1 | 50S ribosomal protein L16 chloroplastic |
| Solyc03g007800.2.1 | Topoisomerase 1-associated factor 1 |
| Solyc07g017700.1.1 | Uncharacterized conserved protein |
| Solyc06g006040.1.1 | Receptor like kinase, RLK |
| Solyc11g069700.1.1 | Elongation factor 1-alpha |
| Solyc06g017860.1.1 | Serine carboxypeptidase |
| Solyc07g006280.2.1 | Senescence-associated protein |
| Solyc06g035940.2.1 | Homeobox-leucine zipper protein PROTODERMAL FACTOR 2 |
| Solyc07g007130.1.1 | NHL repeat-containing protein |
| Solyc04g039670.2.1 | ATP-citrate lyase A-2 |
| Solyc02g089900.1.1 | Receptor-like kinase |
| Solyc07g065900.2.1 | Fructose-bisphosphate aldolase |
| Solyc01g109700.2.1 | Transcription factor |
| Solyc07g008100.2.1 | Genomic DNA chromosome 3 P1 clone MUJ8 |
| Solyc03g005320.2.1 | Fatty acid elongase 3-ketoacyl-CoA synthase |
| Solyc10g079090.1.1 | Chaperone protein dnaJ 6 |
| Solyc12g013710.1.1 | Protochlorophyllide reductase |
| Solyc04g008230.2.1 | Polygalacturonase |
| Solyc05g008820.2.1 | Lipid phosphate phosphatase 3 |
| Solyc02g055370.2.1 | Transcriptional factor B3 family protein |
| Solyc11g006710.1.1 | Cationic amino acid transporter |
| Solyc08g068600.2.1 | Decarboxylase family protein |
| Solyc08g008280.2.1 | WRKY transcription factor-30 |
| Solyc09g015770.2.1 | WRKY transcription factor 6 |
| Solyc06g005170.2.1 | Mitogen-activated protein kinase 3 |
| Solyc03g095770.2.1 | WRKY transcription factor 6 |
| Solyc09g014990.2.1 | WRKY-like transcription factor |
| Solyc10g055760.1.1 | NAC domain protein IPR003441 |
| Solyc01g079830.2.1 | Unknown Protein |
| Solyc06g030470.2.1 | Auxin-regulated protein |
| Solyc10g047530.1.1 | Phototropic-responsive NPH3 family protein |
| Solyc02g083170.2.1 | F-box family protein |

| | |
|--------------------|--|
| Solyc02g089350.2.1 | Gibberellin regulated protein |
| Solyc02g069070.2.1 | Ribonuclease H2 subunit C |
| Solyc01g095530.2.1 | Unknown Protein |
| Solyc06g059710.2.1 | Stearoyl-acyl carrier protein desaturase |
| Solyc07g061880.1.1 | Unknown Protein |

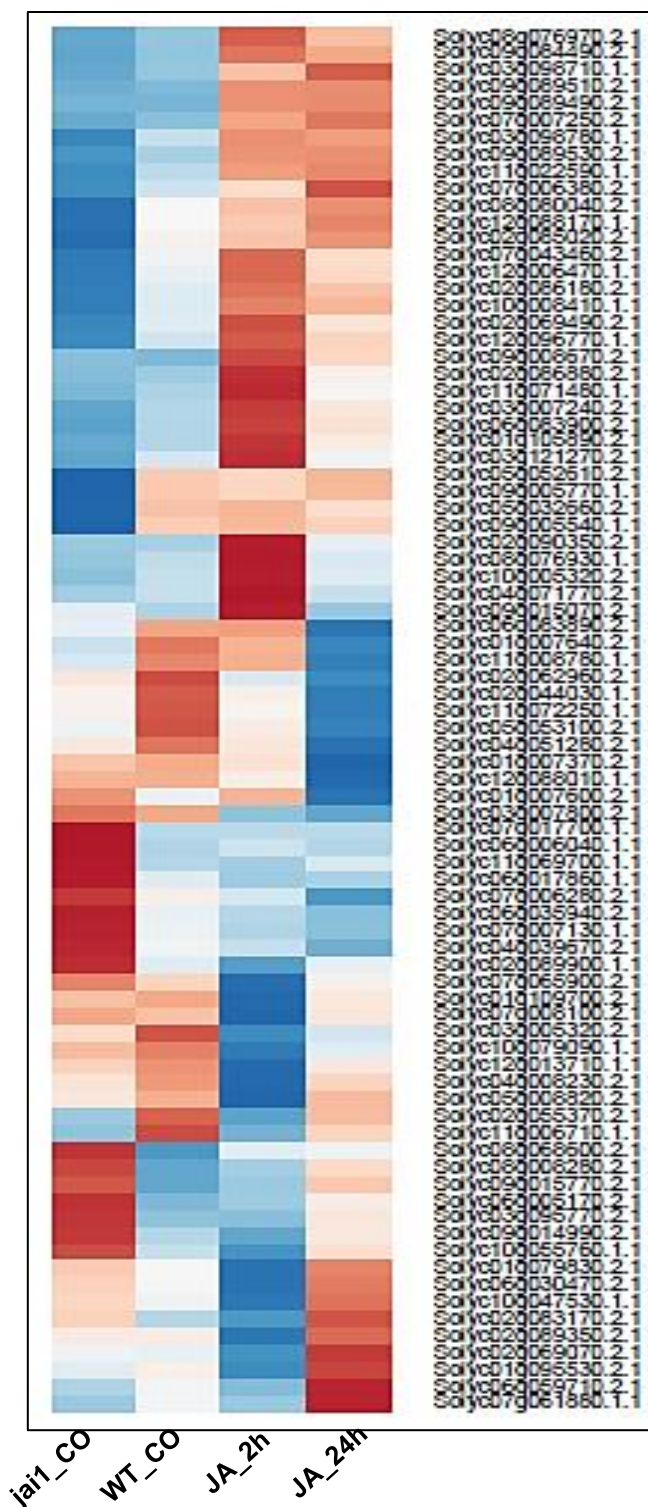
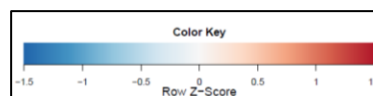


Figure A4: Representation of gene clusters on the heatmap

Clusters depicting highly significant genes that were differentially regulated across treatment conditions with p-values adjusted to Benjamini-Hochberg correction (FDR<0.05). Color key represents Row-Z-Score for each transcription factor that has been scaled and transformed to each treatment condition. Red indicates high expression (log2FC = 1) and blue indicates low expression (log2FC = -1) for each candidate across particular treatment condition, respectively. Transcription factors highlighted with yellow marker were chosen for validation analysis.



6.6.3 Putative MYC2 protein homologs in closely related species

| | | |
|-------------|---|-----|
| AtbHLH14 | MYNLTFSFSLSSSSLLSFTQQTAAIVSSSPDLVLQKLRFFVETS PDRWAYVIFWQKMF | 60 |
| SlMYC2 | MEQLAVSSSPMA-----VAPPPVDVNQVPLGLQMLQYVVKSQPEWWAYAIFWQTSN | 52 |
| StMYC2-like | MEQLLVSSSPMAA-----SLPPPPVDVNQVPLDLQMLQYVVKSQPEWWAYAIFWQTSN | 55 |
| GmMYC2-like | MEELIISPSSSS-----SLVLSLQENPTPTLQKQLQFLLQSQPDWWVYVIFWQASH | 51 |
| PoptrbHLH | MEELIISPSSPS-----SPVLSLQETPP-TLQQLQFIVQNQPDWWSYVIFWQTSN | 50 |
| TcbHLH | MEELIISPSSSS-----SLVFSLQETPPSTLQQLQFVIQSQPDWWAYVIFWQTSN * : * . * * : . . . *** *:::.. : * *.**** | 51 |
| AtbHLH14 | DDQSDRSYLWVDGHFCGNKNNSQENYTTNSI-----E-----C | 95 |
| SlMYC2 | DD-EGKNFLAWGDGYFQGDGVVNNKGGGSSSSSLKSQAQSERKKVIKGIQALMDNGDGT | 111 |
| StMYC2-like | DD-DGKNFLAWGDGYFQGDGVVNNKGGSSSSSSSLKSQAQSERKKVIKGIQALMDNGDGT | 114 |
| GmMYC2-like | DD-NGNLYLSFGEGHFQGTKETSPKSLTI-PTK-----NKF | 85 |
| PoptrbHLH | DD-SGRIFLGWGDGHFQGSKDTSPKNTF-SNSRMTISNSERKRVMKGIQSLIGECHDL | 108 |
| TcbHLH | DE-HGRFLFTWGDGHFQGTKDTSPKLGAN-ISNIPGL--NNERRKVMKGIQALIGDNHDI * : . . : * : : * * * : . . . | 107 |
| AtbHLH14 | E-LMMDGG--DDLELFYAASFY---GE-----DRSPRKEVSDSLVWLTG | 134 |
| SlMYC2 | D--LVDDGDVTDTEWFYVMSLARSFSAGD-----GSVTGKAFGSDDFLWITG | 156 |
| StMYC2-like | D--LVDDGDVTDTEWFYVMSLARSFSAGD-----GSVTGKAFGSDDFLWITG | 159 |
| GmMYC2-like | LMKTPTNDNINDAEWFYVMSLTRSFVNNSSNSTSCSSSSSLPGKSFALGSLVWQNN | 145 |
| PoptrbHLH | DMSLMDGNDATDSEWFYVMSLTRSFSPG-----DGILGKAYTTGSLIWLITG | 154 |
| TcbHLH | DMSMIDGTDITDAEWFYVMSLTRSFAG-----DGIPGKALSTGSLVWLTG . * * * . * : . . . * . . . * . . . | 153 |
| AtbHLH14 | PDELRF-SNYERAKEAGFHGVTLSVIPINNGI IELGSSSEIIQNRNFINRVKSI FGS GK | 193 |
| SlMYC2 | PDQFQLHYSCERAKEAQIHGIQTLVSIPTSNGVFELGSTQLIKQNLVQVQVKSFLCCP | 216 |
| StMYC2-like | PAQFQLHYSCERAKEAQIHGIQTLVCIPTSNGVFELGSTQLIKQNLVQVQVKSFLCCP | 219 |
| GmMYC2-like | RHELQ-FYNCERSNEAHMHG IETLICIPTQNGVEMGSYDTIKQNWNLVQHVKSLFHTSP | 204 |
| PoptrbHLH | GHELQ-FYNCERVKEAQMHG IETLVC IPTSCGVLELGS SSVIRENWGLVQQA KSLF GSD L | 213 |
| TcbHLH | AHELQ-FYNCERAREAQMHA IETLVC IPTSCGVLELGS SEMIRENWGLVQQA KSVF GSD L ::: . . * * . * * : * . . * * . * . * . * . * . * : * : : : . * * . * | 212 |
| AtbHLH14 | TTKHTNQ TGSY---PKPA--VSDH----- | 212 |
| SlMYC2 | -----PIQ-FLEKTISFADIGLV TGLQDDNDYK LRENSRK----- | 251 |
| StMYC2-like | -----PIQ-FLEKSI CFADIGLV TGLQDDNDK LRENSK KQ----- | 255 |
| GmMYC2-like | DP-----VTVQILDDHII SFADIGIVAGIQETKRRKQIT----- | 238 |
| PoptrbHLH | SAYLVPKGP--NNSSEPTQ-FLDRSISFADMGIIAGLQEDCAVDREQKNARETEEANKR | 270 |
| TcbHLH | IGLVPKQSNPNPNLTPGPIQ-FLDRNISFADIGIIAGVQEEASPDNRKTKQENHNNTKK . : : | 271 |
| AtbHLH14 | --SKSGNQQFGSE-----RKRRLKLETRVAAATKEKHHPAVLSHVEAEK | 255 |
| SlMYC2 | -----P-----HPVAK-KRGRKPKGG EDAHMAALNHVEAE R | 283 |
| StMYC2-like | -----P-----QPVVAKKRGRKP--KEDANMAALNHVEAE R | 285 |
| GmMYC2-like | QTAPSKNDNYVDSEHSDSDCPTLPTATPTASEPKRGRKPV LGRE---TPINHVEAE R | 294 |
| PoptrbHLH | NANKPG-LSYLNSEHSDSDFLLAMH--MEKRI PKRGRKPG LGRD---APLNHVEAE R | 323 |
| TcbHLH | DSTKPGQSSYVDSEHSDSDFLLAMN-IEKRTPKRGRKPG LGRE---TPLNHVEAE R : * . : : : . * * * . * | 326 |
| AtbHLH14 | QRREKLNHRFYALRAIVPKVSRMDKASLLSDAVSYIESLKS KIDDELETEI----KMKM | 310 |
| SlMYC2 | QRREKLNHRFYALRSVVPNVSRMDKASLLSDAVSYINQLKAKVDELELQLIDHTKKPKIV | 343 |
| StMYC2-like | QRREKLNHRFYALRSVVPNVSRMDKASLLSDAVSYINQLKAKVDELELQLIDHTKKPKNV | 345 |
| GmMYC2-like | QRREKLNHRFYALRAVVPNVSRMDKASLLSDAVAYINELKAKIEDLESQQPRDSNKKMKT | 354 |
| PoptrbHLH | QRREKLNHRFYALRAVVPNVSRMDKASLLSDAVSYINELKAKVDELESQLERES-KKVKL | 382 |
| TcbHLH | QRREKLNHRFYALRAVVPNVSRMDKASLLSDAVSYINELKAKIEELESQLOREC-KKVKV ***** : . * : ***** : * . * . * . * : : * * : * | 385 |

APPENDICES

| | | |
|-------------|--|-----|
| AtbHLH14 | TETDKLDNSSSNTSPSSVEYQVNQKPSKSNRGS DLEVQVKIVGEEAIIIRVQ TENVNHP TS | 370 |
| SlMYC2 | TESSADNQSATTSSDDQVIKA-A-----NPTAAPEVEVKI VGT DAMIRVQSE NVDYPSA | 397 |
| StMYC2-like | TESSADNQSTTTSSDDQVIKA-----NSTAAPEVEVKI IGT DAMIRVQSE NVDYPSA | 398 |
| GmMYC2-like | EMTDTLDNQSATTSTVVDQSG-SGSRLGLGPLGLEVDVRI VGP DAMVRVQSE NVNHPGA | 413 |
| PoptrbHLH | EVADNLDNQSTTTSV DQSACRP-NSAGGA--GLALEVEIKFV GNDAMIRVQSE NVNYPAS | 439 |
| TcbHLH | EMVDAMDNQSTTTSV DQAARPS-NSSSGTAGSGGLEFDIKIM GNDAMIRVQSE NVNYP SA | 444 |
| | . **.*:.*: *.:*:*:*:*:*:*:* | |
| AtbHLH14 | ALMSALMEMDCRVQHANASRLSQVMVQDVVVLVPEGLRSE DRLR T TLVRTL S L- | 423 |
| SlMYC2 | KLMIALQNLQM QVHHASISSVNHLVLHDVVVRVPQGLSTE DELRTALLTSYDL- | 450 |
| StMYC2-like | KLMIALQNLQM QVHHASISSVNHLVLHDVVVRVPQGLSTE DELRTALLTRLEHH | 452 |
| GmMYC2-like | RLMGALRDLEFQVHHASMSCVNDLMLQDVVVKLPNGMRSEESLKS AII MR L D Q- | 466 |
| PoptrbHLH | RLMCALRELEFQVHHASMSCVNELMLQDVVVRVPDGLRTEEALKSALLGRLE-- | 491 |
| TcbHLH | RLMIALRDLEFQVHHASMSCVNELMLQDIVVRVPDGLRTEEGLKSALLRRLEQ- | 497 |
| | ** ** :: :*:**.* * .:.*:*:*:*:*:*:*:*:*:*:*:*:*:*:*:*: | |

Figure A7: Multiple sequence alignment of putative full-length MYC2 and its homologs.

Putative full-length MYC2 indicating basic Helix-loop-Helix (bHLH) domain highlighted by green for closely related homolog species. Black bars represent bHLH domain showing H5*, E9* and R12* positions important for DNA-binding activity are marked in red, respectively.

6.6.4 Putative PDF2 protein homologs in closely related species

| | | |
|---------------|---|-----|
| PoptrHomeobox | ----- | 0 |
| AtANL2 | MNFGSLFDNTPGGGSGTARLLSGLSYGNHTA-----ATNVLPGGAMAQAAAAASLFSP | 54 |
| StCD2 | MNFGGFLDNNSGGGGAR--IVADIPFNHNSSSNND-NKNNNMPTGAI SQPRL--L--PQS | 53 |
| GmHomeobox | MSFGGLLDNKSGSGGARN-NVSDIPYNNNNVTNTTTTNNDRMPFGAISQPRL--VTTPT | 57 |
| TcHDdomain | MSFGGFLDNNSGGGGAR--IVADIPYSN-----NMPTGAIAPRL--V--SPS | 42 |
| SlPDF2 | ----- | 0 |
| StHomeobox | ----- | 0 |
| PoptrHomeobox | -----MDSHGDMGLLGEHFD--PSLVGRMREDGYESR | 30 |
| AtANL2 | LTKSVYASSGLSLALEQPERGTNRGEASMRNNNNVGGGGDTFD--GSVNRRSREEEHESR | 112 |
| StCD2 | LAKNMFNSPGLSLALQ-TGMEGQNEVTRM-----AENYEGNNSVGRRSREEEPDSR | 103 |
| GmHomeobox | LAKSMFNSGLSLALQ-TNIDGQEDVNRM-----AENTSEPNG-LRRSREDEHESR | 106 |
| TcHDdomain | LAKNMFNSPGLSLALQQPNIDNQDGTMR-----GENFEGSV--GRRSREEEHESR | 91 |
| SlPDF2 | -----MEKSTME | 7 |
| StHomeobox | -----MEDQKDMS | 8 |
| | : | |
| PoptrHomeobox | SGSDNIEGASGEDQDAGDYQRPRKKYNRHTANQIQELESFFKECPHPDEKQRSELSRRLG | 90 |
| AtANL2 | SGSDNVEGISGEDQDAADKPPRKKRYHRHTPQQIQELESFMFKECPHPDEKQRLELSKRLC | 172 |
| StCD2 | SGSDNLEGASGDEQDAADKPPRKKRYHRHTPQQIQELESFKECPHPDEKQRLELSKRLS | 163 |
| GmHomeobox | SGSDNMDGASGDEHDAAADNP RKKRYHRHTPQQIQELEALFKECPHPDEKQRLELSRRLC | 166 |
| TcHDdomain | SGSDNMDGGSDDQDAADNP RKKRYHRHTPQQIQELEALFKECPHPDEKQRLELSKRLC | 151 |
| SlPDF2 | LSNNRDGGVSGDELTSFDGS--SERRHKFSVNIHELESVFKVSSHPEKTKQELATKFS | 65 |
| StHomeobox | EKENENELVSGDELDSQRGK--SSKRMKHSKQIQELEVAFKEDRYPDATIRLELATKLS | 66 |
| | .. **:: : .: :: :**:* * * : * . : * : : | |
| PoptrHomeobox | LESKQIKFWFQNRRTQMKTLERHENAILRQENDKLRAENELLKQNMSPICNCCGGPVV | 150 |
| AtANL2 | LETRQVKFWFQNRRTQMKTLERHENALLRQENDKLRAENMSIREAMRNP ICTNCGGPAM | 232 |
| StCD2 | LETRQVKFWFQNRRTQMKTLERHENSILRQENDKLRAENMSIREAMRNP ICTNCGGPAM | 223 |
| GmHomeobox | LETRQVKFWFQNRRTQMKTLERHENTLLRQENDKLRAENMSIRDAMRNPMSNCGGPAI | 226 |
| TcHDdomain | LETRQVKFWFQNRRTQMKTLERHENSLLRQENDKLRAENMSIRDAMRNP ICTNCGGPAI | 211 |
| SlPDF2 | VDKKQVQFWFQNKRSISKTSERYNKRVLQQENEKLRTEY AAMREVMKKSICDPCRNKDT | 125 |
| StHomeobox | MGSKQVNYWVFNKRSRMKSQSEQHESKLLKQEQYDKLHTEYISMKEMKSPTCGQCHGKTI | 126 |
| | : .:*::**:* * : * * * : * * : * * : * : * . * * . | |
| PoptrHomeobox | P-VPVSYEQQLRIENARLKDELGRVCALANKFLGRPLTSSASPVPPFGSNTKFDLAVGR | 209 |
| AtANL2 | L-GDVSLEEHLRIENARLKDELDRVCNLTKGFLGHHNH-----YNSLELAVGT | 283 |
| StCD2 | I-GEISLEEHLRIENARLKDELDRVCALAGKFLGRPISSLVTSMPMPNSLELGVGN | 282 |
| GmHomeobox | I-GEISLEEHLRIENARLKDELDRVCVLAGKFLGRPVSSL-----PSSLELGMRG | 277 |
| TcHDdomain | I-GDISLEEHLRIENARLKDELDRVCALAGKFLGRPISALATS IAPPMPNSLELGVGS | 270 |
| SlPDF2 | TIRNENVDEKEILNEHARLKDELARIAHADKSLGSSSFLE-GSLTSMMEK--F----- | 176 |
| StHomeobox | SM-NINVDEHQLKNEQAQLEDEVKRLTNEVEKLYDP----- | 161 |
| | . : : : : * : * : * : * : * : * . | |
| PoptrHomeobox | NGYGNLGHDTNPLPMGLDNNGGVMM-----PLMKPIGNAVGNVFPDRSMFVD | 257 |
| AtANL2 | NNNGGHFAF-----PPDFGGGGCL-----PPQQQ---QSTVINGIDQKSVLLE | 324 |
| StCD2 | NGYGGMSNVPTTLPLAPPDFGVGISNSL-----PVPVPSN---RQSTGIERSLERSMYLE | 333 |
| GmHomeobox | NGFAGIPA-ATTLPLG-QDFMGMSVSMNNALAMVSPPTSARAAAAGFDRSVERSMFLE | 335 |
| TcHDdomain | NGFGGLSTVPTTLPLG-PDFGGGITNAL-----PVAPPNRP TTGVTGLDRSVERSMFLE | 323 |
| SlPDF2 | -----GLELNEVDFGKYLSS-----PLPTNLDVTLDKSMLLN | 208 |
| StHomeobox | -----TTSLEGTFDKSTLLN | 176 |
| | . : : * : : | |

APPENDICES

| | | |
|---------------|---|-----|
| PoptrHomeobox | LALAAMDELIKIAQVESPIWIKSLDGGKEVLNHEEYMRTFPPCIGMKPSNFVIEATRESG | 317 |
| AtANL2 | LALTAMDELVKLAQSEELWVKSLDGERDELNQDEYMRTFSS---TKPTGLATEASRTSG | 381 |
| StCD2 | LALAAMEELVKLAQTDEPLWFRSIEGGRELLNHEEYIRFTFTPCIGMRPNSFVSEASRETG | 393 |
| GmHomeobox | LALAAMDELVKIAQTGEPLWMRNVEGGREILNNEEYVRTFTPCIGLRPNFVSEASRENG | 395 |
| TcHdDomain | LALAAMDELVKMAQTDEPLWIRSLLEGGREILNHDEYLRFTFTPCIGMKPGGFVTEASRETG | 383 |
| SlPDF2 | LALDALNELLLKLAMSDEPLWVRNLDGGGEMLNMEYATTFIPIIGIKPSHFTTEATRSGG | 268 |
| StHomeobox | LALDASDELLKLAQNGEPLWFRNLDGGETLNLKEYDSAFTPIISMKEPHFITEATRATC *** * :*:*: * .*:*: :*: * : ** .* * : * : * : * : * | 236 |
| PoptrHomeobox | VVLANSLDLVETLMDVNGWVEMFPSLIARAATIDIVSSGMGGTKSGALQMIHAEFQVISP | 377 |
| AtANL2 | MVIINSLALVETLMDSNRWTEMFPCNVARATTTDVISSGMAGTINGALQLMNAELQVLSP | 441 |
| StCD2 | MVIINSLALVETLMDSNKWAEMFPCLIARTSTTDVISSGMGGTRNGALQLMHAELQVLSP | 453 |
| GmHomeobox | MVIINSLALVETLMDSNRWAEMFPCIIARTSTTEVISSGINGTRNGALQLMHAELQVLSP | 455 |
| TcHdDomain | VVIINSLALVETLMDSTRWAEMFPCMIARTSTTDVISSGMGGTRNGALQLMHAELQVLSP | 443 |
| SlPDF2 | TVVGNLSLTLVEMLMNESQVWEAFPCIIIGKVNTFDVISTGIGEGKSGTLLLIEAELQIISN | 328 |
| StHomeobox | KMVHNSQTLVETLMNKDQWMDMFPFCIVGKTNTIEVISRGISGNKSGALLLIVSELQIISD : : ** *** * : * : * . : : . * : : * * : . * * : : : * : : * | 296 |
| PoptrHomeobox | FVPVRQVKFLRLCKQLAEGVWAVADVSDGNQENLNAQTFVTCRRLPSGCI IQDMNNGCC | 437 |
| AtANL2 | LVPVRNVNFLRFCKQHAEGVWAVVDVSDIDPVRENSGGAP--VIRRLPSGCVVQDMPNGYS | 499 |
| StCD2 | LVPVREVNFLRFCKQHAEGVWAVVDVSDIDTIRETSGAPTYPNCRRLPSGCVVQDMPNGYS | 513 |
| GmHomeobox | LVPVREVNFLRFCKQHAEGVWAVVDVSDIDSIRESSGAPTFVNCRRLPSGCVVQDMPNGYS | 515 |
| TcHdDomain | LVPVREVNFLRFCKQHAEGVWAVVDVSDIDTIRETSGAPTFVNCRRLPSGCVVQDMPNGYS | 503 |
| SlPDF2 | VVPVREIKFLRFCKQHAEDSWIIDVSDTIKEGSQQYKIEKCRRLPSGCI IQDMSNGYS | 388 |
| StHomeobox | MIPSCIEIKLRFCKQHAEGLVWVVDVSDIDTIQKGSQQCEIQSCRRLPSGCI IQDMVDGYS . : * : : * * : : * . * : . * * : * : : * * * * * : : * : * . | 356 |
| PoptrHomeobox | KVTWVEHSEYDES AVHRLYRHLINSGMGFGAQRWIAALQRHYECMAMLLSPTILGEDQTV | 497 |
| AtANL2 | KVTWVEHAHEYDENQIHQLYRPLLRSGLFGFSQRWLATLQRQCECLAII LSSSVTSHDNNTS | 559 |
| StCD2 | KVTWVEHAHEYEEGANHHLYRQLISAGMGFGAQRWVATLQRQCECLAII LMSSTVSARDH-- | 571 |
| GmHomeobox | KVTWVEHAHEYDESQVHQLYRPLLRSGMGFGAQRWVATLQRQCECLAII LMSAAPS RDHSA | 575 |
| TcHdDomain | KVTWVEHAHEYEESQVHQLYRPLLRSGMGFGAQRWVATLQRQCECLAII LMSSTVPTRDHTA | 563 |
| SlPDF2 | KVTWIEHMEYDEIFVDHLYRPLIRAGLFGAQRWMSLQRQSELLRV MASFV-----NST | 443 |
| StHomeobox | KVIWIEHMQYNENHVHHLRPLVKTGLVFGAQRCAIAGLQRQSEFLRMKSFV-----DPT * * * : * * : * * : : * : * * * * : : * * * : * : : * . | 411 |
| PoptrHomeobox | INLGGKSMMLKLARRMVDSFCSGVCASTLHNWGNLV-VESVSEDVRI LTRKI INEPGEPD | 556 |
| AtANL2 | ITPGGRKSMMLKLAQRMTFNFCSGISAPSVHNWSKLT-VGNVDPDVRVMTRKSVDDPGEP | 618 |
| StCD2 | -----TGNVDEDVRVMTRKSVDDPGEP | 594 |
| GmHomeobox | ITAGGRRSMMKLAQRMTNFCAGVCASTVHKWNKLN-AGNVDEDVRVMTRKSVDDPGEP | 634 |
| TcHdDomain | ITASGRRSMLKLAQRMTDNFCAGVCASTLHKWNKLNAGNVDEDVRVMTRKSVDDPGEP | 623 |
| SlPDF2 | VDPKGEIGMGILSQRMTRSFCAVICAT-SHKWITIQKEN--GKDANLMRRNISDAGEPI | 500 |
| StHomeobox | IVSKDHIGIRMLAQSMTRKFC AAVCAT-THKWEIVQLEN--GVDAKLMRRTS IGDHTEPI . * . : : * * : : * | 468 |
| PoptrHomeobox | GIVLSVSTSVWLPVSPQRLDFDLRDEQSRSQWDILSNGGILQEMVQIPKGGHNTVSVL | 616 |
| AtANL2 | GIVLSAATSVWLPAPAPQRLYDFLNRNMRCEWDILSNGGPMQEMAHITKGDQDQ--VSL | 676 |
| StCD2 | GIVLSAATSVWLPVSPQRLDFDLRDERLRSEWDILSNGGPMQEMAHIAKGDHGNVSVL | 654 |
| GmHomeobox | GIVLSAATSVWLPVSPHRLDFDLRDERLRSEWDILSNGGPMQEMAHIAKGDHGNVSVL | 694 |
| TcHdDomain | GIVLSAATSVWLPVSPQRLDFDLRDERLRSEWDILSNGGPMQEM----- | 667 |
| SlPDF2 | GVILSATKTIQLPIKSQLFQFFTNKLRQWDILSCSGAMENI IHINKDENLESSVSVL | 560 |
| StHomeobox | GIVLCAIKTIRLPVKQQLHLEFFFINNKTRSQWDVLSNGPIQELVVRVSKDQNLLESSIYLL * : * . : : * * : * : * : : * * * * * . * : : : | 528 |
| PoptrHomeobox | RSTAVDA-NASDNMLILQETWNDVSGSLVVYAPVDVQSVSVVMNGGDSTYVALLPSGFVI | 675 |
| AtANL2 | RSNAMNA-NQS-SMLILQETCIDASGALVVYAPVDIPAMHVVMNGGDSSYVALLPSGFAV | 734 |
| StCD2 | RASAMNA-NQS-SMLILQETCIDAAGALVVYAPVDIPAMHVVMNGGDSAYVALLPSGFSI | 712 |
| GmHomeobox | RASAINS-NQS-SMLILQETCIDAAGSLVVYAPVDIPAMHVVMNGGDSAYVALLPSGFAI | 752 |
| TcHdDomain | ----- | 667 |
| SlPDF2 | CANGG---ANENNMIFQDTC T DATGSLVVYAVDSSKMNTVMKGGDPSCVELLPNGISI | 617 |
| StHomeobox | RADGDSTSAKQNNMIFQDTC TDTGSLVVYAVTGSQDINMVMKEGDS SFVGLLPNGISI | 588 |

| | | |
|---------------|---|-----|
| PoptrHomeobox | LPGNSFSNGEPNNCNGNPAKRDCDGNSSGGGSFLTQILASNLPSAKLTVESVKTVHNL | 735 |
| AtANL2 | LPDGGIDGGGSGDG-----DQRPVGGGSLLTVAQILVNNLPTAKLTVESVETVNNL | 786 |
| StCD2 | VFDGPGSRGSNG-PS--CNGG--PDQRISGSLLTVAQILVNSLPTAKLTVESVETVNNL | 767 |
| GmHomeobox | VPDGPGSRGPPNGPTSTTNGGDNGVTRVSGSLLTVAQILVNSLPTAKLTVESVETVNNL | 812 |
| TcHDdomain | ----- | 667 |
| SlPDF2 | LPDLSANNN-----KEFGSGSLVTIMFQMLVDNISTADLPQKSIVDANDI | 662 |
| StHomeobox | VQDYSAVDNDND-----IFEKNDNGVYGGSLVTIGFQMLLENLATTSLPKQSIKEANDL | 642 |
| | | |
| PoptrHomeobox | ISCTMQRIKTAFN--- | 748 |
| AtANL2 | ISCTVQKIRAALQCES | 802 |
| StCD2 | ISCTVQKIKAAALQCES | 783 |
| GmHomeobox | ISCTVQKIKAAALHCES | 828 |
| TcHDdomain | ----- | 667 |
| SlPDF2 | ISHTIHKIKSALLI-- | 676 |
| StHomeobox | ICHTIRKIKMALKCK- | 657 |

Figure A8: Multiple sequence alignment of putative full-length MYC2 and its homologs.

Putative full-length PDF2 represents a homeobox domain (HD) domain highlighted in red, aligned with closely related homolog species. START domain of the PDF2 sequence is highlighted in blue.

6.7 Qualitative analysis of monoterpenes and sesquiterpenes

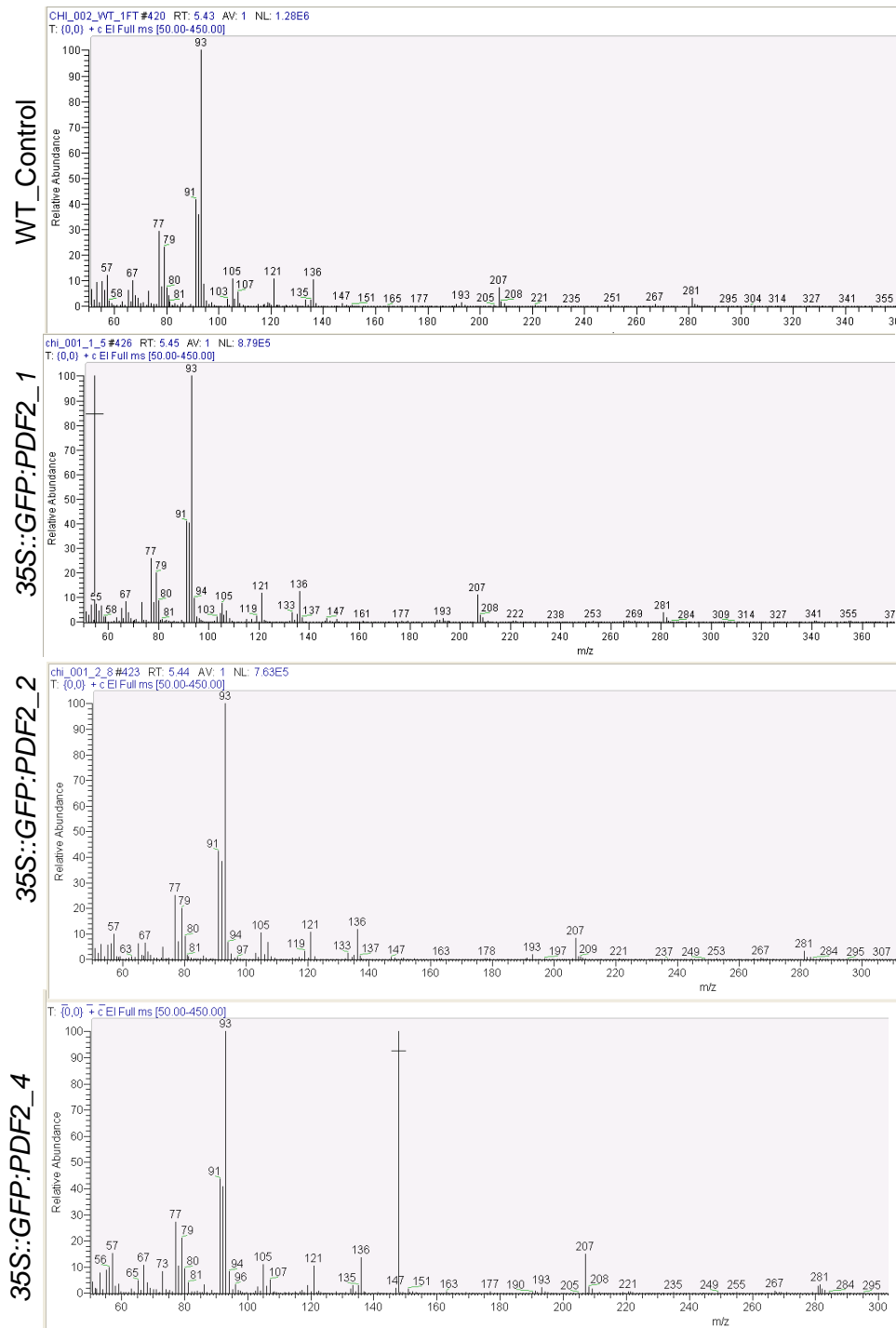


Figure A9: Analysis of the peak area of monoterpenes

Monoterpenes (α – pinene, 3, 4 –Carene with M.W – 136.12 and R.T – 5.42) were analyzed on the GC-MS. α – pinene at the retention time 5.42 was analyzed between WT control and 35S::GFP::PDF2_1/2/4 F1 lines using Xcalibur software.

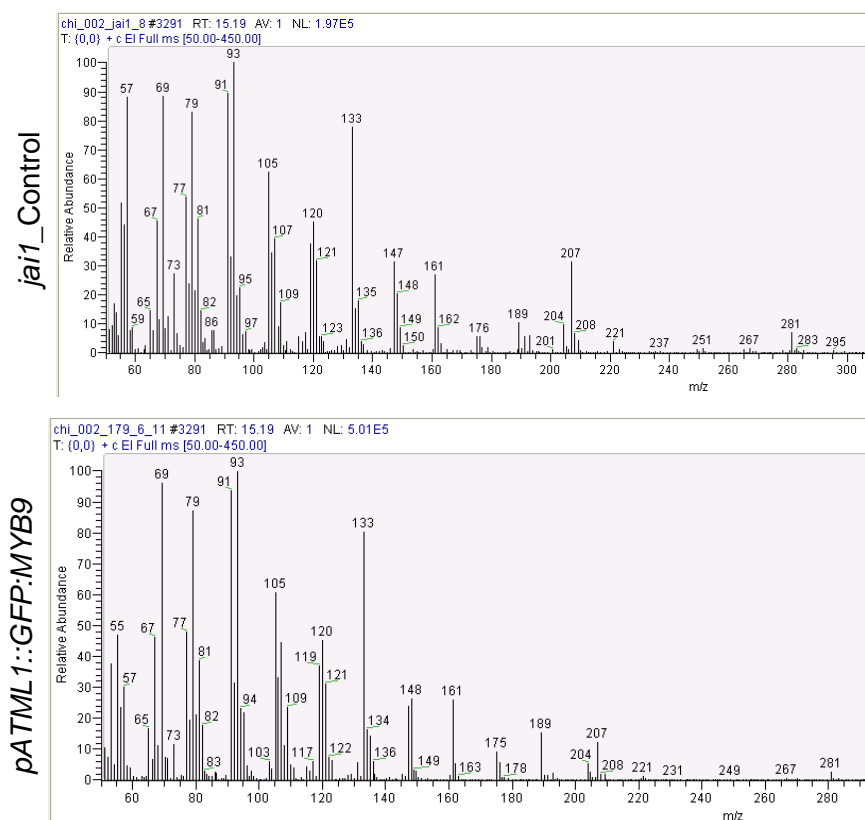


Figure A10: Analysis of the peak area of sesquiterpenes

Sesquiterpenes (β - caryophyllene and α -humelene, M.W – 204.18, R.T – 15.22) detected from the leaf hexane extracts of F1 transgenic lines were analyzed on the GC-MS. β -caryophyllene at the retention time 15.22 was analyzed between *jai1* control and *pATML1::GFP::MYB9* F1 lines using Xcalibur software.

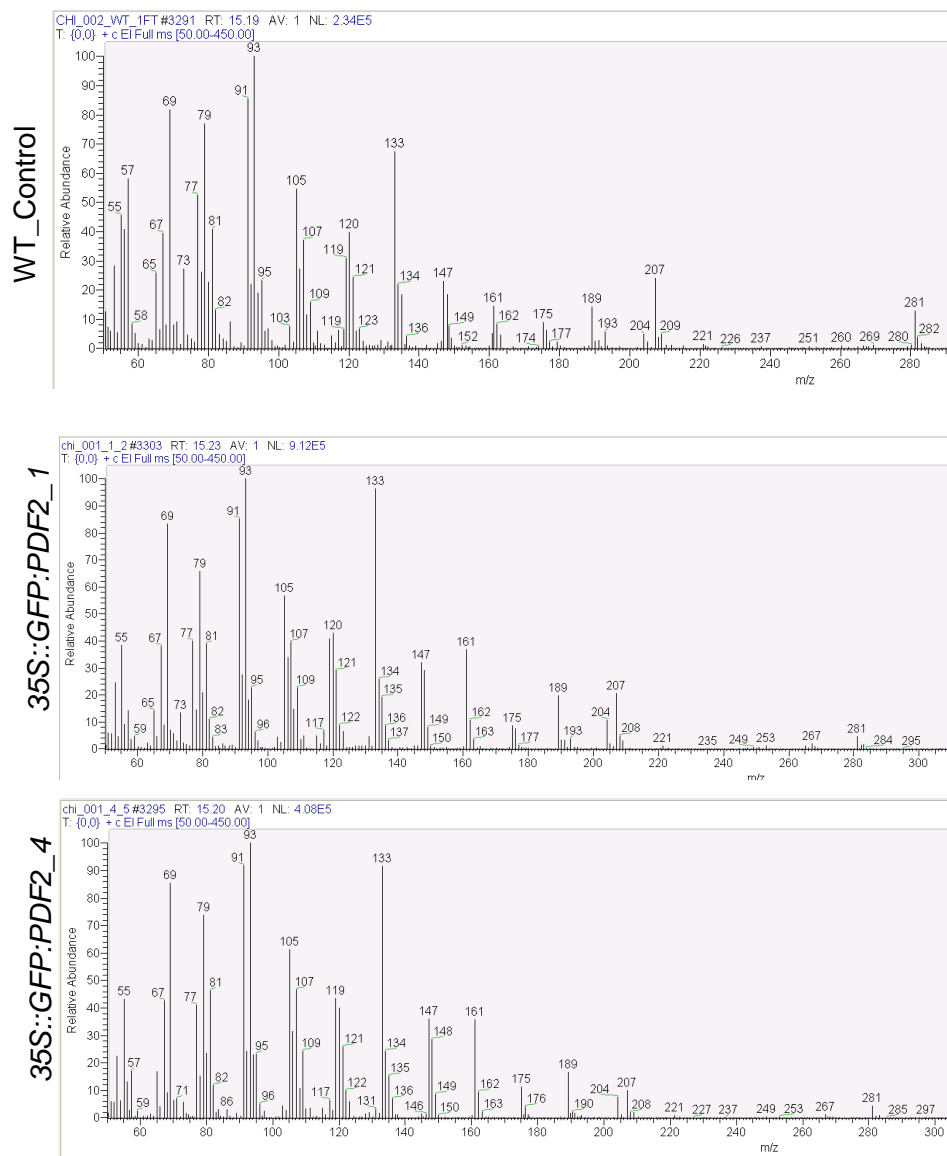


Figure A 11: Analysis of the peak area of sesquiterpenes

Sesquiterpenes (β - caryophyllene and α -humelene, M.W – 204.18, R.T – 15.22) detected from the leaf hexane extracts of F1 transgenic lines were analyzed on the GC-MS. β -caryophyllene at the retention time 15.22 was analyzed between WT control and 35S::GFP::PDF2_1/2/4 F1 lines using Xcalibur software.

BIBLIOGRAPHY

Altschul, S., Gish, W., Miller, W., Myers, E., and Lipman, D. (1990). "Basic local alignment search tool". *Journal of Molecular Biology* **215**, 403-410.

Andersson, B.A., Holman, R.T., Lennart, L., and Stenhagen, G. (1980). Capillary gas chromatograms of leaf volatiles. A possible aid to breeders for pest and disease resistance. *Journal of Agricultural and Food Chemistry* **28**, 985-989.

Abe, M., Takahashi, T., and Komeda, Y. (2001). Identification of a cis-regulatory element for L1 layer-specific gene expression, which is targeted by an L1-specific homeodomain protein. *The Plant Journal* **26**, 487-494.

Abe, M., Katsumata, H., Komeda, Y., and Takahashi, T. (2003). Regulation of shoot epidermal cell differentiation by a pair of homeodomain proteins in *Arabidopsis*. *Development* **130**, 635-643.

Atchley, W.R., and Fitch, W.M. (1997). A natural classification of the basic helix-loop-helix class of transcription factors. *Proceedings of the National Academy of Sciences of the USA* **94**, 5172-5126.

Araki, S., Ito, M., Soyano, T., Nishihama, R., and Machida, Y. (2004). Mitotic cyclins stimulate the activity of c-Myb-like factors for transactivation of G2/M phase-specific genes in tobacco. *Journal of Biological Chemistry* **279**, 32979-32988.

Affolter, M., Schier, A., and Gehring, W.J. (1990). Homeodomain proteins and the regulation of gene expression. *Current Opinion in Cell Biology* **2**, 485-495.

Agrawal, A.A. (1999). Induced responses to herbivory in wild radish: effects on several herbivores and plant fitness. *Ecology* **80**, 1713-1723

Agrawal, A.A. (2000). Benefits and costs of induced plant defense for *Lepidium virginicum* (Brassicaceae). *Ecology* **81**, 1804-1813

Bolger, A.M., Lohse, M., and Usadel, B. (2014). Trimmomatic: a flexible trimmer for Illumina sequence data. *Bioinformatics*. **30**, 2114-2120

Balkunde, R., Pesch, M., and Hulskamp, M. (2010). Trichome patterning in *Arabidopsis thaliana* from genetic to molecular models. *Current Opinion in Developmental Biology* **91**, 299-321.

Balkunde, R., Bouyer, D., and Hulskamp, M. (2011). Nuclear trapping by GL3 controls intercellular transport and redistribution of TTG1 protein in *Arabidopsis*. *Development* **138**, 5039-5048.

Boughton, A.J., Hoover, K., and Felton, G.W. (2005). Methyl jasmonate application induces increased densities of glandular trichomes on tomato, *Lycopersicon esculentum*. *Journal of Chemical Ecology* **31**, 2211-2216.

Behnke, H.D. (1984). Plant trichomes-structure and ultrastructure: general terminology, taxonomic applications, and aspects of trichome-bacterial interaction in leaf tips of *Dioscorea*. *Biology and Chemistry of Plant Trichomes*. New York Plenum Press.

Benz, B.W., and Martin, C.E. (2006). Foliar trichomes, boundary layers, and gas exchange in 12 species of epiphytic *Tillandsia* (Bromeliaceae). *Journal of Plant Physiology* **163**, 648-656.

Bleeker, P.M., Mirabella, R., Diergaarde, P.J., VanDoorn, A., Tissier, A., Kant, M.R., Prins, M., de Vos, M., Haring, M.A., and Schuurink, R.C. (2012). Improved herbivore resistance in cultivated

BIBLIOGRAPHY

tomato with the sesquiterpene biosynthetic pathway from a wild relative. Proceedings of the National Academy of Sciences of the USA **109**, 20124-20129.

Besser, K., Harper, A., Welsby, N., Schauvinhold, I., Slocombe, S., Li, Y., Dixon, R.A., and Broun, P. (2009). Divergent regulation of terpenoid metabolism in the trichomes of wild and cultivated tomato species. *Plant Physiology* **149**, 499-514.

Bergau, N., Bennewitz, S., Syrowatka, F., Hause, G., and Tissier, A. (2015). The development of type VI glandular trichomes in the cultivated tomato *Solanum lycopersicum* and a related wild species *S. habrochaites*. *BMC Plant Biology* **15**, 289.

Buttery, R.G., Ling, L.C., and Light, D.M. (1987). Tomato leaf volatile aroma components. *Journal of Agriculture Food Chemistry* **35**, 1039-1042.

Browse, J. (2009a) Jasmonate passes muster: a receptor and targets for the defense hormone. *Annual Review in Plant Biology* **60**, 183-205.

Browse, J. (2009c). The power of mutants for investigating jasmonate biosynthesis and signaling. *Phytochemistry* **70**, 1539-1546.

Bergau, N., Navarette, Santos A., Henning, A., Balcke, G.U., and Tissier, A. (2016). Autofluorescence as a signal to sort developing glandular trichomes by flow cytometry. *Frontiers in Plant Science* **7**, 949.

Bang, W.Y., Kim, S.W., Jeong, I.S., Koiwa, H., and Bahk, J.D. (2008). The C-terminal region (640-967) of Arabidopsis CPL1 interacts with the abiotic stress- and ABA-responsive transcription factors. *Biochemical and Biophysical Research Communications* **372**, 907-912.

Bostock, R.M. (1999) Signal conflicts and synergies in induced resistance to multiple attackers. *Physiology and Molecular Plant Pathology* **55**, 99-109.

Bailey, P.C., Martin, C., Toledo-Ortiz, G., Quail, P.H., Huq, E., and Heim, M.A, et al. (2003). Update on the basic helix-loop-helix transcription factor gene family in *Arabidopsis thaliana*. *The Plant Cell*. **15**, 2497-502.

Ballester, A.R., Molthoff, J., de Vos, R., Hekkert, B.L., Orzaez, D., Fernández- Moreno, J.P., et al. (2010). Biochemical and molecular analysis of pink tomatoes: deregulated expression of the gene encoding transcription factor SIMYB12 leads to pink tomato fruit color. *Plant Physiology* **152**, 71-84.

Baur, R., Binder, S., and Benz, G. (1991). Non glandular leaf trichomes as short-term inducible defense of the grey alder, *Alnus incana* (L), against the chrysomelid beetle, *Agelastica alni* L. *Oecologia* **87**, 219-226.

Chien, J.C., and Sussex, I.M. (1996). Differential regulation of trichome formation on the adaxial and abaxial leaf surfaces by gibberellins and photoperiod in *Arabidopsis thaliana* (L.) Heynh. *Plant Physiology*. **111**, 1321-1328.

Campos, M.L., Almeida, A., Rossi, M.L., Martinelli, A.P., Junior, C.G.L., Figueira, A., et al. (2009). Brassinosteroids interact negatively with jasmonates in the formation of anti-herbivory traits in tomato. *Journal of Experimental Botany* **60**, 4347-4361.

Choinski J. S., and Wise, R.R. (1999). Leaf growth and development in relation to gas exchange in *Quercus marilandica* Muenchh. *Journal of Plant Physiology* **154**, 302-309.

- Chini, A., Fonseca, S., Fernández, G., Adie, B., Chico, J.M., Lorenzo, O., Garcia-Casado, G., López-Vidriero, I., Lozano, F.M., Ponce, M.R., et al.** (2007). The JAZ family of repressors is the missing link in jasmonate signalling. *Nature* **448**, 666–671.
- Chen, Y.H., Yang, X.Y., He, K., Liu, M.H., Li, J.G., Gao, Z.F., Lin, ZQ., Zhang, Y.F., Wang, X.X., Qiu, X.M., Shen, Y.P., Zhang, L., Deng, X.H., Luo, J.C., Deng, X.W., Chen, Z.L., Gu, H.Y., and Qu, L.J.** (2006a). The MYB transcription factor superfamily of Arabidopsis: expression analysis and phylogenetic comparison with the rice MYB family. *Plant Molecular Biology* **60**, 107-124
- Chen, Y., Chen, Z., Kang, J., Kang, D., Gu, H., and Qin, G.** (2013). *AtMYB14* Regulates Cold Tolerance in *Arabidopsis*. *Plant Molecular Biology Reporter / Isymb*, **31**, 87–97.
- Cui, J.Y., Miao, H., Ding, L.H., Wehner, T.C., Liu, P.N., Wang, Y., Zhang, S.P., and Gu, X.F.** (2016). A new glabrous gene (*csgl3*) identified in trichome development in cucumber (*Cucumis sativus* L.). *PLoS ONE* **11**, e0148422.
- Cui, H., Zhang, S.T., Yang, H.J., Ji, H., and Wang, X.J.** (2011). Gene expression profile analysis of tobacco leaf trichomes. *BMC Plant Biology* **11**, 76.
- Creelman, R.A., and Mullet, J.E.** (1997). Biosynthesis and action of jasmonates in plants. *Annual Reviews of Plant Physiology and Plant Molecular Biology* **48**, 355-381.
- Chung, H.S., Koo, A.J.K., Gao, X., Jayanty, S., Thines, B., Jones, A.D., and Howe, G.** (2008). Regulation and function of Arabidopsis JASMONATE ZIM-domain genes in response to wounding and herbivory. *Plant Physiology* **146**, 952-964.
- Chini, A., Boter, M., and Solano, R.** (2009a). Plant oxylipins: COI1/ JAZs/ MYC2 as the core jasmonic acid-signalling module. *FEBS Journal* **276**, 4682-4692.
- Cipollini, D.F., Purrington, C.B., and Bergelson, J.** (2003). Costs of induced responses in plants. *Basic and Applied Ecology* **4**, 79-89
- de Haan, H.** (1927). Length factors in *Pisum*. *Genetica* **9**, 481-497.
- de Vetten, N., Quattrocchio, F., Mol, J., and Koes, R.** (1997). *an11* locus controlling flower pigmentation in *Petunia* encodes a novel WD-repeat protein conserved in yeast, plants, and animals. *Nature* **373**, 297-300
- Duke, S.O., Canel, C., Rimando, A.M., Tellez, M.R., Duke, M.V., and Paul, R.N.** (2000). Current and potential exploitation of plant glandular trichome productivity. *Advances in Botanical Research* **31**, 121-151.
- Dalin, P., Ågren, J., Björkman, C., Huttunen, P., Kärkkäinen, K.** (2008). Leaf trichome formation and plant resistance to herbivory. Schaller A. (eds) *Induced Plant Resistance to Herbivory*. Springer, Dordrecht
- Digiuni, S., Schellmann, S., Geier, F., Greese, B., Pesch, M., Wester, K., and Hulskamp, M.** (2008). A competitive complex formation mechanism underlies trichome patterning on Arabidopsis leaves. *Molecular Systems Biology*, **4**, 217.
- Dubos, C., Stracke, R., Grotewold, E., Weisshaar, B., Martin, C., and Lepiniec, L.** (2010). MYB transcription factors in Arabidopsis. *Trends in Plant Science* **15**, 573-581.
- Du, H., Zhang, L., Liu, L., Tang, X.F., Yang, W.J., Wu, Y.M., et al.** (2009). Biochemical and molecular characterization of plant MYB transcription factor family. *Biochemistry* **74**, 1-11.

BIBLIOGRAPHY

Dombrecht, B., Xue, G.P., Sprague, S.J., Kirkegaard, J.A., Ross, J.J., Reid, J.B., Fitt, G.P., Sewelam, N., Schenk, P.M., Manners, J.M., and Kazan, K. (2007). MYC2 differentially modulates diverse jasmonate dependent functions in Arabidopsis. *The Plant Cell* **19**, 2225-2245.

Dathe, W., Rönch, H., Preiss, A., Schade, W., Sembdner, G., and Schreiber, K. (1981). Endogenous plant hormones of the broad bean, *Vicia faba* L. (–)-Jasmonic acid, a plant growth inhibitor in pericarp. *Planta* **155**, 530–535.

Dalin, P. (2006). Habitat difference in abundance of willow leaf beetle *Phratora vulgatissima* (Coleoptera: Chrysomelidae): plant quality or natural enemies? *Bulletin of Entomological Research* **96**, 629-635

Dalin, P., and Björkman, C. (2003). Adult beetle grazing induces willow trichome defence against subsequent larval feeding. *Oecologia* **134**, 112-118.

Ehleringer, J., Björkman, O., and Mooney, H.A. (1976). Leaf pubescence: effects on absorptance and photosynthesis in a desert shrub. *Science* **191**, 376-377.

Esen, A. (1978). A simple method for quantitative, semi-quantitative, and qualitative assay of protein. *Annals of Biochemistry*. **89**, 264-273.

Engler, C., Kandzia, R., Marillonnet, S. (2008). A one pot, one step, precision cloning method with high throughput capability. *PLoS ONE* **3**, e3647.

Erb, M., Glauser, G., and Robert, C. (2012). Induced immunity against below ground insect herbivores - activation of defenses in the absence of a jasmonate burst. *Journal of Chemical Ecology* **38**, 629-640.

Fridman, E., Wang, J.H., Iijima, Y., Froehlich, J.E., Gang, D.R., Ohlrogge, J. and Pichersky, E. (2005). Metabolic, genomic, and biochemical analyses of glandular trichomes from the wild tomato species *Lycopersicon hirsutum* identify a key enzyme in the biosynthesis of methylketones. *The Plant Cell* **17**, 1252-1267.

Feller, A., Machemer, K., Braun, E.L., and Grotewold, E. (2011). Evolutionary and comparative analysis of MYB and bHLH plant transcription factors. *The Plant Journal* **66**, 94-116.

Fahn, A. (2000). Structure and function of secretory cells in Plant Trichomes; Hallahan, D.L., Gray, J.C., Eds.; Academic Press: New York, USA p-37.

Fahn, A and Werker, E. (1972). Anatomical mechanisms of seed dispersal. In "seed biology" (T.T Kozlowski, ed.). Academic press, New York, London, 151-221.

Fürstenberg-Hägg, J., Zagrobelny, M., and Bak, S. (2013). Plant defense against insect herbivores. *International Journal of Molecular Sciences* **14**, 10242-10297.

Fonseca, S., Chini, A., Hamberg, M., Adie, B., Porzel, A., Kramell, R., Miersch, O., Wasternack, C., and Solano, R. (2009). (+)-7-iso-Jasmonoyl-L-isoleucine is the endogenous bioactive jasmonate. *Nature Chemical Biology* **5**, 344-350.

Fernandez-Calvo, P., Chini, A., Fernández-Barbero, G., Chico, J.M., Gimenez- Ibanez, S., Geerinck, J., Eeckhout, D., Schweizer, F., Godoy, M., Franco-Zorrilla, J.M., et al. (2011). The Arabidopsis bHLH transcription factors MYC3 and MYC4 are targets of JAZ repressors and act additively with MYC2 in the activation of jasmonate responses. *The Plant Cell* **23**, 701-715.

Ferre-D'Amare, A.R., Pognonec, P., Roeder, R.G., and Burley, S.K. (1994). Structure and function of the b/HLH/Z domain of USF. *EMBO Journal* **13**, 180-189.

- Feenstra, W.J.** (1978). Contiguity of linkage groups 1 and 4, as revealed by linkage relationships of two newly isolated markers dis-1 and dis-2. *Arabidopsis Information Service* **75**, 35-38.
- Grandori, C., Cowley, S.M., James, L.P., and Eisenman, R.N.** (2000). The Myc/Max/Mad network and the transcriptional control of cell behavior. *Annual Review of Cell and Developmental Biology* **16**, 653-699.
- Greenboim-Wainberg, Y., Maymon, I., Borochoy, R., Alvarez, J., Olszewski, N., Ori, N., Eshed, Y., and Weiss D.** (2005). Cross talk between gibberellin and cytokinin: the Arabidopsis GA response inhibitor SPINDLY plays a positive role in cytokinin signaling. *Plant Cell* **17**, 92-102
- Gershenzon, J., McCaskill, D., Rajaonarivony, J.I., Mihaliak, C., Karp, F. and Croteau, R.** (1992) Isolation of secretory cells from plant glandular trichomes and their use in biosynthetic studies of monoterpenes and other gland products. *Annals of Biochemistry* **200**, 130-138.
- Gan, Y., Liu, C., Yu, H., and Broun, P.** (2007a). Integration of cytokinin and gibberellin signalling by *Arabidopsis* transcription factors GIS, ZFP8 and GIS2 in the regulation of epidermal cell fate. *Development* **134**, 2073-2081.
- Gang, D.R., Wang, J., Dudareva, N., Nam, K.H., Simon, J.E., Lewinsohn, E., and Pichersky, E.** (2001). An investigation of the storage and biosynthesis of phenylpropanes in sweet basil. *Plant Physiology* **125**, 539-555.
- Gratao, P.L., Monteiro, C.C., Antunes, A.M., Peres, L.E.P., and Azevedo, R.A.** (2008). Acquired tolerance of tomato (*Lycopersicon esculentum* cv. Micro-Tom) plants to cadmium-induced stress. *Annals of Applied Biology* **153**, 321-333.
- Glas, J.J., Schimmel, B.C.J., Alba, J.M., Escobar-Bravo, R., Schuurink, R.C., and Kant, M.R.** (2012). Plant glandular trichomes as targets for breeding or engineering of resistance to herbivores. *International Journal of Molecular Sciences*, **13**(12), 17077-17103.
- Galmés, J., Medrano, H., and Flexas, J.** (2007). Photosynthesis and photoinhibition in response to drought in a pubescent (var. *minor*) and a glabrous (var. *palaui*) variety of *Digitalis minor*. *Environmental and Experimental Botany* **60**, 105-111.
- Glover, B.J, Perez-Rodriguez, M., and Martin, C.** (1998). Development of several epidermal cell types can be specified by the same MYB-related plant transcription factor. *Development* **125**, 3497-3508
- Goodrich, J., Carpenter, R., and Coen, E.S.** (1992). A common gene regulates pigmentation pattern in diverse plant species. *Cell* **68**, 955–964.
- Hallahan, D.L., West, J.M., Smiley, D.W.M. and Pickett, J.A.** (1998) Nepetalactol oxidoreductase in trichomes of the catmint *Nepeta racemosa*. *Phytochemistry* **48**, 421-427.
- Hooley, R.** (1994). Gibberellins: perception, transduction and responses. *Plant Molecular Biology* **26**, 1529–1555
- Hase, S., Takahashi, S., Takenaka, S., Nakaho, K., Arie, T., Seo S., and Ohashi, Y., and Takahashi, H.** (2008). Involvement of jasmonic acid signaling in bacterial wilt disease resistance induced by biocontrol agent *Pythium oligandrum* in tomato. *Plant Pathology* **57**, 870-876.
- Hülkamp, M., Misera, S., and Jürgens, G.** (1994). Genetic dissection of trichome cell development in Arabidopsis. *Cell* **76**, 555-566.

BIBLIOGRAPHY

Hülskamp, M., and Schnittger, A. (1998). Spatial regulation of trichome formation in *Arabidopsis thaliana*. *Seminars in Cell and Developmental Biology* **9**, 213-220.

Hülskamp, M. (2004). Plant trichomes: a model for cell differentiation. *Nature Reviews Molecular Cell Biology* **5**, 471-480.

Hause, B., Demus, U., Teichmann, C., Parthier, B., and Wasternack, C. (1996). Developmental and tissue-specific expression of JIP-23, a jasmonate-inducible protein of barley. *Plant Cell Physiology* **37**, 641-649.

Harada, E., Kim, J.A., Meyer, A.J., Hell, R., Clemens, S., and Choi, Y.E. (2010). Expression profiling of tobacco leaf trichomes identifies genes for biotic and abiotic stresses. *Plant Cell Physiology* **51**, 1627-1637.

Howe, G., and Jander, G. (2008). Plant immunity to insect herbivores. *Annual Review in Plant Biology* **59**, 41-66.

Howe, G.A., Lightner, J., Browse, J., and Ryan, C.A. (1996). An octadecanoid pathway mutant (JL5) of tomato is compromised in signaling for defense against insect attack. *The Plant Cell* **8**, 2067-2077

Haughn, G.W., and Somerville, C.R. (1988). Genetic control of morphogenesis in *Arabidopsis*. *Developmental Genetics* **9**, 73-89.

Iijima, Y., Nakamura, Y., Ogata, Y., Tanaka, K., Sakurai, N., Suda, K., and Shibata, D. (2008). Metabolite annotations based on the integration of mass spectral information. *The Plant Journal* **54**(5), 949-962.

Iijima, Y., Davidovich-Rikanati, R., Fridman, E., Gang, D.R., Bar, E., Lewinsohn, E., and Pichersky, E. (2004a). The biochemical and molecular basis for the divergent patterns in the biosynthesis of terpenes and phenylpropenes in the peltate glands of three cultivars of basil. *Plant Physiology* **136**, 3724-3736.

Ishida T., Kurata, T., Okada, K., and Wada, T. (2008). A genetic regulatory network in the development of trichomes and root hairs. *Annual Review of Plant Biology* **59**, 364-386.

Isayenkov, S., Mrosk, C., Stenzel, I., Strack, D., and Hause, B. (2005). Suppression of allene oxide cyclase in hairy roots of *Medicago truncatula* reduces jasmonate levels and the degree of mycorrhization with *Glomus intraradices*. *Plant Physiology* **139**, 1404-1410.

Ito, M., Araki, S., Matsunaga, S., Itoh, T., Nishihama, R., Machida, Y., and Watanabe, A. (2001). G2/M-Phase-specific transcription during the plant cell cycle is mediated by c-Myb-Like transcription factors. *The Plant Cell* **13**(8), 1891-1906.

Jones, M.G. (1987). Gibberellins and the pmcera mutant of tomato. *Planta* **172**, 280-284

Jacobsen, S.E., and Olszewski, N.E. (1993). Mutations at the SPINDLY locus of *Arabidopsis* alter gibberellin signal transduction. *The Plant Cell* **5**, 887-896

Jin, J.P., Tian, F., Yang, D.C., Meng, Y.Q., Kong, L., Luo, J.C and Gao, G. (2017). PlantTFDB 4.0: toward a central hub for transcription factors and regulatory interactions in plants. *Nucleic Acids Research* **45**(D1), D1040-D1045.

Jin, J.P., He, K., Tang, X., Li, Z., Lv, L., Zhao, Y., Luo, J.C., and Gao, G. (2015). An *Arabidopsis* transcriptional regulatory map reveals distinct functional and evolutionary features of novel transcription factors. *Molecular Biology and Evolution*, **32**(7), 1767-1773.

- Johnson, H.B.** (1975). Plant pubescence: an ecological perspective. *Botanical Review* **41**, 233-253.
- Javelle, M., Klein-Cosson, C., Vernoud, V., Boltz, V., Maher, C., Timmermans, M., Depege-Fargeix, N., and Rogowsky, P.M.** (2011). Genome-wide characterization of the HD-ZIP IV transcription factor family in Maize: preferential expression in the epidermis. *Plant Physiology* **157**, 790-803.
- Jones, S.** (2004). An overview of the basic helix-loop-helix proteins. *Genome Biology* **5(6)**, 226.
- Koornneef, M., and van der Veen, J.H.** (1980). Induction and analysis of gibberellin-sensitive mutants in *Arabidopsis thaliana* (L.) Heynh. *Theoretical and Applied Genetics* **58**, 257-263.
- Koornneef, M., Elgersma, A., Hanhart, C.J, van Loenen-Martinet, E.P., van Rijn, L., and Zeevaart, J.A.D.** (1985). A gibberellin insensitive mutant of *Arabidopsis thaliana*. *Physiologia Plantarum* **65**, 33-39.
- Krings, M., and Kerp, H.** (1998). Epidermal anatomy of *Barthelopteris germarii* from the Upper Carboniferous and lower Permian of France and Germany. *American Journal of Botany* **85**, 553-562.
- Krings, M., Taylor, T.N., and Kellogg, D.W.** (2002). Touch-sensitive glandular trichomes: a mode of defense against herbivorous arthropods in the Carboniferous. *Evolutionary Ecology* **4**, 779-786.
- Krings, M., Kellogg, D.W., Kerp, H. and Taylor, T.N.** (2003). Trichomes of the seed fern *Blanziopteris praedentata*: implications for plant–insect interactions in the late Carboniferous. *Botanical Journal of the Linnean Society* **141**, 133-149.
- Karabourniotis, G., Kofidis, G., Fasseas, C., Liakoura, V., and Drossopoulos, I.** (1998). Polyphenol deposition in leaf hairs of *Olea europaea* (Oleaceae) and *Quercus ilex* (Fagaceae). *American Journal of Botany* **85**, 1007-1012.
- Khosla, A., Paper, J.M., Bohler, A.P., Bradley, A.M., Neumann, T.R. and Schrick, K.** (2014). HD-zip proteins GL2 and HDG11 have redundant functions in Arabidopsis trichomes, and GL2 activates a positive feedback loop via MYB23. *The Plant Cell* **26**, 2184-2200.
- Kirik, V., Schnittger, A., Radchuk, V., Adler, K., Hülkamp, M., and Baumlein, H.** (2001) Ectopic expression of the Arabidopsis AtMYB23 gene induces differentiation of trichome cells. *Developmental Biology* **235**, 366–377.
- Kirik, V., Simon, M., Hülkamp, M., and Schiefelbein, J.** (2004a). The *ENHANCER OF TRY AND CPC1* gene acts redundantly with *TRIPTYCHON* and *CAPRICE* in trichome and root hair cell patterning in *Arabidopsis*. *Developmental Biology* **268**, 506-513.
- Kirik, V., Simon, M., Wester, K., Schiefelbein, J., and Hülkamp, M.** (2004b). *ENHANCER OF TRY and CPC 2(ETC2)* reveals redundancy in the region specific control of trichome development of *Arabidopsis*. *Plant Molecular Biology* **55**, 389-398.
- Kazan, K., and Manners, J.M.** (2013). MYC2: the master in action. *Molecular Plant* **6**, 686-703.
- Kranz, H.D., Denekamp, M., Greco, R., Jin, H., Leyva, A., Meissner, R.C., Petroni, K., Urzainqui, A., Bevan, M., Martin, C., Smeekens, S., Tonelli, C., Paz-Ares, J., and Weisshaar, B.** (1998). Towards functional characterization of the members of the R2R3-MYB gene family from *Arabidopsis thaliana*. *The Plant Journal* **16**, 263-276
- Kubo, H., Kishi, M., and Goto, K.** (2008). Expression analysis of *ANTHOCYANINLESS2* gene in *Arabidopsis*. *Plant Science* **175**, 853-857.

BIBLIOGRAPHY

- Kang, J., Shi, F., Jones, A.D., Marks, M.D., and Howe, G.A.** (2010). Distortion of trichome morphology by the *hairless* mutation of tomato affects leaf surface chemistry. *Journal of Experimental Botany* **61**, 1053-1064.
- Kobayashi, K., Suzuki, T., Iwata, E., Magyar, Z., Bögre, L. and Ito, M.** (2015). MYB3Rs, plant homologs of Myb oncoproteins, control cell cycle-regulated transcription and form DREAM-like complexes. *Transcription* **6**, 106-111.
- Kanei-Ishii, C., Sarai, A., Sawazaki, T., Nakagoshi, H., He, D.N., Ogata, K., Nishimura, Y., and Ishii, S.** (1990). The tryptophan cluster: a hypothetical structure of the DNA-binding domain of the myb protooncogene product. *Journal of Biological Chemistry* **265**, 19990–19995.
- Kant, M.R., Ament, K., Sabelis, M.W., Haring, M.A., and Schuurink, R.C.** (2004). Differential timing of spider mite-induced direct and indirect defenses in tomato plants. *Plant Physiology* **135**, 483-495.
- Koornneef, M., van der Veen, J.H., Spruit, C.J.P., and Karszen, C.M.** (1981). The isolation and use of mutants with an altered germination behaviour in *Arabidopsis thaliana* and tomato. – In *Induced Mutation - a Tool in Plant Research* (P. Howard Kitto, ed.), 227-232.
- Koornneef, M.** (1981). The complex syndrome of *ttg* mutants. *Arabidopsis Information Service* **18**, 45-51.
- Koornneef, M., Dellaert, L.W.M., and van der Veen, J.H.** (1982). EMS- and radiation-induced mutation frequencies at individual loci in *Arabidopsis thaliana* (L. Heynh). *Mutation Research* **93**, 109-123.
- Lloyd, A.M., Walbot, V., and Davis, R.W.** (1992). *Arabidopsis* and *Nicotiana* anthocyanin production activated by maize anthocyanin-specific regulators, *R* and *C1*. *Science* **258**, 1773-75.
- Langmead, B., Trapnell, C., Pop, M., and Salzberg, S.L.** (2009). Ultrafast and memory-efficient alignment of short DNA sequences to the human genome. *Genome Biology* **10**, R25.
- LOHSE, M., NAGEL, A., HERTER, T., MAY, P., SCHRODA, M., ZRENNER, R., TOHGE, T., FERNIE, A. R., STITT, M. and USADEL, B.** (2014). Mercator: a fast and simple web server for genome scale functional annotation of plant sequence data. *Plant Cell Environment* **37**, 1250-1258.
- Luckwill, L.C.** (1943). *The Genus Lycopersicon: A Historical, Biological, and Taxonomic Survey of the Wild and Cultivated Tomatoes*. Aberdeen, UK: Aberdeen University Press.
- Li, L., Zhao, Y.F., McCaig, B.C., Wingerd, B.A., Wang, J.H., Whalon, M.E., Pichersky, E. and Howe, G.A.** (2004). The tomato homolog of CORONATINEINSENSITIVE1 is required for the maternal control of seed maturation, jasmonate-signaled defense responses, and glandular trichome development. *The Plant Cell* **16**, 126-143.
- Levin, D.A** (1973). The role of trichomes in plant defense. *Quarterly review of biology* **48**, 3-15.
- Lashbrooke, J., Adato, A., Lotan, O., Alkan, N., Tsimbalist, T., Rechav, K., Fernández- Moreno, J.P., Widemann, E., Grausem, B., Pinot, F., and Aharoni, A.** (2015). The Tomato MIXTA-like transcription factor coordinates fruit epidermis conical cell development and cuticular lipid biosynthesis and assembly. *Plant Physiology* **169**, 2553-2571.
- Lian, T.F., Xu, Y.P., Li, L.F., and Su, X.D.** (2017). Crystal structure of tetrameric *Arabidopsis* MYC2 reveals the mechanism of enhanced interaction with DNA. *Cell Reports* **19**, 1334-1342

- Lu, P., Porat, R., Nadeau, J.A., and O'Neill, S.D.** (1996). Identification of a Meristem L1 layer-specific gene in *Arabidopsis* that is expressed during embryonic pattern formation and defines a new class of homeobox genes. *The Plant Cell* **8**, 2155-2168.
- Liu, J., Xia, K.F., Zhu, J.C., Deng, Y.G., Huang, X.L., Hu, B.L., Xu, X., Xu, Z.F.** (2006). The nightshade proteinase inhibitor IIb gene is constitutively expressed in glandular trichomes. *Plant Cell Physiology* **47**, 1274-1284.
- Lorenzo, O., Chico, J.M., Sanchez-Serrano, J.J., and Solano, R.** (2004). JASMONATE-INSENSITIVE1 encodes a MYC transcription factor essential to discriminate between different jasmonate-regulated defense responses in *Arabidopsis*. *The Plant Cell* **16**, 1938-1950.
- Li, Z., Peng, R., Tian, Y., Han, H., Xu, J., and Yao, Q.** (2016). Genome-wide identification and analysis of the MYB transcription factor superfamily in *Solanum lycopersicum*. *Plant Cell Physiology* **57**, 1657-1677.
- Littlewood, T., and Evan, G.I.** (1998). Helix-Loop-Helix transcription factors, 3rd ed. (New York: Oxford University Press).
- Ledent, V., and Vervoort, M.** (2001). The basic helix-loop-helix protein family: Comparative genomics and phylogenetic analysis. *Genome Research* **11**, 754-770.
- Lin, Q., Hamilton, W.D.O., and Merryweather, A.** (1996). Cloning and initial characterization of 14 myb-related cDNAs from tomato (*Lycopersicon esculentum* cv. Ailsa Craig). *Plant Molecular Biology* **30**, 1009-1020.
- Lipsick, J.S.** (1996). One billion years of Myb. *Oncogene* **13**, 223-235.
- Larkin, J. C., Brown, M. L., and Schiefelbein, J.** (2003). How do cells know what they want to be when they grow up? Lessons from epidermal patterning in *Arabidopsis*. *Annual Review of Plant Biology* **54**, 403-430.
- Lee, M.M., and Schiefelbein, J.** (1999). WEREWOLF, a MYB-related protein in *Arabidopsis*, is a position-dependent regulator of epidermal cell patterning. *Cell* **99**, 473-483.
- Lee, M.M., and Schiefelbein, J.** (2002). Cell pattern in the *Arabidopsis* root epidermis determined by lateral inhibition with feedback. *The Plant Cell* **14**, 611-618.
- Li, C.Y., Williams, M.M., Loh, Y.T., Lee, G.I., and Howe, G.A.** (2002). Resistance of cultivated tomato to cell content-feeding herbivores is regulated by the octadecanoid-signaling pathway. *Plant Physiology* **130**, 494-503.
- Larkin, J.C., Oppenheimer, D.G., Pollock, S., and Marks, M.D** (1993). *Arabidopsis* GLABROUS1 gene requires downstream sequences for function. *The Plant Cell* **5**, 1739-1748.
- Maluf, W.R., Campos, G.A., and Cardoso, C.M.** (2001). Relationships between trichome types and spidermite (*Tetranychus evansi*) repellence in tomatoes with respect to foliar zingiberene contents. *Euphytica* **121**, 73-80.
- Murre, C., McCaw, P.S., and Baltimore, D.** (1989). A new DNA-binding and dimerization motif in immunoglobulin enhancer binding, daughterless, MyoD, and myc proteins. *Cell* **56(5)**, 777-783.
- Massari, M.E., and Murre, C.** (2000). Helix-loop-helix proteins: regulators of transcription in eukaryotic organisms. *Molecular Cell Biology* **20(2)**, 429-440.

BIBLIOGRAPHY

- Murakami, Y.** (1972). Dwarfing genes in rice and their relation to gibberellin biosynthesis. - In *Plant Growth Substances 1970* (D, 1, Carr. ed.), Springer-Verlag, Berlin, 16-174.
- Miller, C.O.** (1961). Kinetin and related components in plant growth. *Annual Review of Plant Physiology* **12**, 395–408.
- Meissner, R., Jacobson, Y., Melamed, S., Levyatuv, S., Shalev, G., Ashri, A., Elkind, Y., Levy, A.** (1997). A new model system for tomato genetics. *Plant Journal* **12**, 1465-1472.
- Mathur, J., and Chua, N.** (2000). Microtubule stabilization leads to growth reorientation in *Arabidopsis* trichomes. *The Plant Cell* **12**, 465-477.
- Maffei, M.E.** (2010). Sites of synthesis, biochemistry and functional role of plant volatiles. *South African Journal of Botany* **76**, 612-631.
- Hauser, M.T.** (2014). Molecular basis of natural variation and environmental control of trichome patterning. *Frontiers in Plant Science* **5**, 320.
- Mahmoud, S.S., and Croteau, R.B.** (2002). Strategies for transgenic manipulation of monoterpene biosynthesis in plants. *Trends in Plant Science* **7**, 366-373
- Matías-Hernández, L., Jiang, W., Yang, K., Tang, K., Brodelius, P.E., and Pelaz, S.** (2017). AaMYB1 and its orthologue AtMYB61 affect terpene metabolism and trichome development in *Artemisia annua* and *Arabidopsis thaliana*. *The Plant Journal* **90**, 520-534.
- Meinhardt, H., and Gierer, A.** (1974). Applications of a theory of biological pattern formation based on lateral inhibition. *Journal of Cell Science* **15**, 321-346.
- Meyer, H.M., Teles, J., Formosa-Jordan, P., Refahi, Y., San-Bento, R., Ingram, G., and Roeder, A.H.K.** (2017). Fluctuations of the transcription factor ATML1 generate the pattern of giant cells in the *Arabidopsis* sepal. *eLife*, **6**, e19131.
- Ma, D., Hu, Y., Yang, C., Liu, B., Fang, L., Wan, Q., Liang, W., Mei, G., Wang, L., Wang, H..., Zhang, T.** (2016) Genetic basis for glandular trichome formation in cotton. *Nature Communications* **7**, 10456.
- Masucci, J.D., Rerie, W.G., Foreman, D.R., Zhang, M., Galway, M.E, Marks, M.D., and Schiefelbein, J.** (1996). The homeobox gene GLABRA2 is required for position-dependent cell differentiation in the root epidermis of *Arabidopsis thaliana*. *Development* **122**, 1253–1260.
- Maes, L., Inze, D., and Goossens, A.** (2008). Functional specialization of the TRANSPARENT TESTA GLABRA1 network allows differential hormonal control of laminal and marginal trichome initiation in *Arabidopsis* rosette leaves. *Plant Physiology* **148**.
- Maes, L., van Nieuwerburgh, F.C.W., Zhang, Y., Reed, D.W., Pollier, J., Vande Castele, S.R.F., Inze, D., Covello, P.S., Deforce, D.L.D, Goossens, A.** (2011) Dissection of the phytohormonal regulation of trichome formation and biosynthesis of the antimalarial compound artemisinin in *Artemisia annua* plants. *New Phytologist* **189**, 176-189.
- Mathews, H., Clendennen, S. K., Caldwell, C. G., Liu, X. L., Connors, K., Matheis, N., ... Wagner, D. R.** (2003). Activation tagging in tomato identifies a transcriptional regulator of anthocyanin biosynthesis, modification, and transport. *The Plant Cell* **15**(8), 1689-1703.

- Marks, M.D., Esch, J., Herman, P., Sivakumaran, S., and Oppenheimer, D.** (1991). A model for cell-type determination and differentiation in plants. *Symposia of the Society for Experimental Biology* **45**, 77-87.
- Marks, M.D.** (1997). Molecular genetic analysis of trichome development in *Arabidopsis*. *Annual Review of Plant Physiology and Plant Molecular Biology* **48**, 137-163.
- Nagel, J., Culley, L.K., Lu, Y.P., Liu, E.W., Matthews, P.D., Stevens, J.F., and Page, J.E.** (2008). EST analysis of hop glandular trichomes identifies an O-methyltransferase that catalyzes the biosynthesis of xanthohumol. *The Plant Cell* **20**, 186-200.
- Neff, M.M., Neff, J.D., Chory, J., and Pepper, A.E.** (1998). dCAPS, a simple technique for the genetic analysis of single nucleotide polymorphisms: experimental applications in *Arabidopsis thaliana* genetics. *The Plant Journal* **14**, 387-392.
- Neff, M.M., Turk, E., and Kalishman, M.** (2002) Web-based primer design for Single Nucleotide Polymorphism Analysis. *Trends in Genetics* **18**, 613-615.
- Neer, E.J., Schmidt, C.J., Nambudripad, R., Smith, T.F.,** (1994). The ancient regulatory protein family of WD-repeat proteins. *Nature* **371**, 297-300.
- NOBEL, P.S.** (1999). *Physicochemical and environmental plant physiology*, 2nd ed., San Diego: Academic Press, p 540.
- Nadakuduti, S.S., Pollard, M., Kosma, D.K., Allen, C.Jr, Ohlrogge, J.B, and Barry, C.S.** (2012). Pleiotropic phenotypes of the sticky peel mutant provide new insight into the role of CUTIN DEFICIENT2 in epidermal cell function in tomato. *Plant Physiology* **159**, 945-960.
- Nakamura, M., Katsumata, H., Abe, M., Yabe, N., Komeda, Y., Yamamoto, K.T., and Takahashi, T.** (2006). Characterization of the class IV homeodomain-leucine zipper gene family in *Arabidopsis*. *Plant Physiology* **141**, 1363-1375.
- Oppenheimer, D.G., Herman, P.L., Sivakumaran, S., Esch, J., and Marks, M.D.** (1991). A *myb* gene required for leaf trichome differentiation in *Arabidopsis* is expressed in stipules. *Cell* **67**, 483-493.
- Okabe, Y., Asamizu, E., Saito, T., Matsukura, C., Ariizumi, T., Brès, C., Rothan, C., Mizoguchi, T., and Ezura, H.** (2011). Tomato TILLING Technology: Development of a Reverse Genetics Tool for the Efficient Isolation of Mutants from Micro-Tom Mutant Libraries. *Plant and Cell Physiology* **52(11)**, 1994-2005.
- Ogawa, E., Yamada, Y., Sezaki, N., Kosaka, S., Kondo, H., Kamata, N., Abe, M., Komeda, Y., and Takahashi, T.** (2015). ATML1 and PDF2 play a redundant and essential role in *Arabidopsis* embryo development. *Plant and Cell Physiology* **56**, 1183-1192.
- Pattanaik, S., Patra, B., Singh, S.K., and Yuan, L.** (2014). An overview of the gene regulatory network controlling trichome development in the model plant, *Arabidopsis*. *Frontiers in Plant Science* **5**, 259.
- Park, J.H., Halitschke, R., Kim, H.B., Baldwin, I.T., Feldmann, K. A., and Feyereisen, R.** (2002). A knock-out mutation in allene oxide synthase results in male sterility and defective wound signal transduction in *Arabidopsis* due to a block in jasmonic acid biosynthesis. *The Plant Journal* **31**, 1-12.
- Potts, W.C., and Reid, J.B.** (1983). Internode length in *Pisum*. III. The effect and interaction of the *Na/na* and *Le/le* gene differences on endogenous gibberellin-like substances. *Physiologia. Plantarum* **57**, 448-454.

BIBLIOGRAPHY

Phinney, B.O. (1960). Dwarfing genes in *Zea mays* and their relation to the gibberellins. - In Plant Growth Regulation (R.M. Klein, ed.), pp. 489-501. Ames, Iowa State College.

Pino-Nunes, L.E., Figueira, A.V.O., Tulmann Neto, A., Zsögön, A., Piotto FA, Silva JA and Peres, L.E.P. (2009). Induced Mutagenesis and natural genetic variation in tomato 'Micro-Tom'. *Acta Horticulturae* **821**, 63-72.

Perazza, D., Vachon, G., and Herzog, M. (1998). Gibberellins promote trichome formation by up regulating GLABROUS1 in Arabidopsis. *Plant Physiology* **117**, 375-383.

Peiffer, M., Tooker, J.F., Luthe, D.S., and Felton, G.W. (2009). Plants on early alert: Glandular trichomes as sensors for insect herbivores. *New Phytologist* **184**, 644-656.

Payne, T., Clement, J., Arnold, D., and Lloyd, A. (1999). Heterologous myb genes distinct from GL1 enhance trichome production when overexpressed in *Nicotiana tabacum*. *Development* **126**, 671-682

Payne, T., Zhang, F., and Lloyd, A. (2000). GL3 encodes a bHLH protein that regulates trichome development in Arabidopsis through interaction with GL1 and TTG1. *Genetics* **156**, 1349-1362.

Paz-Ares, J., Ghosal, D., Wienand, U., Peterson, P. and Saedler, H. (1987). The regulatory *cl* locus of *Zea mays* encodes a protein with homology to myb proto-oncogene products and with structural similarities to transcriptional activators. *EMBO Journal* **6**, 3553-3558.

Pullin, A.S., and Gilbert, J.E. (1989). The stinging nettle, *Urtica dioica*, increases trichome density after herbivore and mechanical damage. *Oikos* **54**, 275-280.

Qi, T., Song, S., Ren, Q., Wu, D., Huang, H., Chen, Y., Fan, M., Peng, W., Ren, C., and Xie, D. (2011). The Jasmonate-ZIM-domain proteins interact with the WD-Repeat/bHLH/MYB complexes to regulate Jasmonate mediated anthocyanin accumulation and trichome initiation in *Arabidopsis thaliana*. *The Plant Cell* **23**, 1795-1814.

Richmond, A.E., and Lang, A. (1957). Effect of kinetin on protein content and survival of detached *Xanthium* leaves. *Science* **125**, 650-651.

Robinson, M.D., McCarthy, D.J., and Smyth, G.K. (2010). edgeR: a Bioconductor package for differential expression analysis of digital gene expression data. *Bioinformatics* **26**, 139-140.

Robinson, M.D and Oshlack. (2010). A scaling normalization methods for differential expression analysis of RNA-seq data. *Genome Biology* **11**, R25.

Ramsay, N.A., and Glover, B.J. (2005). MYB-bHLH-WD40 protein complex and the evolution of cellular diversity. *Trends in Plant Science* **10(2)**, 63-70.

Reymond, P., Weber, H., Damond, M., and Farmer, E.E. (2000). Differential gene expression in response to mechanical wounding and insect feeding in *Arabidopsis*. *The Plant Cell* **12**, 707-719.

Rerie, W.G., Feldmann, K.A., and Marks, M.D. (1994). The GLABRA2 gene encodes a homeo domain protein required for normal trichome development in Arabidopsis. *Genes and Development* **8**, 1388-1399.

Riechmann, J.L., and Ratcliffe, O.J. (2000) A genomic perspective on plant transcription factors. *Current Opinion in Plant Biology* **3**, 423-434.

Sallaud, C., Rontein, D., Onillon, S., Jabès, F., Duffé, P., Giacalone, C., Thoraval, S., Escoffier, C., Herbette, G., Leonhardt, N., Causse, M and Tissier, A. (2009). A Novel Pathway for

Sesquiterpene Biosynthesis from Z,Z-Farnesyl Pyrophosphate in the Wild Tomato *Solanum habrochaites*. *The Plant Cell* 21(1), 301-317

Samuels, L., Kunst, L., and Jetter, R. (2008). Sealing plant surfaces: cuticular wax formation by epidermal cells. *Annual Review of Plant Biology* 59, 683-707.

Simmons, A.T. and Gurr, G.M. (2005). Trichomes of *Lycopersicon* species and their hybrids: effects on pests and natural enemies. *Agricultural and Forest Entomology* 7, 265-276.

Swain, S.M., Tseng, T.-S., and Olszewski, N.E. (2001). Altered expression of SPINDLY affects gibberellin response and plant development. *Plant Physiology* 126, 1174-1185.

Swain, S.M., Tseng, T.-S., Thornton, T.M., Gopal Raj, M., and Olszewski, N. (2002). SPINDLY is a nuclear-localized repressor of gibberellin signal transduction expressed throughout the plant. *Plant Physiology* 129, 605-615.

Silverstone, A.L., Tseng, T.-S., Swain, S.M., Dill, A., Jeong, S.Y., Olszewski, N.E., and Sun, T. (2007). Functional analysis of SPINDLY in gibberellin signaling in *Arabidopsis*. *Plant Physiology* 143(2), 987-1000.

Skoog, F., and Miller, C.O. (1957). Chemical regulation of growth and organ formation in plant tissues cultured in vitro. *Symposia of the Society for Experimental Biology*. 54, 118-30.

Silin, Zhong., Je-Gun, Joung., Yi, Zheng., Yun-ru, Chen., Bao, Liu., Ying, Shao., Jenny, Z., Xiang., Zhangjun, Fei., and Giovannoni, J.J. (2011). High-throughput Illumina strand-specific RNA sequencing Library Preparation. *Cold Spring Harbor Protocols*.

Serna, L., and Martin, C. (2006). Trichomes: different regulatory networks lead to convergent structures. *Trends in Plant Science* 11(6), 274-280

Serrani, J.C., Fos, M., Atares, A., and Garcia-Martinez, J.L. (2007). Effect of gibberellin and auxin on parthenocarpic fruit growth induction in the cv MicroTom of tomato. *Journal of Plant Growth Regulation* 26, 211-21.

Schillmiller, A.L., Last, R.L., and Pichersky, E. (2008). Harnessing plant trichome biochemistry for the production of useful compounds. *Plant Journal* 54, 702-711.

Schnittger, A., Folkers, U., Schwab, B., Jürgens, G., and Hülskamp, M. (1999). Generation of a spacing pattern: the role of *TRIPTYCHON* in trichome patterning in *Arabidopsis*. *The Plant Cell* 11, 1105-1116.

Schnittger, A., and Hülskamp, M. (2002). Trichome morphogenesis: A cell-cycle perspective. *Philosophical Transactions of the Royal Society of London. Series B* 357, 823-826.

Schwab, B., Folkers, U., Ilgenfritz, H., and Hülskamp, M. (2000). Trichome morphogenesis in *Arabidopsis*. *Philosophical Transactions of the Royal Society of London. Series B* 355, 879-883.

Schoonhoven, L.M., Jermy, T., and van Loon J.J.A. (1998). *Insect-Plant Biology: From Physiology to Evolution*. Chapman & Hall, London.

Southwood, T.R.E. (1986). Plant surfaces and insects – an overview. In: Juniper BE, Southwood TRE, eds. *Insects and the plant surface* London: Edward Arnold, 1–22.

Suen, P.K., Zhang, S., and Sun, S.S.M. (2015). Molecular characterization of tomato purple acid phosphatase during seed germination and seedling growth under phosphate stress. *The Plant Cell Reports* 34, 981-992.

BIBLIOGRAPHY

- Spyropoulou, E.A., Haring, M.A., Schuurink, R.C.** (2014). RNA sequencing on *Solanum lycopersicum* trichomes identifies transcription factors that activate terpene synthase promoters. *BMC Genomics* **15**, 402.
- Schillmiller, A., Shi, F., Kim, J., Charbonneau, A.L., Holmes, D., Daniel Jones, A., and Last, R.L.** (2010). Mass spectrometry screening reveals widespread diversity in trichome specialized metabolites of tomato chromosomal substitution lines. *The Plant Journal* **62**(3), 391-403.
- Shi, P., Fu, X., Shen, Q., Liu, M., Pan, Q., Tang, Y., Jiang, W., Lv, Z., Yan, T., Ma, Y., Chen, M., Hao, X., Liu, P., Li, L., Sun, X., Tang, K.** (2017). The roles of AaMIXTA1 in regulating the initiation of glandular trichomes and cuticle biosynthesis in *Artemisia annua* L. *New Phytologist* **217**, 261-276.
- Shi, X., Gupta, S., Lindquist, I.E., Cameron, C.T., Mudge, J., and Rashotte, A.M.** (2013). Transcriptome Analysis of Cytokinin Response in Tomato Leaves. *PLoS ONE* **8**(1), e55090.
- Sessions, A., Weigel, D., and Yanofsky, M.F.** (1999). The *Arabidopsis thaliana* *MERISTEM LAYER 1* promoter specifies epidermal expression in meristems and young primordia. *Plant Journal* **20**, 259-263.
- Schweizer, F., Fernández-Calvo, P., Zander, M., Diez-Diaz, M., Fonseca, S., Glauser, G., Lewsey, M.G., Ecker, J.R., Solano, R., and Reymond, P.** (2013). *Arabidopsis* Basic Helix-Loop-Helix transcription factors MYC2, MYC3, and MYC4 regulate glucosinolate biosynthesis, insect performance, and feeding behavior. *The Plant Cell* **25**(8), 3117-3132.
- Sun, X., Gong, S.-Y., Nie, X.-Y., Li, Y., Li, W., Huang, G.-Q., and Li, X.-B.** (2015). A R2R3-MYB transcription factor that is specifically expressed in cotton (*Gossypium hirsutum*) fibers affects secondary cell wall biosynthesis and deposition in transgenic *Arabidopsis*. *Physiologia Plantarum* **154**, 420-432.
- Schmitz, G., Tillmann, E., Carriero, F., Fiore, C., Cellini, F. and Theres, K.** (2002). The tomato Blind gene encodes a MYB transcription factor that controls the formation of lateral meristems. *Proceedings of the National Academy of Sciences of the USA* **99**, 1064-1069.
- Schellmann, S., Schnittger, A., Kirik, V., Wada, T., Okada, K., Beermann, A., Thumfarh, J., Jürgens, G., and Hülskamp, M.** (2002). TRIPTYCHON and CAPRICE mediate lateral inhibition during trichome and root hair patterning in *Arabidopsis*. *EMBO Journal* **21**, 5036-5046.
- Schiefelbein, J.** (2003). Cell-fate specification in the epidermis: a common patterning mechanism in the root and shoot. *Current Opinion in Plant Biology* **6**, 74-78.
- Szymanski, D.B, Jilk, R.A., Pollock, S.M., and Marks, M.D.** (1998). Control of *GL2* expression in *Arabidopsis* leaves and trichomes. *Development* **125**, 1161-1171.
- Szymanski, D.B, Lloyd, A.M., and Marks, M.D.** (2000). Progress in the molecular genetic analysis of trichome initiation and morphogenesis in *Arabidopsis*. *Trends in Plant Science* **5**, 214-219.
- Staswick, P.E., and Tiryaki, I.** (2004). The oxylipin signal jasmonic acid is activated by an enzyme that conjugates it to isoleucine in *Arabidopsis*. *The Plant Cell* **16**, 2117-2127.
- Staswick, P., Su, W., Howell, S.** (1992). Methyl jasmonate inhibition of root growth and induction of a leaf protein are decreased in an *Arabidopsis thaliana* mutant. *Proceedings of the National Academy of Sciences of the USA* **89**, 6837-6840.
- Suza, W., Rowe, M., Hamberg, M., and Staswick, P.** (2010). A tomato enzyme synthesizes (+)-7-iso-jasmonoyl-L-isoleucine in wounded leaves. *Planta* **231**, 717-728.

- Stintzi, A., and Browse, J.** (2000). The *Arabidopsis* male-sterile mutant, *opr3*, lacks the 12-oxophytodienoic acid reductase required for jasmonate synthesis. *Proceedings of the National Academy of Sciences of the USA* **97**, 10625-10630.
- Schaller, A., and Stintzi, A.** (2009). Enzymes in jasmonate biosynthesis: Structure, function, regulation. *Phytochemistry* **70**, 1532-1538.
- Stitz, M., Gase, K., Baldwin, I.T., and Gaquerel, E.** (2011). Ectopic expression of AtJMT in *Nicotiana attenuata*: Creating a metabolic sink has tissue-specific consequences for the jasmonate metabolic network and silences downstream gene expression. *Plant Physiology* **157**, 341-354.
- Stenzel, I., Otto, M., Delker, C., Kirmse, N., Schmidt, D., Miersch, O., Hause, B., and Wasternack, C.** (2012). ALLENE OXIDE CYCLASE (AOC) gene family members of *Arabidopsis thaliana*: tissue- and organ-specific promoter activities and in vivo heteromerization. *Journal of Experimental Botany* **63**, 6125-6138.
- Stenzel, I., Hause, B., Miersch, O., Kurz, T., Maucher, H., Weichert, H., Ziegler, J., Feussner, I., and Wasternack, C.** (2003b). Jasmonate biosynthesis and the allene oxide cyclase family of *Arabidopsis thaliana*. *Plant Molecular Biology* **51**, 895-911.
- Tseng, T.-S., Salome, P.A., McClung, C.R., and Olszewski, N.E.** (2004). SPINDLY and GIGANTEA interact and act in *Arabidopsis thaliana* pathways involved in light responses, flowering, and rhythms in cotyledon movements. *The Plant Cell* **16**, 1550-1563.
- Trapnell, C., Pachter, L., and Salzberg, S.L.** (2009). TopHat: discovering splice junctions with RNA-Seq. *Bioinformatics* **25**, 1105-1111.
- Traw, M.B., and Bergelson, J.** (2003). Interactive effects of jasmonic acid, salicylic acid, and gibberellin on induction of trichomes in *Arabidopsis*. *Plant Physiology* **133**, 1367-1375.
- The Tomato Genome Consortium.** (2012). The tomato genome sequence provides insights into fleshy fruit evolution. *Nature* **485**, 635-641.
- Thimm, O., Bläsing, O., Gibon, Y., Nagel, A., Meyer, S., Krüger, P., Selbig, J., Müller, L.A., Rhee, S.Y. and Stitt, M.** (2004). Mapman: a user-driven tool to display genomics data sets onto diagrams of metabolic pathways and other biological. *The Plant journal* **37**(6), 914-939.
- Tissier, A.** (2012). Glandular trichomes: What comes after expressed sequence tags? *The Plant Journal* **70**, 51-68.
- Tingey, W.M.** (1991). Potato glandular trichomes: defensive activity against insect attack. In: Hedin PA, ed. Naturally occurring pest bioregulators. A.C.S. Symposium Series **449**. Washington, DC: A.C.S. Books, 126-135.
- Tian, D., Tooker, J., Peiffer, M., Chung, S.H., and Felton, G.W.** (2012). Role of trichomes in defence against herbivores: comparison of herbivore response to *wolly* and *hairless* trichome mutants in tomato (*Solanum lycopersicum*). *Planta* **236**, 1053.
- Thines, B., Katsir, L., Melotto, M., Niu, Y., Mandaokar, A., Liu, G., Nomura, K., He, S.Y., Howe, G.A., and Browse, J.** (2007). JAZ repressor proteins are targets of the SCF (COI1) complex during jasmonate signalling. *Nature* **448**, 661-665.
- Toledo-Ortiz, G., Huq, E., and Quail, P.H.** (2003). The *Arabidopsis* basic/helix loop- helix transcription factor family. *The Plant Cell* **15**, 1749-1770.

BIBLIOGRAPHY

- Takada, S., and Jürgens, G.** (2007). Transcriptional regulation of epidermal cell fate in the Arabidopsis embryo. *Development* **134**, 1141-1150.
- Takada, S., Takada, N., and Yoshida, A.** (2013). ATML1 promotes epidermal cell differentiation in Arabidopsis shoots. *Development* **140**, 1919-1923.
- Thaler, J.S.** (1999). Jasmonate-inducible plant defence causes increased parasitism of herbivores. *Nature* **399**, 686-688.
- Traw, M.B., and Dawson, T.E.** (2002a). Differential induction of trichomes by three herbivores of black mustard. *Oecologia* **131**, 526-532.
- Traw, M.B., and Dawson, T.E.** (2002b) Reduced performance of two specialist herbivores (Lepidoptera: Pieridae, Coleoptera: Chrysomelidae) on new leaves of damaged black mustard plants. *Environmental Entomology* **31**, 714-722.
- Uphof, J.C.T.** (1962). Plant hairs. In *Handbuch der Pflanzenanatomie*, Bd. 4, Teil 5 (Finsbauer, K., ed.). Berlin: Borntraeger, pp. 1–292.
- Ueda, J., and Kato, J.** (1980). Isolation and identification of a senescence-promoting substance from wormwood (*Artemisia absinthium* L.) *Plant Physiology* **66**, 246-249.
- Van Der Hoeven, R.S., Monforte, A.J., Breeden, D., Tanksley, S.D. and Steffens, J.C.** (2000). Genetic control and evolution of sesquiterpene biosynthesis in *Lycopersicon esculentum* and *Lycopersicon hirsutum*. *The Plant Cell* **12**, 2283-2294.
- Valkama, E., Koricheva, J., Ossipov, V., Ossipova, S., Haukioja, E., and Pihlaja, K.** (2005). Delayed induced responses of birch glandular trichomes and leaf surface lipophilic compounds to mechanical defoliation and simulated winter browsing. *Oecologia* **146**, 385-393.
- Vollbrecht, E., Veit, B., Sinha, N., and Hake, S.** (1991). The developmental gene *Knotted-1* is a member of a maize homeobox gene family. *Nature* **350**, 241-243.
- Wilkens, R.T., Shea, G.O., Halbreich, S., and Stamp, N.E.** (1996). Resource availability and the trichome defenses of tomato plants. *Oecologia*, **106**, 181-191.
- Wickson, M., and Thimann, K.** (1958). The antagonism of auxin and kinetin in apical dominance. *Physiologia Plantarum* **11**, 62–74
- Wagner, G.J., Wang, E., and Shepherd, R.W.** (2004). New approaches for studying and exploiting an old protuberance, the plant trichome. *Annals of Botany* **93**, 3-11.
- Werker, E.** (2000). Trichome diversity and development. In *Advances in Botanical Research Incorporating Advances in Plant Pathology*, Vol. 31: Plant Trichomes (Hallahan, D.L. and Gray, J.C., eds). San Diego/Boston/ London: Academic Press, pp. 1–35.
- Walker, A.R., Davison, P.A., Bolognesi-Winfield, A.C., James, C.M., Srinivasan, N., Blundell, T.L., Esch, J.J., Marks, M.D., and Gray, J.C.** (1999). The *Transparent Testa Glabra1* locus, which regulates trichome differentiation and anthocyanin biosynthesis in Arabidopsis, encodes a WD40 repeat protein. *The Plant Cell* **11**, 1337-1349.
- Wang, J., Hu, Z., Zhao, T., Yang, Y., Chen, T., Yang, M., and Zhang, B.** (2015). Genome-wide analysis of bHLH transcription factor and involvement in the infection by yellow leaf curl virus in tomato (*Solanum lycopersicum*). *BMC Genomics* **16(1)**, 39.

- Wada, T., Tachibana, T., Shimura, Y and Okada, K.** (1997). Epidermal cell differentiation in *Arabidopsis* determined by a Myb homolog, *CPC*. *Science* **277**, 1113-1116.
- Wada, T., Kurata, T., Tominaga, R., Koshino-Kimura, Y., Tachibana, T., Goto, K., Marks, M.D., Shimura, Y., and Okada, K.** (2002). Role of a positive regulator of root hair development, *CAPRICE*, in *Arabidopsis* root epidermal cell differentiation. *Development* **129**, 5409-5419.
- Wada, T.R., Nukumizu, Y., Sato, S., and Wada, T.** (2013). Control of plant trichome and root-hair development by a tomato (*Solanum lycopersicum*) R3 MYB transcription factor. *PLoS One* **8**, e54019.
- Wasternack, C.** (2007). Jasmonates: An update on biosynthesis, signal transduction and action in plant stress response, growth and development. *Annals of Botany* **100**, 681-697.
- Wasternack, C., and Hause, B.** (2013). Jasmonates: biosynthesis, perception, signal transduction and action in plant stress response, growth and development. An update to the 2007 review in *Annals of Botany*. *Annals of Botany* **111**(6), 1021-1058.
- Xie, D.X., Feys, B.F., James, S., Nieto-Rostro, M., and Turner, J.G.** (1998). *COI1*: an *Arabidopsis* gene required for jasmonate-regulated defense and fertility. *Science* **280**, 1091–1094.
- Yoshida Y., Sano R., Wada T., Takabayashi J. and Okada K.** (2009). Jasmonic acid control of *GLABRA3* links inducible defense and trichome patterning in *Arabidopsis*. *Development* **136**, 1039-1048.
- Xu, Y.H., Liao, Y.C., Lv, F.F., Zhang, Z., Sun, P.W., Gao, Z.H., Hu, K.P., Sui, C., Jin, Y., and Wei, J.H.** (2017). Transcription factor *AsMYC2* controls the jasmonate-responsive expression of *ASS1* regulating sesquiterpene biosynthesis in *Aquilaria sinensis* (Lour.) Gilg. *Plant and Cell Physiology*, **58**(11), 1924-1933.
- Yan, T., Chen, M., Shen, Q., Li, L., Fu, X., Pan, Q., Tang, Y., Shi, P., Lv, Z., Jiang, W., Ma, Y.N., Hao, X., Sun, X., and Tang, K.** (2017). *HOMEODOMAIN PROTEIN 1* is required for jasmonate-mediated glandular trichome initiation in *Artemisia annua*. *New Phytologist* **213**, 1145-1155.
- Yang, Y., Li, R. and Qi, M.** (2000). In vivo analysis of plant promoters and transcription factors by agro-infiltration of tobacco leaves. *The Plant Journal* **22**, 543-551.
- Yoo, S.-D., Cho, Y.-H., and Sheen, J.** (2007). *Arabidopsis mesophyll protoplasts: a versatile cell system for transient gene expression analysis*. *Nature Protocols* **2**, 1565-1572.
- Yang, C.X., Li, H.X., Zhang, J.H., Luo, Z., Gong, P., Zhang, C., Li, J., Wang, T., Zhang, Y., Lu, Y., and Ye, Z.** (2011). A regulatory gene induces trichome formation and embryo lethality in tomato. *Proceedings of the National Academy of Sciences of the USA* **108**, 11836-11841.
- Yan, Y., Stolz, S., Chételat, A., Reymond, P., Pagni, M., Dubugnon, L., and Farmer, E.E.** (2007). A downstream mediator in the growth repression limb of the jasmonate pathway. *The Plant Cell* **19**, 2470-2483.
- Zhong, S., Joung, J.G., Zheng, Y., Chen, Y.R., Liu, B., Shao, Y., Xiang J.Z., Fei, Z., and Giovannoni J.J.** (2011). High-throughput illumina strand-specific RNA sequencing library preparation. *Cold Spring Harbor Protocols* 940–949.
- Zsögön, A., Lambais, M.R., Benedito, V.A., Figueira, A.V.D., and Peres, L.E.P.** (2008). Reduced arbuscular mycorrhizal colonization in tomato ethylene mutants. *Scientia Agricola* **65**, 259-267.

BIBLIOGRAPHY

Zrachya, A., Kumar, P.P., Ramakrishnan, U., Levy, Y., Loyter, A., Arazi, T., Lapidot, M., Gafni, Y. (2007). Production of siRNA targeted against TYLCV coat protein transcripts leads to silencing of its expression and resistance to the virus. *Transgenic Research* **16**, 385-398.

Zimmermann, I.M., Heim M.A., Weisshaar, B., and Uhrig, J.F. (2004) Comprehensive identification of *Arabidopsis thaliana* MYB transcription factors interacting with R/B-like BHLH proteins. *The Plant Journal* **40**, 22-34.

Zhang, F., Yao, J., Ke, J., Zhang, L., Lam, V.Q., Xin, X.F., Zhou, X.E., Chen, J., Brunzelle, J., Griffin, P.R., Zhou, M., Xu, H.E., Melcher, K., He, S.Y. (2015). Structural basis of JAZ repression of MYC transcription factors in jasmonate signalling. *Nature* **525**, 269-273.

Zhang, F., Gonzalez, A., Zhao, M., Payne, T., and Lloyd, A. (2003). A network of redundant bHLH proteins functions in all ITTG1-dependent pathways of *Arabidopsis*. *Development* **130**, 4859-4869.

ACKNOWLEDGEMENTS

Completion of doctoral research was a long journey and I would like to express my sincere regards for everyone who has been a part of this research journey. I would like to express my gratitude to Prof. Dr. Bettina Hause for giving me an opportunity to pursue doctoral research work in her group. It was an honor to be her doctoral student. Her outstanding supervision, critical assessment of thesis work with valuable remarks and providing a good atmosphere at the work place was one of the greatest experiences. I would like to sincerely extend my gratitude to Prof. Dr. Alain Tissier for giving me this wonderful opportunity to work in the project and his helpful suggestions during the research progress.

I am grateful to my collaborators, Prof. Dr. Jim Giovannoni and Dr. Zhangjun Fei for the successful RNA-sequencing at the Boyce Thomson Research institute, Ithaca (USA). I kindly thank Dr. Yoshihiro Okabe at the University of Tsukuba, Japan for the generation of TILLING mutant lines. Further, I express my vote of thanks to Mr. Frank Syrowatka at the ICMS, Halle for analyzing the leaf samples under ESEM.

I would like to extend my gratefulness to Dr. Benedikt Athmer for an in-depth analysis of RNA-seq data, his technical suggestions and introducing bioinformatics platform to analyze the dataset.

I would like to kindly thank Dr. Lennart Eschen-Lippold for introducing interesting techniques, critical remarks on the data and most importantly assessing my dissertation work with valuable remarks.

I would like to express my vote of thanks to Dr. Nick Bergau and Martin Wehse for their preliminary works in this project work, and Dr. Stefan Bennewitz for his technical guidance and fruitful discussions. Further I would like to extend my vote of thanks to PD. Dr Thomas Vogt for his conceptual discussions, technical clarifications, editing my thesis and interesting talks. I would like to thank Dr. Sylvestre Marillonnet for introducing golden gate cloning strategy and Dr. Tom Schreiber for his technical inputs and helpful discussions.

Approximately four years in the lab was a great experience with our lab members. Ulrike Huth, Ramona Schubert, Yulong Li, Heena Yadav, Hagen Stellmach and Dorothea Kleemann for their lively companionship at work and during social events. I thank you each one of you for introducing new techniques or any technical suggestions. It was indeed a great time with you all.

I vow my regards to Dr. Günther Kahlert and Lindsey Köhler at the Systems Biology of Molecular Medicine for taking their time off from busy working schedules and reviewing my thesis work with fruitful remarks. Further, I kindly thank Philip Rebenburg for the summary translation and helpful remarks on the thesis work.

To my beloved parents, Lakshmi and Kemparaju, brothers, Sandeep and Raghavendra, lovely wife Vyshnavi and newly arrived daughter Aadhya. It's a blessing to be in the part of family who have constantly supported and motivated in all the phases of life during doctoral research work. I thank you for being with me in every step of this journey. To all my friends, I thank you all for your companionship, support and motivations.

Curriculum Vitae

Personal Details

First and Last name: Chandan Chiniga Kemparaju
Address: Große Ulrichstraße 40
06108 Halle
Contact Number: +4915773113249
E-Mail address: cchiniga@ipb-halle.de
chandansees@gmail.com
Date of Birth: 08.11.1985 in Hospet (Karnataka, India)
Marital status: Married
Children: 01

Academic Education

08.2013 – Present **Martin-Luther-University, Halle-Wittenberg**
Doctoral researcher at the Leibniz Institute for Plant Biochemistry (IPB), Halle
Jasmonates and Mycorrhiza group
Department of Cell and Metabolic Biology
Doctoral thesis: Identification and Characterization of JA-regulated components involved in the development of glandular trichomes in cultivated tomato

10.2010 – 05.2013 **Rheinische Friedrich-Wilhelms-Universität Bonn**
Master of Science (M.Sc.)
StreamLine – Plant Sciences, Note: 2,1
Master thesis: Genetic characterization of soil microbiome infested with *Trichoderma* and *Verticillium* fungi species to control strawberry wilt symptoms in Brandenburg strawberry fields.

05.2004 – 08.2008 **Visveshwaraya Technological University, Karnataka, India**
Bachelor of Engineering (B.E)
StreamLine – Biotechnology, Note: First Class with Distinction (FCD)

Bachelor thesis: Maize transformation with reporter gene constructs at the Monsanto Research Center, Bengaluru, India

Work Experience

05.2013 – 31.2016

Research Associate

Leibniz Institute for Plant Biochemistry (IPB)

Weinberg 3, Halle (Saale)

AG: Prof. Dr. Bettina Hause – Jasmonates and Mycorrhizha

Department: Cell and Metabolic Biology (SZB)

05.2012 – 04.2013

Research Assistant

Leibniz Center for Agricultural Landscape Research (ZALF) Eberswalderstrasse 86, Müncheberg.

AG: Dr. Peter Lentzsch – Fungal interactions

Department: Landscape Bio-geo-chemistry (LBG) and Plant pathology

01.2012 – 04.2012

Project Intern / Assistant

Max-Planck-Institute for Plant Breeding Research

Carl-von-Linné-Weg 10, Köln.

AG: Prof. Dr. Seth Davis

Department: Plant Developmental Biology

Project title: Functional characterization of circadian clock genes in *Arabidopsis*.

08/2011 - 10/2011

Student Assistant

Rheinische Friedrich-Wilhelms-Universität Bonn

Kirschallee 1, Bonn.

AG: Prof. Dr. Dorothea Bartels

Department: Plant Molecular Physiology

Project title: Analyzing the molecular response between drought-resistant *Craterostigma plantagineum* and drought-sensitive *Lindernia subracemosa*.

10/2008 - 06/2010

Research Associate

Nitya Genomics Center, Bengaluru.

Project title: Effect of environmental factors on the occurrence and distribution of important native medicinal plant species in the Western Ghats, India.

Technical Skills

Molecular biology

Genomic DNA, Plasmid DNA and RNA extraction.

Agarose gel, capillary-gel electrophoresis, SDS-PAGE

| | |
|---------------------|---|
| Protein assays | Protein isolation, Western blot, Co-IP assay |
| Histology | Paraplast, PEG embedding, GUS und <i>in situ</i> hybridization |
| Microbiology | Growth of fungal and bacterial cultures / treatments and sterilizations |
| DNA modification | PCR, qPCR, golden-gate cloning, restriction digestion, ligation RFLP and RAPD |
| Microscopy | Bright field, fluorescence and laser scanning microscope |
| Plant Biotechnology | Maize and tomato transformation and regeneration |
| Metabolomics | GC-MS data analysis |

Conferences / Symposium

| | |
|------|---|
| 2016 | European Plant Science Organization (EPSO) - International conference, Prague, Czech Republic: Poster presentation |
| 2012 | International conference on <i>Verticillium dahliae</i> , Göttingen: participant |
| 2008 | International Conference on “Biotechnology Aspects and Future Trends of Biotechnology”, PESIT, Bengaluru – Active Organizer |
| 2006 | National Symposium on “Future Bio-Tech aspects and its Trends”, PESIT, Bengaluru – Organizer |
| 2005 | National Conference on “Molecular Biology and its Aspects” held at PESIT, Bengaluru -Organizer |

Language ability

| | |
|---------|--|
| Kannada | First language (Mother tongue) |
| English | Very good IELTS: 7.0 |
| German | Good A1, A2 certificate from Goethe Institute B1 certificate from Inlingua language school |

Hobbies

Badminton, travelling and reading

Eidesstattliche Erklärung

Hiermit erkläre ich, dass ich die vorliegende wissenschaftliche Arbeit selbstständig und ohne fremde Hilfe angefertigt habe. Ich erkläre weiterhin, dass ich keine anderen als die von mir angegebenen Quellen und Hilfsmittel benutzt habe und die den Werken wörtlich und inhaltlich entnommenen Stellen als solche kenntlich gemacht habe.

Mit dieser Arbeit bewerbe ich mich erstmals um die Erlangung des Doktorgrades. Diese Arbeit wurde an keiner anderen Fakultät oder Universität zur Begutachtung eingereicht.

Halle (Saale), den 19.06.2018

Chandan Chiniga Kemparaju